

**DEVELOPMENT OF TUNGSTEN NITROSYL ALKYLIDENE COMPLEXES FOR
ACTIVATION OF HYDROCARBONS**

by

Elizabeth Tran

B.Sc. (Hons), University of Ottawa, 1994

A THESIS SUBMITTED IN PARTIAL FULFILLMENT OF THE REQUIREMENTS FOR
THE DEGREE OF DOCTOR OF PHILOSOPHY

in

THE FACULTY OF GRADUATE STUDIES

(Department of Chemistry)

We accept this thesis as conforming to the required standard

THE UNIVERSITY OF BRITISH COLUMBIA

December 2001

© Elizabeth Tran, 2001

In presenting this thesis in partial fulfilment of the requirements for an advanced degree at the University of British Columbia, I agree that the Library shall make it freely available for reference and study. I further agree that permission for extensive copying of this thesis for scholarly purposes may be granted by the head of my department or by his or her representatives. It is understood that copying or publication of this thesis for financial gain shall not be allowed without my written permission.

Department of Chemistry
The University of British Columbia
Vancouver, Canada

Date Dec 11, 2001

Abstract

A series of tungsten alkyls of stoichiometry $\text{Cp}'\text{W}(\text{NO})(\text{R})(\text{R}')$ [$\text{Cp}' = \text{Cp}, \text{Cp}^*$; $\text{R} = \text{CH}_2\text{CMe}_3, \text{CH}_2\text{CMe}_2\text{Ph}, \text{CH}_2\text{SiMe}_3$; $\text{R}' = \text{CH}_2\text{CMe}_3, \text{CH}_2\text{CMe}_2\text{Et}, \text{CH}_2\text{CMe}_2\text{Ph}, \text{CH}_2\text{SiMe}_3, \text{CH}_3, \text{Ph}, \text{Cl}, \text{CH}_2\text{Ph}, \text{OCH}_3, \text{NMe}_2$] is shown by NMR and, in some cases, IR spectroscopies to adopt an α -agostic structure when secondary interactions such as lone pair or π -electron donation are not possible. This was confirmed by X-ray diffraction studies of several of these compounds and by a neutron diffraction study of $\text{Cp}^*\text{W}(\text{NO})(\text{CH}_2\text{CMe}_3)_2$. In each, the agostic interaction is best described as a closed, 3-center, 2-electron bond and serves to give the electron-deficient tungsten center an 18-electron configuration. The complexes in which R and R' are neopentyl-like display fluxional behavior in solution, exhibiting averaged NMR spectra as a result of a competition between R and R' for formation of an α -agostic bond with the metal. This competition is manifested in terms of unusual NMR chemical shifts and coupling constants for the α - CH_2 groups. These data establish that the strength of the $\text{C}-\text{H}\cdots\text{W}$ interaction is dependent on the nature of Cp' , R , and R' . For complexes with $\text{R} = \text{R}'$, it varies in the order $\text{Cp}^* > \text{Cp}$ and $\text{R} = \text{R}' = \text{CH}_2\text{CMe}_3 \approx \text{CH}_2\text{CMe}_2\text{Ph} \geq \text{CH}_2\text{SiMe}_3$. For complexes with $\text{R} \neq \text{R}'$, two trends are observed: First, among all the alkyl ligands studied, the relative α -agostic donor ability is $\text{CH}_2\text{CMe}_3 \geq \text{CH}_2\text{CMe}_2\text{Et} > \text{CH}_2\text{CMe}_2\text{Ph} > \text{CH}_2\text{SiMe}_3 \gg \text{CH}_3$ (CH_2Ph is nonagostic). Second, when $\text{R} = \text{CH}_2\text{CMe}_3$ and $\text{R}' = \text{CH}_2\text{CMe}_3, \text{CH}_2\text{CMe}_2\text{Et}, \text{CH}_2\text{CMe}_2\text{Ph}, \text{CH}_2\text{SiMe}_3, \text{CH}_3, \text{Ph}, \text{Cl}$, or CH_2Ph , the α -agostic donor ability of R decreases as R' is changed from Ph to CH_3 to Cl to CH_2SiMe_3 to $\text{CH}_2\text{CMe}_2\text{Ph}$ to $\text{CH}_2\text{CMe}_2\text{Et}$ to CH_2CMe_3 to CH_2Ph .

The neopentyl complexes, $\text{Cp}'\text{W}(\text{NO})(\text{CH}_2\text{CMe}_3)_2$ [$\text{Cp}' = \text{Cp}, \text{Cp}^*$] and $\text{Cp}^*\text{W}(\text{NO})(\text{CH}_2\text{CMe}_3)(\text{CH}_2\text{Ph})$, undergo facile α -abstraction of neopentane at 60–70 °C to give transiently the 16-electron alkylidene complexes, $[\text{Cp}'\text{W}(\text{NO})(=\text{CHCMe}_3)]$ and $[\text{Cp}^*\text{W}(\text{NO})(=\text{CHPh})]$, respectively. Both $[\text{Cp}'\text{W}(\text{NO})(=\text{CHCMe}_3)]$ and $[\text{Cp}^*\text{W}(\text{NO})(=\text{CHPh})]$ can be trapped with tertiary phosphines in THF solvent to yield the corresponding phosphine adducts as the anti rotamer. In the case of $[\text{Cp}^*\text{W}(\text{NO})(=\text{CHCMe}_3)]$, the trapping can also be effected in neat pyridine or Me_2NEt . $\text{Cp}^*\text{W}(\text{NO})(=\text{CHCMe}_3)(\text{PMe}_3)$ undergoes associative addition reactions with Me_2NH , MeOH , and PhCO_2H to give $\text{Cp}^*\text{W}(\text{NO})(\text{CH}_2\text{CMe}_3)(\text{ER})$ [ER

= NMe₂, OMe, O₂CPh] and free PMe₃. The amido complex is also formed smoothly when [Cp*W(NO)(=CHCMe₃)] is generated in THF in the presence of Me₂NH. When [Cp*W(NO)(=CHCMe₃)] is generated in alkene solvents, it undergoes [2+2] cycloaddition and/or C–H activation reactions depending on the alkene structure. Cycloaddition is observed for acyclic alkenes which lack allylic C–H bonds and for cyclic alkenes with strained C=C bonds. In the case where the acyclic alkenes contain accessible allylic hydrogens, complicated C–H activation product mixtures are formed.

Alkanes and arenes also react readily with [Cp*W(NO)(=CHCMe₃)] at 70 °C by C–H activation. Reactions with alkanes proceed with moderate steric selectivity and produce mixed bis(alkyl), metallacyclobutane, alkene, or allyl complexes depending on the alkane structure. Cp*W(NO)(CH₂CMe₃)(CH₂SiMe₃) is produced in high yield in the reaction with Me₄Si. The major product of the reaction with 1,1,2,2-tetramethylcyclopropane is a metallacycle formed by intermolecular C–H activation followed by γ -cyclometalation. Neohexane and cyclohexane, which are capable of β -elimination, react to give alkene complexes which can be trapped by PMe₃ or Me₂NH. In contrast, alkanes such as pentane and methylcyclohexane react to give Cp*W(NO)(η^3 -allyl)(H) complexes in both the presence and absence of PMe₃. Reactions with arenes are similarly sensitive to steric effects and involve competitive aryl vs benzyl C–H activation. The benzyl-activated products are unstable at 70 °C, decomposing to give benzyldiene complexes that also readily cleave aryl and benzyl C–H bonds.

Mechanistic studies, including isotopic labeling, isotope effect, and kinetic studies, strongly implicate that the thermal decompositions of Cp'W(NO)(CH₂CMe₃)₂ proceed by a reversible, rate-determining α -abstraction process to form the neopentane complex, [Cp'W(NO)(=CHCMe₃)(η^2 -H–CH₂CMe₃)], in which the metal can coordinate interchangeably to the neopentane α - and γ -C–H bonds. Concurrently, the coordinated neopentane dissociates irreversibly from the metal center to yield [Cp'W(NO)(=CHCMe₃)], which can rapidly form adducts with dative ligands or coordinate another hydrocarbon and undergo addition reactions.

The thermal decompositions of the mixed bis(alkyl) complexes, $\text{Cp}^*\text{W}(\text{NO})(\text{CH}_2\text{CMe}_3)(\text{R})$, where $\text{R} = \text{CH}_2\text{CMe}_2\text{Et}$, $\text{CH}_2\text{CMe}_2\text{Ph}$, CH_2SiMe_3 , CH_3 , and Ph , are also reported. These studies show that the pathway by which these compounds decompose is governed primarily by the strengths of the $\text{M}-\text{C}$ bond broken and formed, and that the presence of α -agostic interactions in the ground state has little, if any, effect on the mechanism of decomposition.

Table of Contents

Abstract	ii
Table of Contents	v
List of Figures	xiii
List of Tables	xvi
List of Abbreviations	xix
Acknowledgments	xxii
Dedication	xxiii
 CHAPTER 1: Background, Scope, and Format	 1
1.1 Background	1
1.2 Thesis Outline	2
1.3 Thesis Format	3
1.4 References and Notes	4
 CHAPTER 2: Spectroscopic and Structural Studies of α-Agostic Bonding in Cp'W(NO)(R)(R') Complexes	 6
2.1 Introduction	6
2.2 Experimental Section	9
2.2.1 Methods	9
2.2.2 Reagents	10
2.2.3 Preparation of EtMe ₂ CCH ₂ Br	11
2.2.4 Preparation of PhMe ₂ CCD ₂ Br	11
2.2.5 ¹³ C NMR Data of CpW(NO)(CH ₂ CMe ₃) ₂ (2.1)	12
2.2.6 ¹³ C NMR Data of CpW(NO)(CH ₂ CMe ₂ Ph) ₂ (2.2)	12

2.2.7 MS and ^2H NMR Data of $\text{CpW}(\text{NO})(\text{CD}_2\text{CMe}_2\text{Ph})_2$ (2.2-<i>d</i>₄)	13
2.2.8 ^{13}C NMR Data of $\text{CpW}(\text{NO})(\text{CH}_2\text{SiMe}_3)_2$ (2.3)	13
2.2.9 Improved Preparation of $\text{Cp}^*\text{W}(\text{NO})(\text{CH}_2\text{CMe}_3)_2$ (2.4)	13
2.2.10 Preparation of $\text{Cp}^*\text{W}(\text{NO})(\text{CH}_2\text{CMe}_3)(\text{CD}_2\text{CMe}_3)$ (2.4-<i>d</i>₂)	14
2.2.11 ^{13}C NMR Data of $\text{Cp}^*\text{W}(\text{NO})(\text{CH}_2\text{CMe}_2\text{Ph})_2$ (2.5)	14
2.2.12 ^{13}C Data of $\text{Cp}^*\text{W}(\text{NO})(\text{CH}_2\text{SiMe}_3)_2$ (2.6)	14
2.2.13 Preparation of $\text{Cp}^*\text{W}(\text{NO})(\text{CH}_2\text{CMe}_3)(\text{CH}_2\text{CMe}_2\text{Et})$ (2.7)	14
2.2.14 ^{13}C NMR Data of $\text{Cp}^*\text{W}(\text{NO})(\text{CH}_2\text{CMe}_3)(\text{CH}_2\text{CMe}_2\text{Ph})$ (2.8)	15
2.2.15 ^{13}C and ^1H NOE Difference NMR Data of $\text{Cp}^*\text{W}(\text{NO})(\text{CH}_2\text{CMe}_3)(\text{CH}_2\text{SiMe}_2)$ (2.9)	15
2.2.16 ^{13}C NMR Data of $\text{Cp}^*\text{W}(\text{NO})(\text{CH}_2\text{CMe}_3)(\text{CH}_3)$ (2.10)	15
2.2.17 ^{13}C NMR Data of $\text{Cp}^*\text{W}(\text{NO})(\text{CH}_2\text{CMe}_3)(\text{Ph})$ (2.11)	16
2.2.18 ^{13}C NMR Data of $\text{Cp}^*\text{W}(\text{NO})(\text{CH}_2\text{CMe}_2\text{Ph})(\text{CH}_2\text{SiMe}_3)$ (2.12)	16
2.2.19 ^{13}C NMR Data of $\text{Cp}^*\text{W}(\text{NO})(\text{CH}_2\text{CMe}_2\text{Ph})(\text{CH}_3)$ (2.13)	16
2.2.20 ^{13}C NMR Data of $\text{Cp}^*\text{W}(\text{NO})(\text{CH}_2\text{CMe}_3)(\text{Cl})$ (2.14)	16
2.2.21 Preparation of $\text{Cp}^*\text{W}(\text{NO})(\text{CH}_2\text{CMe}_3)(\text{CH}_2\text{Ph})$ (2.15)	16
2.2.22 Neutron Structure of $\text{Cp}^*\text{W}(\text{NO})(\text{CH}_2\text{CMe}_3)_2$ (2.4) [See also addendum]	17
2.3 Results and Discussion	18
2.3.1 Synthesis	18
2.3.2 Spectroscopic Characterization	20
2.3.2.1 IR Studies	20
2.3.2.2 NMR Studies	21
2.3.3 X-Ray Structural Studies	33
2.3.4 Molecular Orbital Description of the Agostic Bonds	40
2.4 Epilogue	41
2.5 Addendum: Neutron Structure of $\text{Cp}^*\text{W}(\text{NO})(\text{CH}_2\text{CMe}_3)_2$ (2.4) and	

Reinterpretation of Spectroscopic and Structural Trends	44
2.6 References and Notes	48

CHAPTER 3: Thermolysis of $\text{Cp}'\text{W}(\text{NO})(\text{CH}_2\text{CMe}_3)_2$ and

$\text{Cp}^*\text{W}(\text{NO})(\text{CH}_2\text{CMe}_3)(\text{CH}_2\text{Ph})$ Complexes: Generation and Trapping Reactions of $[\text{Cp}'\text{W}(\text{NO})(=\text{CHCMe}_3)]$ and $[\text{Cp}^*\text{W}(\text{NO})(=\text{CHPh})]$ Intermediates

3.1 Introduction	54
3.2 Experimental Section	57
3.2.1 Methods	57
3.2.2 Reagents	58
3.2.3 Preparation of $\text{Cp}'\text{W}(\text{NO})(=\text{CHCMe}_3)(\text{L})$ Complexes [$\text{Cp}' = \text{Cp}$, $\text{L} = \text{PMe}_3$ (3.1), PEt_3 (3.2), $\text{P}(\text{OMe})_3$ (3.3); $\text{Cp}' = \text{Cp}^*$, $\text{L} = \text{PMe}_3$ (3.4), PMe_2Ph (3.5), PEt_3 (3.6), $\text{P}(\text{OMe})_3$ (3.7)]	58
3.2.3.1 Complex 3.1	58
3.2.3.2 Complex 3.2	59
3.2.3.3 Complex 3.3	59
3.2.3.4 Complex 3.4	59
3.2.3.5 Complex 3.5	60
3.2.3.6 Complex 3.6	60
3.2.3.7 Complex 3.7	60
3.2.4 Preparation of $\text{Cp}^*\text{W}(\text{NO})(=\text{CHCMe}_3)(\text{NEtMe}_2)$ (3.8)	61
3.2.5 Preparation of $\text{Cp}^*\text{W}(\text{NO})(=\text{CHCMe}_3)(\text{Py})$ (3.9)	61
3.2.6 Preparation of $\text{Cp}^*\text{W}(\text{NO})(=\text{CHPh})(\text{PMe}_3)$ (3.10)	62
3.2.7 Attempted Trapping of $[\text{Cp}^*\text{W}(\text{NO})(=\text{CHCMe}_3)]$ with THF, Et_2O , Et_3N MeCN, and Me_3CCN	62
3.2.8 Attempted Preparation of $\text{Cp}^*\text{W}(\text{NO})(=\text{CHCMe}_3)(\text{PMe}_3)$ (3.4) in CH_2Cl_2	62
3.2.9 Preparation of $\text{Cp}'\text{W}(\text{NO})(\text{CH}_2\text{CMe}_3)(\text{NMe}_2)$ [$\text{Cp}' = \text{Cp}^*$ (2.17); $\text{Cp}' = \text{Cp}$	

(3.12)]	63
3.2.9.1 Complex 2.17	63
3.2.9.2 Complex 3.12	63
3.2.10 Preparation of $\text{Cp}^*\text{W}(\text{NO})(\text{CHDCMe}_3)(\text{NMe}_2)$ (3.12-d)	64
3.2.11 Reactions of $\text{Cp}^*\text{W}(\text{NO})(=\text{CHCMe}_3)(\text{PMe}_3)$ (3.4) with MeOH, Me ₂ NH, and PhCO ₂ H	64
3.2.11.1 Preparation of $\text{Cp}^*\text{W}(\text{NO})(\text{CH}_2\text{CMe}_3)(\text{OMe})$ (2.16)	64
3.2.11.2 Preparation of $\text{Cp}^*\text{W}(\text{NO})(\text{CH}_2\text{CMe}_3)(\text{NMe}_2)$ (2.17)	64
3.2.11.3 Preparation of $\text{Cp}^*\text{W}(\text{NO})(\text{CH}_2\text{CMe}_3)(\text{O}_2\text{CPh})$ (3.13)	65
3.2.12 Preparation of $\text{Cp}^*\text{W}(\text{NO})[\text{CH}(\text{CMe}_3)\text{CH}_2(\text{CMe}_3)\text{CH}]$ (3.14)	65
3.2.13 Preparation of $\text{Cp}^*\text{W}(\text{NO})[\text{CH}(\text{CMe}_3)\text{CH}(\text{C}_3\text{H}_6)\text{CH}]$ (3.15)	66
3.2.14 Preparation of $\text{Cp}^*\text{W}(\text{NO})[\text{CH}(\text{CMe}_3)\text{CH}(\text{C}_3\text{H}_6)\text{C}(\text{Et})]$ (3.16)	66
3.2.15 Preparation of $\text{Cp}^*\text{W}(\text{NO})[\text{CH}(\text{CMe}_3)\text{CH}(\text{C}_5\text{H}_6)\text{CH}]$ (3.17)	67
3.2.16 Preparation of $\text{Cp}^*\text{W}(\text{NO})(\text{CH}_2\text{CMe}_3)(\eta^3\text{-CH}_2\text{C}(\text{Et})\text{CH}_2)$ (3.18), $\text{Cp}^*\text{W}(\text{NO})(\text{H})(\eta^3\text{-CH}_2\text{C}(\text{Et})\text{CH}_2)$ (3.19) and $\text{Cp}^*\text{W}(\text{NO})(\eta^4\text{-2-methylbutadiene})$ (3.20)	68
3.2.16.1 Complex 3.18	68
3.2.16.2 Complexes 3.19 and 3.20	69
3.2.17 Preparation of $\text{Cp}^*\text{W}(\text{NO})(\eta^3\text{-C}_{10}\text{H}_{18})$ (3.21)	69
3.3 Results and Discussion	71
3.3.1 Trapping of $[\text{Cp}'\text{W}(\text{NO})(=\text{CHCMe}_3)]$ and $[\text{Cp}^*\text{W}(\text{NO})(=\text{CHPh})]$ with Lewis Bases	71
3.3.2 Reactions of $[\text{Cp}'\text{W}(\text{NO})(=\text{CHCMe}_3)]$ and $\text{Cp}^*\text{W}(\text{NO})(=\text{CHCMe}_3)(\text{PMe}_3)$ with Heteroatom-Hydrogen Bonds	78
3.3.3 Reaction of $[\text{Cp}^*\text{W}(\text{NO})(=\text{CHCMe}_3)]$ with Cyclic and Acyclic Alkenes	80
3.3.3.1 [2+2] Cycloaddition	80

3.3.3.2 C–H Bond Activation	88
3.4 Epilogue	96
3.5 References and Notes	100

CHAPTER 4: Selective Activation of Aliphatic and Aromatic C–H Bonds by [Cp*W(NO)(=CHCMe₃)] and Related Complexes

4.1 Introduction	105
4.2 Experimental Section	107
4.2.1 Methods	107
4.2.2 Reagents	107
4.2.3 Preparation of Cp*W(NO)(CH ₂ CMe ₃)(CH ₂ SiMe ₃) (2.9)	107
4.2.4 Preparation of Cp*W(NO)[CH ₂ CMeCMe ₂ CH] (4.1)	108
4.2.5 Preparation of Cp*W(NO)(η^2 -alkene)(PMe ₃) Complexes [alkene = cyclopentene (4.2), cyclohexene (4.3), neohexene (4.4)]	108
4.2.5.1 Complex 4.2	109
4.2.5.2 Complex 4.3	109
4.2.5.3 Complexes 4.4	110
4.2.6 NMR Study of the Thermolysis of 2.4 in Cyclohexane in the Presence of PMe ₃ : Effect of Varying PMe ₃ Concentration	110
4.2.7 NMR Study of the Thermolysis of 2.4 in Neohexane in the Presence of PMe ₃	111
4.2.8 Thermolysis of Cp*W(NO)(CH ₂ CMe ₃)(CH ₂ CMe ₂ Et) (2.7) in Neohexane in the Presence of PMe ₃	111
4.2.9 Thermolysis of Cp*W(NO)(CH ₂ CMe ₃)(CH ₂ CMe ₂ Et) (2.7) in THF in the Presence of PMe ₃	112
4.2.10 Preparation of Cp*W(NO)(cyclohexyl)(NMe ₂) (4.7)	113
4.2.11 Preparation of Cp*W(NO)(η^3 -allyl)(H) Complexes [η^3 -allyl = η^3 -C ₆ H ₉]	

(4.8), η^3 -C ₇ H ₁₁ (4.9), η^3 -C ₈ H ₁₃ (4.10), η^3 -C ₅ H ₉ (4.11)]	113
4.2.11.1 Complexes 4.8	114
4.2.11.2 Complex 4.9 _{endo}	114
4.2.11.3 Complexes 4.10	115
4.2.11.4 Complex 4.11 _{endo}	115
4.2.12 Reactions of 2.4 with Arenes	116
4.2.12.1 Reaction of 2.4 with α,α,α -Trifluorotoluene	116
4.2.12.2 Reaction of 2.4 with Anisole	117
4.2.12.3 Reaction of 2.4 with Toluene	118
4.2.12.4 Reaction of 2.4 with <i>o</i> -Xylene	118
4.2.12.5 Reaction of 2.4 with <i>m</i> -Xylene	120
4.2.12.6 Reaction of 2.4 with <i>p</i> -Xylene	121
4.2.12.7 Reaction of 2.4 with Mesitylene	122
4.2.13 Thermolysis of CpW(NO)(CH ₂ CMe ₃) ₂ (2.1) in Neat Tetramethylsilane, C ₆ D ₆ , and <i>p</i> -Xylene	122
4.2.14 Thermolysis of CpW(NO)(CH ₂ CMe ₃) ₂ (2.1) in Cyclohexane in the Presence of Added PMe ₃	123
4.3 Results and Discussion	123
4.3.1 Reactions of 2.4 with Tetramethylsilane and Alkanes	123
4.3.2 Reactions of 2.4 with Arenes	139
4.3.3 Thermal Reactions of CpW(NO)(CH ₂ CMe ₃) ₂ (2.1) with Aliphatic and Aromatic C–H Bonds: Qualitative Observations	147
4.4 Conclusions	148
4.5 References and Notes	150

CHAPTER 5: Kinetic and Mechanistic Studies of the Generation and C–H

Activation Reactions of the [Cp*W(NO)(=CHCMe₃)] Fragments	157
5.1 Introduction	157
5.2 Experimental Section	160
5.2.1 Methods	160
5.2.2 Reagents	160
5.2.3 NMR and Mass Spectral Data for Cp*W(NO)(CH ₂ CMe ₃)(CD ₂ CMe ₂ Ph) (2.8-d₂)	161
5.2.4 Preparation of (CH ₃) ₂ Si(CD ₃) ₂	161
5.2.5 Preparation of Cp*W(NO)(CH ₂ CMe ₃)(C ₆ D ₅) (2.11-d₅)	162
5.2.6 Kinetic Measurements	162
5.2.7 ¹ H and ² { ¹ H} NMR Analyses of the Thermolysis of (a) 2.1-d₄ and 2.4-d₄ in THF in the Presence of PMe ₃ and (b) 2.4-d₄ in C ₆ D ₆	163
5.2.8 Thermolysis of 2.4 in THF in the Presence of Excess PMe ₃ and C ₆ D ₆	164
5.2.9 GC–MS Analysis of Neopentane Generated from the Thermolysis of (a) 2.1-d₄ and 2.4-d₄ in THF in the Presence of Excess PMe ₃ and (b) 2.4-d₄ in Neat PMe ₃ ...	164
5.2.10 Thermolysis of 2.4 in Si(CD ₃) ₄	164
5.2.11 Thermolysis of 2.4 in C ₆ D ₆	165
5.2.12 Thermolysis of 2.4 in (CH ₃) ₂ Si(CD ₃) ₂	165
5.2.13 Thermolysis of 2.4 in 1:1 C ₆ H ₆ /C ₆ D ₆	166
5.2.14 Thermolysis of 2.4 in 1,3,5-C ₆ H ₃ D ₃ - <i>d</i> ₃	166
5.2.15 Thermolysis of Cp*W(NO)(CH ₂ CMe ₃)(CH ₂ CMe ₂ Ph) (2.8) in THF in the Presence of Added PMe ₃	167
5.2.16 Thermolysis of Cp*W(NO)(CH ₂ CMe ₃)(CD ₂ CMe ₂ Ph) (2.8-d₂) in THF in the Presence of Added PMe ₃	168
5.2.17 Thermolysis of Cp*W(NO)(CHDCMe ₃)[CD ₂ Si(CD ₃) ₃] (2.9-d₁₂) in Si(CH ₃) ₄	169
5.2.18 Thermolysis of Cp*W(NO)(CH ₂ CMe ₃)(CH ₃) (2.10)	169

5.2.19 Thermolysis of $\text{Cp}^*\text{W}(\text{NO})(\text{CH}_2\text{CMe}_3)(\text{C}_6\text{D}_5)$ (2.11-<i>d</i>₅) in C_6D_6	170
5.3 Results and Discussion	170
5.3.1 Isotopic Labeling Studies	170
5.3.2 Isotope Effect Studies	175
5.3.3 Kinetic Studies	178
5.3.4 Thermolyses of Other $\text{Cp}'\text{W}(\text{NO})(\text{R})(\text{R}')$ Complexes: Qualitative Observations	184
5.4 Conclusions	189
5.5 References and Notes	190
APPENDIX	193

List of Figures

Figure 2.1. Nujol-mull IR spectrum of (A) $\text{CpW}(\text{NO})(\text{CH}_2\text{CMe}_2\text{Ph})_2$ (2.2) and (B) $\text{CpW}(\text{NO})(\text{CD}_2\text{CMe}_2\text{Ph})_2$ (2.2-<i>d</i>₄).	21
Figure 2.2. 500-MHz ^1H NMR spectrum of the methylene protons of 2.4 in C_6D_6 at 20 °C.	25
Figure 2.3. Plot of $^1J_{\text{CH}}$ versus δC_α as a function of Cp' and R for complexes 2.1–2.6 ($\text{Cp} = \blacktriangle$; $\text{Cp}^* = \blacksquare$).	26
Figure 2.4. 500-MHz ^1H NMR spectrum of 2.9 in C_6D_6 at 20 °C.	27
Figure 2.5. Schematic representation of 2.9 along the $\text{Cp}^*\text{-W}$ vector. The Cp^* ligand (situated above) is not shown for reasons of clarity.	28
Figure 2.6. Plot of the neopentyl ligand's $^1J_{\text{CH}}$ versus δC_α as a function of R' for complexes 2.7–2.11 and 2.14–2.15	29
Figure 2.7. ORTEP diagrams of (A) $\text{Cp}^*\text{W}(\text{NO})(\text{CD}_2\text{CMe}_3)_2$ (2.4-<i>d</i>₄), (B) $\text{Cp}^*\text{W}(\text{NO})(\text{CH}_2\text{CMe}_3)(\text{CH}_2\text{SiMe}_3)$ (2.9), (C) $\text{Cp}^*\text{W}(\text{NO})(\text{CH}_2\text{CMe}_3)(2,5\text{-C}_6\text{H}_3\text{-Me}_2)$ (2.11'), and (D) $\text{Cp}^*\text{W}(\text{NO})(\text{CH}_2\text{CMe}_3)(\text{NMe}_2)$ (2.17).	36
Figure 2.8. Qualitative molecular orbital diagram for the double α -agostic interaction in $\text{Cp}'\text{W}(\text{NO})(\text{R}')(\text{R}')$ complexes.	41
Figure 2.9. Two views of the neutron structure of $\text{Cp}^*\text{W}(\text{NO})(\text{CH}_2\text{CMe}_3)_2$ (2.4) along with selected bond distances and angles for 2.4 (neutron) and 2.4-<i>d</i>₄ (X-ray).	45
Figure 3.1. ORTEP diagrams and selected bond distances and angles for complexes (A) $\text{CpW}(\text{NO})(=\text{CHCMe}_3)(\text{PMe}_3)$ (3.1) and (B) $\text{Cp}^*\text{W}(\text{NO})(=\text{CHCMe}_3)(\text{PMe}_3)$ (3.4)... ..	77
Figure 3.2. 500-MHz ^1H and 75-MHz $^{13}\text{C}\{^1\text{H}\}$ NMR spectra of 3.16 in CDCl_3	85
Figure 3.3. ORTEP diagrams and bonding parameters for the tungstacyclic rings of (A) $\text{Cp}^*\text{W}(\text{NO})[\text{CH}(\text{CMe}_3)\text{CH}_2\text{CH}(\text{CMe}_3)]$ (3.14), (B)	

Cp*W(NO)[CH(CMe ₃)CH(C ₃ H ₆)CH] (3.15), and (C)	
Cp*W(NO)[CH(CMe ₃)CH(C ₅ H ₆)CH] (3.17).	87
Figure 3.4. ORTEP diagram and selected bond distances and angles of complex	
Cp*W(NO)[η^4 -CH ₂ C(Me)CHCH ₂ C(Me) ₂ CH(Me)] (3.21a).	93
Figure 4.1. ORTEP diagrams and selected bond distances and angles for complexes	
(A) Cp*W(NO)(cyclohexene)(PMe ₃) (4.3) and (B) Cp*W(NO)(neohexene)(PMe ₃)	
(4.4_{syn}).	128
Figure 4.2. ORTEP diagram along with selected bond distances and angles of complex	
Cp*W(NO)(cyclohexyl)(NMe ₂) (4.7).	133
Figure 4.3. ORTEP drawings and selected bond distances and angles of (A)	
Cp*W(NO)(η^3 -C ₇ H ₁₁)(H) (4.9_{endo}) and (B) Cp*W(NO)(η^3 -C ₈ H ₁₃)(H)(4.11_{exo}).	137
Figure 4.4. Variable-temperature 500-MHz ¹ H NMR spectra of 2.11' in toluene- <i>d</i> ₈	
(♦).	143
Figure 5.1. 500-MHz ¹ H NMR spectra of the methylene regions of (A)	
Cp*W(NO)(CH ₂ CMe ₃)(C ₆ H ₅) (2.11) and Cp*W(NO)(CHDCMe ₃)(C ₆ D ₅) (2.11-<i>d</i>₆) and	
(B) Cp*W(NO)(CH ₂ CMe ₃)(2,4,6-C ₆ H ₂ D ₃) (2.11-<i>d</i>₃-H) and	
Cp*W(NO)(CHDCMe ₃)(3,5-C ₆ H ₃ D ₂) (2.11-<i>d</i>₃-D).	177
Figure 5.2. Representative first-order kinetic plots for the decomposition of 2.1 (●)	
and 2.4 (■) in THF in the presence of excess PMe ₃ at 81 °C.	180
Figure 5.3. Eyring plots for the thermal decompositions of 2.1 (●) and 2.4 (■) in	
cyclohexane in the presence of excess PMe ₃	182
Figure 5.4. ORTEP diagram and selected bond distances and angles of complex	
Cp*W(NO)(CH ₂ CMe ₂ - <i>o</i> -C ₆ H ₄)(PMe ₃) (5.1).	186
Figure A1. Plot of the kinetic data for the products of the thermolysis of 2.4 in	
neohexane in the presence of excess PMe ₃ : Cp*W(NO)(=CHCMe ₃)(PMe ₃) (3.4) = ♦;	
Cp*W(NO)(<i>syn</i> -neohexene)(PMe ₃) (4.4_{syn}) = ■; Cp*W(NO)(<i>anti</i> -neohexene)(PMe ₃)	

(4.4_{anti}) = ▲	193
Figure A2. ¹ H- ¹ H EXSY spectrum of Cp*W(NO)(CH ₂ CMe ₃)(C ₆ H ₃ -2,5-Me ₂) (2.11') in toluene- <i>d</i> ₈ at -50 °C:	194
Figure A3. ¹ H NMR spectra of the methylene regions of (A) Cp*W(NO)(CH ₂ CMe ₃)[CH ₂ Si(CH ₃)(CD ₃) ₂] (2.9-<i>d</i>₆-H) and Cp*W(NO)(CHDCMe ₃)[CD ₂ Si(CH ₃) ₂ (CD ₃)] (2.9-<i>d</i>₃-D) [obtained from thermolysis of 2.4 in (CH ₃) ₂ Si(CD ₃) ₂ , <i>k_H/k_D</i> = 1.35(5)], and (B) <i>m</i> - and <i>p</i> -isomers of Cp*W(NO)(CH ₂ CMe ₃)(C ₆ H ₄ Me) and Cp*W(NO)(CHDCMe ₃)(C ₆ D ₄ Me) [obtained from thermolysis of 2.4 in 1:1 toluene/toluene- <i>d</i> ₈ , <i>k_H/k_D</i> = 1.04(5), unpublished]	195

List of Tables

Table 2.1. Selected IR Data for Complexes 2.2 , 2.2-<i>d</i>₄ , 2.5 , and 2.11	21
Table 2.2. Pertinent ¹ H and ¹³ C NMR Data for Complexes 2.1–2.17 in C ₆ D ₆ Unless Otherwise Noted	23
Table 2.3. Selected Bond Distances and Angles for Complexes 2.3 , 2.4-<i>d</i>₄ , 2.9 , 2.11' , and 2.17	37
Table 2.4. Bond Distances and Angles Involving the M–CH ₂ CMe ₃ Fragments of Complexes Cp*W(NO)(CD ₂ CMe ₃) ₂ (2.4-<i>d</i>₄), CpW(=NAd)(CH ₂ CMe ₃) ₂ , ^a and CpNb(=NAr)(CH ₂ CMe ₃) ₂ ^b (The Cp' ligands are not drawn below for clarity)	38
Table 3.1. Selected ¹ H, ¹³ C, and ³¹ P NMR Data for Cp'W(NO)(=CHCMe ₃)(L) and Cp*W(NO)(=CHPh)(PMe ₃) Complexes ^a	75
Table 3.2. Selected Bond Distances and Angles for 3.14 , 3.15 , and 3.17	88
Table 4.1. Selected ¹ H and ¹³ C NMR Data for the η^3 -Allyl Moieties of Complexes 4.8–4.11	136
Table 4.2. Relative Kinetic Selectivities of [Cp*W(NO)(=CHCMe ₃)] and [Cp*W(NO)(=CHAR)] for Activation of Aryl and Benzyl C–H Bonds	145
Table 4.3. Kinetic Selectivities of [Cp*W(NO)(=CHCMe ₃)] for Activation of Aryl C–H Bonds in Monosubstituted Benzenes	146
Table 5.1. Isotopic Composition of Neopentane Derived from Thermal Decompositions of 2.1-<i>d</i>₄ and 2.4-<i>d</i>₄	173
Table 5.2. Rate Constants for the Decompositions of 2.1 and 2.4 as a Function of Phosphine and Phosphine Concentration	179
Table 5.3. Rate Constants for the Thermal Decompositions of 2.1 and 2.4 in the Presence of Excess PMe ₃ ^a	181

Table 5.4. Activation Parameters for the Thermal Decompositions of 2.1 and 2.4 in THF and Cyclohexane in the Presence of Excess PMe_3^a	182
Table 5.5. Rate Constants for Thermolyses of 2.1-<i>d</i>₄ and 2.4-<i>d</i>₄ in the Presence of Excess PMe_3	183
Table A1. Selected IR Spectral Data for Complexes 2.1–2.11^a	193
Table A2. <i>tert</i> -Butyl Ions in the Mass Spectra of Neopentanes	195
Table A3. Crystallographic Data for Complexes 2.4-<i>d</i>₄ , 2.4 , 2.9 , 2.11' , 2.17 , and 3.1 ..	196
Table A4. Crystallographic Data for Complexes 3.4 , 3.14 , 3.15 , 3.17 , and 3.21a	197
Table A5. Crystallographic Data for Complexes 4.3 , 4.4_{syn} , 4.7 , 4.9_{endo} , 4.11_{exo} , and 5.1	198
Table A6. Fractional coordinates and equivalent isotropic displacement parameters for $\text{Cp}^*\text{W}(\text{NO})(\text{CD}_2\text{CMe}_3)_2$ (2.4-<i>d</i>₄)	199
Table A7. Fractional coordinates and equivalent isotropic displacement parameters for $\text{Cp}^*\text{W}(\text{NO})(\text{CH}_2\text{CMe}_3)_2$ (2.4)	200
Table A8. Fractional coordinates and equivalent isotropic displacement parameters for $\text{Cp}^*\text{W}(\text{NO})(\text{CH}_2\text{CMe}_3)(\text{CH}_2\text{SiMe}_3)$ (2.9)	201
Table A9. Fractional coordinates and equivalent isotropic displacement parameters for $\text{Cp}^*\text{W}(\text{NO})(\text{CH}_2\text{CMe}_3)(\text{C}_6\text{H}_3\text{-2,5-Me}_2)$ (2.11')	202
Table A10. Fractional coordinates and equivalent isotropic displacement parameters for $\text{Cp}^*\text{W}(\text{NO})(\text{CH}_2\text{CMe}_3)(\text{NMe}_2)$ (2.17)	203
Table A11. Fractional coordinates and equivalent isotropic displacement parameters for $\text{CpW}(\text{NO})(=\text{CHCMe}_3)(\text{PMe}_3)$ (3.1)	204
Table A12. Fractional coordinates and equivalent isotropic displacement parameters for $\text{Cp}^*\text{W}(\text{NO})(=\text{CHCMe}_3)(\text{PMe}_3)$ (3.4)	205
Table A13. Fractional coordinates and equivalent isotropic displacement parameters for $\text{Cp}^*\text{W}(\text{NO})[\text{CH}(\text{CMe}_3)\text{CH}_2(\text{CMe}_3)\text{CH}]$ (3.14)	206

Table A14. Fractional coordinates and equivalent isotropic displacement parameters for Cp*W(NO)(C ₁₀ H ₁₈) (3.15)	207
Table A15. Fractional coordinates and equivalent isotropic displacement parameters for Cp*W(NO)(C ₁₂ H ₁₈) (3.17)	208
Table A16. Fractional coordinates and equivalent isotropic displacement parameters for Cp*W(NO)(η^3 -C ₁₀ H ₁₈) (3.21a)	209
Table A17. Fractional coordinates and equivalent isotropic displacement parameters for Cp*W(NO)(cyclohexene)(PMe ₃) (4.2)	210
Table A18. Fractional coordinates and equivalent isotropic displacement parameters for Cp*W(NO)(neohexene)(PMe ₃) (4.4 _{syn})	211
Table A19. Fractional coordinates and equivalent isotropic displacement parameters for Cp*W(NO)(cyclohexyl)(NMe ₂) (4.7)	212
Table A20. Fractional coordinates and equivalent isotropic displacement parameters for Cp*W(NO)(η^3 -C ₇ H ₁₁)(H) (4.9 _{endo})	213
Table A21. Fractional coordinates and equivalent isotropic displacement parameters for Cp*W(NO)(η^3 -C ₈ H ₁₃)(H) (4.11 _{exo})	214
Table A22. Fractional coordinates and equivalent isotropic displacement parameters for Cp*W(NO)(CH ₂ CMe ₂ - <i>o</i> -C ₆ H ₄)(PMe ₃) (5.1)	215

List of Abbreviations

Å	angstrom, 10^{-10} m
Ad	adamantyl
anal.	analysis
APT	attached proton test $^{13}\text{C}\{^1\text{H}\}$ NMR
Ar	argon or aryl
atm	atmosphere(s)
bp	boiling point
br	broad
Bu	butyl
°C	degree Celsius
^{13}C	carbon-13
$^{13}\text{C}\{^1\text{H}\}$	proton-decoupled ^{13}C
cal	calorie
calcd	calculated
C_6D_6	benzene- d_6
CDCl_3	chloroform- d_1
CD_2Cl_2	dichloromethane- d_2
CH_2CMe_3	neopentyl
$\text{CH}_2\text{CMe}_2\text{Ph}$	neophyl
CI	chemical ionization
cm^{-1}	wavenumbers
COSY	Correlated 2D NMR Spectroscopy
Cp	$\eta^5\text{-C}_5\text{H}_5$, cyclopentadienyl
Cp*	$\eta^5\text{-C}_5\text{Me}_5$, permethylated Cp
Cp'	Cp or Cp*
$^{\circ}\text{Pr}$	cyclopropyl
δ	NMR chemical shift in ppm
d	doublet or day(s)
DMF	dimethylformamide
Δ	heat (thermolysis)
EI	electron impact
Et	ethyl
Et_2O	diethyl ether

eu	entropy unit (cal/K·mol)
g	gram(s)
GC	gas chromatography
ΔG^\ddagger	free energy of activation
h	Planck's constant
^1H	proton
^2H	deuterium
ΔH^\ddagger	enthalpy of activation
HMQC	Heteronuclear Multiple Quantum Coherence
HMBC	Heteronuclear Multiple Bond Coherence
Hz	Hertz
IR	infrared spectroscopy or spectrum
J	coupling constant
$^nJ_{AB}$	n-bond coupling constant between atoms A and B
K	degree Kelvin or equilibrium constant
kcal	kilocalorie
kJ	kilojoule(s)
k_{obs}	observed rate constant
LUMO	lowest unoccupied molecular orbital
m	multiplet
<i>m</i>	meta
M	molar or mega
m/z	mass-to-charge ratio
Me	methyl
MeCN	acetonitrile
mg	milligram(s)
mL	millilitre(s)
min	minute(s)
mmol	millimole
mol	mole
MS	mass spectrometry
ν	infrared stretching frequency
NMR	nuclear magnetic resonance
NOE	nuclear Overhauser effect
<i>o</i>	ortho
ORTEP	Oak Ridge Thermal Ellipsoid Program

<i>p</i>	para
^{31}P	phosphorus-31
$^{31}\text{P}\{^1\text{H}\}$	^1H -decoupled phosphorus
Ph	phenyl
Pr	propyl
ppm	parts per million
q	quartet
ΔS^\ddagger	entropy of activation
s	singlet
t	triplet
THF	tetrahydrofuran
UV-vis	ultraviolet-visible
^{183}W	tungsten-183

Acknowledgments

I would like to take this opportunity to thank those people without whose help this thesis would not have been possible. I first would like to thank Dave Burkey, Sean Lumb, Steve Sayers, Miguel Romero, Jim Nieman, and the late Prof. Larry Weiler for numerous helpful discussions, and especially Dave Burkey for showing me how to be a better technical writer. My sincerest thanks also go to the following members of my guidance committee: Prof. Mike Fryzuk for constructive criticisms of Chapters 2, 3, and 5, Prof. Derek Gates for proof-reading the Abstract and Chapter 1, and Prof. Chris Orvig for assuming the role of acting supervisor and for ensuring that this thesis be defended.

My appreciation must also go to Ms. Liane Darge, Mrs. Marietta Austria, Mr. Peter Borda, Mr. Marshall Lapawa, Ms. Lina Madilao, and Dr. Nick Burlinson for technical assistance and/or training. I also would like to thank the following collaborators: Prof. Bob Bau of USC and Dr. Sax A. Mason of Institut Laue-Langevin in Grenoble for the neutron structure reported in Chapter 2; Dr. Tom Koetzle of Brookhaven National Lab, Prof. Bob Bau and Dr. Manfred Bortz of USC, and Drs. Art Schultz and Rebecca Miller of Argonne National Lab for an attempted but unsuccessful neutron diffraction study; and Drs. Victor Young, Jr. and Maren Pink of the University of Minnesota, Prof. Fred Einstein and Dr. Ray Batchelor of Simon Fraser University, and the late Dr. Steve Rettig of UBC for the X-ray structures reported in Chapters 2–5.

To Profs. Maurice Brookhart of the University of North Carolina and Pete Wolczanski of Cornell, I would like express my gratitude for a helpful discussion concerning the work in Chapters 2 and 5, respectively. My deep appreciation also goes to Prof. Ed Piers and the late Prof. Larry Weiler for advice, and to Prof. Tony Durst of the University of Ottawa and Dr. Prabat Arya of NRC for introducing me to chemical research and for continued guidance.

Finally, I must acknowledge the constant love and support shown to me by my parents and family and the unwavering encouragement shown to me by my friends. I am especially indebted to my brothers, John and Chuck, for computer assistance and conversation, and my friends, Hoa, Judy, Ellie, Gunjeet, and Kamla, for making me feel blessed.

To my loving parents

CHAPTER 1

Background, Scope, and Format

1.1 Background	1
1.2 Thesis Scope	2
1.3 Thesis Format	3
1.4 References and Notes	4

1.1 Background

An ongoing goal of research in the Legzdins group has been the development of organotransition-metal nitrosyl complexes as specific and selective reagents for organic and organometallic transformations of practical significance.¹ In particular, major efforts have been directed toward the synthesis, characterization, and reactivity studies of the molybdenum and tungsten complexes $\text{Cp}'\text{M}(\text{NO})\text{R}_2$ ($\text{Cp}' = \text{Cp}, \text{Cp}^*$ and $\text{R} = \text{alkyl, aryl}$).² These complexes are formally d^4 , 16-electron species. They are monomeric and possess a three-legged piano-stool structure in which the $\text{M}-\text{NO}$ linkage is essentially linear. In this configuration, the metal d_{xy} and d_{xz} orbitals are significantly stabilized by backbonding to the nitrosyl π^* orbitals, while the $d_{x^2-y^2}$ orbital (= LUMO) remains high in energy and available for bonding to additional ligands.³

In general, the molybdenum and tungsten $\text{Cp}'\text{M}(\text{NO})\text{R}_2$ complexes exhibit reactivity patterns that are very similar. Although most are relatively air-stable and thermally stable as solids, their solution chemistry is quite diverse. For example, in addition to forming 1:1 metal-centered adducts with small Lewis bases and isonitrosyl adducts with Lewis acids,⁴ they both react readily with oxygen^{4,5} to form the bis(oxo) complexes, $\text{Cp}'\text{M}(=\text{O})_2\text{R}$, and with sulfur,⁴ isocyanides,⁴ NO ,⁴ CO ,⁶ and heterocumulenes to form products arising from insertion into the $\text{M}-\text{C}$ σ -bonds. More interestingly, however, are their reactions with water⁷ and hydrogen,^{8,9}

which vary depending on the identity of the metal. For example, while exposure of $\text{Cp}^*\text{Mo}(\text{NO})(\text{CH}_2\text{SiMe}_3)_2$ to H_2 leads to the formation of $[\text{Cp}'\text{Mo}(\text{NO})(\text{CH}_2\text{SiMe}_3)](\mu\text{-N})[\text{Cp}'\text{Mo}(\text{O})(\text{CH}_2\text{SiMe}_3)]$,⁸ the same reaction with the tungsten analogue produces the hydride complex, $\text{Cp}^*\text{W}(\text{NO})(\text{CH}_2\text{SiMe}_3)(\text{H})$, as a short-lived species.⁹ The objective of this thesis is to investigate further the chemistry of the tungsten bis(alkyl) complexes. In particular, research has been focused on the structures and thermal reactivity of these compounds.

1.2 Thesis Outline

This thesis is divided into five chapters, each of which is self-contained, and an appendix section. Chapter 2 reports a systematic spectroscopic and structural investigation of a series of $\text{Cp}'\text{W}(\text{NO})(\text{R})(\text{R}')$ complexes, where R = alkyl, and R' = alkyl, aryl, chloride, alkoxide, or amide. In contrast to previous reports,² this study shows that, in the absence of secondary interactions such as lone pair or π -electron donation, these complexes are in fact electronically saturated species due to the presence of an α -agostic C–H interaction. These interactions exist in both the solid and solution states and give rise to a number of unusual spectroscopic and structural features that have allowed the strength of the $\alpha\text{-C-H}\cdots\text{W}$ interaction to be established as a function of Cp' , R , and R' .

Thermolysis of the neopentyl complexes, $\text{Cp}'\text{W}(\text{NO})(\text{CH}_2\text{CMe}_3)_2$ [$\text{Cp}' = \text{Cp}, \text{Cp}^*$] and $\text{Cp}^*\text{W}(\text{NO})(\text{CH}_2\text{CMe}_3)(\text{CH}_2\text{Ph})$, leads to extrusion of neopentane and formation of $[\text{Cp}'\text{W}(\text{NO})(=\text{CHCMe}_3)]$ and $[\text{Cp}^*\text{W}(\text{NO})(=\text{CHPh})]$, respectively, as reactive intermediates. The reactivity of these alkylidene intermediates with a range of trapping agents forms the basis of Chapter 3. The reactions of $[\text{Cp}'\text{W}(\text{NO})(=\text{CHCMe}_3)]$ and $[\text{Cp}^*\text{W}(\text{NO})(=\text{CHPh})]$ with L , where L = tertiary phosphine, pyridine, or tertiary amine, afford $\text{Cp}'\text{W}(\text{NO})(=\text{CHCMe}_3)(\text{L})$ and $\text{Cp}^*\text{W}(\text{NO})(=\text{CHPh})(\text{L})$ complexes. Both $[\text{Cp}^*\text{W}(\text{NO})(=\text{CHCMe}_3)]$ and its PMe_3 adduct undergo addition reactions with REH substrates to form complexes of the type, $\text{Cp}^*\text{W}(\text{NO})(\text{CH}_2\text{CMe}_3)(\text{ER})$ [$\text{ER} = \text{NR}_2, \text{OR}, \text{OC}(\text{O})\text{R}$]. Alkenes also react readily with $[\text{Cp}^*\text{W}(\text{NO})(=\text{CHCMe}_3)]$. These reactions, however, lead to complicated product mixtures resulting from $[2+2]$ cycloaddition and/or C–H activation depending on the alkene structure.

The products for both types of reactions are discussed, and mechanisms are proposed for their formation.

Chapter 4 is an extension of Chapter 3 and is concerned with the alkane and arene C–H activation reactions of $[\text{Cp}^*\text{W}(\text{NO})(=\text{CHCMe}_3)]$, and to a lesser extent the Cp analogue. The reactions of $[\text{Cp}^*\text{W}(\text{NO})(=\text{CHCMe}_3)]$ with alkanes proceed with moderate steric selectivity and are typically followed by rapid rearrangement transformations that result in overall dehydrogenation of the alkane. The reactions with arenes are similarly sensitive to steric effects and involve competitive aryl vs benzyl C–H activation. The benzyl-activated products are thermally unstable at the temperature at which they are formed, decomposing to give neopentane and benzyldiene complexes that also readily cleave aryl and benzyl C–H bonds.

Finally, Chapter 5 reports a detailed mechanistic investigation of the chemistry described in Chapters 3 and 4. Specifically, the kinetics of the thermal decompositions of $\text{Cp}'\text{W}(\text{NO})(\text{CH}_2\text{CMe}_3)_2$ in the presence of phosphines are presented, along with the results of an isotope effect and an isotope labeling study, which not only provide further support for the intermediacy of $[\text{Cp}'\text{W}(\text{NO})(=\text{CHCMe}_3)]$ but which also provide strong evidence for the involvement of $\sigma\text{-C-H}$ complexes in the formation and C–H activation reactions of these coordinatively unsaturated alkylidene species. The thermal decompositions of the mixed bis(alkyl) complexes, $\text{Cp}^*\text{W}(\text{NO})(\text{CH}_2\text{CMe}_3)(\text{R})$, where $\text{R} = \text{CH}_2\text{CMe}_2\text{Et}$, $\text{CH}_2\text{CMe}_2\text{Ph}$, CH_2SiMe_3 , CH_3 , and Ph , are also presented. These studies show that the pathway by which these compounds decompose is governed primarily by the strengths of the M–C bond broken and formed, and that the presence of α -agostic interactions in the ground state has little, if any, effect on the mechanism of decomposition.

1.3 Thesis Format

This thesis is formatted in a manner similar to that described in the Ph. D. thesis of former group member, J. E. Veltheer,¹⁰ with Chapters 2 through 5 having five major sections. For a given Chapter X, the sections are: **X.1** Introduction, **X.2** Experimental Section, **X.3** Results and

Discussion, **X.4** Epilogue or Conclusions, and **X.5** References and Notes. Subsections of these categories are numbered using legal outlining procedures, e.g. **X.1.1**, **X.1.1.1**, **X.1.2**, **X.1.2.1**, etc. In each chapter, all new compounds prepared are catalogued numerically. For example, those in Chapter 2 are referred to as **2.1, 2.2**, **2.3**, and so on. Schemes, figures, and equations are similarly sequenced. The standard experimental methodologies outlined in Section 2.2.1 apply to the entire thesis. An Appendix is also included which contains tables of crystallographic data, etc.

1.4 References and Notes

- (1) For a recent comprehensive discussion of transition-metal nitrosyl chemistry, see: Richter-Addo, G. G.; Legzdins, P. *Metal Nitrosyls*; Oxford University Press: New York, 1992.
- (2) Legzdins, P.; Veltheer, J. E. *Acc. Chem. Res.* **1993**, *26*, 41, and references therein.
- (3) (a) Legzdins, P.; Rettig, S. J.; Sánchez, L.; Bursten, B. E.; Gatter, M. G. *J. Am. Chem. Soc.* **1985**, *107*, 1411. (b) Bursten, B. E.; Cayton, R. H. *Organometallics* **1987**, *6*, 2004.
- (4) Legzdins, P.; Sánchez, L. *Organometallics* **1988**, *7*, 2394.
- (5) Legzdins, P.; Phillips, E. C.; Sánchez, L. *Organometallics* **1989**, *8*, 940.
- (6) Debad, J. D.; Legzdins, P.; Batchelor, R. J.; Einstein, F. W. B. *Organometallics* **1993**, *12*, 2094.
- (7) (a) Legzdins, P.; Rettig, S. J.; Ross, K. J.; Veltheer, J. E. *J. Am. Chem. Soc.* **1991**, *113*, 4361. (b) Legzdins, P.; Lundmark, P. J.; Phillips, E. C.; Rettig, S. J.; Veltheer, J. E. *Organometallics* **1992**, *11*, 2991.
- (8) Debad, J. D.; Legzdins, P.; Reina, R.; Young, M. A.; Batchelor, R. J.; Einstein, F. W. B. *Organometallics* **1994**, *13*, 4315.

- (9) (a) Legzdins, P.; Martin, J. T.; Einstein, F. W. B.; Jones, R. H. *Organometallics* **1987**, *6*, 1826. (b) Debad, J. D.; Legzdins, P.; Batchelor, R. J.; Einstein, F. W. B. *Organometallics* **1992**, *13*, 6.
- (10) J. E. Veltheer, Ph. D. Thesis, 1993, University of British Columbia.

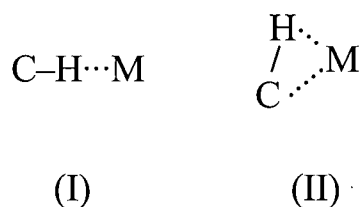
CHAPTER 2

Spectroscopic and Structural Studies of α -Agostic Bonding in $\text{Cp}'\text{W}(\text{NO})(\text{R})(\text{R}')$ Complexes

2.1 Introduction	6
2.2 Experimental Section	9
2.3 Results and Discussion	18
2.4 Epilogue	41
2.5 Addendum: Neutron Structure of $\text{Cp}^*\text{W}(\text{NO})(\text{CH}_2\text{CMe}_3)_2$ (2.4) and Reinterpretation of Spectroscopic and Structural Data	44
2.6 References and Notes	48

2.1 Introduction

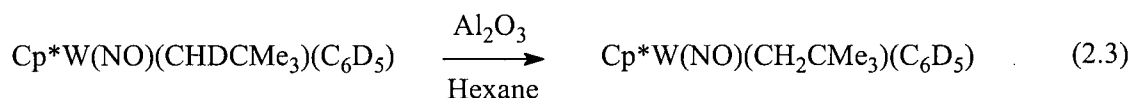
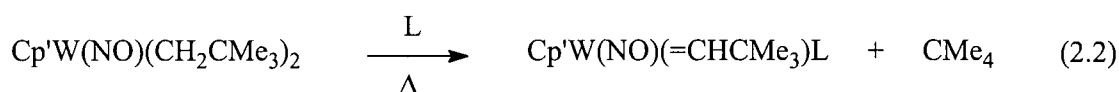
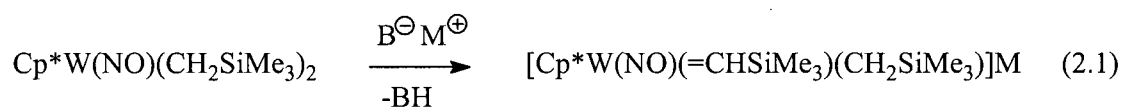
The interaction between a *ligand* C–H bond and an electronically unsaturated metal center is called an *agostic* interaction.¹ First observed in the late 1960s by Ibers,² Shaw,³ and Trofimenko,⁴ such an interaction has since become increasingly widespread, existing not only in transition-metal complexes but also in complexes of the lanthanide and actinide series. In all cases the C–H moiety acts as a weak two-electron donor to the metal, forming a three-center, two-electron bond whose strength and geometry depend upon the energy of the vacant metal orbital and the steric and conformational effects of the molecule. In general, the energy of an agostic interaction is 10–20 kcal mol^{–1},^{5,6} while its geometry varies from a linear or open arrangement (I) to a canted side-on or closed structure (II) in which the H atom is closer to the metal. The bonding, on the other hand, is best described in terms of two synergistic components: (1) a σ -type interaction that involves C–H (σ)-to-metal direct donation, and (2) a π -type interaction that involves metal-to-C–H (σ^*) back donation.



It has been proposed that the driving force for the formation of an agostic C-H \cdots M interaction is to reduce the electron deficiency of the metal and to stabilize what would otherwise be an unsaturated species.⁷ While this interaction is often benign, its strength can be such as to have a marked effect on the chemical properties of the coordinated C-H bond and the reactivity of the molecule. For example, it is now well established that agostic C-H binding can significantly weaken the C-H bond and increase its Brønsted acidity,⁸ thereby rendering it susceptible to a wide range of C-H activation reactions.^{8d,9,10,11} In other instances, the coordinated C-H bond never becomes broken; instead, it plays an important role in lowering the activation barrier and in influencing the stereochemical outcome of chemical transformations such as Ziegler-Natta-type polymerization of alkenes^{12,13} and alkynes.¹⁴

In general, agostic C-H \cdots M linkages may be detected in the solid state by X-ray and neutron diffraction studies and in solution by IR and NMR spectroscopic methods. Keys to the structural identification of these links are short M \cdots H and M \cdots C distances, a lengthening of the coordinated C-H bond, and (in certain cases) a geometrical distortion of the ligand that contains this group. Spectroscopically, the anomalous chemical shifts of the agostic H and C atoms and the reduced values of the $^1J_{\text{CH}}$ coupling constant evident in the NMR spectra and the ν_{CH} stretching frequency of the coordinated C-H bond in the IR spectra are most diagnostic of C-H binding. The latter two parameters, in particular, have also proven important in determining the degree of agosticity of a C-H \cdots M interaction, especially when comparisons are made for members of a related series of compounds. Typically, these $^1J_{\text{CH}}$ and ν_{CH} values fall in the ranges 50–100 Hz and 2300–2700 cm⁻¹, respectively, compared to 120–130 Hz and 2900–3100 cm⁻¹ for the corresponding unperturbed C-H groups.¹

This chapter describes the results of a spectroscopic and X-ray structural study of a series of d^2 tungsten alkyl complexes of the type $\text{Cp}'\text{W}(\text{NO})(\text{R})(\text{R}')$, where Cp' represents a cyclopentadienyl or pentamethylcyclopentadienyl ring, R is an alkyl ligand that contains α -H atoms, and R' is either an alkyl group, an aryl moiety, or a potential multi-electron donor ligand. The principal objectives of this work are to determine the solution and solid-state structures of these compounds and to rationalize some of their chemical behavior which typically involves the cleavage of an α -C-H bond. As depicted in eqs 2.1–2.3, this may proceed by deprotonation¹⁵ as reported recently by Legzdins and Sayers, or it may involve H-atom abstraction¹⁶ or exchange as described in the ensuing chapters of this thesis.



In this chapter it will be demonstrated that $\text{Cp}'\text{W}(\text{NO})(\text{R})(\text{R}')$ complexes, which lack π or lone-pair donation, are *not* 16-electron complexes as had previously been inferred,¹⁷ but are in fact more electronically rich due to the presence of *at least* one α -agostic C-H interaction. In particular, it will be established that these interactions not only exist in both the solution and solid states but also vary in strength and multiplicity depending on the nature of Cp' , R , and R' . For example, when R and R' are both bulky alkyl ligands containing α -H atoms, the molecule assumes a structure in which *two* α -C-H units from different alkyl ligands form three-center, two-electron bonds with tungsten.

Examples of multiple agostic C-H bonds in a mononuclear complex are rare, with the majority occurring in transition-metal complexes with very low electron count^{18,19} or

complexes of the rare earth elements.^{20,21,22} Indeed, it was not until very recently that three 16-electron transition metal complexes containing multiple agostic bonds were discovered and reported. Interestingly, these complexes, which include the bis(methyl) complex, (ⁱPr₂-2,6-C₆H₃N=)₂MoMe₂,²³ and the bis(neopentyl) compounds, CpW(≡CAd)(CH₂CMe₃)₂²⁴ (Ad = 1-adamantyl) and CpNb(=NAr)(CH₂CMe₃)₂ (Ar = C₆H₃-2,6-ⁱPr₂),²⁵ also possess α-agostic structures. The first complex has been proposed to contain four α-agostic interactions based on neutron-diffraction data, while the second and third complexes have been shown to exhibit two such interactions. A comparison of the structure of these latter complexes with that of the Cp'W(NO)(R)(R') bis(alkyl) systems will therefore also be presented.

2.2 Experimental Section

2.2.1 Methods

The experimental methodologies described in this chapter apply to the entire thesis. All reactions and subsequent manipulations of air- and/or water-sensitive compounds were performed under anaerobic and anhydrous conditions under an atmosphere of pre-purified dinitrogen or argon. Purification of these gases was achieved by sequential passage over MnO on vermiculite and activated 4-Å molecular sieves. Conventional glovebox and Schlenk techniques were utilized throughout. The specific glovebox used in this work was an Innovative Technology dual-station glovebox.

IR spectra were recorded at room temperature as solutions in NaCl cells or as Nujol mulls between KCl plates on an ATI Mattson Genesis Series FT-IR spectrophotometer using WinFIRST 2.0 software. NMR spectra were obtained at room temperature unless otherwise noted on either a Varian XL (300 MHz, ¹H), Bruker WH (400 MHz, ¹H), or Bruker AMX (500 MHz, ¹H) spectrometer. Where necessary, selective homonuclear decoupling, ¹H NOE difference, ¹³C(APT), gated ¹³C{¹H}, ¹H-¹H COSY, ¹H-¹³C HMQC, and ¹H-¹³C HMBC experiments were carried out to correlate and assign ¹H and ¹³C signals. ¹H and ¹³C chemical shifts are recorded in ppm, relative to the residual proton or natural-abundance carbon signal(s)

of the solvent employed. $^2\text{H}\{^1\text{H}\}$ NMR signals are referenced to $\text{C}_6\text{H}_5\text{D}$ (δ 7.15). All coupling constants are reported in Hz.

Mrs. M. T. Austria and Ms. L. K. Darge of the UBC NMR laboratory assisted in obtaining some NMR data. Low-resolution mass spectra (EI, 70 eV, probe temperature 150 °C) were recorded by Mr. M. Lapawa and Ms. L. Madilao of the UBC mass spectrometry facility using a Kratos MS-50 spectrometer. Elemental analyses were performed by Mr. P. Borda of this Department. Reported yields are not optimized unless specified.

2.2.2 Reagents

Hexanes, pentane, THF, and Et_2O were distilled from Na/benzophenone ketyl under dinitrogen. Deuterated solvents were purchased from Cambridge Isotope Laboratories (all >99.9 atom % D) and then degassed and vacuum-transferred from Na/benzophenone ketyl (C_6D_6), Na (toluene- d_8), or activated 4-Å molecular sieves (CD_2Cl_2). Celite and neutral alumina I were oven-dried (>130 °C) and cooled under vacuum prior to use. KH (Alfa, 50% in oil) was washed with hexanes and dried in vacuo prior to use. Dialkylmagnesium reagents $\text{R}_2\text{Mg}(\text{dioxane})$ ($\text{R} = \text{Me}, \text{CH}_2\text{CMe}_3, \text{CH}_2\text{SiMe}_3, \text{CH}_2\text{CMe}_2\text{Ph}$) were prepared by modified literature procedures²⁶ using 2.2 equiv of dioxane; the titre of each was determined by back-titration with 0.10 N aqueous HCl using phenolphthalein as indicator. With the exception of $\text{Cp}^*\text{W}(\text{NO})(\text{CH}_2\text{CMe}_3)_2$ (**2.4**), the known complexes **2.1–2.6**^{27,28} and **2.8–2.14**^{29,30} were prepared according to published procedures. The complexes $\text{Cp}^*\text{W}(\text{NO})(\text{CH}_2\text{CMe}_3)(\text{OMe})$ (**2.16**), $\text{Cp}^*\text{W}(\text{NO})(\text{CH}_2\text{CMe}_3)(\text{NMe}_2)$ (**2.17**), and $\text{Cp}^*\text{W}(\text{NO})(\text{CH}_2\text{CMe}_3)(\text{C}_6\text{H}_3\text{-2,5-Me}_2)$ (**2.11'**) were prepared as described in Sections 3.2.2 and 4.2.2. For brevity, the complete ^1H NMR data of the known complexes are excluded since they do not differ significantly from those reported in the literature and since they are not necessary for the analysis. The α -proton and α -carbon signals that are listed in Table 2.2 are also omitted to avoid redundancy.

2.2.3. Preparation of EtMe₂CCH₂Br

To a 1-L, three-necked round-bottomed flask containing LiAlH₄ (6.30 g, 166 mmol) and connected to a condenser and a 100-mL addition funnel was added THF (400 mL) by cannula. The stirred grey suspension was cooled to -78 °C and was then treated dropwise with a 50-mL THF solution of 2,2-dimethylbutyric acid (18.9 g, 163 mmol) via addition funnel. Once the addition was complete, the resulting mixture was stirred at -78 °C for 45 min and at room temperature for ca. 1.5 d, whereupon no noticeable change occurred. In air, the reaction mixture was cooled to 0 °C and quenched successively with 3N aqueous NaOH (25 mL) and water (200 mL). The white precipitate formed was removed by filtration, and the filtrate was extracted with Et₂O (200 mL). The aqueous layer was re-extracted with Et₂O (3 × 150 mL). The combined organic layers were reduced in volume on a rotary evaporator, washed with water (2 × 30 mL), dried over MgSO₄, filtered, and concentrated in vacuo. The crude mixture was distilled in air at 140–150 °C to obtain the desired 2,2-dimethylbutanol as a viscous, pale yellow liquid (16.0 g, 98 % yield). To a portion of this alcohol (13.0 g, 0.127 mmol) was added dry DMF (75 mL). The resulting solution was cooled to 0 °C, and then the sequential slow addition of *n*-Bu₃P (50.0 mL, 200 mmol) by cannula, and Br₂ (7.0 mL, 200 mmol) by disposable syringe were effected. After being stirred for 3.5 h in the dark, the bright orange solution was distilled in air at 140–205 °C. The pale yellow distillate was extracted with water. The bottom organic layer was re-extracted with water (2 × 10 mL), dried over MgSO₄, and filtered. The filtrate was next distilled from P₂O₅ under Ar (1 atm) at ~150–200 °C to obtain the desired alkyl bromide as a colorless liquid (6.50 g, 31% yield). Conversion of this alkyl bromide to the corresponding dialkyl Mg reagent was carried out in a manner analogous to that described for the preparation of (Me₃CCH₂)₂Mg·(dioxane).

2.2.4 Preparation of PhMe₂CCD₂Br

To a THF (350 mL) mixture of KH (6.85 g, 171 mmol, 3 equiv) at -10 °C was added dropwise PhCH₂CO₂Me (8.0 mL, 56.8 mmol) by cannula. The resulting clear, colorless solution over white solids was stirred at ambient temperatures for 2 h, after which time it was

re-cooled to $-10\text{ }^{\circ}\text{C}$. Freshly distilled MeI (28.0 mL, 450 mmol) was added slowly via dropping funnel over a period of 1 h, causing the reaction solution to become pale yellow. This mixture was stirred at room temperature for another 2 d, whereupon the solution became clear and colorless. Working in air, the reaction mixture was filtered through a plug of Celite ($5 \times 10\text{ cm}$). The filtrate was concentrated in vacuo, and then distilled under reduced pressure to obtain pure $\text{PhCMe}_2\text{CO}_2\text{Me}$ as a clear, colorless liquid (4.22 g, 80 % yield). Reduction of this ester (4.22 g, 23.7 mmol) with LiAlD_4 (0.498 g, 11.9 mmol) in Et_2O (200 mL) based on the procedure for the preparation of $\text{Me}_3\text{CCD}_2\text{OH}$ led to the isolation of $\text{PhCMe}_2\text{CD}_2\text{OH}$ as a slightly viscous colorless liquid (3.60 g, 99% yield) after simple distillation under reduced pressure. This alcohol (3.60 g, 23.7 mmol) was then converted to the bromo derivative by treatment with *n*-Bu₃P (8.85 mL, 35.6 mmol, 1.5 equiv) and excess Br_2 (1.71 mL, 33.2 mmol, 1.4 equiv) in DMF as described above. The bromide product was purified by flash chromatography on silica gel (230-400 mesh, $3 \times 10\text{ cm}$) using pure hexanes ($R_f = 0.55$) as the eluting solution and isolated as a colorless liquid (2.46 g, 48% yield). The bromide was then converted into the desired magnesium reagent in the usual manner.

2.2.5 ^{13}C NMR Data of $\text{CpW}(\text{NO})(\text{CH}_2\text{CMe}_3)_2$ (2.1)

Gated $^{13}\text{C}\{^1\text{H}\}$ NMR (75 MHz, C_6D_6) δ 34.3 (q, $^1J_{\text{CH}} = 124$, CMe_3), 39.4 (s, CMe_3), 101.2 (d, $^1J_{\text{CH}} = 178$, C_5H_5).

2.2.6 ^{13}C NMR Data of $\text{CpW}(\text{NO})(\text{CH}_2\text{CMe}_2\text{Ph})_2$ (2.2)

Gated $^{13}\text{C}\{^1\text{H}\}$ NMR (75 MHz, C_6D_6) δ 32.7 (q, $^1J_{\text{CH}} = 125$, CMeMe), 33.5 (q, $^1J_{\text{CH}} = 125$, CMeMe), 46.1 (s, CMe_2), 101.4 (d, $^1J_{\text{CH}} = 178$, C_5H_5), 125.6 (d, $^1J_{\text{CH}} = 159$, Ar CH), 126.0 (d, $^1J_{\text{CH}} = 156$, Ar CH), 128.3 (d, $^1J_{\text{CH}} = 158$, Ar CH), 152.8 (s, C_{ipso}).

2.2.7 MS and ^2H NMR Data of $\text{CpW}(\text{NO})(\text{CD}_2\text{CMe}_2\text{Ph})_2$ (2.2-*d*₄)

MS (LREI, m/z) 549 [M^+ , ^{184}W]. $^2\text{H}\{^1\text{H}\}$ (77 MHz, C_6H_6) δ -1.05 (br s, 2D, WCD_2), 3.55 (br s, 2D, WCD_2).

2.2.8 ^{13}C NMR Data of $\text{CpW}(\text{NO})(\text{CH}_2\text{SiMe}_3)_2$ (2.3)

Gated $^{13}\text{C}\{^1\text{H}\}$ NMR (75 MHz, C_6D_6) δ 2.8 (q, $^1J_{\text{CH}} = 118$, SiMe_3), 101.5 (d, $^1J_{\text{CH}} = 178$, C_5H_5).

2.2.9 Improved Preparation of $\text{Cp}^*\text{W}(\text{NO})(\text{CH}_2\text{CMe}_3)_2$ (2.4)

To a Schlenk flask containing a mixture of $\text{Cp}^*\text{W}(\text{NO})\text{Cl}_2$ (909 mg, 2.16 mmol) and $(\text{Me}_3\text{CCH}_2)_2\text{Mg}\cdot(\text{dioxane})$ (277 mg, 2.16 mmol) at $-196\text{ }^\circ\text{C}$ was added THF ($\sim 40\text{ mL}$) by vacuum transfer. The resulting brown mixture was thawed and stirred at $\sim 10\text{ }^\circ\text{C}$ for 20 min, during which time it became a dark purple solution. THF was then removed in vacuo, and the flask was returned to the glovebox, charged with additional $(\text{Me}_3\text{CCH}_2)_2\text{Mg}\cdot(\text{dioxane})$ (277 mg, 2.16 mmol), and reconnected to a high vacuum line. Et_2O was then added by vacuum transfer at $-196\text{ }^\circ\text{C}$. The resulting mixture was thawed and stirred at room temperature for 30 min, during which time a red solution containing a pale yellow precipitate formed. Next, the solvent was removed in vacuo and the residue was extracted with 5:1 hexanes/ Et_2O (30 mL). The extracts were filtered through alumina I ($3 \times 2\text{ cm}$) supported on a medium-porosity frit. The alumina column was washed with additional 5:1 hexanes/ Et_2O until the filtrate was colorless. Diminishing the volume of the combined filtrates under reduced pressure, followed by cooling to $-30\text{ }^\circ\text{C}$ for 2 d afforded **2.4** (684 mg, 65% yield in 3 crops) as dark wine-red needles.

Anal. Calcd. for $\text{C}_{20}\text{H}_{37}\text{NOW}$: C, 48.89; H, 7.59; N, 2.85. Found: C, 48.63; H, 7.73; N, 2.77. MS (LREI, m/z) 491 [M^+ , ^{184}W]. ^1H NMR (500 MHz, C_6D_6) δ 1.32 (s, 18H, CMe_3),

1.54 (s, 15H, C_5Me_5). Gated $^{13}C\{^1H\}$ NMR (75 MHz, C_6D_6) δ 9.9 (q, $^1J_{CH} = 128$, C_5Me_5), 34.7 (q, $^1J_{CH} = 124$, CMe_3), 39.2 (s, CMe_3), 110.2 (s, C_5Me_5).

2.2.10 Preparation of $Cp^*W(NO)(CH_2CMe_3)(CD_2CMe_3)$ (2.4- d_2)

This complex was prepared in the same manner as described for the synthesis of **2.4** but using $(Me_3CCD_2)Mg \cdot (dioxane)$ for the second alkylation step. The only exception was that the hexanes/ Et_2O extracts were filtered through a pad of Celite rather than alumina I. MS (LREI, m/z) 493 [M^+ , ^{184}W]. IR (cm^{-1} , Nujol) no reduced $\nu_{C\alpha-H}$ observed. Gated $^{13}C\{^1H\}$ NMR spectra obtained at -80 and $+20$ °C were identical to that of **2.4** at $+20$ °C.

2.2.11 ^{13}C NMR Data of $Cp^*W(NO)(CH_2CMe_2Ph)_2$ (2.5)

Gated $^{13}C\{^1H\}$ NMR (75 MHz, C_6D_6) δ 9.4 (q, $^1J_{CH} = 127$, C_5Me_5), 32.4 (q, $^1J_{CH} = 125$, $CMeMe$), 33.8 (q, $^1J_{CH} = 125$, $CMeMe$), 45.9 (s, CMe_2), 109.7 (s, C_5Me_5), 125.5 (d, $^1J_{CH} = 159$, Ar CH), 126.4 (d, $^1J_{CH} = 157$, Ar CH), 128.4 (d, $^1J_{CH} = 158$, Ar CH), 153.2 (s, C_{ipso}).

2.2.12 ^{13}C Data of $Cp^*W(NO)(CH_2SiMe_3)_2$ (2.6)

Gated $^{13}C\{^1H\}$ NMR (75 MHz, C_6D_6) δ 2.9 (q, $^1J_{CH} = 117$, $SiMe_3$), 9.9 (q, $^1J_{CH} = 127$, C_5Me_5), 110.2 (s, C_5Me_5).

2.2.13 Preparation of $Cp^*W(NO)(CH_2CMe_3)(CH_2CMe_2Et)$ (2.7)

To a mixture of $Cp^*W(NO)(CH_2CMe_3)Cl$ (375 mg, 0.823 mmol) and $(EtMe_2CCH_2)_2Mg \cdot (dioxane)$ (128 mg, 0.823 mmol) at -196 °C was added Et_2O (10 mL) by vacuum transfer. The resulting contents were thawed and stirred at ambient temperature for 10 min, during which time the mixture changed from purple to deep red. The solvent was then removed in vacuo. The residue was triturated with pentane (3×5 mL) and filtered through

Celite. The dark red filtrate was reduced in volume at room temperature and then stored at -30°C overnight to obtain **2.7** as shiny rust-colored crystals (279 mg, 67% yield).

Anal. Calcd. for $\text{C}_{21}\text{H}_{39}\text{NO}$: C, 49.91; H, 7.78; N, 2.77. Found: C, 49.63; H, 7.73; N, 2.77. IR (cm^{-1}) ν_{NO} 1576 (s). MS (LREI, m/z) 505 [M^+ , ^{184}W]. ^1H NMR (500 MHz, C_6D_6) δ 0.97 (t, $^3J_{\text{HH}} = 7.5$, 3H, CH_2Me), 1.23 (s, 3H, CMeMe), 1.38 (s, 9H, CMe_3), 1.42 (s, 3H, CMeMe), 1.52 (s, 15H, C_5Me_5), 1.63 (m, 2H, CH_2Me). $^{13}\text{C}\{^1\text{H}\}$ NMR (75 MHz, C_6D_6) δ 9.78 (q, $^1J_{\text{CH}} = 125$, CH_2Me), 9.83 (q, $^1J_{\text{CH}} = 127$, C_5Me_5), 30.9 (q, $^1J_{\text{CH}} \sim 125$, CMeMe), 31.1 (q, $^1J_{\text{CH}} = 124$, CMeMe), 34.4 (q, $^1J_{\text{CH}} = 124$, CMe_3), 39.2 (s, CMe_3), 39.5 (t, $^1J_{\text{CH}} = 124$, CH_2Me), 41.2 (s, CMe_2Et), 109.6 (s, C_5Me_5).

2.2.14 ^{13}C NMR Data of $\text{Cp}^*\text{W}(\text{NO})(\text{CH}_2\text{CMe}_3)(\text{CH}_2\text{CMe}_2\text{Ph})$ (**2.8**)

Gated $^{13}\text{C}\{^1\text{H}\}$ NMR (75 MHz, C_6D_6) δ 9.7 (q, $^1J_{\text{CH}} = 127$, C_5Me_5), 32.6 (q, $^1J_{\text{CH}} = 125$, CMeMe), 34.0 (q, $^1J_{\text{CH}} = 124$, CMeMe), 34.2 (q, $^1J_{\text{CH}} = 124$, CMe_3), 39.6 (s, CMe_3), 45.4 (s, CMe_2), 109.7 (s, C_5Me_5), 125.5 (d, $^1J_{\text{CH}} = 159$, Ar CH), 126.3 (d, $^1J_{\text{CH}} = 157$, Ar CH), 128.4 (d, $^1J_{\text{CH}} = 158$, Ar CH), 153.6 (s, C_{ipso}).

2.2.15 ^{13}C and ^1H NOE Difference NMR Data of $\text{Cp}^*\text{W}(\text{NO})(\text{CH}_2\text{CMe}_3)(\text{CH}_2\text{SiMe}_2)$ (**2.9**)

Gated $^{13}\text{C}\{^1\text{H}\}$ NMR (75 MHz, C_6D_6) δ 2.8 (q, $^1J_{\text{CH}} = 117$, SiMe_3), 9.8 (q, $^1J_{\text{CH}} = 127$, C_5Me_5), 34.2 (q, $^1J_{\text{CH}} = 124$, CMe_3), 39.8 (s, CMe_3), 109.8 (s, C_5Me_5). ^1H NOEDS (400 MHz, C_6D_6) irradi. at -2.12 ppm, NOEs at $\delta -1.29$ and 3.28 ; irradi. at -1.29 ppm, NOEs at $\delta -2.12$ and 1.07 ; irradi. at 1.07 ppm, NOE at $\delta -1.29$; irradi. at 3.28 ppm, NOE at $\delta -2.12$.

2.2.16 ^{13}C NMR Data of $\text{Cp}^*\text{W}(\text{NO})(\text{CH}_2\text{CMe}_3)(\text{CH}_3)$ (**2.10**)

Gated $^{13}\text{C}\{^1\text{H}\}$ NMR (75 MHz, C_6D_6) δ 9.6 (q, $^1J_{\text{CH}} = 127$, C_5Me_5), 33.9 (q, $^1J_{\text{CH}} = 124$, CMe_3), 40.3 (s, CMe_3), 109.5 (s, C_5Me_5).

2.2.17 ^{13}C NMR Data of $\text{Cp}^*\text{W}(\text{NO})(\text{CH}_2\text{CMe}_3)(\text{Ph})$ (2.11)

Gated $^{13}\text{C}\{^1\text{H}\}$ NMR (75 MHz, CD_2Cl_2) δ 10.2 (q, $^1J_{\text{CH}} = 127$, C_5Me_5), 33.5 (q, $^1J_{\text{CH}} = 124$, CMe_3), 41.4 (s, CMe_3), 111.4 (s, C_5Me_5), 127.2 (d, $^1J_{\text{CH}} = 158$, Ar CH), 128.3 (d, $^1J_{\text{CH}} = 159$, Ar CH), 136.9 (d, $^1J_{\text{CH}} = 155$, Ar CH), 181.0 (s, WC_{ipso}).

2.2.18 ^{13}C NMR Data of $\text{Cp}^*\text{W}(\text{NO})(\text{CH}_2\text{CMe}_2\text{Ph})(\text{CH}_2\text{SiMe}_3)$ (2.12)

Gated $^{13}\text{C}\{^1\text{H}\}$ (75 MHz, C_6D_6) δ 2.8 (q, $^1J_{\text{CH}} = 118$, SiMe_3), 9.6 (q, $^1J_{\text{CH}} = 127$, C_5Me_5), 32.8 (q, $^1J_{\text{CH}} = 125$, CMeMe), 33.0 (q, $^1J_{\text{CH}} = 125$, CMeMe), 46.1 (s, CMeMe), 110.0 (s, C_5Me_5), 125.7 (d, $^1J_{\text{CH}} = 159$, Ar CH), 126.3 (d, $^1J_{\text{CH}} = 156$, Ar CH), 128.3 (d, $^1J_{\text{CH}} = 156$, Ar CH), 153.3 (s, C_{ipso}).

2.2.19 ^{13}C NMR Data of $\text{Cp}^*\text{W}(\text{NO})(\text{CH}_2\text{CMe}_2\text{Ph})(\text{CH}_3)$ (2.13)

Gated $^{13}\text{C}\{^1\text{H}\}$ NMR (75 MHz, C_6D_6) δ 9.4 (q, $^1J_{\text{CH}} = 127$, C_5Me_5), 31.7 (q, $^1J_{\text{CH}} = 121$, CMeMe), 33.1 (q, $^1J_{\text{CH}} = 121$, CMeMe), 46.7 (s, CMe_2), 109.6 (s, C_5Me_5), 125.5 (d, $^1J_{\text{CH}} = 159$, Ar CH), 126.4 (d, $^1J_{\text{CH}} = 158$, Ar CH), 128.2 (d, $^1J_{\text{CH}} = 157$, Ar CH), 152.7 (s, C_{ipso}).

2.2.20 ^{13}C NMR Data of $\text{Cp}^*\text{W}(\text{NO})(\text{CH}_2\text{CMe}_3)(\text{Cl})$ (2.14)

Gated $^{13}\text{C}\{^1\text{H}\}$ NMR (75 MHz, C_6D_6) δ 9.8 (q, $^1J_{\text{CH}} = 127$, C_5Me_5), 33.7 (q, $^1J_{\text{CH}} = 124$, CMe_3), 39.1 (s, CMe_3), 112.6 (s, C_5Me_5).

2.2.21 Preparation of $\text{Cp}^*\text{W}(\text{NO})(\text{CH}_2\text{CMe}_3)(\text{CH}_2\text{Ph})$ (2.15)

To a mixture of $\text{Cp}^*\text{W}(\text{NO})(\text{CH}_2\text{CMe}_3)\text{Cl}$ (162 mg, 0.356 mmol) and $(\text{PhCH}_2)_2\text{Mg}\cdot(\text{dioxane})$ (60 mg, 0.356 mmol) in a Schlenk tube at -196°C was added Et_2O (20 mL) by vacuum transfer. The resulting contents were thawed and stirred at ambient

temperature for ca. 15 min, during which time the mixture changed from purple to orange. The solvent was then removed in vacuo. The residue was redissolved in Et₂O and filtered through a small plug of alumina I. The alumina column was washed with an additional 2 mL of Et₂O. The combined dark orange filtrates were reduced in volume at room temperature, an operation that resulted in the formation of a small amount of orange crystals. Toluene (1 mL) was then added, and the resulting homogeneous solution was stored at -30 °C overnight to induce the precipitation of **2.15** as orange crystals (136 mg, 75% yield).

Anal. Calcd. for C₂₁H₃₉NO: C, 51.67; H, 6.51; N, 2.74. Found: C, 51.79; H, 6.59; N, 2.65. IR (cm⁻¹) ν_{NO} 1539 (s). MS (LREI, *m/z*) 511 [M⁺, ¹⁸⁴W]. ¹H NMR (300 MHz, C₆D₆) δ 1.15 (s, 9H, CMe₃), 1.55 (s, 15H, C₅Me₅), 6.88 (m, 3H, H_o, H_m), 7.28 (pseudo t, ³J_{HH} = 6.9, 1H, H_p). Gated ¹³C{¹H} NMR (75 MHz, CD₂Cl₂) At 20 °C: δ 10.4 (q, ¹J_{CH} = 127, C₅Me₅), 33.9 (q, ¹J_{CH} = 123, CMe₃), 38.8 (s, CMe₃), 109.5 (s, C₅Me₅), 127.0 (d, ¹J_{CH} = 158, C_p), 129.3 (d, ¹J_{CH} = 158, C_o or C_m), 131.6 (d, ¹J_{CH} = 158, C_o or C_m), 133.2 (C_{ipso}). At -80 °C: δ 10.2 (q, ¹J_{CH} = 127, C₅Me₅), 33.2 (q, ¹J_{CH} = 122, CMe₃), 36.4 (s, CMe₃), 107.8 (s, C₅Me₅), 117.2 (s, C_{ipso}), 129.2 (d, ¹J_{CH} = 159, C_o or C_m), 129.7 (d, ¹J_{CH} = 160, C_p), 133.1 (d, ¹J_{CH} = 159, C_o or C_m).

2.2.22 Neutron Structure of Cp*W(NO)(CH₂CMe₃)₂ (2.4) [See also Addendum]

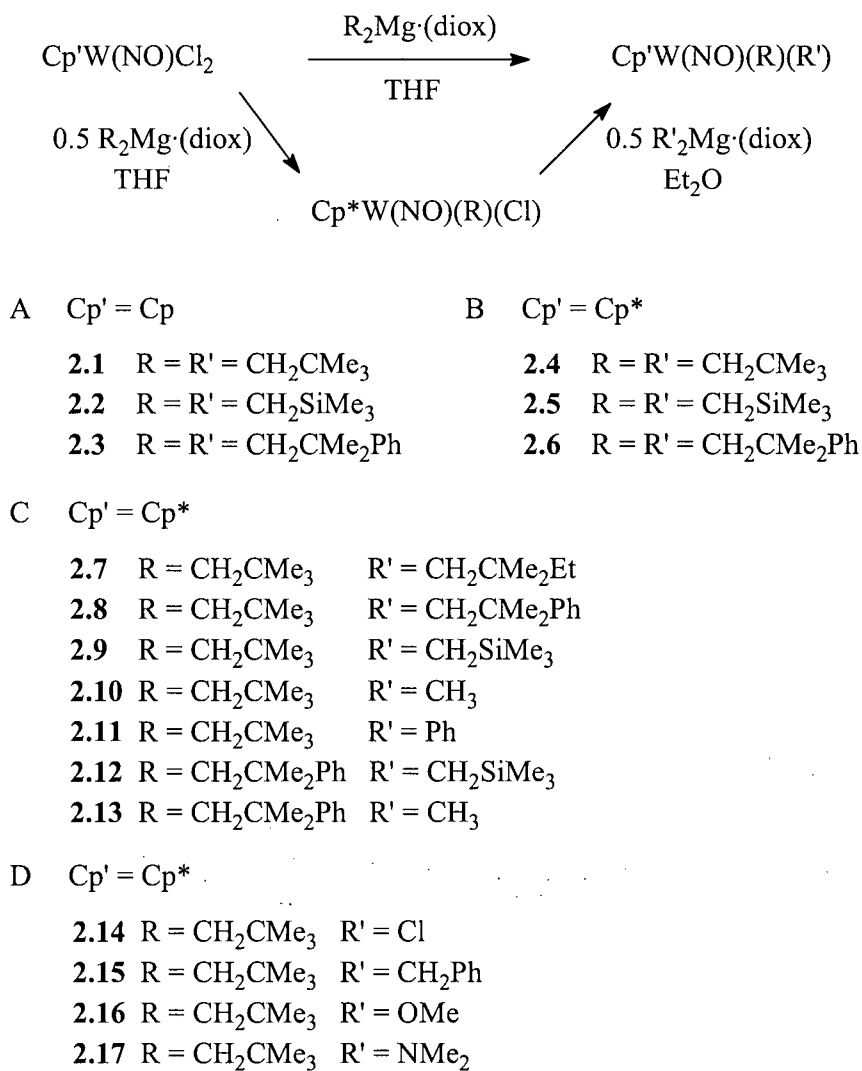
Single crystals of **2.4** were grown from Et₂O/pentane solution at -30 °C. Neutron diffraction data were collected at the Institut Laue-Langevin in Grenoble, France on instrument D19 using 4° × 64° area detector. Under an inert atmosphere, a red-brown crystal with approximate dimensions 4.8 × 1.8 × 0.48 mm was mounted inside a thin-walled quartz tube, jammed between two plugs of quartz wool to prevent slippage. It was then placed inside a Displex cryostat and slowly cooled. At ~100 K, the crystal appeared to undergo a reversible phase transition, and consequently the temperature was raised to 120 K for the subsequent data collection. Data were collected with neutrons of wavelengths 1.5365(2) Å and integrated in three dimensions: a total of 4644 reflections emerged to give a final data set of 2940 unique reflections (R_{merge} = 4.6%) which were used in the subsequent structure analysis.

2.3 Results and Discussion

2.3.1 Synthesis

A list of the $\text{Cp}'\text{W}(\text{NO})(\text{R})(\text{R}')$ complexes selected for this investigation, including the synthetic routes to the bis(alkyl) species, is outlined in Scheme 2.1. These complexes are divided into four groups based on the nature of Cp' , R , and R' . With the exception of **2.4**,

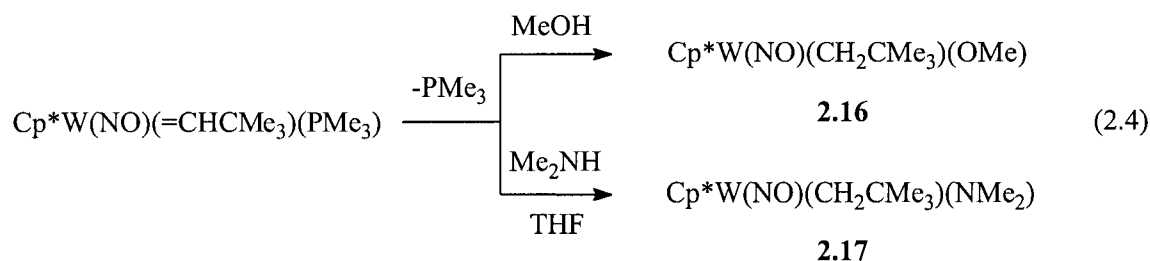
Scheme 2.1



2.16, and **2.17**, the known complexes **2.1–2.6**^{27,28} and **2.8–2.14**^{29,30} were prepared according to literature procedures, while the new complexes **2.7** and **2.15** were prepared in 67% and 75% isolated yields by analogous methods.

The synthesis of **2.4** as reported previously²⁸ involves metathesis of $\text{Cp}^*\text{W}(\text{NO})\text{Cl}_2$ with 1 equiv of $(\text{Me}_3\text{CCH}_2)_2\text{Mg}\cdot(\text{dioxane})$ in THF. This method, unfortunately, affords the desired wine-red product in only 27–31% yield at best. A more efficient one-pot synthesis was thus developed for the work described here. This new approach, which reproducibly provides **2.4** in yields as high as 65–73%, is analogous to that for the synthesis of the mixed bis(alkyl) species and involves sequential use of THF and Et_2O as solvents. The role of Et_2O is unclear at the moment.³¹

In contrast to the formation of complexes **2.1–2.15**, the preparation of $\text{Cp}^*\text{W}(\text{NO})(\text{CH}_2\text{CMe}_3)(\text{OMe})$ (**2.16**) and $\text{Cp}^*\text{W}(\text{NO})(\text{CH}_2\text{CMe}_3)(\text{NMe}_2)$ (**2.17**) by metathesis routes have met with little success. The reactions of $\text{Cp}^*\text{W}(\text{NO})(\text{CH}_2\text{CMe}_3)\text{Cl}$ with NaOMe or LiNMe_2 in either THF or Et_2O , for example, proceeded with only partial conversion and led to an intractable mixture of products containing <20% of **2.16** and **2.17**, respectively. Complexes **2.16** and **2.17** were thus prepared as shown in eq 2.4. This alternative method, which is described in full detail in Chapter 3, involves the use of the alkylidene complex, $\text{Cp}^*\text{W}(\text{NO})(=\text{CHCMe}_3)(\text{PMe}_3)$, as the starting material and offers the following three attractive features: (1) it is quantitative (>97% NMR yield), (2) it is unaffected by the presence of excess alcohol or amine, and (3) it produces volatile PMe_3 as the only by-product.



2.3.2 Spectroscopic Characterization

With the exception of complexes **2.7** and **2.15–2.17**, the spectral data of complexes **2.1–2.6** and **2.8–2.14** have previously been reported.^{27–30} These reported data, however, are incomplete and have not been fully interpreted. For example, the anomalous spectral features of these complexes have been neither identified nor examined by previous investigators.^{27–30} The objective of this section is to discuss the spectral properties of all complexes listed in Scheme 2.1 and, in particular, to address and interpret the unusual spectral features that these complexes exhibit including those that had earlier been overlooked. These data not only show that in most cases these compounds contain *at least* one α -agostic C–H bond, but also that the strength of each of these bonds is dependent on the nature of the alkyl ligands and the effective electron density at the metal. In this section, a discussion of the IR data will be presented first, followed by a discussion of the ^1H and ^{13}C NMR data of complexes of groups A and B, and of groups C and D, respectively.

2.3.2.1 IR Studies

The first indication that several complexes of the type $\text{Cp}'\text{W}(\text{NO})(\text{R})(\text{R}')$ contain an α -agostic structure comes from the Nujol-mull IR spectra of complexes **2.2**, **2.5**, and **2.11**, which show intense ν_{NO} and weak, broad ν_{CH} stretching vibrations at $1547\text{--}1558\text{ cm}^{-1}$ and $2478\text{--}2715\text{ cm}^{-1}$, respectively (Table 2.1). The extraordinarily low ν_{CH} is consistent with the presence of a C–H bond whose strength is diminished due to a strong interaction with an electron-deficient metal center.¹ For complex **2.2**, the ν_{CH} absorption appears as a broad band with two maxima that, as would be expected for an α -agostic complex, is shifted to $1992\text{--}2142\text{ cm}^{-1}$ upon substitution of the four α -H atoms by deuterium atoms (Figure 2.1). It is also ca. 220 and 170 cm^{-1} higher in energy than that of the Cp^* complexes **2.5** and **2.11**, respectively, a feature that can be attributed to there being less electron density at this metal center for $\text{M}(\text{d}_\pi)\text{-to-C-H}(\sigma^*)$ backbonding.³² Since the extent of backbonding is the chief factor affecting the C–H bond order, and hence the ν_{CH} value, it can be concluded that the latter compounds have stronger agostic interactions.

Table 2.1. Selected IR Data for Complexes **2.2**, **2.2-*d*₄**, **2.5**, and **2.11**^a

Cmpd No.	R	R'	Nujol ^b	
			ν_{NO}	ν_{CH}
2.2	CH ₂ CMe ₂ Ph	CH ₂ CMe ₂ Ph	1558 (s)	2686, 2715 (br w)
2.2-<i>d</i>₄	CD ₂ CMe ₂ Ph	CD ₂ CMe ₂ Ph	1556 (s)	2148, 2038, 1992 (w)
2.5	CH ₂ CMe ₂ Ph	CH ₂ CMe ₂ Ph	1547 (s)	2478 (br w)
2.11	CH ₂ CMe ₃	Ph	1547 (s)	2529 (br w)

^a ν in cm⁻¹. ^bs = strong; w = weak; br = broad.

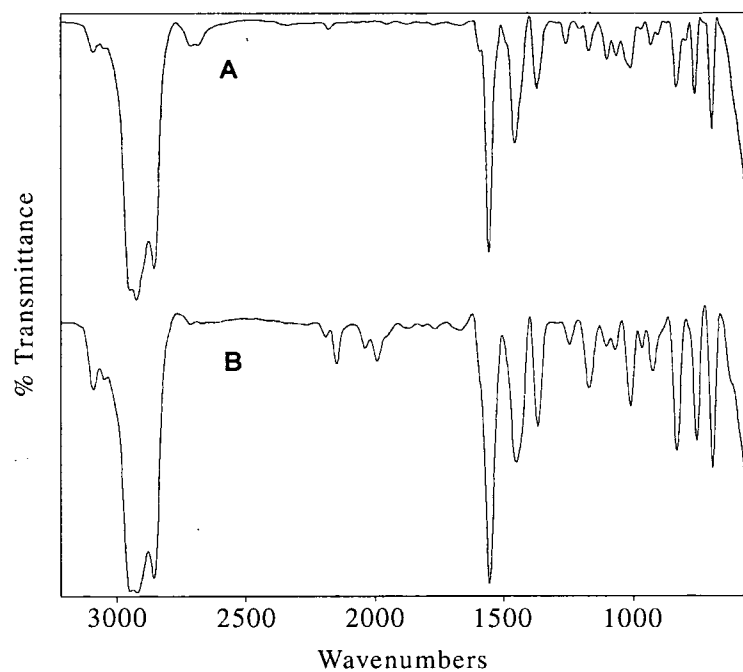


Figure 2.1. Nujol-mull IR spectrum of (A) CpW(NO)(CH₂CMe₂Ph)₂ (**2.2**) and (B) CpW(NO)(CD₂CMe₂Ph)₂ (**2.2-*d*₄**).

2.3.2.2 NMR Studies

The room-temperature ¹H and ¹³C NMR spectra of complexes **2.1–2.17** in C₆D₆, and of **2.11** and **2.15** in CD₂Cl₂ have been examined. In general, these data are in agreement with

previously reported observations and assignments except for those pertaining to the α -moieties of the alkyl ligands. Several spectral parameters of the α -H and α -C atoms are unusual, and provide further evidence for the presence of α -agostic interactions in these complexes. As summarized in Table 2.2, these include the ^1H and ^{13}C chemical shifts, the ^1H – ^1H chemical shift differences, the ^1H – ^1H , ^1H – ^{13}C , and ^1H – ^{183}W coupling constants. The NMR properties of complexes in groups A and B differ from those of group C, which differ in turn from those of group D. Each of these cases will therefore be discussed separately.

As previously reported, the ^1H and ^{13}C NMR spectra of complexes in groups A and B (i.e. **2.1**–**2.6**) are all similar and are consistent with the compounds possessing a three-legged piano-stool molecular structure in which a mirror plane renders the two alkyl groups chemically equivalent.^{27,28} Noteworthy, however, are the two sets of resonances integrating for 2H each due to the diastereotopic methylene protons. In contrast to literature reports, these appear as an AA'XX'Z splitting pattern (where $Z = ^{183}\text{W}$, $I = 1/2$, 14% abundance) rather than as a pattern for an A_2B_2 ²⁹ or A_2X_2 ²³ spin system (see Figure 2.2 for the ^1H NMR spectrum of the methylene regions of **2.4**). Thus, for each complex one of the methylene resonances is a slightly distorted doublet that appears at δ 2 to 4 and shows a $^2J_{\text{HH}}$ coupling constant of 11–12 Hz; while the other resonance is a prominent pseudodoublet that is highly shielded (δ –0.5 to –1.5) and exhibits additional splittings due to coupling of these protons to tungsten ($^2J_{\text{HW}} \approx 8$ –13 Hz)³³ as well as to each other ($^4J_{\text{HH}} \approx 1$ –4 Hz).³² In general, a four-bond H–H coupling across a metal center, a large chemical shift difference for the diastereotopic methylene resonances ($2.79 < \Delta\delta_{\text{HH}} < 5.12$ for **2.1**–**2.6**), and a high-field shift for one of these resonances are spectral manifestations of strong agostic interactions.¹ A negative ^1H chemical shift, in particular, is often characteristic of a hydrogen atom that is *hydridic* in nature due to coordination to a metal. For comparison, the W–H chemical shifts of $\text{Cp}^*\text{W}(\text{NO})(\eta^3\text{-allyl})(\text{H})$ ^{34a} and $\text{CpW}(\text{NO})(\text{H})(\text{I})(\text{PR}_3)$ ^{31b} have also been found to occur ca. δ –0.5 to –2, while $^4J_{\text{HH}}$ values of ca. 1–3 Hz have been reported for the double α -C–H agostic complex, $\text{CpW}(\equiv\text{CAd})(\text{CH}_2\text{CMe}_3)_2$,²⁴ the single α -C–H agostic complexes $\text{Cp}^*\text{Ta}(\text{=CHPh})(\text{CH=PPH}_3)\text{Cl}$ ³⁵ and $[\eta^5\text{-C}_5(\text{CMe}_3)(\text{CH}_2\text{CMe}_3)_2(\text{CH}_2\text{CMe}_2\text{CH}_2)_2]\text{TaCl}_2$,³⁶ and the β -Si–H agostic complex $\text{Cp}_2\text{Zr}(\text{H})(\text{N}^t\text{BuSiMe}_2\text{H})$.³⁷

Table 2.2. Pertinent ^1H and ^{13}C NMR Data for Complexes 2.1–2.17 in C_6D_6 Unless Otherwise Noted

Cmpd No.	$^1\text{H}^a$		$^{13}\text{C}^b$				
	R		R'		R	R'	
	δH (mult, $^2J_{\text{HHb}}$, $^4J_{\text{HHb}}$, $^2J_{\text{HW}}$)	δH (mult, $^2J_{\text{HH}}$)	δH (mult, $^2J_{\text{HHb}}$, $^4J_{\text{HHb}}$, $^2J_{\text{HW}}$)	δH (mult, $^2J_{\text{HH}}$)	δC_α ($^1J_{\text{CH}}$)	δC_α ($^1J_{\text{CH}}$)	
2.1	CH ₂ CMe ₃	CH ₂ CMe ₃	-1.54 (dd, 11.4, 3.5, 8.0)	3.58 (d, 11.4)	5.12 (dd, 103, 122, 90 ^c)	91.4	-
2.2	CH ₂ CMe ₂ Ph	CH ₂ CMe ₂ Ph	-0.98 (dd, 11.1, 3.0) ^d	3.66 (d, 10.8)	4.63 (dd, 103, 124, 93 ^c)	93.8	-
2.3	CH ₂ SiMe ₃	CH ₂ SiMe ₃	-0.56 (d, 8.4) ^d	2.23 (d, 8.4)	2.79 (dd, 104, 118, 83 ^c)	60.8	-
2.4	CH ₂ CMe ₃	CH ₂ CMe ₃	-1.43 (dd, 12.5, 3.5, 11.1)	2.74 (d, 12.5)	4.17 (dd, 99, 122, 95 ^c)	95.3	-
2.5	CH ₂ CMe ₂ Ph	CH ₂ CMe ₂ Ph	-1.17 (d, 12.0) ^d	2.93 (d, 12.3)	4.10 (dd, 99, 123)	99.0	-
2.6	CH ₂ SiMe ₃	CH ₂ SiMe ₃	-1.47 (d, 11.1, 8.0)	1.54 (d, 11.1)	3.01 (dd, 100, 117)	62.7	-
2.7	CH ₂ CMe ₃	CH ₂ CMe ₂ Et	-1.52 (dd, 13.0, 3.3, 13.4)	2.85 (d, 13.0)	4.37 (dd, 13.3, 3.3, 13.1)	96.6	92.4
2.8	CH ₂ CMe ₃	CH ₂ CMe ₂ Ph	-2.26 (dd, 12.3, 2.6, ~12.0)	3.20 (d, 12.3)	5.46 (dd, 13.2, 2.6, ~12.5)	102.0	92.6

2.9	CH ₂ CMe ₃	CH ₂ SiMe ₃	-2.12 (dd, 12.8, 1.9, 10.9)	3.28 (d, 12.8)	5.40 (dd, 12.0, 2.2, 10.9)	-1.29 (d, 12.0)	2.36	106.0	51.1 (dd, 102, 114)
2.10	CH ₂ CMe ₃	CH ₃	-3.15 (dq, 12.4, 1.6) ^d	4.13 (d, 12.4)	7.28 (d, 1.7) ^d	0.53	-	120.9	29.2 (q, 123, 97 ^c)
2.11^e	CH ₂ CMe ₃	Ph	-2.05 ^f (d, 11.4) ^d	4.50 ^f (d, 11.4) ^d	6.55	-	-	124.9	181.0 (dd, 87, 124)
2.12	CH ₂ CMe ₂ Ph	CH ₂ SiMe ₃	-1.55 (dd, 12.6, 2.1) ^g	3.35 (d, 12.6)	4.90 (dd, 11.1, 2.1) ^g	-1.51 (d, 11.1)	2.69	104.5	55.1 (dd, 101, 116, 88 ^c)
2.13	CH ₂ CMe ₂ Ph	CH ₃	-2.75 (dq, 12.0, 1.4) ^c	4.29 (d, 12.3)	7.04 (d, 1.5) ^d	0.54	-	121.7	29.5 (q, 123)
2.14	CH ₂ CMe ₃	Cl	-0.32 (d, 13.2, 11.4)	3.36 (d, 13.2)	3.68	-	-	96.7	-
2.15	CH ₂ CMe ₃	CH ₂ Ph	-2.37 ^f (d, 13.2, 11.1)	2.19 ^f (d, 13.2)	4.56 (d, 8.4)	2.22 (d, 8.4)	0.76	89.6 ^e	52.2 ^e (t, 132, 33 ^c)
2.16	CH ₂ CMe ₃	NMe ₂	0.87 (d, 13.5)	1.00 (d, 13.5)	0.13	-	-	60.8 ^{e,h} (t, 117)	44.9 ^{e,h} (t, 143)
2.17	CH ₂ CMe ₃	OMe	1.26 (d, 14.3)	1.39 (d, 14.3)	0.13	-	-	60.7 (t, 118)	- (t, 118)
						-	-	32.8	-
						-	-	(t, 120)	

^aRecorded at 500 MHz unless otherwise noted. ^bRecorded at 75 MHz. ^c J_{CW} . ^d J_{HW} could not be determined due to poor resolution. ^eIn CD₂Cl₂. ^fRecorded at 300 MHz. ^g J_{HW} could not be determined due to peak overlap. ^hAt -80 °C.

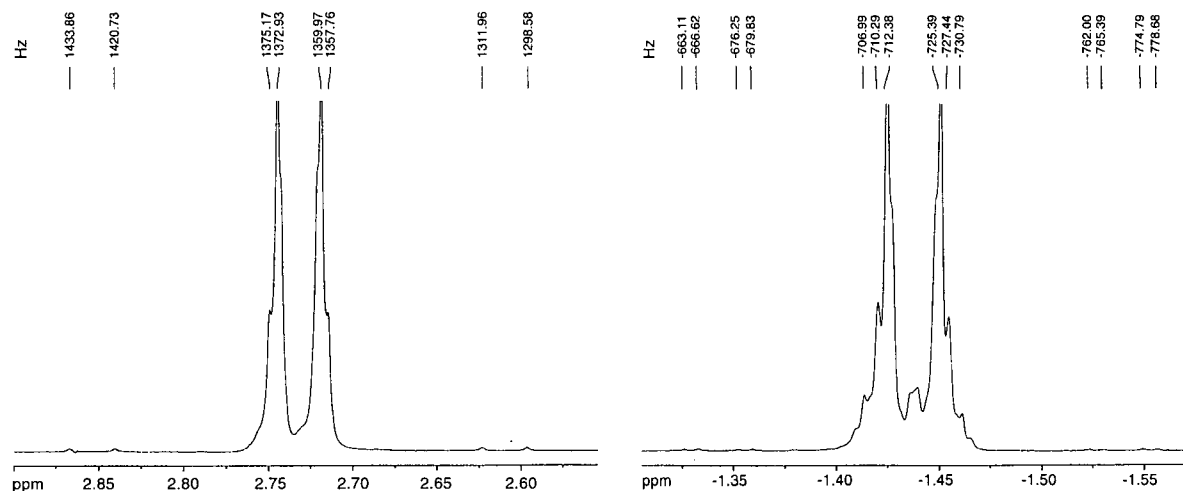


Figure 2.2. 500-MHz ^1H NMR spectrum of the methylene protons of **2.4** in C_6D_6 at 20 $^\circ\text{C}$.

In the gated $^{13}\text{C}\{^1\text{H}\}$ NMR spectra of **2.1**–**2.6**, the α -carbons of each complex resonate as a doublet of doublets with a normal and a reduced ^{13}C – ^1H coupling constant ($^1J_{\text{CH}}$) of 117–124 Hz and 99–104 Hz, respectively. In all instances, the latter is associated with the upfield methylene protons as judged from the ^{13}C satellites in the ^1H NMR spectra. As illustrated in Figure 2.3, it is also inversely proportional to the chemical shift of the α -carbon resonances (δ_{C}) and is consistently smaller for Cp^* complexes and for complexes containing the neopentyl and neophyl ligands. As noted in the introduction, a low $^1J_{\text{CH}}$ value is indicative of $\text{C}-\text{H}\cdots\text{M}$ interaction, and can be attributed to $\text{C}-\text{H}$ bond weakening. A ^{13}C chemical shift to higher frequency as $^1J_{\text{CH}}$ decreases, on the other hand, is suggestive of a geometrical distortion and an increase in sp^2 character at this carbon. That the latter is likely the case is based on Schrock's studies of the α -agostic interactions in a series of neopentyl and neopentylidene complexes of the type $\text{Ta}(\text{CH}_2\text{CMe}_3)_x\text{Cl}_y$ ($x = 1-3$, $y = 2-4$)³⁸ and $\text{Ta}(=\text{CHCMe}_3)_2(\text{PMe}_3)_2(\text{R})$ ($\text{R} = \text{alkyl}$).³⁹ These studies show that as the $^1J_{\text{CH}}$ of the neopentyl and neopentylidene ligands decrease, the ^{13}C shifts of the α -carbon of these ligands move to higher and lower frequencies, respectively, consistent with the α -carbon of the neopentyl ligand becoming more sp^2 -hybridized and the α -carbon of the neopentylidene ligand becoming more sp -hybridized.

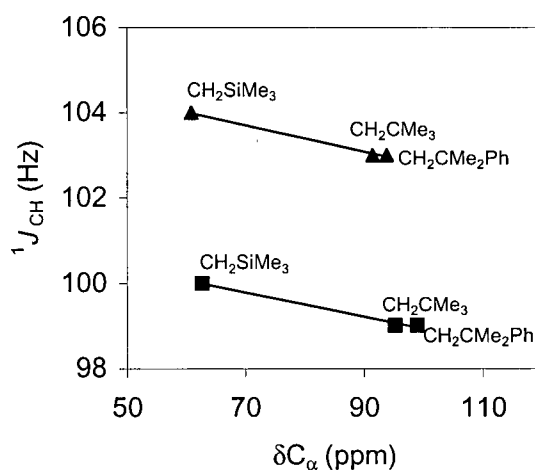


Figure 2.3. Plot of $^1J_{CH}$ versus δC_α as a function of Cp' and R for complexes **2.1–2.6** (Cp = \blacktriangle ; Cp* = \blacksquare).

The above data thus not only indicate that the *upfield* methylene hydrogens in **2.1–2.6** are agostic but also establish that the degree of agostic bonding in these complexes varies with Cp' and R. Assuming that a reduction in $^1J_{CH}$ value is representative of the strength of the agostic interaction, the order for decreasing degree of agostic bonding in **2.1–2.6** is as follows: Cp' = Cp* > Cp and R = CH₂CMe₃ \approx CH₂CMe₂Ph > CH₂SiMe₃. That a stronger α -agostic interaction is observed for more electron-rich metal centers and for sterically more bulky alkyl ligands is not unprecedented. Indeed, similar steric and electronic effects have been observed by Schrock and co-workers in their spectroscopic and structural studies of α -agostic alkylidene complexes.⁴⁰

In contrast to complexes of groups A and B, the complexes of group C are chiral and, as such, they show not only separate NMR signals for each of the α -carbons and α -methylene protons but also different splitting patterns for the latter depending upon the nature of R and R'. For complexes **2.7**, **2.8**, **2.9**, and **2.12** (i.e. R \neq R' = CH₂CMe₃, CH₂CMe₂Et, CH₂CMe₂Ph, or CH₂SiMe₃), the α -protons of each alkyl ligand resonate as a doublet and a doublet of doublets at ca. δ 1.1 to 4.3 and δ -0.5 to -2.8, respectively. Again, as observed for the

symmetrical bis(alkyl) species, the splittings of the upfield resonances are due to geminal coupling as well as four-bond ^1H – ^1H and two-bond ^1H – ^{183}W couplings. This is clearly illustrated by the ^1H NMR spectrum of **2.9** shown in Figure 2.4.

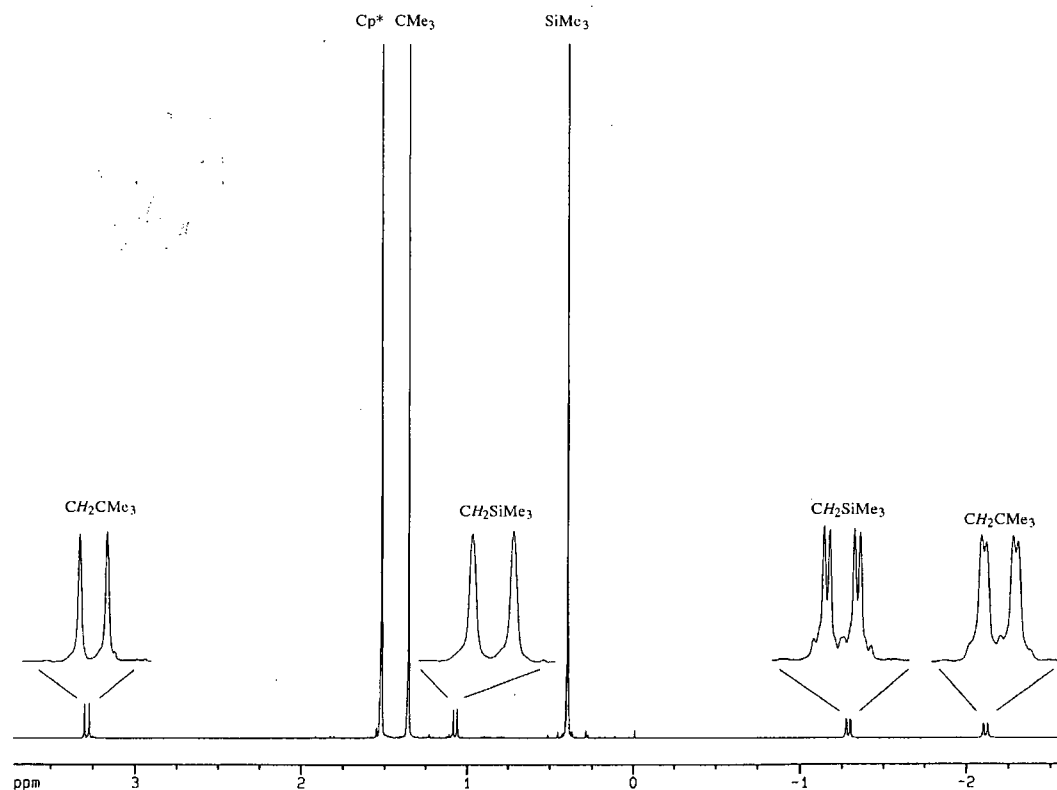


Figure 2.4. 500-MHz ^1H NMR spectrum of **2.9** in C_6D_6 at 20 $^\circ\text{C}$.

In order to establish the stereochemical relationship of the α -methylene protons, an NOE difference experiment on complex **2.9** has been performed. The results of this experiment show that the protons that give rise to the upfield doublets of doublets are on average in close proximity to each other. Thus, if it can be assumed on the basis of steric grounds that the β -moiety of each alkyl ligand is directed away from the Cp^* ligand, then the upfield protons must be situated *trans* to the NO ligand as shown in Figure 2.5:

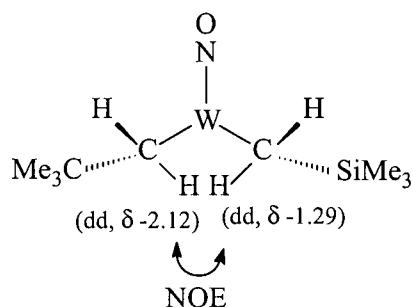


Figure 2.5. Schematic representation of **2.9** along the Cp*-W vector. The Cp* ligand (situated above) is not shown for reasons of clarity.

For complexes **2.10** and **2.13** in which $R = \text{CH}_2\text{CMe}_3$ or $\text{CH}_2\text{CMe}_2\text{Ph}$ and $R' = \text{CH}_3$, the methyl-ligand proton signals are observed at δ 0.5 as a doublet, while the methylene proton signals are observed at ca. δ 4.2 and δ -3.0 as a doublet and a doublet of quartets. Of significance here is that the chemical shift difference for the two methylene resonances (i.e. $\Delta\delta_{\text{HH}}$) is even *greater* than those of the bis(alkyl) species described above, and that the chemical shift for the methyl resonance appears to be *normal*, being roughly mid-way between the methylene signals. In the case of the phenyl complex **2.11** (i.e. $R' = \text{Ph}$), a pair of diastereotopic methylene doublets with a similarly large chemical shift difference is again observed.

A comparison of the ^1H NMR data of complexes **2.7–2.13** reveals that the magnitude of the chemical shift difference for each pair of methylene resonances ($\Delta\delta_{\text{HH}}$) is dependent upon two variables. First, it depends on the identity of the alkyl ligand, decreasing in the following order: $\text{CH}_2\text{CMe}_3 > \text{CH}_2\text{CMe}_2\text{Et} > \text{CH}_2\text{CMe}_2\text{Ph} > \text{CH}_2\text{SiMe}_3$. Second, it decreases as the neighboring alkyl group becomes more neopentyl-like. For example, for complexes **2.7–2.11** the $\Delta\delta_{\text{HH}}$ value of the neopentyl ligand decreases as R' is varied from CH_3 and Ph to CH_2SiMe_3 to $\text{CH}_2\text{CMe}_2\text{Ph}$ to $\text{CH}_2\text{CMe}_2\text{Et}$. Similarly, the $\Delta\delta_{\text{HH}}$ value of the neophyl ligand in complexes **2.12** and **2.13** decreases as R' is varied from CH_3 to CH_2SiMe_3 . The observation of $\Delta\delta_{\text{HH}}$ values which are not only large but also ligand-dependent strongly indicates that these trends are neither by accident nor a consequence of diamagnetic anisotropy. A more

reasonable explanation is that a large $\Delta\delta_{\text{HH}}$ value is caused by coordination of one of the methylene C–H bonds to the metal center and that the magnitude of this spectral parameter is primarily affected by the strength of this coordination.

In the gated $^{13}\text{C}\{^1\text{H}\}$ NMR spectra of complexes **2.7–2.13**, each α -methylene carbon resonance appears at low field (δ 55–122) as a doublet of doublets with normal and reduced $^1J_{\text{CH}}$ values similar to those of the symmetrical bis(alkyl) species. By contrast, the α -methyl signal of complexes **2.10** and **2.13** each appears as a high-field quartet (δ 29) with a normal $^1J_{\text{CH}}$ value of 123 Hz. Comparison of the chemical shift (δ_{C}) and the reduced $^1J_{\text{CH}}$ values of the α -methylene groups in **2.7–2.13** reveals that they too are ligand dependent and that they follow essentially the same trends as determined from the ^1H NMR data. Although the differences are small, it is nevertheless noticeable that δ_{C} is shifted to higher field while $^1J_{\text{CH}}$ decreases as the alkyl ligand is varied from CH_2SiMe_3 to $\text{CH}_2\text{CMe}_2\text{Ph}$ to $\text{CH}_2\text{CMe}_2\text{Et}$ and CH_2CMe_3 . The same changes are also observed on changing the neighboring alkyl group. For example, comparison of the $^1J_{\text{CH}}$ values of the neopentyl ligand in complexes **2.7–2.11** shows that it decreases as R' is varied from $\text{CH}_2\text{CMe}_2\text{Ph}$ to CH_2SiMe_3 to CH_3 to Ph (Figure 2.6).

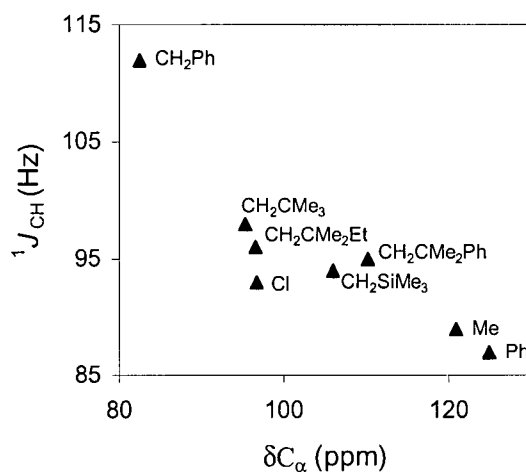


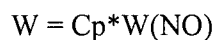
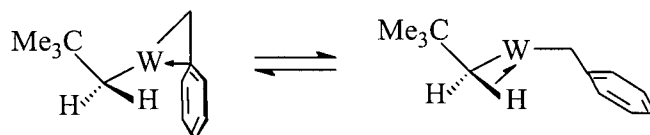
Figure 2.6. Plot of the neopentyl ligand's $^1J_{\text{CH}}$ versus δC_{α} as a function of R' for complexes **2.7–2.11** and **2.14–2.15**.

The observation of a normal δ_{H} , a high-field δ_{C} , and a normal $^1J_{\text{CH}}$ for the methyl ligand in complexes **2.10** and **2.13** suggests that this ligand is weakly agostic at best, if at all. It thus can be concluded that each of these compounds, along with the phenyl complex **2.11**, possesses essentially *one* agostic interaction and that this interaction involves a neopentyl or a neophyl $\alpha\text{-C-H}$ bond. In the case of complexes **2.7–2.9** and **2.12–2.13**, the observation of large $\Delta\delta_{\text{HH}}$ and low $^1J_{\text{CH}}$ values for *both* alkyl ligands can be rationalized by considering that an $\alpha\text{-C-H}$ bond in *each* ligand is involved in agostic bonding, though not necessarily simultaneously (see later). Furthermore, the fact that one alkyl ligand has a larger $\Delta\delta_{\text{HH}}$ and a lower $^1J_{\text{CH}}$ than the other strongly suggests that these agostic interactions are unequal. Thus, on the basis of the ^1H and ^{13}C NMR spectral trends described above, it can be concluded that the degree of agosticity of a given alkyl ligand is optimized when the neighboring alkyl ligand is small and/or lacks α -hydrogens and that the neopentyl ligand is the best agostic donor among the alkyl ligands investigated in this study.

In contrast to complexes of groups A–C, the complexes of group D all contain a potential π -donating ligand and exhibit NMR spectra consistent with the presence of an α -agostic interaction for some but not for other complexes. For the chloro complex **2.14**, both its ^1H and ^{13}C NMR spectra display methylene signals with chemical shifts and coupling constants ($\Delta\delta_{\text{HH}} = 3.68$ ppm, $^1J_{\text{CH}} = 93, 131$ Hz) indicative of a highly distorted α -agostic neopentyl ligand. The presence of lone-pair electrons on the chlorine atom thus has no effect on the ability of the neopentyl to form a three-center, two-electron bond with tungsten. A similar lack of effects by Cl ligands has been reported for the titanium methyl complex, $(\text{dmpe})(\text{Cl})_3\text{Ti}(\text{CH}_3)$,⁴¹ which has been assigned an α -agostic structure by neutron diffraction, and for the α -agostic niobium alkyl species, $\text{Tp}^*\text{Nb}(\text{Cl})(\text{R})(\text{PhC}\equiv\text{CMe})$ ($\text{R} = \text{CH}_3, \text{CH}_2\text{CH}_3, \text{CH}_2\text{SiMe}_3$).⁴²

For the benzyl complex **2.15**, the situation is not as straightforward. For example, although the neopentyl methylene protons give rise to two distinct doublets at $\delta -2.37$ and 2.19 ($^2J_{\text{HH}} = 13.2$ Hz, $\Delta\delta_{\text{HH}} = 4.56$ ppm) and although the upfield signal also exhibits coupling to tungsten ($^2J_{\text{HW}} = 11.1$ Hz), the corresponding carbon, however, resonates as a triplet with a

chemical shift (δ 89.6 in CD_2Cl_2 or 82.6 in C_6D_6) and coupling constant ($^1J_{\text{CH}} = 112$ Hz) that are more consistent with the average for an agostic and a nonagostic neopentyl methylene moiety. For comparison, the corresponding δ_{C} and $^1J_{\text{CH}}$ values for complexes **2.1**, **2.4**, **2.7–2.11**, and **2.14** in C_6D_6 are in the ranges δ 91–125 and 87–103 Hz, respectively. The NMR signals for the benzyl ligand are similarly unusual. For example, the chemical shifts (δ 2.22 and 2.98, $\Delta\delta_{\text{HH}} = 0.76$ ppm) and coupling constants ($^2J_{\text{HH}} = 8.4$ Hz) of the methylene proton signals of this ligand are intermediate for an η^1 -benzyl (δ 0–1, $^2J_{\text{HH}} \sim 10$ Hz) and an η^2 -benzyl (δ 2–3, $^2J_{\text{HH}} \sim 5$ –7 Hz) ligands.^{26,43} The same trend is also observed for the ipso and methylene carbon resonances, which occur at δ 133.2 and δ 51.6 (t, $^1J_{\text{CH}} = 134$ Hz). For comparison, the ^{13}C shifts for the ipso carbon of η^1 -benzyl and η^2 -benzyl groups in structurally related complexes are in the regions δ 150–160 and δ 110–120, respectively.^{26,39} Taken together, these data can be rationalized in terms of the following equilibrium in which the neopentyl and benzyl ligands of **2.15** are rapidly exchanging their modes of attachment to the tungsten center at room temperature.



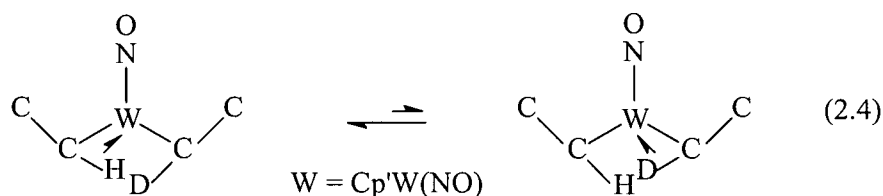
In support of this proposal, the NMR spectra of **2.15** are temperature-dependent. Cooling a sample to -80 °C causes the gated $^{13}\text{C}\{^1\text{H}\}$ NMR spectrum to change as follows. First, the signal due to the neopentyl methylene carbon is shifted upfield by ca. 30 ppm while its $^1J_{\text{CH}}$ coupling constant is increased to 117 Hz, a value that is characteristic of a nonagostic neopentyl ligand. Second, the signals for both the benzyl methylene (δ 44.9) and benzyl ipso (δ 117.2) carbons are similarly shifted to lower frequencies. Importantly, the chemical shift of the latter is in the region associated with static η^2 -benzyl ligands, while the $^1J_{\text{CH}}$ coupling constant (143 Hz) for the former is consistent with considerable sp^2 character at this carbon.^{26,37} On the basis of these spectral observations it can be concluded that (1) the low-temperature limiting structure for **2.15** is that in which the benzyl ligand is coordinated to

tungsten in an η^2 -fashion and the neopentyl ligand is nonagostic, and (2) at room temperature this η^2 -benzyl-metal interaction is fluxional, thereby allowing an α -C-H bond of the neopentyl ligand to compete for coordination.

Finally, in contrast to the NMR spectra of complexes **2.1–2.15**, the NMR spectra of the neopentyl complexes $\text{Cp}^*\text{W}(\text{NO})(\text{CH}_2\text{CMe}_3)(\text{OMe})$ (**2.16**) and $\text{Cp}^*\text{W}(\text{NO})(\text{CH}_2\text{CMe}_3)(\text{NMe}_2)$ (**2.17**) display *normal* chemical shifts and coupling constants for the α -methylene protons and carbons. The $^1J_{\text{CH}}$ values of 118 Hz for **2.16** and 120 Hz for **2.17**, in particular, are indicative of nonagostic structures for these compounds. In the ^1H NMR spectrum of **2.17**, the methyl substituents of the NMe_2 ligand give rise to two sharp singlets at δ 2.59 and 3.71, which remain unchanged even when heated to 100 °C. This suggests that the amido ligand is functioning as a π -donor. The lack of agostic interactions in this complex and in **2.16** therefore can be attributed to the inability of an α -C-H bond on the neopentyl group to compete with the lone-pairs of electrons on N and O for metal coordination.

The results presented thus far clearly show that in the absence of efficient π -donation, alkyl complexes, $\text{Cp}'\text{W}(\text{NO})(\text{R})(\text{R}')$, possess an α -agostic structure in solution. When R is a sterically bulky alkyl ligand and R' is CH_3 , Ph, or Cl, the metal center approaches a closed-shell configuration by forming a strong three-center, two-electron bond with one α -C-H bond. When R and R' are both bulky alkyl moieties, the metal center is coordinated to two α -C-H groups, one from each alkyl ligand. The nature of the agostic interaction(s) in these latter complexes is not clear-cut, however. The fact that a reduced $^1J_{\text{CH}}$ is observed for *both* alkyl ligands can be interpreted in terms of either a rapid site exchange of an α -H atom of one alkyl ligand and an α -H atom of the other for successive interaction with the metal center, or a *simultaneous* interaction of both α -H atoms. In order to distinguish between these two possibilities, a variable-temperature NMR study of the partially deuterated complex, $\text{Cp}^*\text{W}(\text{NO})(\text{CH}_2\text{CMe}_3)(\text{CD}_2\text{CMe}_3)$ (**2.4-d₂**), was performed. Since the zero-point energy of a C-H bond is higher than that of a C-D bond and since this energy difference is greatest when the two bonds are nonagostic, there is a thermodynamic preference for the former to coordinate to the metal. Thus, if two α -C-H bonds from different alkyl ligands are indeed

competing with each other for the metal, then cooling a solution of **2.4-*d*₂** should cause the equilibrium to shift in favor of the α -C–H agostic form (eq 2.4), and should lead to an asymmetric structure with a reduction in $^1J_{\text{CH}}$.



Both the ^1H and the gated $^{13}\text{C}\{^1\text{H}\}$ NMR spectra of **2.4-*d*₂** have been investigated at several temperatures from -80 to $+20$ °C. As in the case of **2.4**, the spectra of **2.4-*d*₂** are consistent with there being a mirror plane in the molecule, even down to -80 °C. In addition, they show that the $^1J_{\text{CH}}$ for the α -carbons are invariant not only to partial deuterium substitution but also to temperature. These findings thus provide strong support that **2.4-*d*₂** and related bis(alkyl) complexes possess a time-averaged structure (see later) in which *two* α -C–H bonds are coordinated to the metal center.

2.3.3 X-Ray Structural Studies

The first $\text{Cp}'\text{W}(\text{NO})(\text{R})(\text{R}')$ complex to have been structurally characterized by X-ray diffraction is the group A complex, $\text{CpW}(\text{NO})(\text{CH}_2\text{SiMe}_3)_2$ (**2.3**).³¹ Although the α -H atoms were not located, the structure exhibits two features that are characteristic of α -agostic species. First, the $\text{W}-\text{C}_\alpha$ distances (2.103(9) and 2.108(9) Å) are significantly shorter than simple tungsten-carbon single bonds, which are typically 2.18–2.25 Å. Second, the $\text{W}-\text{C}_\alpha-\text{Si}$ angles ($125.5(5)^\circ$ and $127.1(5)^\circ$) are more obtuse than those observed in nonagostic systems. In order to confirm that these unusual features are structural consequences of α -agostic bonding and to compare the conformational preference of the alkyl ligands in this complex to those in complexes of groups B–D, X-ray crystallographic analyses of the following four compounds have been performed: $\text{Cp}^*\text{W}(\text{NO})(\text{CD}_2\text{CMe}_3)_2$ (**2.4-*d*₄**), $\text{Cp}^*\text{W}(\text{NO})(\text{CH}_2\text{CMe}_3)(\text{CH}_2\text{SiMe}_3)$

(**2.9**), $\text{Cp}^*\text{W}(\text{NO})(\text{CH}_2\text{CMe}_2)(\text{C}_6\text{H}_3\text{-2,5-Me}_2)$ (**2.11'**), and $\text{Cp}^*\text{W}(\text{NO})(\text{CH}_2\text{CMe}_3)(\text{NMe}_2)$ (**2.17**). **2.4-d₄** and **2.17** are examples of complexes from groups B and D, respectively, while **2.9** and **2.11'** are representative of group C. The last is a structural analogue of **2.11** whose synthesis and spectroscopic characterization are discussed in Chapter 4.

The above four compounds were chosen because (1) X-ray quality crystals of each could easily be obtained; (2) they each contain a neopentyl ligand, which according to NMR studies, should be significantly distorted and should provide a more clear-cut situation than the (trimethylsilyl)methyl ligands in **2.3**; and (3) by sharing the neopentyl ligand they not only allow for direct comparison between complexes, but also for comparison with several related agostic neopentyl complexes reported in the literature. Shown in Figures 2.7 are the ORTEP representations of the solid-state molecular structures of **2.4-d₄**, **2.9**, **2.11'**, and **2.17**. The relevant bond distances and angles, along with those of **2.3**, are listed in Table 2.3.

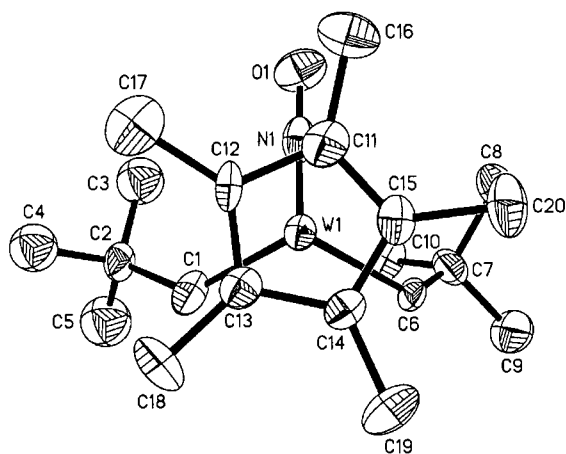
Comparison of the structures of **2.4-d₄**, **2.9**, **2.11'**, and **2.17**, with **2.3** shows that they all share a three-legged piano-stool geometry about tungsten and that the intramolecular dimensions involving the $\text{Cp}'\text{-W}$ and W-NO portions in each molecule are unremarkable. In all cases, the Cp' ligands are coordinated in an η^5 fashion while the W-NO linkages are essentially linear with W-N distances (ca. 1.76 Å) and W-N-O angles (ca. 166.9–169.5°) in the range found for other $\text{Cp}'\text{W}(\text{NO})$ -containing systems.^{27,39} This indicates that the NO ligands are functioning as formal three-electron donors and that there is considerable $\text{W} \rightarrow \text{NO}$ backbonding. An examination of the W-alkyl fragments reveals that (1) they each adopt a conformation almost identical to that in **2.3**; that is, for all complexes the alkyl ligands are obtuse and oriented with their β -moieties pointing in the general direction of the NO ligand but away from the plane formed by the Cp' (centroid), the metal, and the NO ligand (Figure 2.7a); and (2) the degree of distortion in each case varies depending upon the alkyl group and the effective electron density at the metal.

For complex **2.4-d₄**, one of the *tert*-butyl groups is disordered over two positions in a 0.54:0.46 ratio. The quaternary carbon could be refined anisotropically, but the methyls could

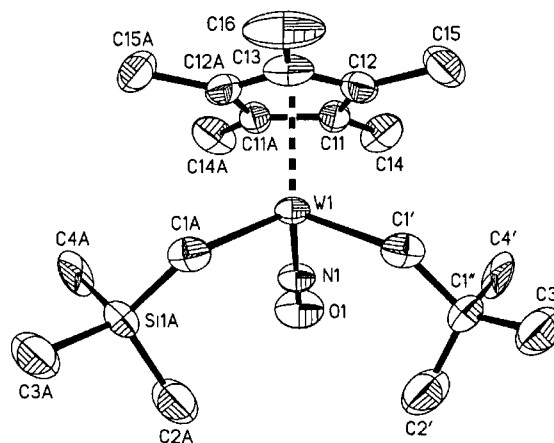
not. Comparison of the bonding parameters of the neopentyl ligands in **2.4-d₄** reveals that they are inequivalent. Thus, while the W(1)–C(2) distance of 2.169(10) Å and W(1)–C(1)–C(2) angle of 126.9(6)° are within the range observed for the alkyl ligands of **2.3**, the corresponding distance (2.101(10) Å) and angle (134.0(7)°) for the neighboring neopentyl group indicate an even greater distortion. For comparison, the M–C_α–C_β angles in the bis(neopentyl) complexes CpW(≡CAd)(CH₂CMe₃)₂²⁴ and CpNb(=NAr)(CH₂CMe₃)₂,²⁵ in which the presence of *two* α-agostic interactions has been confirmed by X-ray diffraction, are 134.8(4)° and 132.5–131.2°, respectively (Table 2.4).

In order to gain conclusive evidence that **2.4-d₄** also has an α-agostic structure, the positions of the α-D atoms were located during the structure refinement. This was achieved by placing the D atoms in idealized positions and then allowing the orientations of the resulting C–D bonds to refine freely. Summarized in Table 2.4 are the bonding parameters of the W–CD₂CMe₃ fragments in **2.4-d₄**. Noteworthy is that while the W–C(1)–D(1b) and W–C(6)–D(6a) angles are *normal*, the W–C(1)–D(1a) and W–C(6)–D(6b) angles of 82.1° and 94.1°, respectively, are significantly contracted from tetrahedral and are consistent with these D's being drawn toward the metal. That this is indeed the case is confirmed by the short W···D(1a) and W···D(6b) distances of 2.25 and 2.45 Å and the relatively lengthened C(1)–D(1a) and C(6)–D(6b) distances of 1.11 and 1.04 Å. For comparison, the M–C_α–H bond angles in the alkylidyne and imido complexes mentioned above are 93° and 86.5–89.4°, while the corresponding C–H···M distances are 2.42 and 2.32–2.41 Å, respectively (Table 2.4). In **2.4-d₄**, the D atom nearest to tungsten is associated with the more acute W–C_α–D angle and the more obtuse W–C_α–C_β angle. Taken together, these observations not only strongly suggest that this complex contains *two* α-agostic interactions in the solid state, one from each neopentyl ligand, but also show that one of the interactions is stronger than the other and that each of these interactions is indeed the primary cause for the significant angular deformation at the α-carbons.

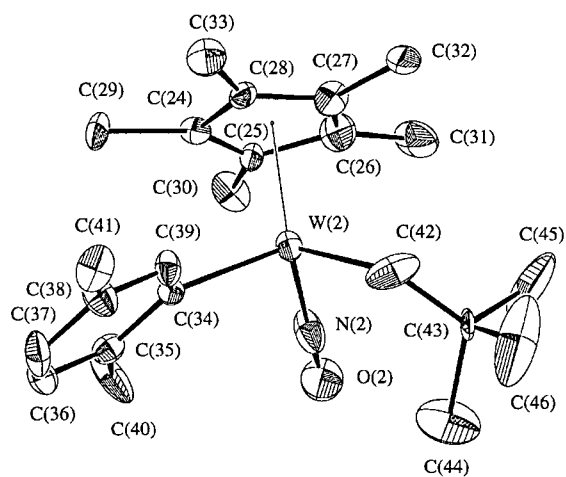
A



B



C



D

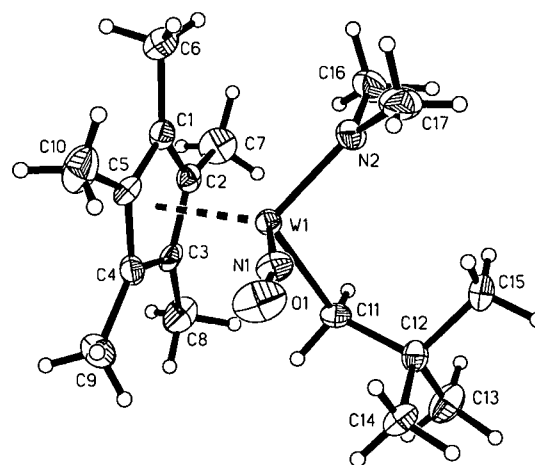
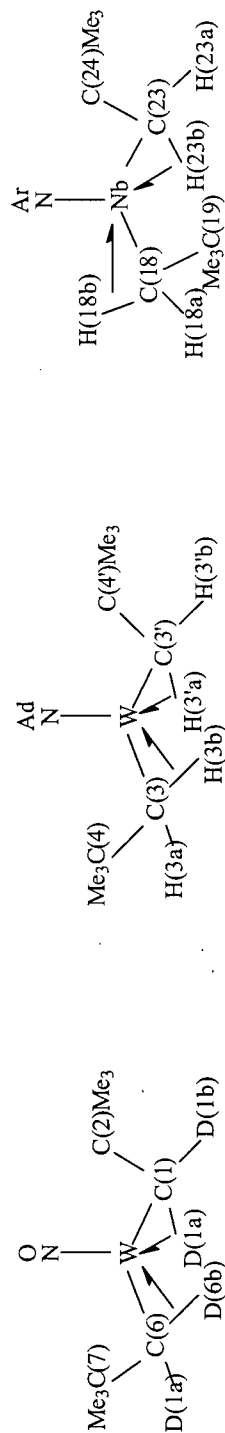


Figure 2.7. ORTEP diagrams of (A) $\text{Cp}^*\text{W}(\text{NO})(\text{CD}_2\text{CMe}_3)_2$ (**2.4-*d*₄**), (B) $\text{Cp}^*\text{W}(\text{NO})(\text{CH}_2\text{CMe}_3)(\text{CH}_2\text{SiMe}_3)$ (**2.9**), (C) $\text{Cp}^*\text{W}(\text{NO})(\text{CH}_2\text{CMe}_3)(2,5\text{-C}_6\text{H}_3\text{-Me}_2)$ (**2.11'**), and (D) $\text{Cp}^*\text{W}(\text{NO})(\text{CH}_2\text{CMe}_3)(\text{NMe}_2)$ (**2.17**).

Table 2.3. Selected Bond Distances and Angles for Complexes 2.3, 2.4-*d*₄, 2.9, 2.11', and 2.17

2.3	2.4- <i>d</i> ₄	2.9	2.11'	2.17	
Bond Distances (Å)					
W(1)–C(1)	2.103(9)	W(1)–C(1)	W(1)–C(19)	W(1)–C(11)	2.186(4)
W(1)–C(2)	2.108(9)	W(1)–C(6)	W(1)–C(11)	W(1)–N(2)	1.931(4)
W(1)–N(1)	1.757(8)	W(1)–N(1)	W(1)–N(1)	W(1)–N(1)	1.777(4)
C(1)–Si(1)	1.858(11)	C(1')–C(1'')	C(19)–C(20)	C(1)–C(2)	1.537(7)
C(2)–Si(2)	1.822(10)	C(6)–C(7)	N(1)–O(1)	N(1)–O(1)	1.230(5)
N(1)–O(1)	1.226(10)	N(1)–O(1)			
Bond Angles (°)					
W(1)–N(1)–O(1)	169.5(6)	W(1)–N(1)–O(1)	W(1)–N(1)–O(1)	W(1)–N(1)–O(1)	166.9(4)
N(1)–W(1)–C(1)	97.7(4)	N(1)–W(1)–C(1)	N(1)–W(1)–C(19)	N(1)–W(1)–C(11)	98.4(2)
N(1)–W(1)–C(2)	95.7(4)	N(1)–W(1)–C(6)	N(1)–W(1)–C(11)	N(1)–W(1)–N(2)	98.1(2)
C(1)–W(1)–C(2)	109.6(4)	C(1)–W(1)–C(6)	C(11)–W(1)–C(19)	N(2)–W(1)–C(11)	103.1(2)
W(1)–C(1)–Si(1)	125.5(5)	W(1)–C(1)–C(2)	W(1)–C(11)–C(12)	W(1)–N(2)–C(16)	121.4(4)
W(1)–C(2)–Si(2)	127.1(5)	W(1)–C(6)–C(7)	W(1)–C(11)–C(16)	W(1)–N(2)–C(17)	128.5(5)
			W(1)–C(19)–C(20)	W(1)–C(11)–C(12)	122.9(3)

Table 2.4. Bond Distances and Angles Involving the M-CH₂CMe₃ Fragments of Complexes Cp*W(NO)(CD₂CMe₃)₂ (2.4-d₄), CpW(=NAd)(CH₂CMe₃)₂,^a and CpNb(=NAr)(CH₂CMe₃)₂^b (The Cp' ligands are not drawn below for clarity)



Cp*W(NO)(CD ₂ CMe ₃) ₂ (2.4-d₄)	CpW(=NAd)(CH ₂ CMe ₃) ₂			CpNb(=NAr)(CH ₂ CMe ₃) ₂					
	Bond Distances (Å)								
W–C(1)	2.101(10)	W–C(6)	2.169(8)	W–C(3)	2.159(7)	Nb–C(23)	2.215(3)	Nb–C(18)	2.174(3)
W–D(1a)	2.25(10)	W–D(6b)	2.45(9)	W–H(3a)	2.42(7)	Nb–H(23a)	2.32(3)	Nb–H(18a)	2.40(3)
C(1)–D(1a)	1.110	C(6)–D(6b)	1.042	C(3)–H(3a)	0.98				
C(1)–D(1b)	0.839	C(6)–D(6a)	0.896	C(3)–H(3b)	0.93				
	Bond Angles (°)								
W–C(1)–C(2)	134.0(7)	W–C(6)–C(7)	126.9(6)	W–C(3)–C(4)	134.8(4)	Nb–C(23)–C(24)	132.5(3)	Nb–C(18)–C(19)	131.2(2)
W–C(1)–D(1a)	82.1	W–C(6)–D(6b)	94.1	W–C(3)–H(3a)	93	Nb–C(23)–H(23a)	89.4	Nb–C(18)–H(a)	86.5
W–C(1)–D(1b)	101.4	W–C(6)–D(6a)	102.2	W–C(3)–H(3b)	109	Nb–C(23)–H(23b)	107.0	Nb–C(18)–H(b)	107.3
D(1a)–C(1)–D(1b)	108.4	D(6a)–C(6)–D(6b)	104.2			H(a)–C(23)–H(b)	109.6	H(a)–C(18)–H(b)	105.3

^aThe two neopentyl groups are crystallographically equivalent; Ad = 1-adamantyl. ^bAr = C₆H₃-2,6-ⁱPr₂.

In contrast to **2.4-*d*₄**, the alkyl groups of **2.9** initially appeared equivalent due to a crystallographically imposed mirror plane. The structure thus had to be refined using high-resolution data. By restraining the W–C_α bonds to having the same bond length within a 0.010 Å esd and all atoms in the disordered groups to having identical anisotropic displacement parameters, the Si–C and C–C bond lengths were successfully refined independently and a chemically reasonable structure was obtained (Figure 2.7b). The important feature to note about this structure is that the neopentyl ligand (W–C_α–C_β = 133.3(11)°) is more severely distorted than the (trimethylsilyl)methyl ligand (W–C_α–Si_β = 119.1(7)°), a fact that is consistent with the NMR data which suggest that the former has a stronger agostic interaction.

In the case of complex **2.11'**, the asymmetric unit contains two molecules which are virtually mirror images of each other, one of which is shown in Figure 2.7c. Like the bis(alkyl) complexes **2.4-*d*₄** and **2.9**, the neopentyl ligand of **2.11'** also exhibits a markedly short W–C_α distance (2.084(11) Å) and a large W–C_α–C_β angle (133.9(8)°). That the latter is in the range observed for **2.4-*d*₄** and **2.9** implies a similar degree of agostic bonding for all three systems.

For complex **2.17**, on the other hand, hydrogen bonding between the Cp* ligand of one molecule and the NO ligand of another occurs. This is evident from the C(6)–H(6b)···O(1) distance of 2.555 Å and C(6)–H(6b)···O(1) angle of 167.8°. Examination of the amido ligand reveals that the N atom adopts a planar geometry with bonding parameters consistent with it functioning as a π-donor. For example, the W–NMe₂ distance of 1.931(4) Å is indicative of considerable multiple bond character in this linkage, while the N(1)–W(1)–N(2)–C(16) and N(1)–W(1)–N(2)–C(17) torsion angles of 177.5(4)° and –5.9(5)°, respectively, are of proper magnitude for maximum π-bonding. The neopentyl ligand displays a *normal* W–C_α distance of 2.186(4) Å and a W–C_α–C_β angle (122.9(3)°) that is substantially less than that in **2.4-*d*₄**, **2.9**, and **2.11'**. Thus, although the W–C_α–C_β angle deviates from the ideal 109° for sp³-hybridized centers, it is more likely that this deviation is a consequence of the intrinsic steric

repulsion between the *tert*-butyl group and the rest of the molecule rather than α -agostic bonding.

2.3.4 Molecular Orbital Description of the Agostic Bonds

As noted in Chapter 1, $\text{Cp}'\text{W}(\text{NO})(\text{R})(\text{R}')$ bis(alkyl) complexes are formally 16-electron species which possess a low-lying unoccupied molecular orbital (LUMO) that is approximately $d_{x^2-y^2}$ in character.⁴⁴ Although the orbital is situated such that three of its four lobes are suitably oriented for bonding to additional ligands, the spectroscopic and structural data presented above, however, show that only the lobe that is straddled by the alkyl ligands is involved in α -agostic bonding.

For complexes in which there is only one $\alpha\text{-C-H}\cdots\text{W}$ interaction, donation of an electron pair from a C-H bond gives the metal a configuration approaching 18 electrons. For complexes in which two such interactions are present, the bonding situation is more complicated, for the metal now has an electron count of 20 electrons. In general, transition-metal complexes with greater than an 18-electron count are oxidatively unstable since antibonding orbitals are used to accommodate the excess electron density.⁴⁵ Two representative examples of such complexes are cobaltocene and nickelocene, which are a 19- and 20-electron complexes, respectively.⁴⁶ In the case of the $\text{Cp}'\text{W}(\text{NO})(\text{R})(\text{R}')$ bis(alkyl) complexes, however, the formation of a double α -agostic interaction need not result in the antibonding orbitals being occupied. This is possible by considering the molecular orbital model shown in Figure 2.8. In this model, which is analogous to that proposed previously by Schrock and co-workers for the alkylidyne bis(neopentyl) system mentioned above,²³ mixing of two $\alpha\text{-C-H}$ σ orbitals with the metal-based LUMO leads to formation of C-H-W bonding, nonbonding, and antibonding molecular orbitals. Since there are only two pairs of C-H σ electrons, only the bonding and nonbonding molecular orbitals will be occupied.

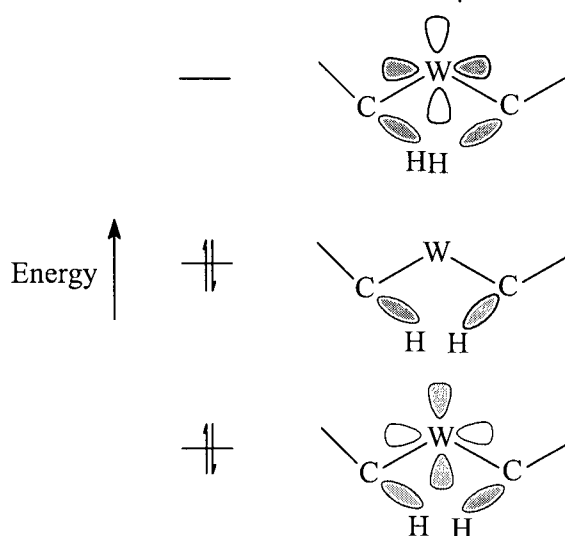


Figure 2.8. Qualitative molecular orbital diagram for the double α -agostic interaction in $\text{Cp}'\text{W}(\text{NO})(\text{R}')(\text{R}')$ complexes.

2.4 Epilogue

In summary, a series of 17 alkyl complexes of the type $\text{Cp}'\text{W}(\text{NO})(\text{R})(\text{R}')$ have been systematically studied by IR and NMR spectroscopies. The X-ray structures of several of these species have also been determined. The picture that emerges from these studies is that these compounds adopt an α -agostic structure when secondary interactions such as lone pair or π -electron donation are not possible. Thus, with the exception of the alkoxo and amido complexes, **2.16** and **2.17**, in which the metal center attains an 18-electron configuration via lone-pair donation from the O and N atoms, the remaining complexes exhibit α -methylene agostic interactions of varying strengths and multiplicities.

In solution the α -agostic interactions give rise to a number of unusual spectroscopic features for each α -methylene moiety. Most noteworthy are (1) a negative ^1H shift for one of the methylene protons, indicating the presence of an α -agostic interaction between this hydrogen and the tungsten, (2) reduced ν_{CH} and $^1J_{\text{CH}}$ values, consistent with a weakening of

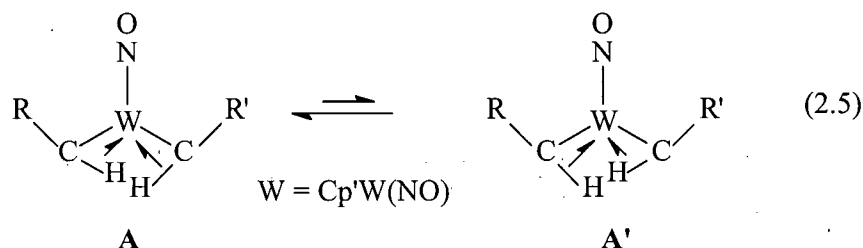
the α -C-H bond, and (3) a ^{13}C shift to higher frequency as $^1J_{\text{CH}}$ decreases, indicating an increase in sp^2 character and a geometrical distortion at this carbon. In the solid state, these α -agostic interactions lead to shortened W-C $_{\alpha}$ bonds and markedly obtuse W-C $_{\alpha}$ -C(Si) $_{\beta}$ angles. That these abnormal structural features are indeed consequences of α -agostic bonding has been confirmed by the X-ray structure of complex **2.4-d₄**, in which all four D atoms were located. Although the uncertainties associated with the metrical parameters of these atoms are large, it nevertheless is clear that one C-D bond on each methylene group is normal while the other is agostic.

Two types of α -agostic complexes have been established. In one type, which includes complexes in which R = CH₂CMe₃ and R' = Ph, CH₃, Cl, or CH₂Ph, *one* α -agostic interaction involving the neopentyl ligand is observed. The order for the increasing degree of α -agostic bonding among these complexes based on the magnitude of the $^1J_{\text{CH}}$ value is R' = PhCH₂ < Cl < CH₃ < Ph. That the benzyl complex contains the weakest α -agostic interaction is consistent with the fact that in this complex the neopentyl α -C-H bond has to compete with the π -system of the benzyl ligand for the vacant metal orbital. In the case of the phenyl complex, the interaction between the α -C-H bond and the metal is strongest because the phenyl ligand can only act as a σ -donor.

The second type of α -agostic complexes is significantly more striking, for *two* α -agostic interactions from different alkyl ligands are present. On the basis of the NMR data, the strength of these interactions varies as follows. First, among all the alkyl ligands studied, the order of decreasing α -agostic donor ability is CH₂CMe₃ \geq CH₂CMe₂Et > CH₂CMe₂Ph > CH₂SiMe₃. Second, for a series of Cp* complexes in which R = CH₂CMe₃ and R' = CH₂CMe₃, CH₂CMe₂Et, CH₂CMe₂Ph, or CH₂SiMe₃, the degree of α -agosticity of R decreases as R' is changed from CH₂SiMe₃ to CH₂CMe₂Ph to CH₂CMe₂Et to CH₂CMe₃. Third, for a series of Cp and Cp* complexes in which R = R', the agostic interactions in the Cp* series are consistently stronger than those in the Cp analogues, a fact that can be ascribed to there being a greater degree of metal-to-C-H (σ^*) backbonding in the former complexes. A similar

phenomenon has been well established for related η^2 -H₂ compounds, whose existence can only be detected when the metal has d electrons for back-donation.⁴⁷

Although the trends above clearly show that in solution the α -agostic interactions in Cp'W(NO)(R)(R') complexes are unequal when $R \neq R'$ and that the degree of agosticity of a given alkyl group changes as R' is varied, this is not entirely true in the solid state as the neopentyl ligands in complexes Cp*W(NO)(CH₂CMe₃)(CH₂SiMe₃) (**2.9**) and Cp*W(NO)(CH₂CMe₃)(C₆H₃-2,5-Me₂) (**2.11'**) are *equally* distorted. Furthermore, although the NMR data of complexes in which $R = R'$ indicate a plane of symmetry in solution and therefore imply that the agostic interactions are equal, the solid-state structure of **2.4-d₄** shows it to contain an asymmetric structure in which one neopentyl group is not only markedly more distorted than the other but is also equally distorted compared to that in **2.9** and **2.11'**. Taken together, these results suggest that (1) *in the solid state*, regardless of whether $R = R'$ or $R \neq R'$, the double α -agostic interactions in Cp'W(NO)(R)(R') bis(alkyl) complexes are unequal and do *not* vary as a function of the neighboring alkyl group, and (2) *in solution*, they exist as time-averaged structures due equilibration of the type shown in eq 2.5.



The observation that only the (trimethylsilyl)methyl and neopentyl-like ligands are agostic suggests that steric factors play an important role in the occurrence of agostic interactions. This is not surprising since in order to minimize steric crowding at the metal, the $\text{W}-\text{C}_\alpha-\text{C}_\beta$ would have to widen, thereby placing an α -C-H bond close the metal. Among the ligands studied, the neopentyl is the most agostic. The reason for this selectivity is not clear. It appears not to be solely steric in origin, since if this were the case, then the CH₂CMe₂Et and CH₂CMe₂Ph (neophyl) ligands, which are larger than the neopentyl ligand, would be expected

to have stronger α -agostic interactions. Furthermore, although it could be argued that the neophyl ligand has a weaker agostic bond because of the electronic effects of the phenyl substituent, this is also unlikely since the strengths of the agostic bond of this ligand and of the neopentyl ligand are identical when the neighboring alkyl group of both complexes is neophyl or neopentyl, respectively, or when it is a methyl or a trimethylsilylmethyl group.

Finally, the reason why two α -agostic interactions are formed, when one is sufficient for electronic saturation, is also uncertain. Given the fact these interactions only occur in complexes in which both alkyl ligands are bulky, steric factors again appear to play an active role in making these interactions feasible.

2.5 Addendum: Neutron Structure of $\text{Cp}^*\text{W}(\text{NO})(\text{CH}_2\text{CMe}_3)_2$ (**2.4**) and Reinterpretation of Spectroscopic and Structural Data

As noted above, the position of hydrogens as determined by X-ray diffraction is subject to appreciable error. This is due to the fact that peaks due to hydrogen atoms are typically near the noise level of the electron-density maps. Thus, in order to unambiguously establish the multiplicity of the α -agostic interaction in **2.4**, a neutron diffraction study of this complex was undertaken. This was achieved at 120 K and yielded the results shown in Figure 2.9. As was found in the X-ray analysis of **2.4-d₄**, one of the *tert*-butyl groups in **2.4** exhibits packing disorder — the three methyl groups at C(2) thus had to be refined as two sets of half-methyls, approximately equally populated and related to each other by a 60° rotation about the C(1)–C(2) bond. This disorder, fortunately, has no effect on the atomic positions of the neopentyl methylene groups.

As illustrated in Figure 2.9, the neutron structure of **2.4** and the X-ray structure of **2.4-d₄** are very similar, differing significantly only in the extent by which the C(1)–H(1A) and C(6)–H(6B) bonds distort. Thus, as in **2.4-d₄** the neopentyl ligands in **2.4** are also distorted from regular tetrahedral geometry at C(1) and C(6). The W(1)–C(1)–C(2) angle and the

		2.4- <i>d</i> ₄	2.4
--	--	----------------------------	-----

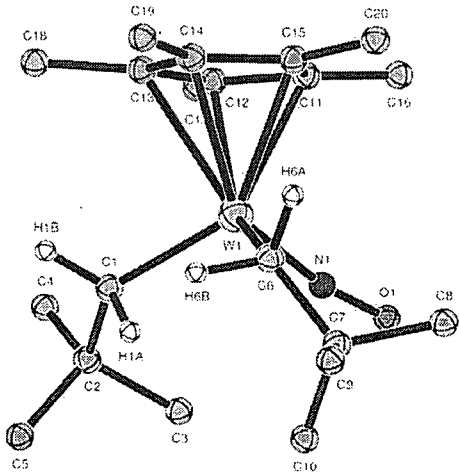
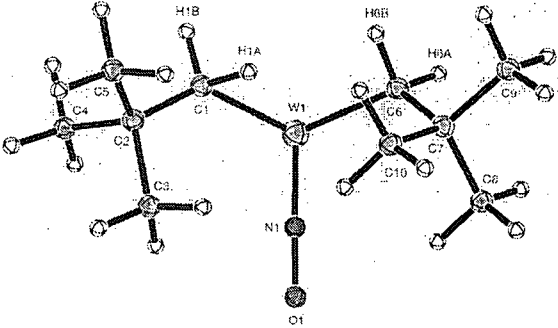
	W(1)–N(1)	1.752(9)	1.785(3)
	W(1)–C(1)	2.101(10)	2.110(3)
	W(1)–C(6)	2.169(8)	2.175(3)
	C(1)–C(2)	1.528(13)	1.538(3)
	C(6)–C(7)	1.482(13)	1.542(3)
	N(1)–O(1)	1.244(9)	1.228(3)
	W(1)···H(1A)	2.25(10)	2.233(6)
	W(1)···H(1B)	N/A	2.693(6)
	W(1)···H(6A)	N/A	2.745(6)
	W(1)···H(6B)	2.45(9)	2.582(6)
	C(1)–H(1A)	1.110	1.153(6)
	C(1)–H(1B)	0.839	1.070(8)
	C(6)–H(6A)	0.896	1.094(6)
	C(6)–H(6B)	1.042	1.083(7)
	W(1)–C(1)–C(2)	134.0(7)	133.4(2)
	W(1)–C(6)–C(7)	126.9(6)	125.4(2)
	W(1)–C(1)–H(1A)	82.1	80.6(3)
	W(1)–C(1)–H(1B)	101.4	111.5(3)
	W(1)–C(6)–H(6A)	102.2	109.7(3)
	W(1)–C(6)–H(6B)	94.1	99.3(3)
	H(1A)–C(1)–H(1B)	108.4	103.9(5)
	H(6A)–C(6)–H(6B)	104.2	103.6(5)
	W(1)–N(1)–O(1)	168.7(7)	169.1(2)
	N(1)–W(1)–C(1)	98.7(4)	99.4(2)
	N(1)–W(1)–C(6)	98.8(4)	99.42(14)
	C(1)–W(1)–C(6)	106.4(4)	106.48(14)

Figure 2.9. Two views of the neutron structure of Cp*W(NO)(CH₂CMe₃)₂ (**2.4**) along with selected bond distances and angles for **2.4** (neutron) and **2.4-*d*₄** (X-ray).

W(1)–C(1) distance are $133.4(2)^\circ$ and $2.110(3) \text{ \AA}$, respectively, and are essentially identical to those found in **2.4-d₄**. In contrast, the W(1)–C(6)–C(7) angle of $125.4(2)^\circ$ and the W(1)–C(6) distance of $2.175(3) \text{ \AA}$ are now only slightly outside the ranges observed in Cp*W(NO)(CH₂CMe₃)(NMe₂) (see Table 2.3 above) and (dmpe)W(≡CCMe₃)(=CHCMe₃)(CH₂CMe₃),⁴⁸ which do not contain an α -agostic neopentyl ligand.

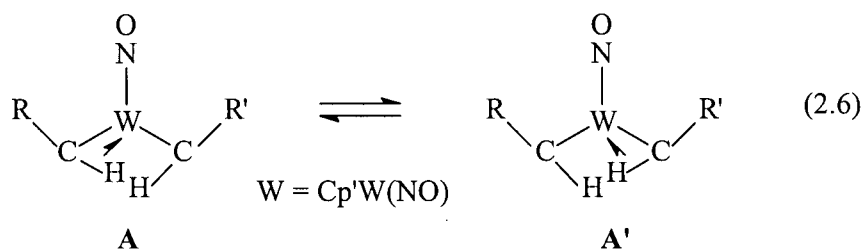
With regard to the four methylene hydrogens, the bonding parameters associated with H(1B) and H(6A) are unexceptional, as expected.⁴⁹ H(1A) and H(6B), on the other hand, are bent toward the metal center such that the W(1)–C(1)–H(1A) and W(1)–C(6)–H(6B) angles are significantly smaller and larger, respectively, than in **2.4-d₄**. The W(1)–C(6)–H(6B) angle is $99.3(3)^\circ$ and can be compared to analogous angles of $104.2(6)^\circ$ and $101.1(5)^\circ$ for the anagostic CH₂CMe₃ group in Cp*₂Th(CH₂CMe₃)₂,²² and $95.7(8)^\circ$ and $94.0(13)^\circ$ in Cp*La[CH(SiMe₃)₂]₂,⁵⁰ which does not exhibit α -agostic C–H interactions with the metal center. Consequently, the W(1)⋯H(6B) distance is $2.582(6) \text{ \AA}$, which is too long for there to be a genuine agostic interaction.⁵¹ Consistent with this contention, the C(6)–H(6B) bond does not lie in the plane containing the metal LUMO⁴⁴ [N(1)–W(1)–C(6)–H(6B) = $-132.6(4)^\circ$] and the C(6)–H(6B) distance is in the range expected for normal aliphatic C–H bonds.

In contrast to H(6B), the W(1)–C(1)–H(1A) angle is $80.6(3)^\circ$ and the W(1)⋯H(1A) distance is $2.233(6) \text{ \AA}$, which is only $\sim 0.34 \text{ \AA}$ longer than the average dihydrogen W–H distance ($1.89(1) \text{ \AA}$) in the neutron structure of W(CO)₃(P^{*i*}Pr₃)₂(η^2 -H₂).⁴⁷ An agostic interaction must be responsible for this short distance since both C(1) and H(1A) lie in the plane containing the metal LUMO [N(1)–W(1)–C(1)–H(1A) = $87.7(4)^\circ$] and since C(1)–H(1A) = $1.153(6) \text{ \AA}$, which is among the longest C–H bonds ever to be definitively characterized.^{1a,52} Thus, in contrast to the X-ray structure of **2.4-d₄** where the presence of two α -C–H⋯W interactions, one from each neopentyl ligand, is strongly suggested, the neutron structure of **2.4** establishes that only *one* such interaction, in fact, exists.

On the basis of the close similarity between the neutron structure of **2.4** and the X-ray structures of $\text{CpW(NO)(CH}_2\text{SiMe}_3)_2$ (**2.3**), $\text{Cp}^*\text{W(NO)(CH}_2\text{CMe}_3)(\text{CH}_2\text{SiMe}_3)$ (**2.9**), and $\text{Cp}^*\text{W(NO)(CH}_2\text{CMe}_3)(\text{C}_6\text{H}_3\text{-2,5-Me}_2)$ (**2.11'**), it can therefore be concluded that **2.3**, **2.9**, and **2.11'** each also contain only one α -agostic C–H interaction. The observation that the neopentyl ligands in **2.9** and **2.11'** are equally distorted compared to the agostic neopentyl ligand in **2.4** strongly suggests that *in the solid state* the agostic interactions in these three complexes are comparable in strength.

The $\alpha\text{-C-H}\cdots\text{W}$ interaction in **2.4** (and by analogy in **2.3**, **2.9**, and **2.11'**) is best described as a closed, three-center, two-electron bond and serves to give the electron-deficient tungsten center an effective closed-shell configuration. This finding implies that *in solution* the fluxional process illustrated in eq 2.6 is in fact responsible for the averaging of the alkyl ligands in **2.4** and in other $\text{Cp}'\text{W(NO)(R)(R')}$ bis(alkyl) complexes and that this exchange process is fast on the NMR time scale even at low temperatures. It also implies that, for a series of Cp^* complexes in which $\text{R} = \text{CH}_2\text{CMe}_3$ and $\text{R}' = \text{CH}_2\text{CMe}_3$, $\text{CH}_2\text{CMe}_2\text{Et}$, $\text{CH}_2\text{CMe}_2\text{Ph}$, or CH_2SiMe_3 , the observed $^1J_{\text{CH}}$ values for R and R' vary because of the change in position of this equilibrium depending on the nature of R'. That is, they change because R is a better α -agostic donor than R' and not because it binds more strongly than R'. Consistent with this new proposal, when

First, among all the alkyl ligands studied, the order of decreasing α -agostic donor ability is $\text{CH}_2\text{CMe}_3 \geq \text{CH}_2\text{CMe}_2\text{Et} > \text{CH}_2\text{CMe}_2\text{Ph} > \text{CH}_2\text{SiMe}_3$. Second, for a series of Cp^* complexes in which $\text{R} = \text{CH}_2\text{CMe}_3$ and $\text{R}' = \text{CH}_2\text{CMe}_3$, $\text{CH}_2\text{CMe}_2\text{Et}$, $\text{CH}_2\text{CMe}_2\text{Ph}$, or CH_2SiMe_3 , the degree of α -agosticity of R decreases as R' is changed from CH_2SiMe_3 to $\text{CH}_2\text{CMe}_2\text{Ph}$ to $\text{CH}_2\text{CMe}_2\text{Et}$ to CH_2CMe_3 . Third, for a series of Cp and Cp^* complexes in which $\text{R} = \text{R}'$, the agostic interactions in the Cp^* series are consistently stronger than those in the Cp analogues, a fact that can be ascribed to there being a greater degree of metal-to-C–H (σ^*) backbonding in the former complexes.



2.6 References and Notes

- (1) For reviews, see: (a) Brookhart, M.; Green, M. L. H. *J. Organomet. Chem.* **1983**, 250, 395. (b) Brookhart, M.; Green, M. L. H.; Wong, L.-L. *Prog. Inorg. Chem.* **1988**, 36, 1. (c) Crabtree, R. H.; Hamilton, D. G. *Adv. Organomet. Chem.* **1988**, 28, 299. (d) Crabtree, R. H. *Angew. Chem. Int. Ed. Engl.* **1993**, 32, 789.
- (2) LaPlaca, S. J.; Ibers, J. A. *Inorg. Chem.* **1965**, 4, 778.
- (3) Bailey, N. A.; Jenkins, J. M.; Mason, R.; Shaw, B. L. *J. Chem. Soc. Chem. Comm.* **1965**, 237.
- (4) Trofimenko, S. *J. Am. Chem. Soc.* **1967**, 89, 6288.
- (5) (a) Cotton, F. A.; Stanislawski, A. G. *J. Am. Chem. Soc.* **1974**, 96, 5074. (b) Burger, B. J.; Thompson, M. E.; Cotter, W. D.; Bercaw, J. E. *J. Am. Chem. Soc.* **1990**, 112, 1566.
- (6) (a) Kawamura-Kuribayashi, H.; Koga, N.; Morokuma, K. *J. Am. Chem. Soc.* **1992**, 114, 2359. (b) Lohrenz, J. C. W.; Woo, T. K.; Ziegler, T. *J. Am. Chem. Soc.* **1995**, 117, 12793. (c) Margl, P.; Lohrenz, J. C. W.; Ziegler, T.; Blochl, P. E. *J. Am. Chem. Soc.* **1996**, 118, 4434.
- (7) Eisenstein, O.; Jean, Y. *J. Am. Chem. Soc.* **1985**, 107, 1177.

- (8) For examples, see: (a) Lamanna, W.; Brookhart, M. *J. Am. Chem. Soc.* **1981**, *103*, 989. (b) Lamanna, W.; Brookhart, M.; Humphrey, M. B. *J. Am. Chem. Soc.* **1982**, *104*, 2117. (c) Crabtree, R. H.; Lavin, M. *J. Chem. Soc., Chem. Commun.* **1985**, 794. (d) Kanamori, K.; Broderick, W. E.; Jordan, R. F.; Willett, R. D.; Legg, J. I. *J. Am. Chem. Soc.* **1986**, *108*, 7122. (e) Vigalok, A.; Uzan, O.; Shimon, L. J. W.; Ben-David, Y.; Martin, J. M. L.; Milstein, D. *J. Am. Chem. Soc.* **1998**, *120*, 12539.
- (9) For reviews, see: (a) ref. 1. (b) Hall, C.; Perutz, R. N. *Chem. Rev.* **1996**, *96*, 3125.
- (10) (a) Turner, H. W.; Schrock, R. R. *J. Am. Chem. Soc.* **1982**, *104*, 2331. (b) Turner, H. W.; Schrock, R. R.; Fellman, J. D.; Holmes, S. J. *J. Am. Chem. Soc.* **1983**, *105*, 4942.
- (11) Blomberg, M. R. A.; Brandemark, U.; Siegbahn, P. E. M. *J. Am. Chem. Soc.* **1983**, *105*, 5557.
- (12) Grubbs, R. H.; Coates, G. W. *Acc. Chem. Res.* **1996**, *29*, 85.
- (13) Piers, W. E.; Bercaw, J. E. *J. Am. Chem. Soc.* **1990**, *112*, 9406.
- (14) Katz, T. J.; Sivavec, T. M. *J. Am. Chem. Soc.* **1985**, *107*, 737.
- (15) (a) Legzdins, P.; Sayers, S. F. *Organometallics* **1996**, *15*, 3907. (b) Legzdins, P.; Sayers, S. F. *Chem. Eur. J.* **1997**, *3*, 1579.
- (16) Tran, E.; Legzdins, P. *J. Am. Chem. Soc.* **1997**, *119*, 5071.
- (17) Legzdins, P.; Veltheer, J. E. *Acc. Chem. Res.* **1993**, *26*, 41, and references therein.
- (18) Mena, M.; Pellinghelli, M. A.; Royo, P.; Serrano, R.; Tiripicchio, A. *J. Chem. Soc., Chem. Commun.* **1996**, 1118.
- (19) (a) Huang, D.; Streib, W. E.; Eisenstein, O.; Caulton, K. G. *Angew. Chem. Int. Ed. Engl.* **1997**, *36*, 2004. (b) Cooper, A. C.; Streib, W. E.; Eisenstein, O.; Caulton, K. G. *J. Am. Chem. Soc.* **1997**, *119*, 9069. (c) Ujaque, G.; Cooper, A. C.; Maseras, F.;

- Eisenstein, O.; Caulton, K. G. *J. Am. Chem. Soc.* **1998**, *120*, 361. (d) Huang, D.; Streib, W. E.; Bollinger, J. C.; Caulton, K. G.; Winter, R. F.; Scheiring, T. *J. Am. Chem. Soc.* **1999**, *121*, 8087.
- (20) van der Heijden, H.; Schaverien, C. J.; Orpen, A. G. *Organometallics* **1989**, *8*, 255.
- (21) Jeske, G.; Lauke, H.; Mauermann, J.; Swepston, P. N.; Schumann, H.; Marks, T. J. *J. Am. Chem. Soc.* **1985**, *107*, 8091.
- (22) Bruno, J. W.; Smith, G. M.; Marks, T. J.; Fair, C. K.; Schultz, A. J.; Williams, J. M. *J. Am. Chem. Soc.* **1986**, *108*, 40.
- (23) Poole, A. D.; Williams, D. N.; Kenwright, A. M.; Gibson, V. C.; Clegg, W.; Hockless, D. C. R.; O'Neil, P. A. *Organometallics* **1993**, *12*, 2549.
- (24) Warren, T. H.; Schrock, R. R.; Davis, W. M. *J. Organomet. Chem.* **1998**, *569*, 125.
- (25) Cole, J. M.; Gibson, V. C.; Howard, J. A. K.; McIntyre, G. J.; Walker, G. L. P. *Chem. Commun.* **1998**, 1829.
- (26) Dryden, N. H.; Legzdins, P.; Trotter, J.; Yee, V. C. *Organometallics* **1991**, *10*, 2857.
- (27) Legzdins, P.; Rettig, S. J.; Sánchez, L. *Organometallics* **1988**, *7*, 2394.
- (28) Debad, J. D.; Legzdins, P.; Rettig, S. J.; Veltheer, J. E. *Organometallics* **1993**, *12*, 2714.
- (29) Dryden, N. H.; Legzdins, P.; Rettig, S. J.; Veltheer, J. E. *Organometallics* **1992**, *11*, 2583.
- (30) Debad, J. D.; Legzdins, P.; Batchelor, R. J.; Einstein, F. W. B. *Organometallics* **1993**, *12*, 2094.
- (31) Although their identities have not yet been unambiguously established, the side-products based on their brown and forest green colors are presumably the bridging

nitrido complexes, $\text{Cp}^*\text{W}(\text{NO})(\text{Cl})(\mu\text{-N})[\text{Cp}^*\text{W}(=\text{O})\text{Cl}]^{29\text{a}}$ and $\text{Cp}^*\text{W}(\text{NO})(\text{CH}_2\text{CMe}_3)(\mu\text{-N})[\text{Cp}^*\text{W}(=\text{O})\text{Cl}]^{29\text{b}}$ formed by reduction of the starting material and the mono(alkyl) intermediate, $\text{Cp}^*\text{W}(\text{NO})\text{Cl}_2$ and $\text{Cp}^*\text{W}(\text{NO})(\text{CH}_2\text{CMe}_3)\text{Cl}$, respectively. See: (a) Legzdins, P.; Ross, K. J.; Sayers, S. F.; Rettig, S. J. *Organometallics* **1997**, *16*, 190. (b) Debad, J. D.; Legzdins, P.; Reina, R.; Young, M. A.; Batchelor, R. J.; Einstein, F. W. B. *Organometallics* **1994**, *13*, 4315.

- (32) Wood, C. D.; McLain, S. J.; Schrock, R. R. *J. Am. Chem. Soc.* **1978**, *101*, 3210.
- (33) In principle, the coupling between the upfield protons to tungsten and to each other could also be considered as one-bond and three-bond couplings, respectively, owing to the agostic interactions. However, such consideration would be misleading because true one-bond tungsten-hydrogen couplings in $\text{Cp}^*\text{W}(\text{NO})$ -containing complexes are all >100 Hz,³³ while three-bond $^1\text{H}\text{--}^1\text{H}$ couplings across a transition-metal center are typically >7 Hz.^{33\text{a}}} Furthermore, that the long-range $^1\text{H}\text{--}^1\text{H}$ coupling could be due to W (the letter, *not* tungsten) coupling can also be ruled out, since such couplings are usually >3 Hz for cyclic systems and <0.5 Hz for acyclic ones.^{33\text{b}}} (a) Wenzel, T. T.; Bergman, R. G. *J. Am. Chem. Soc.* **1986**, *108*, 4856. (b) For a comprehensive review, see: Barfield, M.; Chakrabarti, B. *Chem. Rev.* **1969**, *69*, 757.
- (34) (a) See chapters 3 and 4 of this thesis. (b) Legzdins, P.; Martin, J. T.; Oxley, J. C. *Organometallics* **1985**, *4*, 1263.
- (35) Messerle, L. W.; Jennische, P.; Schrock, R. R.; Stucky, G. *J. Am. Chem. Soc.* **1980**, *102*, 6744.
- (36) van der Heijden, H.; Gal, A. W.; Pasman, P.; Orpen, A. G. *Organometallics* **1985**, *4*, 1847.
- (37) Procopio, L. J.; Carroll, P. J.; Berry, D. H. *J. Am. Chem. Soc.* **1994**, *116*, 177.

- (38) Fellmann, J. D.; Schrock, R. R.; Traficante, D. D. *Organometallics* **1982**, *1*, 481.
- (39) Fellmann, J. D.; Schrock, R. R.; Rupprecht, G. A. *J. Am. Chem. Soc.* **1981**, *103*, 5752.
- (40) Schultz, A. J.; Brown, R. K.; Williams, J. M.; Schrock, R. R. *J. Am. Chem. Soc.* **1981**, *103*, 169, and references therein.
- (41) Dawoodi, Z.; Green, M. L. H.; Mtetwa, V. S. B.; Prout, K.; Schultz, A. J.; Williams, J. M.; Koetzle, T. F. *J. Chem. Soc. Dalton Trans.* **1986**, 1629.
- (42) Etienne, M.; Mathieu, R.; Donnadieu, B. *J. Am. Chem. Soc.* **1997**, *119*, 3218.
- (43) Legzdins, P.; Jones, R. H.; Phillips, E. C.; Yee, V. C.; Trotter, J.; Einstein, F. W. B. *Organometallics* **1991**, *10*, 1002.
- (44) (a) Legzdins, P.; Rettig, S. J.; Sánchez, L.; Bursten, B. E.; Gatter, M. G. *J. Am. Chem. Soc.* **1985**, *107*, 1411. (b) Bursten, B. E.; Cayton, R. H. *Organometallics* **1987**, *6*, 2004.
- (45) Lauer, J. W.; Hoffmann, R. *J. Am. Chem. Soc.* **1976**, *98*, 1729.
- (46) Green, M. L. H. In *Organometallic Compounds*, 3rd ed; Methuen and Co. Ltd.: London, 1968, Vol. 2, pp 90–164.
- (47) Kubas, G. J. *Acc. Chem. Res.* **1988**, *21*, 120.
- (48) Churchill, M. R.; Youngs, W. J. *Inorg. Chem.* **1979**, *18*, 2454.
- (49) (a) Kuchitsu, K. *J. Chem. Phys.* **1968**, *49*, 4456. (b) Bartell, M. S.; Kuchitsu, K.; De Neui, R. J. *J. Chem. Phys.* **1965**, *35*, 1211.
- (50) (a) Klooster, W. T.; Brammer, L.; Schaverien, C. J.; Budzelaar, P. H. M. *J. Am. Chem. Soc.* **1999**, *121*, 1381. (b) Schaverien, C. J.; Budzelaar, P. H. M., private communication.

- (51) For comparison, the agostic $\text{CH}\cdots\text{W}$ distance in $\text{W}(\text{CO})_3(\text{PCy}_3)_2$ is about 2.27 \AA^{51a} and the agostic $\text{CH}\cdots\text{Mo}$ distance in $[\text{Et}_2\text{B}(\text{pz})_2][\eta^3\text{-CH}_2\text{C}(\text{Ph})\text{CH}_2](\text{CO})_2\text{Mo}$ appears to be $2.27(8) \text{ \AA}$ and possibly as short as about 2.15 \AA^{51b} : (a) Wasserman, H. J.; Kubas, G. J.; Ryan, R. R. *J. Am. Chem. Soc.* **1986**, *108*, 2294. (b) Cotton, F. A.; LaCour, T.; Stanislawski, A. G. *J. Am. Chem. Soc.* **1974**, *96*, 754.
- (52) Brown, R. K.; Williams, J. M.; Schultz, A. J.; Stucky, G. D.; Ittel, S. D.; Harlow, R. L. *J. Am. Chem. Soc.* **1980**, *102*, 981.

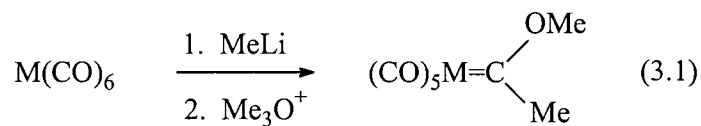
CHAPTER 3

Thermolysis of $\text{Cp}'\text{W}(\text{NO})(\text{CH}_2\text{CMe}_3)_2$ and $\text{Cp}^*\text{W}(\text{NO})(\text{CH}_2\text{CMe}_3)(\text{CH}_2\text{Ph})$ Complexes: Generation and Trapping Reactions of $[\text{Cp}'\text{W}(\text{NO})(=\text{CHCMe}_3)]$ and $[\text{Cp}^*\text{W}(\text{NO})(=\text{CHPh})]$ Intermediates

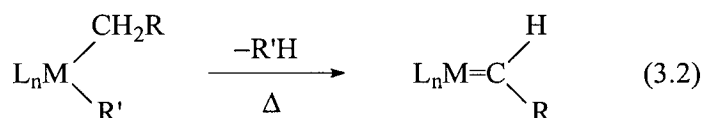
3.1 Introduction	54
3.2 Experimental Section	57
3.3 Results and Discussion	71
3.4 Epilogue	96
3.5 References and Notes	100

3.1 Introduction

The first transition-metal complexes to contain a direct metal-carbon double bond were prepared in the mid-1960s.¹ Since then, thousands have been reported and, in general, tend to fall into one of three distinct classes based on their mode of reactivity. The first two classes are complexes called Fischer-type carbenes² and Schrock-type alkylidenes,³ named after their discoverers. Fischer-type carbene complexes are mostly generated by alkylation of a metal-bound carbonyl ligand (eq 3.1), are electrophilic, and have found widespread utility in the cyclopropanation of alkenes.⁴ In addition, the metal in these complexes is usually in a low oxidation state, while the carbene carbon is often stabilized by a heteroatom.



Schrock-type alkylidene complexes, on the other hand, are nucleophilic and are prepared almost exclusively by α -hydrogen abstraction routes (eq 3.2).⁵ They are also key intermediates in numerous important stoichiometric and catalytic transformations. These include formation of metallacycles via 2+2 cycloaddition reactions with unsaturated organic substrates,³ alkene metathesis,⁶ ring-opening metathesis polymerization,⁷ acyclic diene⁸ and alkyne⁹ polymerizations, ring-closing metathesis,¹⁰ and carbonyl olefinations.¹¹



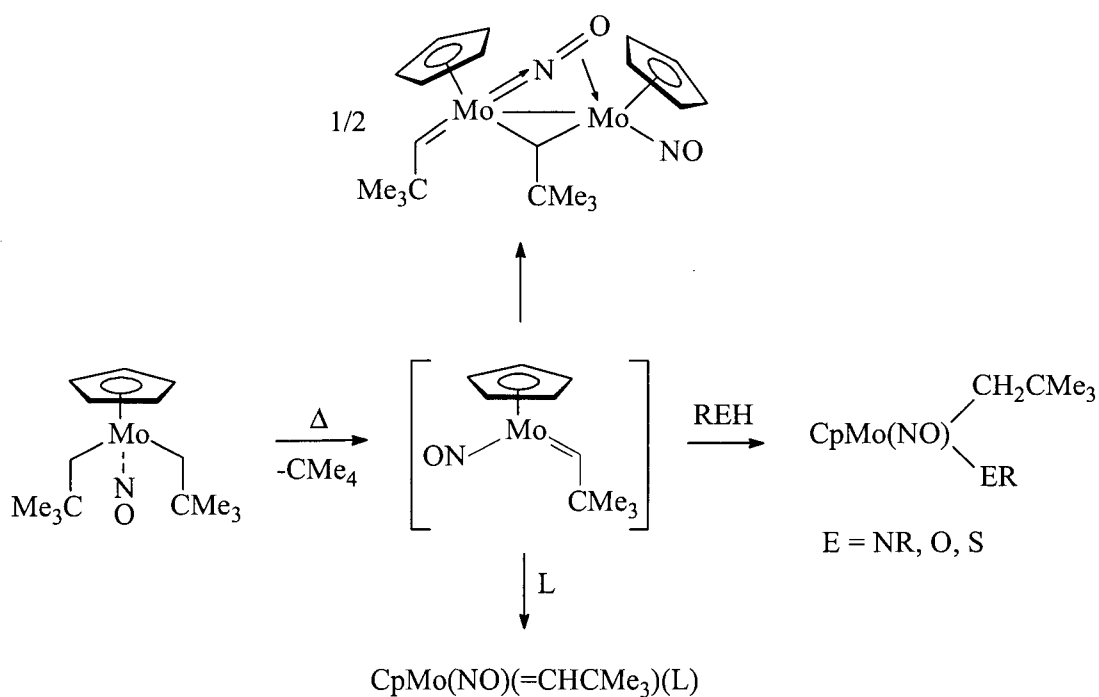
The difference in the chemical reactivity between Fischer carbene and Schrock alkylidene complexes can be attributed to a difference in the bonding within their metal-carbon double bonds.¹² In Fischer carbene complexes, this bonding is a composite of electron donation from a doubly occupied orbital on the carbene ligand and a π -back-donation from a filled metal d orbital. The M=C bond in alkylidene complexes, in contrast, is best considered in terms of an ethylene-like covalent interaction (i.e. one in which the electrons are nearly equally distributed between the metal fragment and the alkylidene moiety).

Finally, the third class of M=C complexes is amphiphilic, reacting as both electrophiles and nucleophiles. Examples include $(\text{CO})_2(\text{Ph}_3\text{P})_2\text{Ru}(=\text{CF}_2)$,¹³ which reacts with HCl and CH_3NH_2 to give $(\text{CO})_2(\text{Ph}_3\text{P})_2\text{Ru}(\text{CF}_2\text{H})\text{Cl}$ and $(\text{CO})_2(\text{Ph}_3\text{P})_2\text{Ru}(\text{CNCH}_3)$, respectively, and $\text{Cp}(\text{CO})_2\text{Re}(=\text{CHCH}_2\text{CH}_2\text{CMe}_3)$,¹⁴ which reacts with HCl and PMe_3 to produce $\text{Cp}(\text{CO})_2\text{Re}(\text{CH}_2\text{CH}_2\text{CH}_2\text{CMe}_3)\text{Cl}$ and zwitterionic $\text{Cp}(\text{CO})_2\text{Re}[\text{CH}(\text{PMe}_3)\text{CH}_2\text{CH}_2\text{CMe}_3]$.

The investigation into M=C complexes by the Legzdins group began in the early 1990s with the discovery that the molybdenum bis(alkyl) complex, $\text{CpMo}(\text{NO})(\text{CH}_2\text{CMe}_3)_2$, decomposes at room temperature to give a bimetallic species with a unique bridging $\eta^1:\eta^2\text{-NO}$ ligand (Scheme 3.1).¹⁵ The reaction presumably proceeds via α -elimination of neopentane and formation of the putative complex $\text{CpMo}(\text{NO})(=\text{CHCMe}_3)$. Although this 16-electron

intermediate exists only transiently, it can be trapped by coordination to various Lewis bases. It can also add heteroatom-hydrogen bonds to its Mo=C linkage in manner consistent with it being nucleophilic at carbon.¹⁶

Scheme 3.1



Subsequent to the discovery of the molybdenum neopentylidene system, anionic alkylidene complexes of the type $[\text{Cp}^*\text{M(NO)(=CHSiMe}_3\text{)(CH}_2\text{SiMe}_3)]^-\text{M}'^+$ [$\text{M} = \text{Mo, W}$; $\text{M}' = \text{Na, Li}$] have been prepared by deprotonation of an alkyl ligand of $\text{Cp}^*\text{M(NO)(CH}_2\text{SiMe}_3)_2$.¹⁷ While these 18-electron compounds exhibit interesting structures, their chemistry, unfortunately, has been limited to only protonation reactions that lead to the starting material.

As a continuation of the development of unsaturated alkylidene complexes containing the $\text{Cp}^*\text{M(NO)}$ fragment, the thermal decompositions of a series of tungsten bis(alkyl)

complexes of the type $\text{Cp}'\text{W}(\text{NO})(\text{CH}_2\text{CMe}_3)(\text{R})$, where $\text{Cp}' = \text{Cp}$ or Cp^* and $\text{R} = \text{CH}_2\text{CMe}_3$, $\text{CH}_2\text{CMe}_2\text{Et}$, $\text{CH}_2\text{CMe}_2\text{Ph}$, CH_2SiMe_3 , CH_3 , Ph , or CH_2Ph , have been investigated. Of these compounds, the neopentyl complexes $\text{Cp}'\text{W}(\text{NO})(\text{CH}_2\text{CMe}_3)_2$ and $\text{Cp}^*\text{W}(\text{NO})(\text{CH}_2\text{CMe}_3)(\text{CH}_2\text{Ph})$ have been found to undergo α -abstraction to generate neopentane and the transient alkylidene complexes $[\text{Cp}'\text{W}(\text{NO})(=\text{CHCMe}_3)]$ and $[\text{Cp}^*\text{W}(\text{NO})(=\text{CHPh})]$, respectively. The decompositions of the remaining complexes, in contrast, are complicated by alternative and/or competing reactions, each of which will be discussed in subsequent chapters of this thesis.

In the present chapter several aspects of the chemistry of the above unsaturated tungsten(II) alkylidene complexes, which have allowed the similarities and differences between the molybdenum and tungsten systems and the Cp and Cp^* systems to be established, are described. These include (1) the trapping reactions of these species with Lewis bases, (2) the reactions of the neopentylidene species and their PMe_3 adducts with substrates containing heteroatom-hydrogen bonds, and (3) the reactions of the Cp^* neopentylidene intermediate with cyclic and acyclic alkenes, which in an unprecedented manner lead not only to novel 2+2 cycloaddition complexes but also to a wide range of structurally diverse C–H bond-activation products. The ability of the neopentylidene species $[\text{Cp}^*\text{W}(\text{NO})(=\text{CHCMe}_3)]$ to activate alkane C–H bonds has recently been reported,¹⁸ full details of this chemistry are described in Chapters 4 and 5.

3.2 Experimental Section

3.2.1 Methods

The synthetic methodologies employed throughout this thesis are described in detail in section 2.2.1. GC-MS analyses were performed by Ms. L. Madilao of the UBC mass spectrometry facility using a Carlo Erba GC and Kratos MS-80 unit. Unless otherwise noted all thermolyses were carried out in thick-walled glass vessels or J. Young NMR tubes immersed in an oil bath at 60–70 °C for ca. 1.5–2 d.

3.2.2 Reagents

The complexes $\text{CpW}(\text{NO})(\text{CH}_2\text{CMe}_3)_2$ (**2.1**), $\text{Cp}^*\text{W}(\text{NO})(\text{CH}_2\text{CMe}_3)_2$ (**2.4**), and $\text{Cp}^*\text{W}(\text{NO})(\text{CH}_2\text{CMe}_3)(\text{CH}_2\text{Ph})$ (**2.15**) were prepared as described in Section 2.2.1. PMe_3 , PMe_2Ph , PEt_3 , $\text{P}(\text{OMe})_3$, EtNMe_2 , Et_3N , neohexene, 2-methyl-1-butene, 2-methyl-2-butene, cyclopentene (Aldrich), ethylcyclopentene (Wiley Organics), and norbornadiene (Eastman Kodak) were dried over sodium and vacuum-transferred prior to use. Acetonitrile and *tert*-butylnitrile (Aldrich) were distilled from CaH_2 . Pyridine (BDH) and methanol (Aldrich) were dried over activated 4-Å molecular sieves. Me_2NH (99.9%, Aldrich) was used as received. Benzoic acid (Fisher) was recrystallized from hexanes, and then dried under vacuum at room temperature.

3.2.3 Preparation of $\text{Cp}'\text{W}(\text{NO})(=\text{CHCMe}_3)(\text{L})$ Complexes [$\text{Cp}' = \text{Cp}$, $\text{L} = \text{PMe}_3$ (**3.1**), PEt_3 (**3.2**), $\text{P}(\text{OMe})_3$ (**3.3**); $\text{Cp}' = \text{Cp}^*$, $\text{L} = \text{PMe}_3$ (**3.4**), PMe_2Ph (**3.5**), PEt_3 (**3.6**), $\text{P}(\text{OMe})_3$ (**3.7**)]

Complexes **3.1–3.7** were prepared in a similar manner using the appropriate Lewis base. An exception is that the thermolyses for the preparation of the Cp complexes were carried out at ca. 65 °C for 1 d, while those for the Cp^* series were effected at ca. 75 °C for 2 d. The preparation of **3.4** is described as a representative example. To a Pyrex bomb containing **2.4** (172 mg, 0.350 mmol) were added sequentially THF (2 mL) and PMe_3 (>10 equiv) by vacuum transfer. The resulting wine-red mixture was heated at 75 °C for 2 d, during which time it became a yellow-brown solution. Next, the organic volatiles were removed in vacuo, and the residue was extracted with 4:1 hexanes/ Et_2O (10 mL). The extracts were filtered through Celite (1 × 1 cm), which was washed with additional 4:1 hexanes/ Et_2O until the filtrate was colorless. Diminishing the volume of the combined filtrates in vacuo, followed by cooling to –30 °C for 2 d afforded **3.4** (147 mg, 85 % yield) as yellow plates.

3.2.3.1 Complex 3.1 was isolated as dark yellow blocks (93% yield) from Et_2O at –30 °C.

Anal. Calcd. for $C_{13}H_{24}NOPW$: C, 36.72; H, 5.69; N, 3.29. Found: C, 36.89; H, 5.84; N, 3.19. IR (cm^{-1}) ν_{NO} 1520 (s). MS 425 [M^+ , ^{184}W]. 1H NMR (300 MHz, C_6D_6) δ 1.09 (d, $^2J_{HP} = 9.6$, 9H, PMe_3), 1.43 (s, 9H, CMe_3), 5.26 (d, $J_{HP} = 1.2$, 5H, C_5H_5). $^{13}C\{^1H\}$ NMR (75 MHz, C_6D_6) δ 21.0 (d, $^1J_{CP} = 34$, PMe_3), 32.1 (CMe_3), 52.7 (CMe_3), 96.4 (C_5H_5).

3.2.3.2 Complex 3.2 was isolated as pale yellow clusters (57% yield) from 1:5 hexanes/ Et_2O at $-30^\circ C$.

Anal. Calcd. for $C_{16}H_{30}NOPW$: C, 41.13; H, 6.47; N, 3.00. Found: C, 41.28; H, 6.41; N, 3.01. IR (cm^{-1}) ν_{NO} 1514 (s). MS 467 [M^+ , ^{184}W]. 1H NMR (300 MHz, $CDCl_3$) δ 1.02 (m, 9H, CH_2CH_3), 1.12 (s, 9H, CMe_3), 1.6–1.9 (m, 6H, CH_2CH_3), 5.62 (d, $J_{HP} = 0.9$, 5H, C_5H_5). $^{13}C\{^1H\}$ NMR (75 MHz, $CDCl_3$) δ 7.9 (CH_2CH_3), 21.6 (d, $^1J_{CP} = 31$, CH_2CH_3), 31.6 (CMe_3), 52.4 (CMe_3), 96.5 (C_5H_5).

3.2.3.3 Complex 3.3. The formation of this complex in THF was not clean. A black precipitate also formed, which was removed by filtration through alumina I (1×1 cm). The filtrate was then concentrated in vacuo to obtain relatively pure **3.3** as judged by 1H NMR spectroscopy.

1H NMR (300 MHz, $CDCl_3$) δ 1.14 (s, 9H, CMe_3), 3.57 (d, $^3J_{HP} = 12.0$, 9H, OCH_3), 5.70 (d, $J_{HP} = 1.2$, 5H, C_5H_5). $^{13}C\{^1H\}$ NMR (75 MHz, $CDCl_3$) δ 30.9 (CMe_3), 52.0 (CMe_3), 52.3 (OCH_3), 96.8 (C_5H_5).

3.2.3.4 Complex 3.4. Anal. Calcd. for $C_{18}H_{34}NOPW$: C, 43.65; H, 6.92; N, 2.83. Found: C, 43.62; H, 7.00; N, 2.78. IR (cm^{-1}) ν_{NO} 1513 (s). MS 495 [M^+ , ^{184}W]. 1H NMR (300 MHz, C_6D_6) δ 1.06 (d, $^2J_{HP} = 9.0$, 9H, PMe_3), 1.43 (s, 9H, CMe_3), 1.87 (s, 15H, C_5Me_5). $^{13}C\{^1H\}$ NMR (75 MHz, C_6D_6) δ 11.0 (C_5Me_5), 19.7 (d, $^1J_{CP} = 32$, PMe_3), 32.0 (CMe_3), 52.2 (CMe_3), 106.3 (C_5Me_5).

3.2.3.5 Complex 3.5 is highly soluble in hydrocarbon solvents, but can be isolated as a tan solid by storing a concentrated pentane/Et₂O mixture at -30 °C for 1–2 months. The purity of this material, however, was ca. 90% at best.

IR (cm⁻¹) 1509 (s). MS 557 [M⁺, ¹⁸⁴W]. ¹H NMR (300 MHz, CD₂Cl₂) δ 1.15 (s, 9H, CMe₃), 1.82 (s, 15H, C₅Me₅), 1.72 (s, 3H, PMe₂), 1.75 (s, 3H, PMe₂), 7.4 (m, 5H, Ph). ¹³C{¹H} NMR (75 MHz, CD₂Cl₂) δ 10.6 (C₅Me₅), 19.9 (PMeMe), 20.4 (PMeMe), 31.5 (CMe₃), 32.6 (CMe₃), 107.0 (C₅Me₅), 128.8 (d, *J*_{CP} = 10, C_{o/m}), 130.2 (C_p), 130.9 (d, *J*_{CP} = 11, C_{o/m}), 136.9 (C_{ipso}).

3.2.3.6 Complex 3.6 was isolated as pale yellow blocks (74% yield) from a 3:1 mixture of hexanes/Et₂O at -30 °C.

Anal. Calcd. for C₂₁H₄₀NOPW: C, 46.94; H, 7.50; N, 2.61. Found: C, 47.34; H, 7.50; N, 2.81. IR (cm⁻¹) ν_{NO} 1527 (s). MS 537 [M⁺, ¹⁸⁴W]. ¹H NMR (500 MHz, CDCl₃) δ 0.76 (pent, ³*J*_{HH} = 7.6, ²*J*_{HP} = 9.0, 9H, CH₂CH₃), 1.43 (m, 6H, CH₂CH₃), 1.87 (s, 15H, C₅Me₅). ¹³C{¹H} NMR (75 MHz, CDCl₃) δ 7.6 (CH₂CH₃), 10.9 (C₅Me₅), 19.0 (d, ¹*J*_{CP} = 29, CH₂CH₃), 31.7 (CMe₃), 52.2 (CMe₃), 106.3 (C₅Me₅).

3.2.3.7 Complex 3.7 was isolated as pale yellow plates (51% yield) from a 3:1 mixture of hexanes/Et₂O at -30 °C.

Anal. Calcd. for C₁₈H₃₄NO₄PW: C, 39.79; H, 6.31; N, 2.58. Found: C, 39.67; H, 6.33; N, 2.53. IR (cm⁻¹) ν_{NO} 1527 (s). MS 543 [M⁺, ¹⁸⁴W]. ¹H NMR (300 MHz, CDCl₃) δ 1.12 (s, 9H, CMe₃), 2.02 (s, 15H, C₅Me₅), 3.50 (d, ³*J*_{HP} = 11.7, 9H, P(OMe)₃). ¹³C{¹H} NMR (75 MHz, CDCl₃) δ 10.6 (C₅Me₅), 31.1 (CMe₃), 51.8 (OMe), 52.6 (CMe₃), 107.3 (C₅Me₅).

3.2.4 Preparation of $\text{Cp}^*\text{W}(\text{NO})(=\text{CHCMe}_3)(\text{NEtMe}_2)$ (**3.8**)

A wine-red solution of **2.4** (62 mg, 0.13 mmol) in EtNMe_2 (2 mL) was heated in the dark at 70 °C for 2 d, during which time it became brown-yellow. In the presence of room light, the organic volatiles were removed in vacuo to obtain a brown oil which was redissolved in hexanes (2 mL) and filtered through Celite (1 × 1 cm). The filtrate was concentrated and then cooled at -30 °C for several days to induce the deposition of **3.8** as dark yellow crystals (22 mg, 35% yield).

Anal. Calcd. for $\text{C}_{19}\text{H}_{36}\text{N}_2\text{OW}$: C, 46.35; H, 7.37; N, 5.69. Found: C, 46.08; H, 7.44; N, 5.66. IR (cm^{-1}) ν_{NO} 1512 (s). MS 492 [M^+ , ^{184}W]. ^1H NMR (300 MHz, C_6D_6) δ 0.75 (t, $^3J_{\text{HH}} = 7.4$, 3H, CH_2CH_3), 1.55 (s, 9H, CMe_3), 1.80 (s, 15H, C_5Me_5), 2.00 (m, 2H, CH_2CH_3), 2.30 (s, 3H, NMe), 2.40 (s, 3H, NMe). $^{13}\text{C}\{^1\text{H}\}$ NMR (75 MHz, C_6D_6) δ 10.8 (C_5Me_5), 11.3 (CH_2CH_3), 33.0 (CMe_3), 33.9 (CMe_3), 55.8 (NMe), 56.9 (NMe), 60.7 (CH_2CH_3), 106.8 (C_5Me_5).

3.2.5 Preparation of $\text{Cp}^*\text{W}(\text{NO})(=\text{CHCMe}_3)(\text{Py})$ (**3.9**)

In a manner similar to the preparation of **3.8**, a solution of **2.4** (56 mg, 0.11 mmol) in pyridine (3 mL) was heated in the dark at 70 °C for 2 d, during which time it became orange-brown. In the presence of light, the organic volatiles were removed in vacuo to obtain a brown oil which was extracted into Et_2O (1 mL) and then cooled to -30 °C. Orange-brown crystals of **3.9** formed after 1 d (15 mg, 27% yield) and were isolated by removing the mother liquor with a pipet.

Anal. Calcd. for $\text{C}_{20}\text{H}_{30}\text{N}_2\text{OW}$: C, 48.20; H, 6.07; N, 5.62. Found: C, 48.13; H, 5.97; N, 5.47. IR (cm^{-1}) ν_{NO} 1551 (s). MS 498 [M^+ , ^{184}W]. ^1H NMR (300 MHz, C_6D_6) δ 1.63 (s, 9H, CMe_3), 1.79 (s, 15H, C_5Me_5), 6.08 (pseudo t, $^3J_{\text{CH}} = 6.4$, 2H, H_m), 6.48 (t, $^3J_{\text{HH}} = 8.5$, 1H, H_p), 8.29 (d, $^3J_{\text{HH}} = 6.5$, 2H, H_o). $^{13}\text{C}\{^1\text{H}\}$ NMR (75 MHz, C_6D_6) δ 10.4 (C_5Me_5), 33.9 (CMe_3), 49.0 (CMe_3), 107.3 (C_5Me_5), 124.6 ($\text{C}_{o/m}$), 136.3 (C_p), 156.1 ($\text{C}_{o/m}$).

3.2.6 Preparation of $\text{Cp}^*\text{W}(\text{NO})(=\text{CHPh})(\text{PMe}_3)$ (**3.10**)

Complex **3.10** was prepared from $\text{Cp}^*\text{W}(\text{NO})(\text{CH}_2\text{CMe}_3)(\text{CH}_2\text{Ph})$ in a manner analogous to that described for the preparation of $\text{Cp}^*\text{W}(\text{NO})(=\text{CHCMe}_3)(\text{PMe}_3)$. It was crystallized from 5:1 $\text{Et}_2\text{O}/\text{THF}$ at $-30\text{ }^\circ\text{C}$ and isolated as brown-orange rods (65% yield, 2 crops).

Anal. Calcd. for $\text{C}_{20}\text{H}_{30}\text{NOPW}$: C, 46.62; H, 5.87; N, 2.72. Found: C, 46.42; H, 5.69; N, 2.95. MS 515 $[\text{M}^+, ^{184}\text{W}]$. ^1H NMR (400 MHz, CD_2Cl_2) δ 1.34 (d, $^2J_{\text{HP}} = 8.7$, 9H, PMe_3), 2.12 (s, 15H, C_5Me_5), 7.03 (t, $^3J_{\text{HH}} = 7.3$, 1H, H_p), 7.22 (t, $^3J_{\text{HH}} = 7.6$, 2H, H_m), 7.56 (d, $^3J_{\text{HH}} = 7.6$, 2H, H_o). $^{13}\text{C}\{^1\text{H}\}$ NMR (75 MHz, CD_2Cl_2) δ 11.1 (C_5Me_5), 17.6 (d, $^1J_{\text{CP}} = 34$, PMe_3), 108.4 (C_5Me_5), 125.5 (C_p), 128.4 (C_m), 128.8 (C_o), 154.1 (d, $^3J_{\text{CP}} = 4$, C_{ipso}).

3.2.7 Attempted Trapping of $[\text{Cp}^*\text{W}(\text{NO})(=\text{CHCMe}_3)]$ with THF, Et_2O , Et_3N MeCN, and Me_3CCN

Each of these reactions was carried out in a manner similar to the preparation of **3.8** and **3.9** using the appropriate trapping agent. In all cases the ^1H NMR spectrum of the crude reaction mixture revealed either decomposition or a plethora of intractable *non-alkylidene* products.

3.2.8 Attempted Preparation of $\text{Cp}^*\text{W}(\text{NO})(=\text{CHCMe}_3)(\text{PMe}_3)$ (**3.4**) in CH_2Cl_2

In a manner similar to the preparation of **3.4** in THF, a dichloromethane solution (2 mL) of **2.4** (48 mg, 0.098 mmol) and excess PMe_3 was heated at $70\text{ }^\circ\text{C}$ for 2 d, during which time a pale green-yellow precipitate formed and the reaction solution became orange. The organic volatiles were then removed in vacuo to obtain a residue, which upon addition of Et_2O gave a pale yellow solid and an orange solution. The solid (presumably a complex mixture of phosphonium chlorides based on FAB mass spectrometry) was removed by filtration.

Concentration of the filtrate followed by cooling to $-30\text{ }^{\circ}\text{C}$ for 2 d provided $\text{Cp}^*\text{W}(\text{NO})(\text{PMe}_3)\text{Cl}_2$ (**3.11**) (12 mg, 25% yield) as brown-orange needles.

MS 420 $[\text{M}^+ - \text{PMe}_3, ^{184}\text{W}]$. ^1H NMR (300 MHz, C_6D_6) δ 1.63 (d, $^2J_{\text{HP}} = 10.5$, 9H, PMe_3), 2.03 (s, 15H, C_5Me_5). $^{13}\text{C}\{^1\text{H}\}$ NMR (75 MHz, C_6D_6) δ 10.5 (C_5Me_5), 13.4 (d, $^1J_{\text{CP}} = 34$, PMe_3), 113.2 (C_5Me_5). $^{31}\text{P}\{^1\text{H}\}$ NMR (121 MHz, C_6D_6) δ 12.0 ($^1J_{\text{PW}} = 251$).

3.2.9 Preparation of $\text{Cp}'\text{W}(\text{NO})(\text{CH}_2\text{CMe}_3)(\text{NMe}_2)$ [$\text{Cp}' = \text{Cp}^*$ (**2.17**); $\text{Cp}' = \text{Cp}$ (**3.12**)]

3.2.9.1 Complex 2.17. To a thick-walled Pyrex bomb containing **2.4** (47 mg, 0.096 mmol) was added THF (10 mL) and Me_2NH (3-5 equiv from a calibrated gas bulb) by vacuum transfer. The resulting mixture was thawed and heated at $70\text{ }^{\circ}\text{C}$ for 2 d, during which time its color darkened. The organic volatiles were then removed in vacuo to obtain a residue, which was extracted into 2:1 hexanes/ Et_2O and filtered through Celite ($1 \times 1\text{ cm}$). Concentration of the filtrate followed by cooling to $-30\text{ }^{\circ}\text{C}$ for 2 d provided **2.17** as orange-yellow needles (43 mg, 91% yield).

Anal. Calcd. for $\text{C}_{17}\text{H}_{32}\text{N}_2\text{OW}$: C, 43.97; H, 6.95; N, 6.03. Found: C, 43.89; H, 7.09; N, 5.91. IR (cm^{-1}) ν_{NO} 1566 (s). MS 464 $[\text{M}^+, ^{184}\text{W}]$. ^1H NMR (500 MHz, C_6D_6) δ 0.94 (AB q, $^2J_{\text{HH}} = 13.5$, 2H, WCH_2), 1.37 (s, 9H, CMe_3), 1.65 (s, 15H, C_5Me_5), 2.59 (s, 3H, NMe), 3.71 (s, 3H, NMe). $^{13}\text{C}\{^1\text{H}\}$ NMR (125 MHz, C_6D_6) δ 9.52 (C_5Me_5), 34.5 (CMe_3), 42.2 (CMe_3), 51.3 (NMe), 57.7 (WCH_2), 59.8 (NMe), 109.8 (C_5Me_5).

3.2.9.2 Complex 3.12 (yellow-orange blocks, 93% yield) was prepared from **2.1** in a manner similar to that described for **2.17** except that the thermolysis was effected at $65\text{ }^{\circ}\text{C}$ for 1 d.

Anal. Calcd. for $\text{C}_{12}\text{H}_{22}\text{N}_2\text{OW}$: C, 36.56; H, 5.63; N, 7.11. Found: C, 36.85; H, 5.77; N, 7.17. IR (cm^{-1}) ν_{NO} 1602 (s). MS 394 $[\text{M}^+, ^{184}\text{W}]$. ^1H NMR (300 MHz, C_6D_6) δ 1.32 (s, 9H, CMe_3), 1.50 (AB q, $^2J_{\text{HH}} = 12.7$, 2H, WCH_2), 2.62 (NMe), 3.68 (NMe), 5.14 (C_5H_5).

$^{13}\text{C}\{^1\text{H}\}$ NMR (75 MHz, C_6D_6) δ 34.3 (CMe_3), 37.4 (CMe_3), 47.5 (WCH_2), 56.0 (NMe), 59.5 (NMe), 102.5 (C_5H_5).

3.2.10 Preparation of $\text{CpW}(\text{NO})(\text{CHDCMe}_3)(\text{NMe}_2)$ (**3.12-d**)

This compound was prepared from $\text{CpW}(\text{NO})(\text{CD}_2\text{CMe}_3)_2$ and Me_2NH in a manner analogous to that described for **3.12**. The procedure afforded **3.12-d** in >95% yield as judged by ^1H NMR spectroscopy.

^1H NMR (300 MHz, C_6D_6) δ 1.32 (s, 9H, CMe_3), 1.50 (br s, 1H, WCHD), 2.62 (NMe), 3.68 (NMe), 5.14 (C_5H_5). $^{13}\text{C}\{^1\text{H}\}$ NMR (75 MHz, C_6D_6) δ 34.3 (CMe_3), 37.4 (CMe_3), 46.9 (t, $^1J_{\text{CD}} = 18.5$, WCHD), 56.0 (NMe), 59.6 (NMe), 102.5 (C_5H_5).

3.2.11 Reactions of $\text{Cp}^*\text{W}(\text{NO})(=\text{CHCMe}_3)(\text{PMe}_3)$ (**3.4**) with MeOH , Me_2NH , and PhCO_2H

3.2.11.1 Preparation of $\text{Cp}^*\text{W}(\text{NO})(\text{CH}_2\text{CMe}_3)(\text{OMe})$ (2.16**).** To a sample of **3.4** (10 mg, 0.020 mmol) in an NMR tube was added methanol by vacuum transfer. The resulting solution was left at room temperature for 6 h, whereupon the once yellow solution appeared red. The organic volatiles were then removed in vacuo, and an NMR sample in C_6D_6 was prepared. The ^1H NMR spectrum of the crude reaction mixture revealed the quantitative conversion of **3.4** into **2.16**.

^1H NMR (500 MHz, C_6D_6) δ 1.33 (AB q, $^2J_{\text{HH}} = 14.3$, 2H, WCH_2), 1.41 (s, 9H, CMe_3), 1.57 (s, 15H, C_5Me_5), 4.75 (s, 3H, OMe). $^{13}\text{C}\{^1\text{H}\}$ NMR (75 MHz, C_6D_6) δ 9.1 (C_5Me_5), 32.8 (WCH_2), 34.0 (CMe_3), 36.8 (CMe_3), 70.0 (OMe), 111.6 (C_5Me_5).

3.2.11.2 Preparation of $\text{Cp}^*\text{W}(\text{NO})(\text{CH}_2\text{CMe}_3)(\text{NMe}_2)$ (2.17**).** A solution of **3.4** (12 mg, 0.024 mmol) in THF (0.5 mL) was treated with excess Me_2NH by vacuum transfer. The resulting solution was heated at 70 °C for 1 d, during which time it slowly turned yellow-

orange. The organic volatiles were then removed in vacuo. The ^1H NMR spectrum of the crude reaction mixture in C_6D_6 revealed the quantitative conversion of **3.4** into **2.17**.

3.2.11.3 Preparation of $\text{Cp}^*\text{W}(\text{NO})(\text{CH}_2\text{CMe}_3)(\text{O}_2\text{CPh})$ (3.13). To an NMR tube containing **3.4** (17 mg, 0.034 mmol) and benzoic acid (4 mg, 1 equiv) was added C_6D_6 (0.5 mL) by vacuum transfer. Upon thawing, the color of the mixture immediately changed from yellow to orange. The ^1H NMR spectrum indicated clean conversion to **3.13**, whose identity was confirmed by comparison of its NMR spectra to those of an authentic sample.¹⁹

3.2.12 Preparation of $\text{Cp}^*\text{W}(\text{NO})[\text{CH}(\text{CMe}_3)\text{CH}_2(\text{CMe}_3)\text{CH}]$ (3.14)

To a Pyrex bomb containing **2.4** (909 mg, 2.16 mmol) was added neohexene (3 mL) by vacuum transfer. The mixture was heated at 70 °C for 2 d, during which time it became orange-yellow. The organic volatiles were then removed in vacuo to obtain a yellow solid, which was redissolved in 4:1 hexanes/ Et_2O (1 mL) and cooled to -30 °C. Yellow needles of **3.14** (903 mg, 97% yield in 2 crops), which were suitable for an X-ray diffraction study, formed after 2 d and were isolated by removing the mother liquor with a pipet.

Anal. Calcd. for $\text{C}_{21}\text{H}_{31}\text{NOW}$: C, 50.10; H, 7.41; N, 2.78. Found: C, 49.87; H, 7.40; N, 2.76. IR (cm^{-1}) ν_{NO} 1518 (s). MS 503 [M^+ , ^{184}W]. ^1H NMR (300 MHz, CDCl_3) δ -2.29 (td, $^2J_{\text{HH}} = 4.5$, $^3J_{\text{HH}} = 10.2$, 1H, H_β syn to Cp^*), -1.01 (pseudo q, $^2J_{\text{HH}} = 4.5$, $^3J_{\text{HH}} = 6.0$, 1H, H_β anti to Cp^*), 1.09 (s, 18H, CMe_3), 1.91 (s, 15H, C_5Me_5), 3.92 (dd, $^3J_{\text{HH}} = 6.0$, 10.2, 2H, WCH). $^{13}\text{C}\{^1\text{H}\}$ NMR (75 MHz, CDCl_3) δ -4.8 (CH_2), 10.3 (C_5Me_5), 32.2 (CMe_3), 43.2 (s, CMe_3), 108.8 (C_5Me_5), 124.2 ($^1J_{\text{CW}} = 124$, WCH). NOEDS (400 MHz, CDCl_3) irrad. at 1.91 ppm (Cp^*), NOE at δ 3.92 (H_α); irrad. at 3.92 ppm (H_α), NOEs at δ -2.29 (H_β), 1.22 (CMe_3), 1.65 (Cp^*).

3.2.13 Preparation of $\text{Cp}^*\text{W}(\text{NO})[\text{CH}(\text{CMe}_3)\text{CH}(\text{C}_3\text{H}_6)\text{CH}]$ (**3.15**)

A solution of **2.4** (68 mg, 0.13 mmol) in cyclopentene (4 mL) was heated at 70 °C for 2 d, during which time it became orange-yellow. The organic volatiles were then collected by vacuum transfer and analyzed by GC-MS, which showed, in addition to neopentane (m/z 57) and the solvent (m/z 70), the presence of 3-cyclopentylcyclopentene (m/z 136) and 1,1'-bicyclopentyl (m/z 138). The identity of the latter two compounds was confirmed by comparison of their mass spectral fragmentation patterns with those of authentic samples.²⁰ Their yields, unfortunately, could not be estimated due to partial peak overlap in the GC trace. Extraction of the crude reaction mixture into Et_2O , followed by filtration through Celite (1 × 1 cm) and cooling to -30 °C for several days provided **3.15** as orange crystals (30 mg, 45% yield).

Anal. Calcd. for $\text{C}_{20}\text{H}_{33}\text{NOW}$: C, 49.29; H, 6.83; N, 2.87. Found: C, 49.59; H, 7.03; N, 2.89. MS 485 [M^+ , ^{184}W]. ^1H NMR (500 MHz, CDCl_3) δ -0.37 (septet, $^3J_{\text{HH}} = 5.3, 10.2$, 1H, H_β), 0.38 (m, 1H, CH_2), 1.00 (s, 9H, CMe_3), 1.75 (m, 1H, CH_2), 2.00 (s, 15H, C_5Me_5), 2.04 (m, 1H, CH_2), 2.32 (m, 1H, CH_2), 2.46 (m, 1H, CH_2), 2.61 (m, 1H, CH_2), 3.29 (d, $^3J_{\text{HH}} = 5.1$, 1H, CHCMe_3), 7.68 (m, 1H, WCH). $^{13}\text{C}\{^1\text{H}\}$ NMR (75 MHz, CDCl_3) δ 10.4 (C_5Me_5), 15.5 (β CH), 32.1 (CMe_3), 33.4 (CH_2), 37.2 (CH_2), 40.6 (CH_2), 41.2 (CMe_3), 109.5 (C_5Me_5), 115.3 (CHCMe_3), 141.8 (WCH).

3.2.14 Preparation of $\text{Cp}^*\text{W}(\text{NO})[\text{CH}(\text{CMe}_3)\text{CH}(\text{C}_3\text{H}_6)\text{C}(\text{Et})]$ (**3.16**)

A solution of **2.4** (33 mg, 0.049 mmol) in ethylcyclopentene (4 mL) was heated at 75 °C for 2 d, during which time it became orange-yellow. The organic volatiles were then collected by vacuum transfer and analyzed by GC-MS, which showed in addition to neopentane and the solvent (m/z 96) the presence of a complex mixture of unidentifiable products with parent peaks at m/z 98, 134, 136, 164, and 166. Examination of the crude reaction mixture by ^1H NMR spectroscopy indicated the presence of **3.16** and a trace amount of decomposition products. This mixture was then triturated with pentane (3 × 5 mL) and

filtered through alumina I (1×1 cm). The alumina column was washed with additional 5:1 pentane/Et₂O until the filtrate was colorless. Diminishing the volume of the combined filtrates under reduced pressure followed by cooling to -30 °C for several days afforded **3.16** as orange-yellow crystals (6 mg, 17% yield).

MS 515 [M^+ , ^{184}W]. 1H NMR (500 MHz, CDCl₃) δ -0.62 (quint, $^3J_{HH} = 5.4, 10.6$, 1H, H $_{\beta}$), 0.47 (m, 1H, C_aH₂), 1.01 (s, 9H, CMe₃), 1.11 (t, $^3J_{HH} = 7.2$, 3H, CH₂CH₃), 1.76 (m, $^3J_{HH} = 5.4, 11.7$, 1H, C_bH₂), 1.98 (s, 15H, C₅Me₅), 2.13 (m, 1H, C_cH₂), 2.27 (m, 1H, C_cH₂), 2.35 (m, 2H, C_aH₂, C_bH₂), 2.48 (m, 1H, C_dH₂), 3.08 (m, 1H, C_dH₂), 3.12 (d, $^3J_{HH} = 5.4$, 1H, WCH). $^{13}C\{^1H\}$ NMR (75 MHz, CDCl₃) δ 10.3 (C₅Me₅), 17.0 (CH₂CH₃), 27.4 (β CH), 32.1 (CMe₃), 33.4 (C_aH₂), 37.9 (C_bH₂), 40.9 (CMe₃), 42.9 (C_cH₂), 46.9 (C_dH₂), 109.2 (C₅Me₅), 113.2 (WCH), 173.2 (WC). NOEDS (400 MHz, CDCl₃): irradi. at δ 1.01 , NOEs at -0.62 and 3.12 ppm.

3.2.15 Preparation of Cp*W(NO)[CH(CMe₃)CH(C₅H₆)CH] (**3.17**)

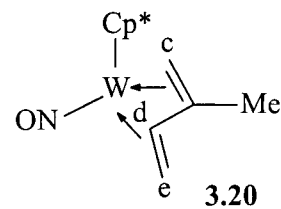
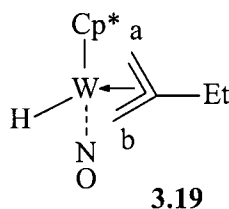
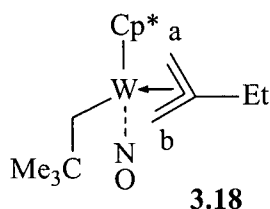
A solution of **2.4** (24 mg, 0.049 mmol) in norbornadiene (~ 2 mL) was heated at 70 °C for 2 d, during which time it became pale orange. The organic volatiles were then removed in vacuo, leaving an insoluble white material (presumably products of the ring-opening polymerization of norbornadiene) and an orange crystalline solid. The latter was extracted into Et₂O (3 mL) and filtered through Celite (1×1 cm). Concentration of the filtrate followed by cooling to -30 °C for several days provided **3.17** as orange blocks. These blocks, which were suitable for an X-ray crystallographic analysis, were obtained in 32% yield (8 mg).

MS 511 [M^+ , ^{184}W]. 1H NMR (500 MHz, C₆D₆) δ -0.12 (m, $J_{HH} = 2.3, 6.6$, 1H, H $_{\beta}$), 0.02 (d, $J_{HH} = 8.9$, 1H, CH₂), 1.25 (m, $J_{HH} = 8.8, 2.6$, 1H, CH₂), 2.38 (s, 1H, CH), 2.78 (s, 1H, CH), 3.09 (d, $^3J_{HH} = 6.2$, 1H, CHCMe₃), 5.94 (dd, $J_{HH} = 3.0, 5.2$, 1H, =CH), 6.18 (dd, $J_{HH} = 3.1, 5.5$, 1H, =CH), 6.94 (dd, $J_{HH} = 2.9, 7.2$, 1H, WCH). $^{13}C\{^1H\}$ NMR (125 MHz, C₆D₆) δ 10.4 (C₅Me₅), 18.0 (β CH), 32.9 (CMe₃), 34.1 (CMe₃), 43.6 (CH), 45.3 (CH₂), 47.5 (CH), 108.9 (C₅Me₅), 122.1 (CHCMe₃), 131.6 (WCH), 135.8 (=CH), 142.3 (=CH).

3.2.16 Preparation of $\text{Cp}^*\text{W}(\text{NO})(\text{CH}_2\text{CMe}_3)(\eta^3\text{-CH}_2\text{C}(\text{Et})\text{CH}_2)$ (3.18**), $\text{Cp}^*\text{W}(\text{NO})(\text{H})(\eta^3\text{-CH}_2\text{C}(\text{Et})\text{CH}_2)$ (**3.19**) and $\text{Cp}^*\text{W}(\text{NO})(\eta^4\text{-2-methylbutadiene})$ (**3.20**).**

In a manner similar to the preparation of **3.14**, a solution of **2.4** (58 mg, 0.118 mmol) in 2-methyl-1-butene (2 mL) was heated at 70 °C for 2 d, during which time it became yellow-brown. The organic volatiles were then collected by vacuum transfer and were examined by GC-MS, which showed the presence of neopentane (m/z 57), the solvent (m/z 70), and a trace amount of an unidentifiable material whose mass is equivalent to two C_5H_{10} units. Analysis of the crude reaction mixture by ^1H NMR spectroscopy indicated that **3.18**, **3.19**, and **3.20** (in ~1.2:1:0.4 ratio) were formed in a combined yield of 60–75%; the remaining products could not be ascertained due to inadequate signal-to-noise of their signals and to spectral overlap. Next, the NMR mixture was taken to dryness, extracted into pentane, and filtered through alumina I (1 × 1 cm). The alumina column was washed with additional 4:1 pentane/ Et_2O until the filtrate was colorless. Concentration of the combined filtrates followed by cooling to –30 °C for several days afforded **3.18** (13 mg, 22% yield) as sticky white rosettes. The pale yellow mother liquor was then reduced in volume and stored at –30 °C for 2 d to induce the deposition of **3.18**, **3.19**, and **3.20** as yellow crystals in a ratio of ~1:2:1.

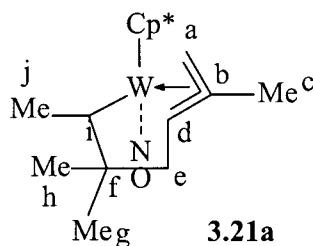
3.2.16.1 Complex 3.18. Anal. Calcd. for $\text{C}_{20}\text{H}_{37}\text{NOW}$: C, 49.09; H, 7.21; N, 2.86. Found: C, 48.96; H, 7.14; N, 2.86. IR (cm^{-1}) ν_{NO} 1565 (s). MS 489 [M^+ , ^{184}W]. ^1H NMR (500 MHz, CDCl_3) δ 0.75 (d, $J_{\text{HH}} = 2.7$, 1H, C_aH_2), 0.96 (s, 9H, CMe_3), 1.03 (d, $^2J_{\text{HH}} = 12.8$, 1H, WCH_2), 1.23 (t, $^3J_{\text{HH}} = 7.7$, 3H, CH_2CH_3), 1.60 (d, $^2J_{\text{HH}} = 12.8$, 1H, WCH_2), 1.81 (s, 15H, C_5Me_5), 1.89 (br s, 1H, C_bH_2), 2.22 (d, $J_{\text{HH}} = 2.7$, 1H, C_aH_2), 2.25 (m, 2H, CH_2CH_3), 3.64 (d, $J_{\text{HH}} = 3.9$, 1H, C_bH_2). $^{13}\text{C}\{^1\text{H}\}$ NMR (75 MHz, CDCl_3) δ 10.2 (C_5Me_5), 17.6 (CH_2CH_3), 27.6 (WCH_2), 29.5 (CH_2CH_3), 34.4 (CMe_3), 37.2 (CMe_3), 42.5 (C_aH_2), 74.2 (C_bH_2), 107.2 (C_5Me_5), 135.6 (4° C). NOES (400 MHz, C_6D_6) irradi. at δ 0.75, NOEs at 1.81, 2.22 ppm; irradi. at δ 1.23, NOEs at 2.22, 2.25 ppm; irradi. at δ 3.64, NOEs at 0.96, 1.60, 1.89 ppm.



3.2.16.2 Complexes 3.19 and 3.20. IR (cm^{-1}) ν_{NO} 1590 (s), 1565 (s, br); ν_{WH} 1888 (w). MS **3.19**: 416 [$\text{M}^+ - \text{H}_2$, ^{184}W]. ^1H NMR (500 MHz, C_6D_6) δ **3.19**: -0.88 (s, $^1J_{\text{HW}} = 118$, 1H, WH), 0.45 (s, 1H, C_aH_2), 0.75 (s, 1H, C_bH_2), 1.09 (t, $^3J_{\text{HH}} = 7.5$, 3H, CH_2CH_3), 1.78 (s, 15H, C_5Me_5), 2.20 (m, 1H, CH_2CH_3), 2.50 (m, 1H, CH_2CH_3), 2.96 (br s, 1H, C_aH_2), 4.15 (br s, 1H, C_bH_2). **3.20**: 0.95 (dd, $^2J_{\text{HH}} = 4.0$, $^3J_{\text{HH}} = 0.9$, 1H, C_cH_2), 1.1 (obscured by CH_2CH_3 of **3.19**, 1H, C_dH), 1.75 (s, 15H, C_5Me_5), 2.04 (s, 3H, CH_3), 2.3 (obscured by CH_2CH_3 of **3.19**, 1H, C_eH_2), 3.14 (dd, $^2J_{\text{HH}} = 4.0$, $^3J_{\text{HH}} = 14.0$, 1H, C_eH_2), 3.29 (dd, $^2J_{\text{HH}} = 4.0$, $^5J_{\text{HH}} = 0.7$, 1H, C_cH_2). $^{13}\text{C}\{^1\text{H}\}$ NMR (75 MHz, C_6D_6) δ **3.19**: 10.7 (C_5Me_5), 14.9 (CH_2CH_3), 27.2 (WCH_2), 31.0 (CH_2CH_3), 35.0 (CMe_3), 37.6 (CMe_3), 46.2 (C_aH_2), 53.0 (C_bH_2), 104.7 (C_5Me_5), 124.6 (4°C). **3.20**: 9.9 (C_5Me_5), 18.8 (CH_3), 50.7 (C_cH_2), 55.5 (C_eH_2), 80.5 (C_dH), 106.5 (C_5Me_5), 115.8 (4°C).

3.2.17 Preparation of $\text{Cp}^*\text{W}(\text{NO})(\eta^3\text{-C}_{10}\text{H}_{18})$ (**3.21**)

A solution of **2.4** (73 mg, 0.149 mmol) in 2-methyl-2-butene (2 mL) was heated at 70°C for 2 d, during which time it became yellow-orange. The organic volatiles were then collected by vacuum transfer and were analyzed by GC-MS, which showed peaks due to neopentane and the solvent. Examination of the crude reaction mixture by ^1H NMR spectroscopy revealed the presence of **3.21a-c** in a relative yield of about 2:1:0.8 along with unidentified products. Next, the NMR mixture was taken to dryness, extracted into pentane, and filtered through Celite (1×1 cm). Concentration of the filtrate followed by cooling to -30°C for 2 d provided **3.21** as pale yellow crystals (30 mg, 41% yield). X-ray quality crystals of **3.21a** were obtained by recrystallizing this batch of crystals from a mixture of 5:1 pentane/toluene at -30°C .



Anal. Calcd. for $C_{20}H_{33}NOW$: C, 49.29; H, 6.83; N, 2.87. Found: C, 48.98; H, 6.77; N, 2.95. IR (cm^{-1}) ν_{NO} 1585, 1621, 1651 (s). MS 487 [M^+ , ^{184}W]. 1H NMR (500 MHz, C_6D_6) δ **3.21a**: 0.41 (d, $^2J_{HH} = 2.7$, 1H, C_aH_2 anti), 0.93 (s, 3H, C_gH_3), 1.22 (s, 3H, C_hH_3), 1.50 (obscured, 1H, C_iH), 1.59 (s, 15H, C_5Me_5), 1.85 (dd, $J_{HH} = 4.2, 9.5$, 1H, C_eH_2), 1.94 (d, $^3J_{HH} = 7.5$, 3H, C_jH_3), 1.94 (d, $^2J_{HH} = 3.1$, 1H, C_aH_2 syn), 2.38 (s, 3H, C_cH_3), 2.56 (t, $^2J_{HH} = 10.3$, 1H, C_eH_2), 2.66 (dd, $^3J_{HH} = 4.9, 10.1$, 1H, C_dH). **3.21b**: 0.38 (d, $^2J_{HH} = 2.7$, 1H, C_aH_2 anti), 0.87 (s, 3H, CH_3), 1.19 (s, 3H, CH_3), 1.67 (s, 15H, C_5Me_5), 1.55 (obscured, 3H, CH_3), 1.61 (obscured, 1H, CH_2), 2.01 (obscured, 1H, CH_2), 2.08 (d, $^2J_{HH} = 3.0$, 1H, C_aH_2 syn), 2.25 (s, 3H, C_cH_3), 2.51 (q, $^3J_{HH} = 7.9$, 1H, C_iH), 2.67 (obscured, 1H, C_dH). **3.21c**: 0.49 (d, $^2J_{HH} = 2.7$, 1H, C_aH_2 anti), 0.77 (d, $^3J_{HH} = 7.1$, 3H, CH_3), 1.52 (s, 15H, C_5Me_5), 1.89 (obscured, 1H, CH), 1.97 (obscured, 1H, CH_2), 2.05 (m, 1H, C_dH), 2.22 (s, 3H, CH_3), 2.36 (d, $^2J_{HH} = 2.8$, 1H, C_aH_2 syn). $^{13}C\{^1H\}$ NMR (75 MHz, C_6D_6) δ **3.21a**: 10.2 (C_5Me_5), 18.2 (C_cH_3), 24.3 (C_jH_3), 28.9 (C_gH_3), 31.7 (C_hH_3), 41.1 (C_eH_2), 42.2 (C_iH), 44.4 (C_aH_2), 60.1 (C_f), 90.6 (C_dH), 106.2 (C_5Me_5), 128.8 (C_b). **3.21b**: 42.6 (C_aH_2), 61.9 (C_f), 96.1 (C_dH), 123.94 (C_b). **3.21c**: 48.1 (C_aH_2), 76.6 (C_dH), 123.92 (C_b). Remaining signals for **3.21b** and **3.21c**: 9.8, 10.7 (C_5Me_5), 14.3, 18.0, 18.4, 19.5, 26.0, 30.3 (CH_3), 37.3, 35.7 (CH), 32.4, 43.3 (CH_2), 106.9 (C_5Me_5). NOEDS (400 MHz, C_6D_6) **3.21a**: irradi. at 0.41 ppm (C_aH_2), NOEs at δ 1.92 (C_aH_2), 2.66 (C_dH); irradi. at 0.93 ppm (C_gH_3), NOEs at 1.22, 1.85, 2.65; irradi. at 1.22 ppm (C_hH_3), NOEs at δ 0.93, 1.92 (C_jH_3), 2.55; irradi. at 1.67 ppm, NOEs at δ 0.41, 0.93; irradi. 2.38 ppm (C_cH_3), NOEs at δ 1.22, 1.92 (C_aH_2); irradi. at 2.65 ppm, NOEs at δ 0.41, 0.93, 1.85.

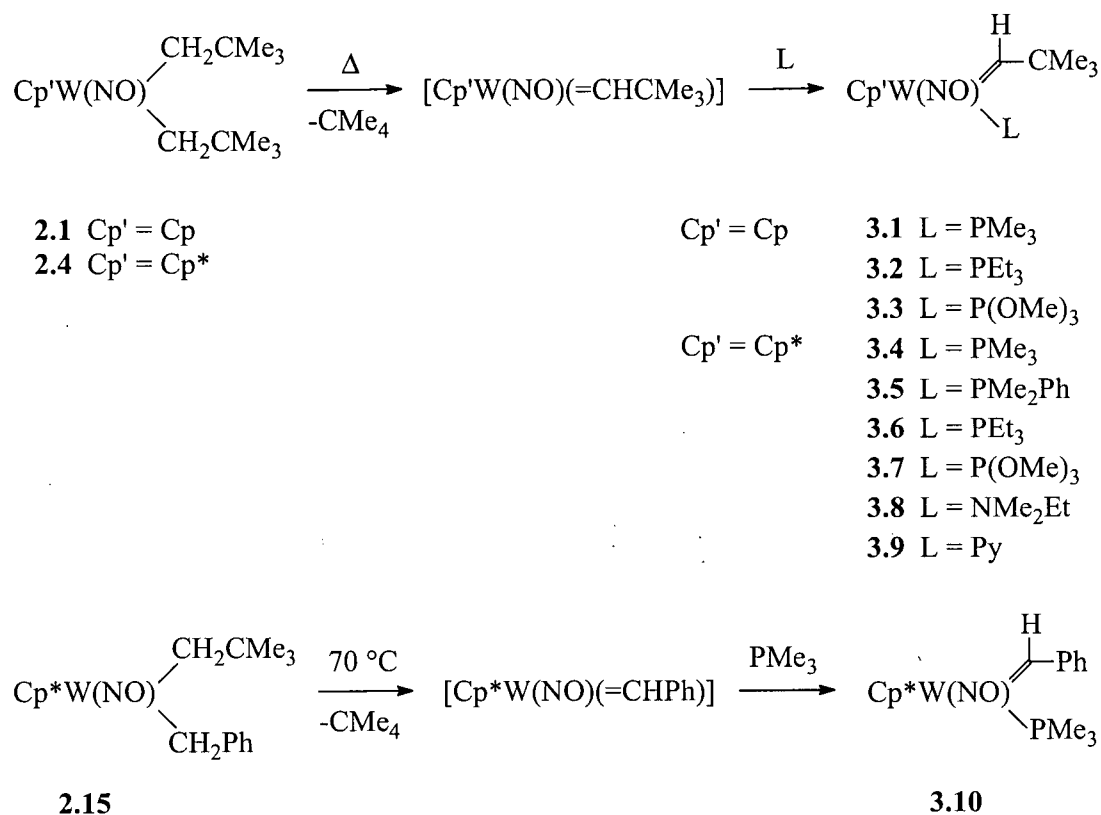
3.3 Results and Discussion

3.3.1 Trapping of $[\text{Cp}'\text{W}(\text{NO})(=\text{CHCMe}_3)]$ and $[\text{Cp}^*\text{W}(\text{NO})(=\text{CHPh})]$ with Lewis Bases

In analogy to the behavior of the molybdenum bis(neopentyl) complex, $\text{CpMo}(\text{NO})(\text{CH}_2\text{CMe}_3)_2$, studied earlier,¹⁵ the thermolysis of the tungsten bis(alkyl) analogues $\text{Cp}'\text{W}(\text{NO})(\text{CH}_2\text{CMe}_3)_2$ [$\text{Cp}' = \text{Cp}$ (**2.1**), Cp^* (**2.4**)] and $\text{Cp}^*\text{W}(\text{NO})(\text{CH}_2\text{CMe}_3)(\text{CH}_2\text{Ph})$ (**2.15**) occurs exclusively by an α -abstraction process that yields neopentane and the transient neopentylidene and benzylidene intermediates $[\text{Cp}'\text{W}(\text{NO})(=\text{CHCMe}_3)]$ and $[\text{Cp}^*\text{W}(\text{NO})(=\text{CHPh})]$. Three features of the generation and subsequent trapping of these tungsten alkylidene intermediates contrast sharply with the molybdenum reactions, however. First, unlike $\text{CpMo}(\text{NO})(\text{CH}_2\text{CMe}_3)_2$, which decomposes in several hours at room temperature, the tungsten bis(alkyl) precursors are thermally robust, decomposing in solution only under forcing conditions: ca. 15 h at 60 °C for **2.1** and 2 d at 70 °C for **2.4** and **2.15**. Second, thermolysis of solutions of **2.1** or **2.4** in the absence of a trapping agent does not produce a bridging alkylidene complex as observed for the molybdenum system but rather leads to decomposition. Third, while the molybdenum reactions may be conducted in a range of solvents including hexanes, Et_2O , and dichloromethane, the reactions of the tungsten complexes are highly solvent sensitive *and* depend on the nature of the trapping ligand.

In general, the tungsten alkylidene complexes (only the neopentylidene systems were studied in detail) are readily trapped by Lewis bases (L) such as phosphines, phosphites, and amines, as shown in Scheme 3.2, but not with acetonitrile, *tert*-butylnitrile, Et_2O , THF, or Me_2S . The observation of the tungsten ligand-trapped products, however, depends on the steric bulk and donor strength of L and on the type of Cp' ligand. For complex **2.1**, adduct formation leading to complexes **3.1–3.3** is observed with PMe_3 , PEt_3 , and $\text{P}(\text{OMe})_3$, while an intractable mixture of products is observed upon reaction with pyridine. Complex **2.4**, in contrast, reacts with not only PMe_3 , PMe_2Ph , PEt_3 , and $\text{P}(\text{OMe})_3$, but also with dimethylethylamine and pyridine, yielding complexes **3.4–3.9** in high yields, a behavior that is

Scheme 3.2

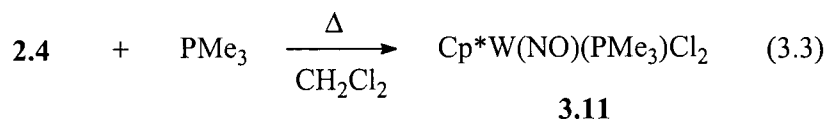


more analogous to the CpMo bis(neopentyl) system.¹⁵ However, unlike the molybdenum system, which is relatively insensitive to the steric bulk of the trapping ligands, decomposition is observed when the tungsten complexes **2.1** and **2.4** are independently thermolyzed in the presence of sterically encumbered PPh₃ or when **2.4** is reacted with bulky triethylamine.

The fact that the [CpMo(NO)(=CHCMe₃)] and [Cp*W(NO)(=CHCMe₃)] intermediates can be trapped by amines but not the CpW analogue, even though the electronic properties of this species are more comparable with those of the molybdenum system, strongly suggests that it is not the trapping of the unsaturated neopentylidene species that depends on the nature of L and Cp'. A more reasonable explanation is that it is the effect of L and Cp' on the stability of the ligand-trapped products that determines whether these complexes will be observed and

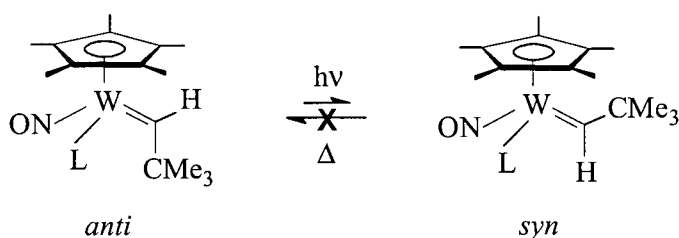
isolated. On the basis of the above observations, this stability decreases as the size and donating ability of L increases and decreases, respectively. It also decreases when Cp' is changed from Cp* to Cp. Thus, unlike the CpMo system, which forms isolable pyridine and PPh₃ adducts, analogous CpW products are not observed presumably not because they are not formed but because they decompose at the temperature required for **2.1** to extrude neopentane.

As noted above, the observation of the tungsten ligand-trapped alkylidene complexes is also markedly dependent on the choice of solvent. This is due to the fact that the unsaturated alkylidene intermediates are highly reactive not only toward dative ligands but also toward most solvents. For reactions involving amine ligands, the amine must also function as the solvent in order to avoid competitive side-product formation and decomposition. For reactions with phosphine and phosphite ligands, on the other hand, THF but not Et₂O or acetonitrile may be used as solvent without deleterious effects. Use of sterically hindered 2,2,4,4-tetramethylpentane for the reaction of **2.4** with PMe₃ is also equally effective. Changing this solvent to cyclohexane or other less encumbered aliphatic hydrocarbon solvents, however, yields a mixture of products in which the desired neopentylidene adduct **3.4** is formed in moderate yields at best, due to competitive reaction of the [Cp*W(NO)(=CHCMe₃)] intermediate with the C–H bonds of the solvent (see Chapter 4). Finally, the reaction of **2.4** with PMe₃ in dichloromethane does not lead to alkylidene products; rather, a complex mixture of compounds, in which Cp*W(NO)(Cl)₂(PMe₃) (**3.11**) is the major (and only identified) product, is observed (eq 3.3). The identity of **3.11** was established by NMR and mass spectroscopies and by comparison to an authentic sample prepared from reaction of Cp*W(NO)Cl₂ with PMe₃. The mechanism by which **3.11** forms remains unclear, since the reaction also generates a large amount of insoluble phosphonium chlorides due to rapid reaction between PMe₃ and dichloromethane at 70 °C.



All alkylidene complexes outlined in Scheme 3.2 are 18-electron species. They are yellow to brown-orange materials that are readily soluble in aromatic and ethereal solvents and that, although they may be handled briefly in air as solids, are moisture sensitive in solution. With the exception of **3.3**, the phosphine and phosphite adducts can be crystallized from hexanes/Et₂O and are stable as solids for months at room temperature and to substitution by weaker σ -donors. The amine adducts, in contrast, are unstable in the solid state, decomposing over several days at $-30\text{ }^{\circ}\text{C}$ in the absence of light. In the presence of excess PMe₃, the pyridine adduct **3.10** slowly and quantitatively converts to the PMe₃ adduct **3.4**. In C₆D₆ solutions, the Cp and Cp* phosphine adducts show little degradation after being heated for 1 d at 100 and 120 $^{\circ}\text{C}$, respectively, whereas the amine adducts are sensitive to concentration effects. For example, in dilute C₆D₆ solutions, complex **3.9** may be heated to 70 $^{\circ}\text{C}$ for 16 h or stored at 25 $^{\circ}\text{C}$ for ca. 1 week in the dark with only trace amounts of decomposition and no reaction with solvent. In concentrated solutions, it decomposes over a period of days at room temperature to intractable products, presumably via bimolecular pathways. For comparison, the CpMo pyridine adduct can be crystallized and isolated, but at room temperature it decomposes slowly in solution to give largely the asymmetric dimer [CpMo(NO)(CHCMe₃)]₂ (Scheme 3.1). The CpMo phosphine analogues, in contrast, show no sign of decomposition even upon heating in C₆D₆ at 180 $^{\circ}\text{C}$ for 24 h.

Each of the complexes **3.1–3.10** was generated and isolated as a single isomer, which on the basis of ¹H NMR and X-ray data is the anti rotamer in which the alkylidene substituent points away from the Cp' ligand (see below). The syn rotamer was sometimes also observed in trace amounts (~5–10%) when solution or solid samples of the anti isomers were exposed to room light for more than several days. In the absence of light, no syn products could be detected, even at elevated temperatures. Thus, in contrast to many other alkylidene complexes including the CpMo(NO)(=CHCMe₃)(L) system, which can undergo syn and anti rotamer interconversion thermally,²¹ the syn and anti rotamers of the tungsten alkylidene complexes reported here can only be interconverted photochemically.



All alkylidene complexes in Scheme 3.2 were fully characterized by ^1H and ^{13}C NMR spectroscopies and in the case of complexes **3.1** and **3.4** also by X-ray diffraction. The ^1H and ^{13}C NMR spectra of complexes **3.1**–**3.10** are similar to those of their molybdenum counterparts (Table 3.1). For the phosphine and phosphite adduct complexes, the alkylidene H_α and C_α resonances appear as doublets due to coupling to phosphorus. For complexes containing a mixture of syn and anti rotamers, two sets of H_α resonances, which differ in chemical shift by up to 1.4 ppm, are observed. The higher-field resonances are assigned to the anti isomers since the α -hydrogen atoms in these complexes are closer the Cp' ligand and are

Table 3.1. Selected ^1H , ^{13}C , and ^{31}P NMR Data for $\text{Cp}'\text{W}(\text{NO})(=\text{CHCMe}_3)(\text{L})$ and $\text{Cp}^*\text{W}(\text{NO})(=\text{CHPh})(\text{PMe}_3)$ Complexes^a

Complex	H_α		C_α			^{31}P	
	δ^b	$^3J_{\text{HP}}^b$	δ	$^1J_{\text{CH}}$	$^1J_{\text{CP}}$	δ^c	$^1J_{\text{PW}}$
$\text{CpW}(\text{NO})(=\text{CHCMe}_3)(\text{PMe}_3)$ (3.1) ^c	12.00 (13.27)	3.0(5.4)	282.6	114	10	−5.1 (−1.5)	455
$\text{CpW}(\text{NO})(=\text{CHCMe}_3)(\text{PEt}_3)$ (3.2)	12.10	3.0	285.5	117	10	31.4	435
$\text{CpW}(\text{NO})(=\text{CHCMe}_3)[\text{P}(\text{OMe})_3]$ (3.3)	12.80	3.0					
$\text{Cp}^*\text{W}(\text{NO})(=\text{CHCMe}_3)(\text{PMe}_3)$ (3.4) ^c	11.25 (12.81)	3.6 (4.8)	282.8	111	9	−6.5 (−2.9)	449
$\text{Cp}^*\text{W}(\text{NO})(=\text{CHCMe}_3)(\text{PMe}_2\text{Ph})$ (3.5) ^d	11.27 (12.64)	3.3 (4.0)	285.4	113	9	9.8 (7.6)	446
$\text{Cp}^*\text{W}(\text{NO})(=\text{CHCMe}_3)(\text{PEt}_3)$ (3.6)	11.25 (12.47)	3.6 (4.5)	285.5	112	9	25.0	430
$\text{Cp}^*\text{W}(\text{NO})(=\text{CHCMe}_3)[\text{P}(\text{OMe})_3]$ (3.7)	11.91 (13.30)	3.0 (3.9)	296.3	116	13	24.5 (19.0)	675
$\text{Cp}^*\text{W}(\text{NO})(=\text{CHCMe}_3)(\text{NMe}_2\text{Et})$ (3.8) ^c	10.10		257.9	116			
$\text{Cp}^*\text{W}(\text{NO})(=\text{CHCMe}_3)(\text{Py})$ (3.9) ^c	10.63 (12.32)		264.4	116			
$\text{Cp}^*\text{W}(\text{NO})(=\text{CHPh})(\text{PMe}_3)$ (3.10) ^d	11.79	3.8	261.2	119	9	−6.5	443

^aAnti rotamer in CDCl_3 unless otherwise noted. ^bAnti rotamer (syn rotamer). ^cIn C_6D_6 . ^dIn CD_2Cl_2 .

therefore more shielded.

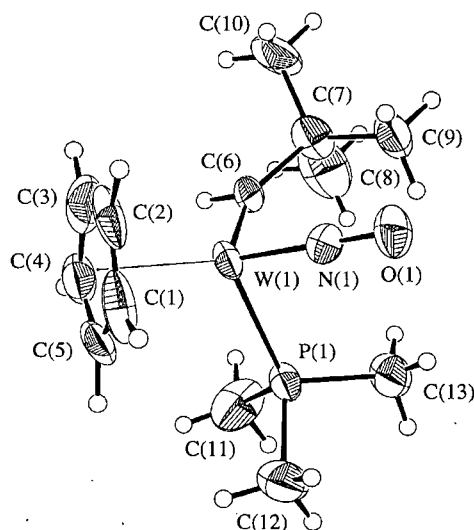
Other notable features of the ^1H and ^{13}C NMR data of **3.1–3.10** are the $^1J_{\text{CH}}$ coupling constants and the chemical shifts of the resonances of the alkylidene α -CH moieties. For all complexes, the $^1J_{\text{CH}}$ values are low (111–119 Hz)²² and fall within the range characteristic of 18-electron alkylidene complexes in which steric interaction between the substituent on the α -carbon atom and the metal fragment renders the $\text{M}=\text{C}_\alpha-\text{C}_\beta$ angles large.²³ That this is indeed the case has been confirmed by an X-ray structural determination of complexes **3.1** and **3.4** (see later).

Both the chemical shifts of the alkylidene H_α and C_α resonances of **3.1–3.10** move progressively upfield as L varies in the series L = phosphite, phosphine, pyridine, amine. The same also happens to the H_α resonance on replacing Cp by Cp*. The fact that an upfield shift is observed on replacing the phosphite or Cp ligand with the more electron-donating (and therefore more shielding) phosphine or Cp* group is undoubtedly electronic in origin, but why the pyridine and amine ligands, which are sterically unremarkable and are poorer donors, give rise to the furthest upfield resonances is unclear at the moment.

Finally, it should also be noted that the ^1H NMR spectra of the pyridine and benzylidene complexes **3.9** and **3.10** each display only three sets of resonances for the pyridine and benzylidene ring protons, thereby implying that these rings are rotating rapidly on the NMR time scale at 25 °C.

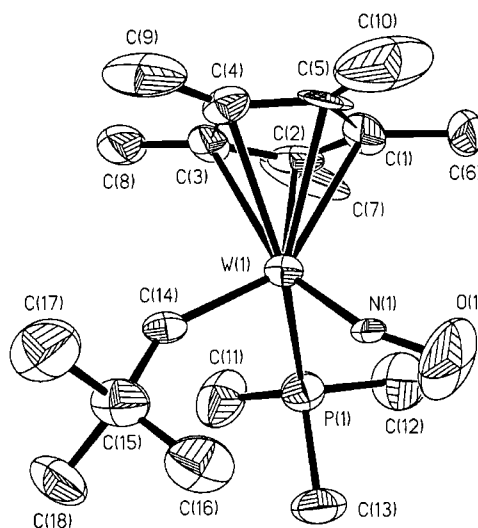
The solid-state molecular structures of the neopentylidene complexes **3.1** and **3.4**, as determined by X-ray diffraction, are shown in Figure 3.1, along with selected bond distances and angles. Noteworthy is that the NO ligand in each complex is essentially linear, while the orientation of the neopentylidene ligand, with the substituents parallel to the NO moiety ($\text{N}-\text{W}-\text{C}_\alpha-\text{C}_\beta$ torsion angle $\sim 0^\circ$) and the *tert*-butyl group pointing away from the Cp' ligand (i.e. the anti orientation), is as expected for a conformation involving maximum $\text{W}=\text{C}$ π -bonding and minimum steric interactions.²⁴ The $\text{W}-\text{C}_\alpha$ distances of 1.93–1.96 Å are typical of

A



N(1)–O(1)	1.24(1) Å
W(1)–N(1)	1.77(1) Å
W(1)–C(6)	1.93(2) Å
W(1)–P(1)	2.418(4) Å
W(1)–N(1)–O(1)	175.3(10)°
P(1)–W(1)–N(1)	91.3(4)°
P(1)–W(1)–C(6)	93.4(4)°
N(1)–W(1)–C(6)	101.2(5)°
W(1)–C(6)–C(7)	140(1)°

B



N(1)–O(1)	1.22(2) Å
W(1)–N(1)	1.774(14) Å
W(1)–C(14)	1.961(9) Å
W(1)–P(1)	2.555(4) Å
W(1)–N(1)–O(1)	163.3(14)°
P(1)–W(1)–N(1)	91.0(5)°
P(1)–W(1)–C(14)	93.8(6)°
N(1)–W(1)–C(14)	98.7(7)°
W(1)–C(6)–C(7)	140.7(11)°

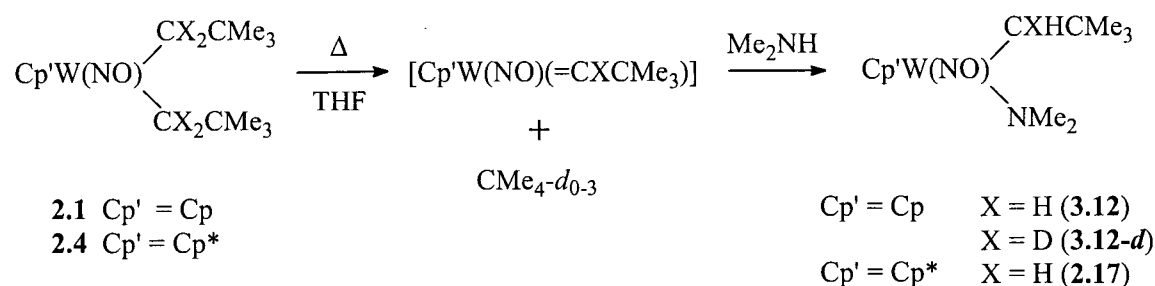
Figure 3.1. ORTEP diagrams and selected bond distances and angles for complexes (A) $\text{CpW}(\text{NO})(=\text{CHCMe}_3)(\text{PMe}_3)$ (**3.1**) and (B) $\text{Cp}^*\text{W}(\text{NO})(=\text{CHCMe}_3)(\text{PMe}_3)$ (**3.4**).

W–C double bonds, while the W–C_α–C_β angles of 140° are obtuse for sp²-hybridized centers, confirming the results of the NMR studies. For comparison, the corresponding bond distances and angles in isoelectronic CpMo(NO)(=CHCMe₃)(PMePh₂) and [CpRe(NO)(=CHPh)(PPh₃)] [PF₆]^{21a} complexes are 1.950(3) and 1.949(6) Å, and 140.8(3) and 136.2(5)°, respectively.

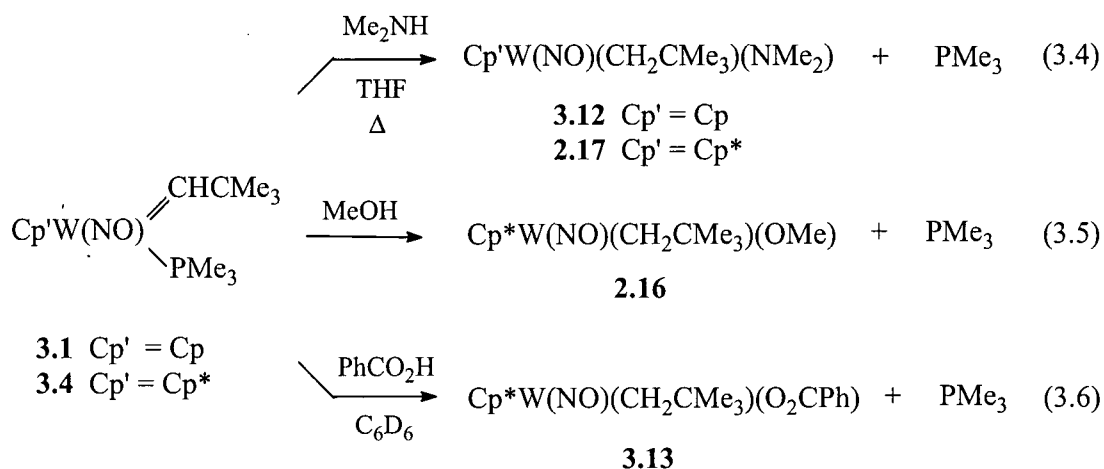
3.3.2 Reactions of [Cp'W(NO)(=CHCMe₃)] and Cp*W(NO)(=CHCMe₃)(PMe₃) with Heteroatom-Hydrogen Bonds

In analogy with the molybdenum chemistry, the thermolysis of the tungsten bis(neopentyls) **2.1** and **2.4** in the presence of amines with accessible N–H bonds results in the quantitative formation of amido-alkyl complexes Cp'W(NO)(CH₂CMe₃)(NR₂). For example, thermolysis of a THF solution of **2.1** at 60 °C for 1 d or of **2.4** at 70 °C for 2 d in the presence of excess dimethylamine leads exclusively to the corresponding neopentyl amido complexes **3.12** and **2.17** as shown in Scheme 3.3. Heating the α-deuterated complex CpW(NO)(CD₂CMe₃)₂ (**2.1-d₄**) under similar conditions yields the monodeuterated species **3.12-d**, for which the ¹H NMR spectrum shows a broad singlet at δ 1.50 and the ¹³C {¹H} NMR spectrum a triplet at δ 46.9 (¹J_{CH} = 18.5 Hz) due to the neopentyl α-proton and α-carbon atom, respectively. This result thus demonstrates that **2.1** and **2.4** react with amine N–H bonds via the neopentylidene [CpW(NO)(=CHCMe₃)] and [Cp*W(NO)(=CHCMe₃)] intermediates.

Scheme 3.3



Stronger protic acids such as alcohols²⁵ and carboxylic acids¹⁹ do not react with **2.1** or **2.4** via the intermediacy of alkylidene complexes. Although O–H bond cleavage leading to formation of neopentyl alkoxo and carboxylato complexes is observed, these reactions instead proceed rapidly by protonolysis of a neopentyl ligand in the starting material. Formal addition of O–H and even N–H bonds across a W=C linkage, however, can be observed when amines, alcohols, and carboxylic acids are reacted with the ligand-trapped complexes $\text{Cp}'\text{W}(\text{NO})(=\text{CHCMe}_3)(\text{L})$. For example, as shown in eq 3.4–3.6 when complex **3.4** is treated with dimethylamine, methanol, or benzoic acid, loss of PMe_3 occurs with quantitative formation of the amido complex **2.17**, the alkoxo complex **2.16**, and the known carboxylate complex **3.13**,¹⁹ respectively. For comparison, of the known $\text{CpMo}(\text{NO})(=\text{CHCMe}_3)(\text{L})$ systems, only the pyridine adduct shows any degree of substitutional lability toward substrates that function as both a Lewis base and a Brønsted acid.¹⁶ Qualitatively, the rate of the tungsten reactions varies with the acidity of the organic compounds, with benzoic acid reacting immediately upon contact at ca. 10 °C, methanol in several hours at room temperature, and dimethylamine in 1–2 days at 70 °C. Substrates with moderate acidity but lack a donor function are not sufficiently reactive toward **3.4**. For example, phenylacetylene and methyl acetate, which have significantly lower pK_a values than dimethylamine, do not react.²⁶



Since the coordinatively unsaturated $[\text{Cp}^*\text{W}(\text{NO})(=\text{CHCMe}_3)]$ complex is highly reactive toward the C–H bonds of hydrocarbon solvents even in the presence of excess

PMe_3 ,¹⁸ the fact that the PMe_3 adduct **3.4** is stable upon thermolysis in benzene for several days at 70–80 °C strongly suggests that loss of PMe_3 prior to heteroatom-hydrogen bond addition is unlikely. More probable is that the reaction proceeds via an *associative* mechanism in which a *net* addition of the heteroatom-hydrogen bond across the $\text{W}=\text{C}$ bond in **3.4** occurs prior to and/or concurrently with phosphine dissociation. Since **3.4** is a coordinatively saturated, 18-electron complex, this addition reaction could occur in one of three ways: (a) by initial protonolysis of the α -carbon atom, followed by coordination of the heteroatom to tungsten and dissociation of phosphine; (b) by an $\text{S}_{\text{N}}2$ -like displacement of the phosphine as the heteroatom-hydrogen bond is added across the alkylidene functionality; or (c) by an $\eta^5\text{--}\eta^3$ ring slippage or $\eta^3\text{--}\eta^1$ NO isomerization to open a coordination site, followed by heteroatom coordination, phosphine loss, and heteroatom-hydrogen bond addition. While the above results do not allow these possibilities to be distinguished, initial protonolysis is not unreasonable for the reaction with benzoic acid, for it would explain why this substrate, which is a poorer donor than dimethylamine and methanol, reacts instantaneously upon contact.

3.3.3 Reactions of $[\text{Cp}^*\text{W}(\text{NO})(=\text{CHCMe}_3)]$ with Cyclic and Acyclic Alkenes

In addition to its reactions with Lewis bases and heteroatom-hydrogen bonds, the transient $[\text{Cp}^*\text{W}(\text{NO})(=\text{CHCMe}_3)]$ complex reacts readily with cyclic and acyclic alkenes, leading to [2+2] cycloaddition and/or C–H activation products depending upon the structure of the alkene.

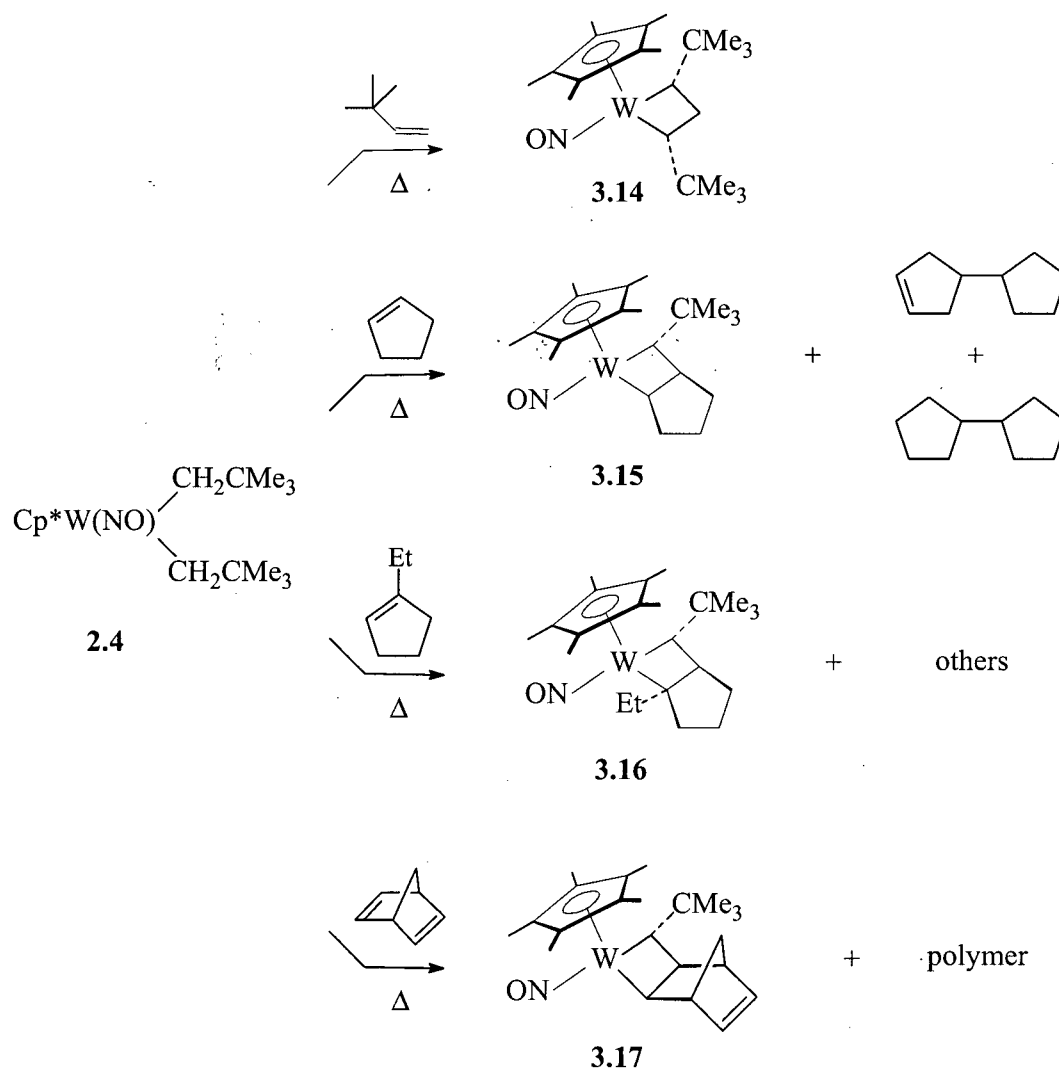
3.3.3.1 [2+2] Cycloaddition

As shown in Scheme 3.4, heating **2.4** in neohexene at 70 °C for 2 d affords the tungstacyclobutane complex **3.14** as the sole product as judged by ^1H NMR spectroscopy. Complex **3.14** is an orange-yellow solid which can be crystallized in 97% yield from hexanes/ Et_2O at –30 °C and which, in contrast to analogous acyclic bis(alkyl) complexes, is remarkably stable. For example, it is unaffected by air and moisture in the solid and solution

states and is inert to protic acids such as methanol. It is also stable to thermolysis (70 °C, 12 h) in toluene in the presence of excess PMe_3 .

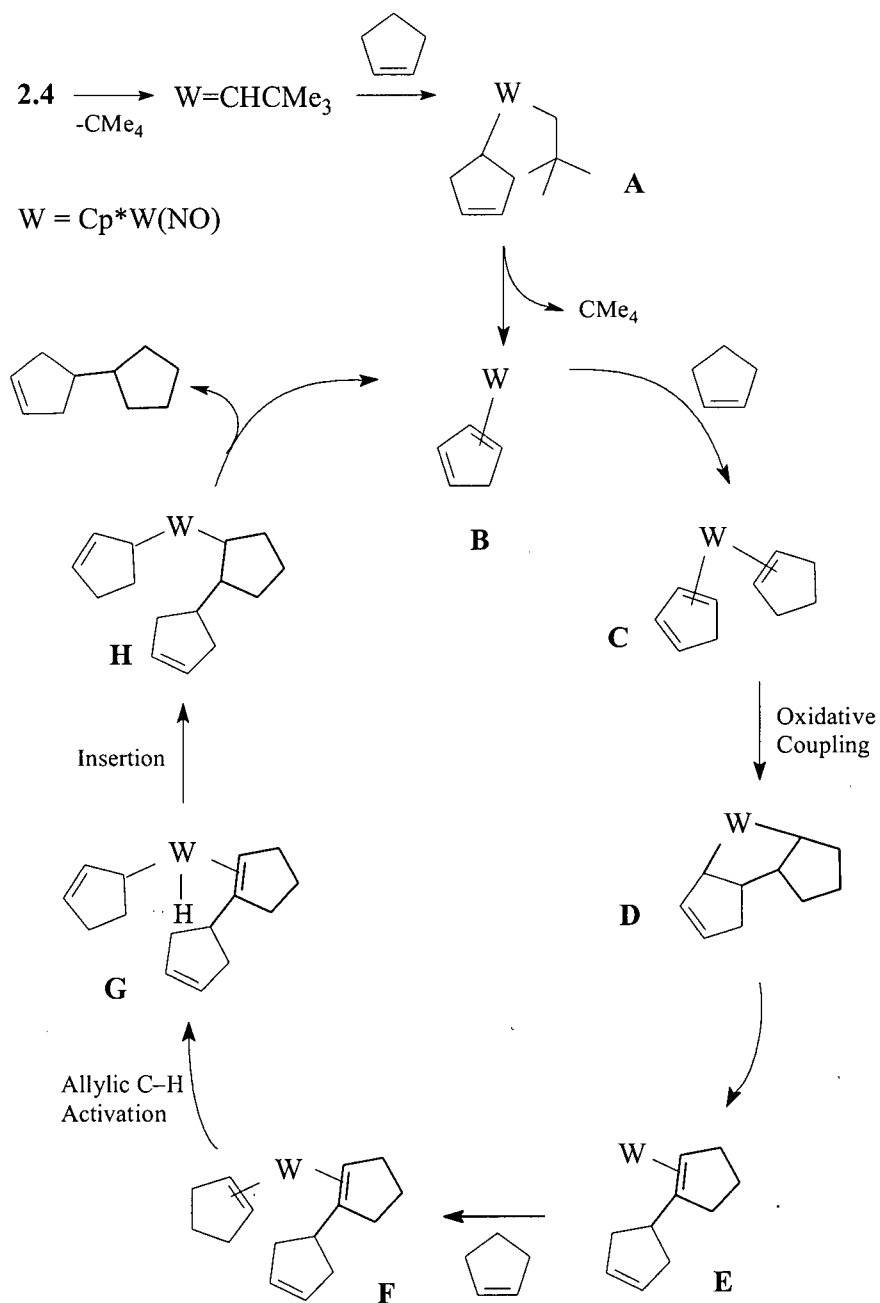
When **2.4** is heated in cyclopentene, ethylcyclopentene, or norbornadiene, the corresponding metallacycles **3.15**, **3.16**, and **3.17** are isolated in 45%, 17%, and 32% crystallized yields, respectively. These reactions, however, are accompanied by decomposition, formation of complex mixtures of organometallic side products, and formation of the following organic byproducts, which unfortunately could not be quantified. The reaction with norbornadiene, for example, is complicated by precipitation (particularly in concentrated solutions) of a white, amorphous, rubbery polymer that is presumably polynorbornadiene. This polymer is insoluble in all standard organic solvents, making its removal from the reaction vessel impossible²⁷ and the isolation of **3.17** generally difficult. In the reaction with ethylcyclopentene, no polymeric products could be detected. Instead, GC–MS analysis of the volatiles reveals the presence of two major organic products whose identity remains to be determined but whose masses (m/z 166 and 164) suggest that they are formed respectively by coupling of a neopentylidene ligand to an ethylcyclopentene molecule and by dehydrogenation of this coupled product. The mechanism of the coupling reaction is unknown, but appears *not* to involve initial [2+2] cycloaddition of ethylcyclopentene to the $[\text{Cp}^*\text{W}(\text{NO})(=\text{CHCMe}_3)]$ intermediate (see later) since the product of this metathesis process would be expected to have a mass greater than 166. Finally, in the cyclopentene reaction, neither polymers nor coupled products analogous to those generated in the ethylcyclopentene reaction could be detected. Instead, products consistent with the dimerization of cyclopentene are observed. Thus, GC–MS analysis of the volatiles reveals the presence of 3-cyclopentylcyclopentene (m/z 136) and 1,1'-bicyclopentyl (m/z 138) as the major organic species. These were identified by comparison of their mass spectral fragmentation patterns with those of authentic samples reported in the literature.²⁰

Scheme 3.4



A plausible mechanism for the formation of 3-cyclopentylcyclopentene is shown in Scheme 3.5. The initial step is addition of a methylene C–H bond of cyclopentene (most likely at the allylic position based on results described below) across the $\text{W}=\text{C}$ bond of $[\text{Cp}^*\text{W}(\text{NO})(=\text{CHCMe}_3)]$. This leads to the neopentyl cyclopentenyl intermediate **A**, which undergoes β -H abstraction to form the 16-electron alkene complex **B**. A catalytic cycle then

Scheme 3.5



ensues, which involves formation of the metallacyclopentane complex **E** by coordination and subsequent oxidative coupling of a second molecule of cyclopentene. Complex **E** then undergoes β -H abstraction, followed by allylic C-H activation of a third molecule of cyclopentene to give **G**. Alkene insertion into the W-H bond of **G** then yields intermediate **H**. From **H**, 3-cyclopentylcyclopentene is liberated and **B** regenerated upon β -H abstraction. The formation of cyclopentene trimers is not observed presumably because coupling between a monomer and a dimer is sterically unfavorable.

Like **3.14**, complexes **3.15–3.17** are orange, sparingly to moderately soluble in aliphatic hydrocarbon solvents, and stable indefinitely at 25 °C under dinitrogen. They also can be handled for long periods in air and, in the case of **3.15**, heated in C_6D_6 for 12 h at 70 °C, without noticeable decomposition. Spectroscopically, the metallacyclobutane ligands of **3.14–3.17** are all similar; the 1H and ^{13}C NMR spectra of **3.16** in $CDCl_3$ are shown in Figure 3.2 as representative examples. Like the vast majority of early transition-metal metallacyclobutane complexes,²⁸ the H_β and C_β resonances of **3.14–3.17** are found upfield in the range δ -2.29 to -0.12 and δ -4.8 to 27.4, respectively, while downfield shifts are observed for the H_α and C_α resonances at δ 3.09–7.68 and δ 113.2–141.8. The presence of a plane of symmetry in complex **3.14** is indicated by the observation of identical *tert*-butyl groups and a single WCH signal in the 1H and ^{13}C NMR spectra. That the *tert*-butyl groups point away from the Cp* ligand has been confirmed by an NOE difference experiment, which shows a strong enhancement of the H_α resonance upon irradiation of the Cp* signal, and vice versa. In the 1H NMR spectrum of **3.14**, the H_α resonance appears as a doublet of doublets with $^3J_{HH} = 6.0$ and 10.2 Hz due to coupling to the *trans*- and *cis*- β protons, respectively. In **3.15**, **3.16**, and **3.17**, the $^3J_{HH}$ coupling constants between the $CHCMe_3$ and β protons are 5.1–7.2 Hz, suggesting that they are *trans* to one another. Similar *cis*- and *trans*-coupling constants have been reported previously for other metallacyclobutane systems.^{28b}

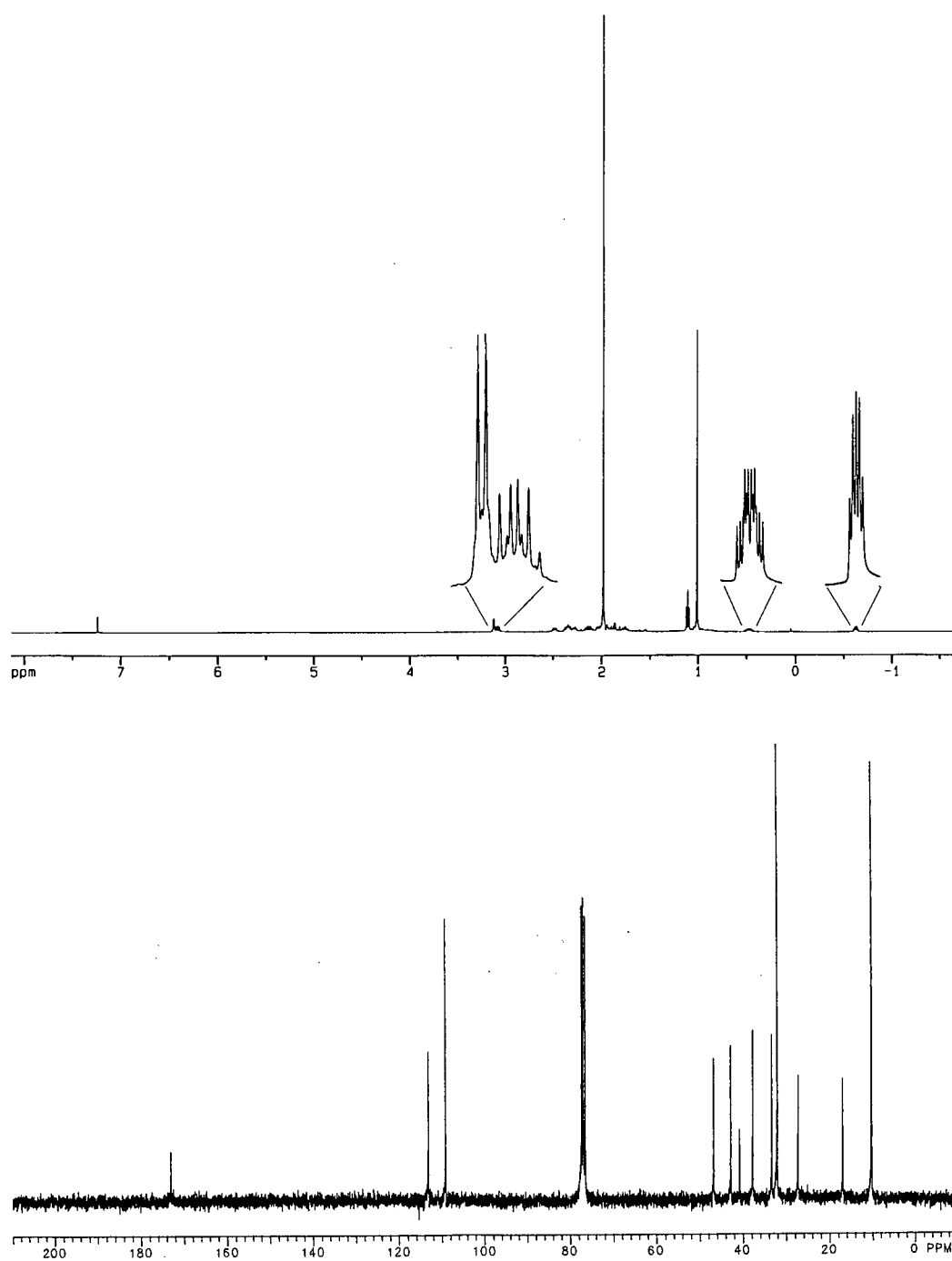


Figure 3.2. 500-MHz ¹H and 75-MHz ¹³C{¹H} NMR spectra of **3.16** in CDCl₃.

Complexes **3.14**–**3.17** are the first Cp'M(NO)-containing metallacyclobutanes to be synthesized, a class of compounds which to date cannot be accessed by traditional metathesis routes.²⁹ In order to confirm the stereochemical assignments and to gain detailed structural information of these compounds, the solid-state molecular structures of **3.14**, **3.15**, and **3.17** were established by X-ray diffraction studies. Shown in Figure 3.2 are the ORTEP representations of these structures; selected bond distances and angles are listed in Table 3.2. As expected from the NMR experiments, the *tert*-butyl groups in **3.14** are *cis* to one another, while the *tert*-butyl groups in **3.15** and **3.17** are *trans* to the β -substituents. For all three complexes, the NO ligand is essentially linear while the tungstacyclic ring is nearly planar and symmetric. Noteworthy is that the majority of the metrical parameters of the tungstacyclic rings in **3.14**, **3.15**, and **3.17** are virtually identical (Figure 3.2). The W–C $_{\alpha}$ –C $_{\beta}$ –C $_{\alpha}$ torsion angles are 10.3(4)°, –0.3(4)°, and –7.5(3)°, respectively, while the W–C $_{\alpha}$ (2.071–2.098 Å) and W...C $_{\beta}$ (2.37 Å) distances and C $_{\alpha}$ –W–C $_{\alpha}$ angles (84–85°) are in the range often observed for d⁰ tungstacyclobutane complexes.^{28a,30} The most unusual aspects of the tungstacyclic rings are the C $_{\alpha}$ –C $_{\beta}$ bond distances. In **3.14**, these distances (1.63 Å) lie at the long end of the range found for transition-metal metallacyclobutane complexes (1.54–1.63 Å). In **3.15** and **3.17**, the C $_{\alpha}$ –C $_{\beta}$ distances belonging to the alkene fragment are 1.702(6) and 1.671(7) Å, respectively, and are the longest reported to date.

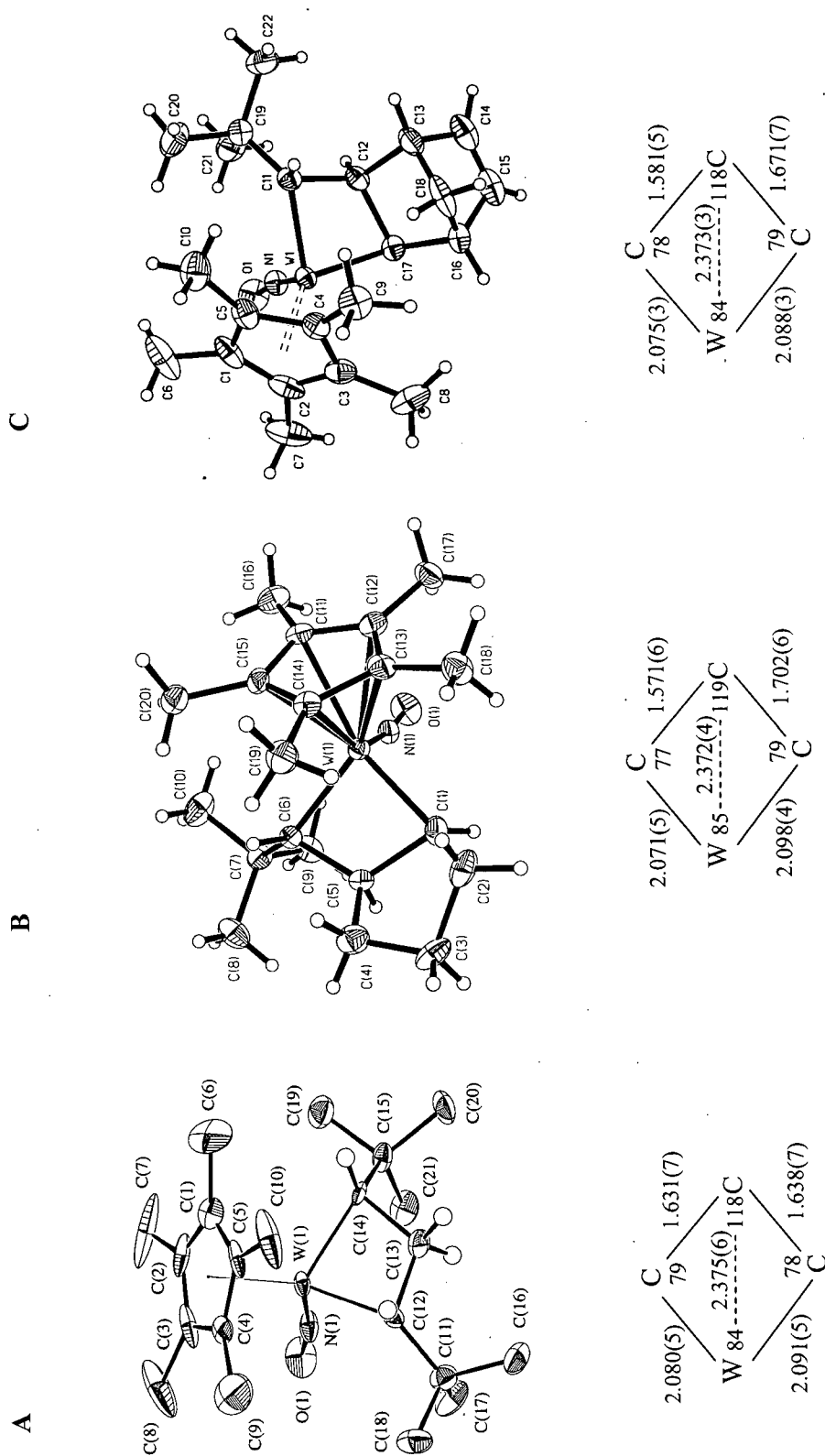


Figure 3.3. ORTEP diagrams and bonding parameters for the tungstacyclic rings of (A) $\text{Cp}^*\text{W}(\text{NO})[\text{CH}(\text{CMe}_3)\text{CH}_2\text{CH}(\text{CMe}_3)]$ (3.14), (B) $\text{Cp}^*\text{W}(\text{NO})[\text{CH}(\text{CMe}_3)\text{CH}(\text{C}_3\text{H}_6)\text{CH}]$ (3.15), and (C) $\text{Cp}^*\text{W}(\text{NO})[\text{CH}(\text{CMe}_3)\text{CH}(\text{C}_5\text{H}_6)\text{CH}]$ (3.17)

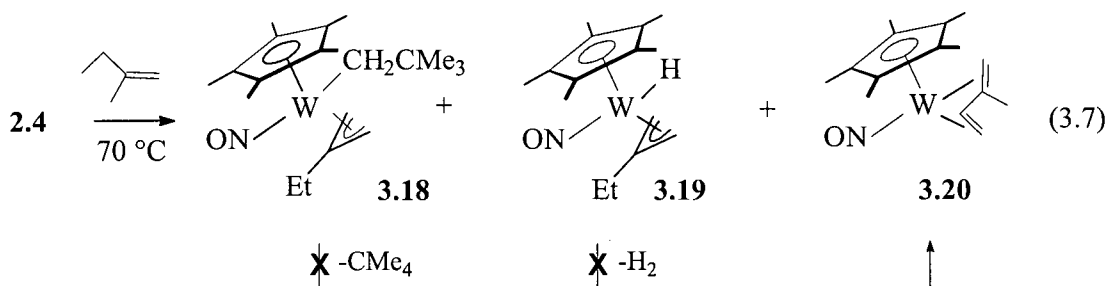
Table 3.2. Selected Bond Distances and Angles for **3.14**, **3.15**, and **3.17**

3.14		3.15		3.17	
Bond Distances (Å)					
N(1)–O(1)	1.230(5)	N(1)–O(1)	1.239(5)	N(1)–O(1)	1.227(3)
W(1)–N(1)	1.767(4)	W(1)–N(1)	1.763(4)	W(1)–N(1)	1.771(3)
W(1)–C(12)	2.091(5)	W(1)–C(6)	2.098(4)	W(1)–C(11)	2.088(3)
W(1)–C(14)	2.080(5)	W(1)–C(1)	2.071(5)	W(1)–C(17)	2.075(3)
W(1)–C(13)	2.375(6)	W(1)–C(5)	2.372(4)	W(1)–C(12)	2.373(3)
C(12)–C(13)	1.638(7)	C(5)–C(6)	1.571(6)	C(11)–C(12)	1.581(5)
C(13)–C(14)	1.631(7)	C(1)–C(5)	1.702(6)	C(12)–C(17)	1.671(5)
Bond Angles (°)					
O(1)–N(1)–W(1)	168.3(4)	O(1)–N(1)–W(1)	169.0(3)	O(1)–N(1)–W(1)	168.7(3)
C(12)–W(1)–C(14)	84.3(2)	C(1)–W(1)–C(6)	85.0(2)	C(11)–W(1)–C(17)	84.13(12)
W(1)–C(12)–C(13)	78.1(3)	W(1)–C(1)–C(5)	77.2(2)	W(1)–C(11)–C(12)	79.3(2)
W(1)–C(14)–C(13)	78.6(3)	W(1)–C(6)–C(5)	79.1(2)	W(1)–C(17)–C(12)	77.8(2)
C(12)–C(13)–C(14)	117.8(4)	C(1)–C(5)–C(6)	118.7(4)	C(11)–C(12)–C(17)	118.1 (3)
W(1)–C(12)–C(11)	133.5(3)	W(1)–C(6)–C(7)	131.5(3)	W(1)–C(11)–C(19)	132.0(2)

3.3.3.2 C–H Bond Activation

In contrast to the alkene reactions described above, the thermolysis of **2.4** in acyclic alkenes possessing allylic C–H bonds leads primarily to C–H bond activation products. For example, thermolysis of **2.4** in neat 2-methyl-1-butene at 70 °C for 2 d results in formation of a 6:5:4 mixture of the η^3 -allyl neopentyl complex **3.18**, η^3 -allyl hydride complex **3.19**, and η^4 -*trans*-diene complex **3.20** along with several intractable Cp*-containing products, which do not display NMR resonances characteristic of metallacyclobutane complexes (eq 3.7). GC–MS analysis of the volatile products shows neopentane and a barely detectable compound whose mass equals the sum of a neopentylidene ligand and a 2-methyl-1-butene molecule.

Monitoring of the reaction by ^1H NMR spectroscopy reveals that **3.18**–**3.20** are formed in a final combined yield of 60–70% and in a constant ratio over the course of the reaction. Complexes **3.18**–**3.20** can be heated in 2-methyl-1-butene, 2-methyl-2-butene, or benzene at 70–80 °C for 3–4 d without decomposition, rearrangement, or reaction with the solvent. These observations thus demonstrate that these complexes are thermally robust and are produced by independent pathways.

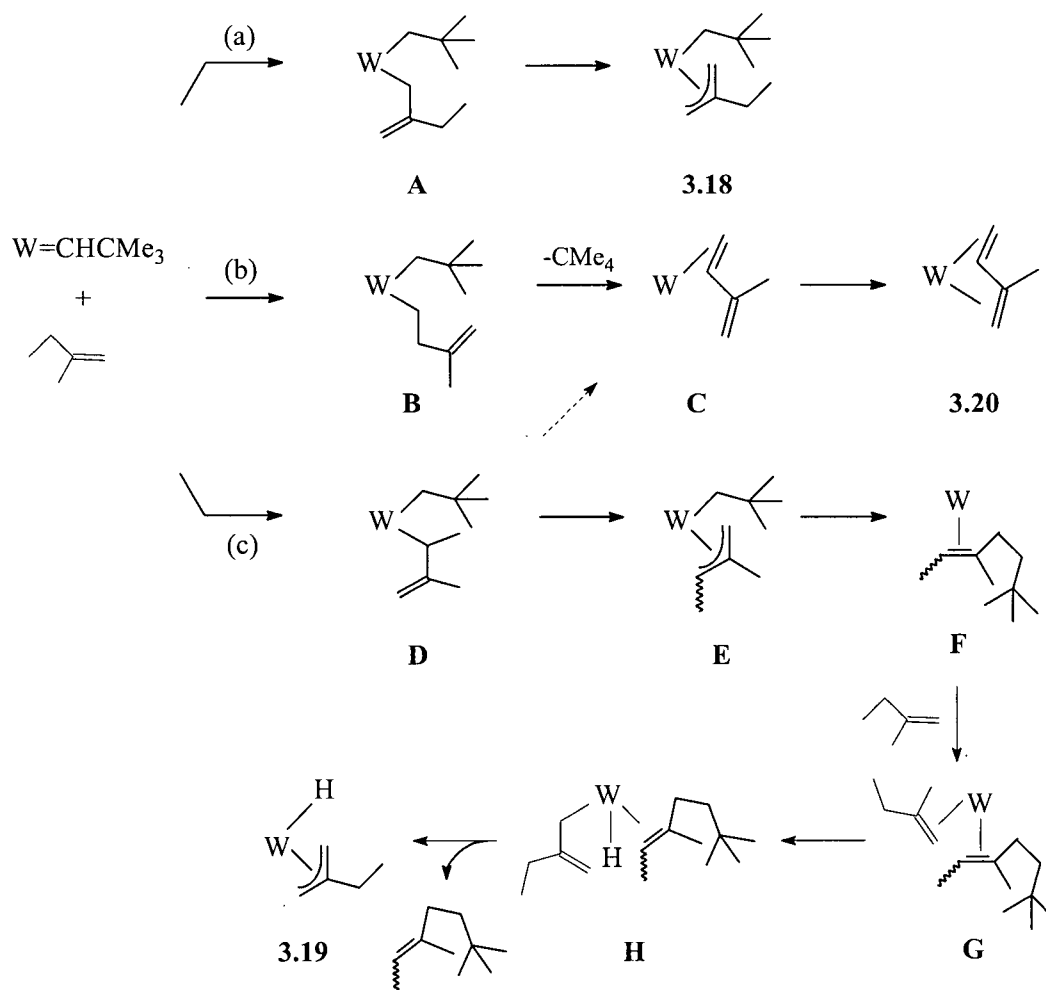


Complex **3.18** is a sticky off-white solid whose formation is consistent with initial allylic C–H activation by $[\text{Cp}^*\text{W}(\text{NO})(=\text{CHCMe}_3)]$, followed by an η^1 - to η^3 -allyl conversion as shown in Scheme 3.6a. Although highly soluble in hydrocarbon solvents, **3.18** can be isolated in 20% yield by chromatography on alumina I, followed by painstaking crystallization from pentane/Et₂O at –30 °C. It can also be fully characterized by spectroscopic and analytical techniques. In addition to resonances attributable to the Cp* and neopentyl ligands, the ^1H and ^{13}C NMR spectra of **3.18** display characteristic patterns indicative of the presence of an η^3 -allyl moiety.³¹ Due to the chirality at the metal center, two sets of diastereotopic syn and anti proton resonances are observed in the ^1H NMR spectrum; these appear at δ 2.22 and 3.64 and δ 0.75 and 1.89, respectively. In the $^{13}\text{C}\{^1\text{H}\}$ NMR spectrum, the terminal carbons resonate at δ 42.5 and 74.2, while the signal for the central carbon appears at δ 135.6. An endo conformation was assigned based on the results of an ^1H NOE difference experiment, which shows a strong enhancement of the Cp* signal upon irradiation of the signal for the anti proton at δ 0.75. This assignment is consistent with the observation that the anti protons, being closer to the Cp* ligand, are more shielded and therefore resonate at higher field than the syn protons.

In contrast to **3.18**, the η^3 -allyl hydride and η^4 -*trans*-diene complexes **3.19** and **3.20** could not be isolated free of **3.18** and each other. They were therefore identified on the basis of IR and $^1\text{H}/^{13}\text{C}$ NMR spectroscopies, aided by HMQC and COSY experiments. Spectroscopically, **3.20** is very similar to the previously reported $\text{CpMo}(\text{NO})(\text{trans-}\eta^4\text{-2-methylbutadiene})^{32}$ complex. Of note are the upfield shifts of the diene protons at δ 0.95, 1.1, 2.3, and 3.29, which are indicative of not only η^4 -bonding but also significant π -backbonding from the tungsten metal. For complex **3.19**, its IR and NMR characteristics are similar to those of the $\text{Cp}^*\text{W}(\text{NO})(\eta^3\text{-allyl})(\text{H})$ complexes described in Chapter 4. Key to its structural assignment as a hydride complex is a weak W–H stretch at 1888 cm^{-1} in the Nujol-mull IR spectrum and a singlet integrating for one proton at δ -0.88 ($^1J_{\text{WH}} = 118\text{ Hz}$) in the ^1H NMR spectrum (C_6D_6).

The formation of complex **3.20** presumably occurs by initial C–H bond cleavage at the non-allylic methyl and/or (though less likely) the allylic methylene carbon, followed by β -abstraction and coordination of the pendant C=C bond (Scheme 3.6b). The formation of complex **3.19**, on the other hand, can be rationalized by the reaction sequence shown in Scheme 3.6c. According to this multistep mechanism, which also yields an organic byproduct whose mass equals the sum of a neopentylidene ligand and a 2-methyl-1-butene molecule, allylic C–H activation at the methylene position, followed by η^1 - to η^3 -allyl conversion first takes place to yield an η^3 -allyl neopentyl intermediate **E**. In order to relieve allylic strain due to substitution at the terminal carbon, **E** rearranges to alkene adduct **F** by a reductive C–C coupling process similar to that proposed recently by Ipaktschi and coworkers for the conversion of $\text{CpW}(\text{NO})(\eta^3\text{-allyl})(\eta^1\text{-alkynyl})$ complexes to η^2 -alkene- η^2 -allene complexes.^{29b} **F** then reacts with another equivalent of 2-methyl-1-butene to yield **3.19** via a reaction pathway analogous to that proposed above for the formation of 3-cyclopentylcyclopentene. An exception is that formation of the η^1 -allyl-hydride- η^2 -alkene complex **H** is followed by η^1 - to η^3 -allyl conversion with concomitant displacement of the alkene ligand rather than by insertion of the alkene into the W–H bond. This proposed mechanism assumes that (1) allylic C–H activation of the alkene ligand in **F** is slow compared to coordination of a second molecule of 2-methyl-1-butene and (2) for steric reasons, allylic C–H activation of the 2-

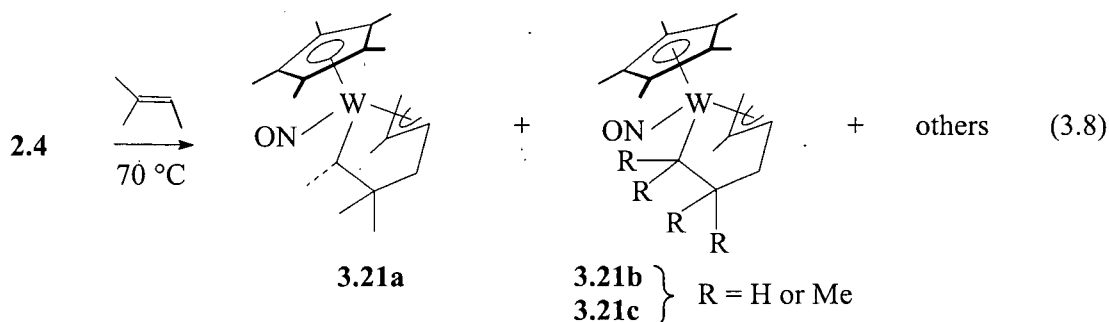
Scheme 3.6



methyl-1-butene ligand in **G** is faster than allylic C–H activation of the trisubstituted alkene as well as alkene-alkene coupling.

The thermolysis of **2.4** in neat 2-methyl-2-butene at 70 °C for 2 d, in contrast, is cleaner than the 2-methyl-1-butene reaction. It affords neopentane as the only detectable organic byproduct and shows little evidence, if any, in the ^1H NMR spectrum of the crude reaction mixture for formation of allyl neopentyl, allyl hydride, or diene complexes as described above. It produces instead a mixture of three major organometallic products in

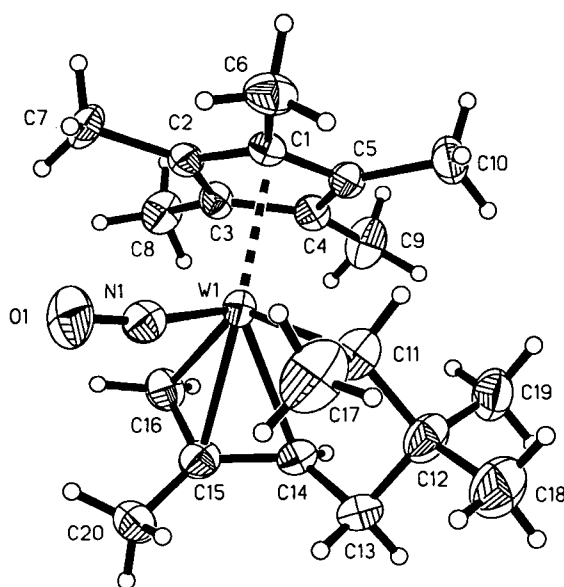
70–80% yield in a ratio of ~10:5:4, the most abundant of which is $\text{Cp}^*\text{W}(\text{NO})[\eta^4\text{-CH}_2\text{C}(\text{Me})\text{CHCH}_2\text{C}(\text{Me})_2\text{CH}(\text{Me})]$ (**3.21a**) in which two molecules of 2-methyl-2-butene have coupled (eq 3.8).



Neither complex **3.21a** nor the second (**3.21b**) and third (**3.21c**) products could be separated from one another. All three compounds were therefore characterized as a mixture, obtained by crystallization from a concentrated pentane solution of the crude products at $-30\text{ }^\circ\text{C}$. The identity of **3.21a** was established on the basis of ^1H and ^{13}C NMR spectroscopies, aided by COSY, HMQC, HMBC, and NOE difference experiments, and confirmed by X-ray diffraction. In its ^1H NMR spectrum, **3.21a** gives rise to 11 signals due to the 11 different types of protons. Most prominent are the signals at δ 1.50 due to the W–CH proton and at δ 0.41, 1.98, and 2.66 due to the CH_2 and CH protons of the $\eta^3\text{-CH}_2\text{C}(\text{Me})\text{CH}$ moiety. In the ^{13}C NMR spectrum, the corresponding carbon resonances are found at δ 42.2, 44.4, and 90.6.

Shown in Figure 3.4 is an ORTEP diagram of the solid-state molecular structure of **3.21a** along with selected bond distances and angles. As expected from the NMR experiments, the structure contains a $[\text{CH}(\text{CH}_3)\text{C}(\text{CH}_3)_2\text{CH}_2\text{CH}(\text{CH}_3)\text{CH}_2]$ ligand, bonded by a W–alkyl and a W– η^3 -allyl interaction. Noteworthy are the following two features. First, the W–C(11) distance ($2.307(7)\text{ \AA}$) is at the long end of the range for W–C single bonds. Second, the allyl moiety is coordinated in an endo, syn fashion and shows no $\eta^3 \rightarrow \sigma, \eta^2$ distortion typically observed in $(\eta^3\text{-allyl})(\text{nitrosyl})$ tungsten and -molybdenum systems such as $\text{CpM}(\text{NO})(\eta^3\text{-allyl})(\text{halide})$ [$\text{M} = \text{Mo},^{33} \text{W}^{34}$], $\text{CpW}(\text{NO})(\eta^3\text{-allyl})(\eta^1\text{-alkynyl})$,^{29b} and

TpMo(NO)(η^3 -allyl)(CO).³⁵ That the latter is the case is evidenced by the fact that the C(14)–C(15) (1.396(9) Å) and C(15)–C(16) (1.420(9) Å) distances are similar and in the range intermediate of double and single bonds. A reasonable explanation for this is that **3.21a** is sufficiently electron-rich to allow the metal to back-donate to both allylic C–C bonds.



N(1)–O(1)	1.225(6) Å
W(1)–N(1)	1.765(5) Å
W(1)–C(11)	2.307(7) Å
W(1)–C(16)	2.239(6) Å
W(1)–C(15)	2.372(6) Å
W(1)–C(14)	2.382(6) Å
C(15)–C(16)	1.420(9) Å
C(14)–C(15)	1.396(9) Å
O(1)–N(1)–W(1)	170.7(5)°
C(12)–C(11)–W(1)	114.8(4)°
C(14)–C(15)–C(16)	113.8(6)°
C(15)–C(14)–C(13)	127.5(6)°

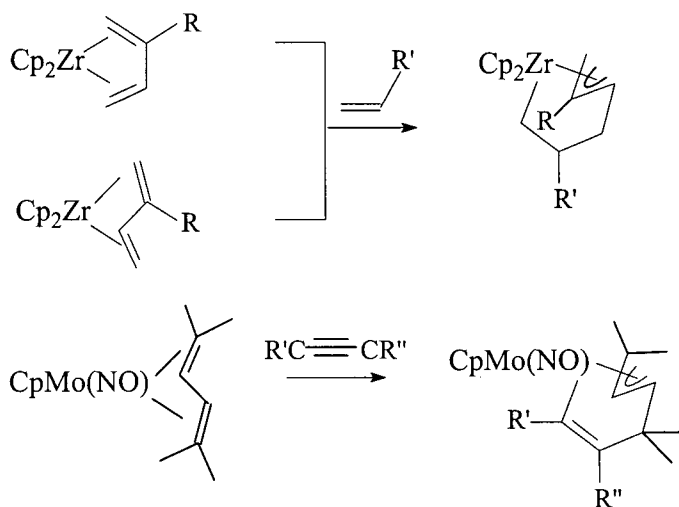
Figure 3.4. ORTEP diagram and selected bond distances and angles of complex Cp*W(NO)[η^4 -CH₂C(Me)CHCH₂C(Me)₂CH(Me)] (**3.21a**).

For complexes **3.21b** and **3.21c**, complete assignment of their ¹H and ¹³C NMR resonances, unfortunately, proves not possible due to severe spectral overlap. Nevertheless, both compounds appear to be isomers of **3.21a** on the basis of the following observations. First, their NMR and IR spectroscopic data are, for the most part, similar to those of **3.21a** (see the Experimental Section). For example, that each complex also contains an η^3 -CH₂C(Me)CH moiety is clearly indicated by the presence of CH₂ and CH signals in the ¹H NMR spectrum at δ 0.38, 2.08, and 2.67 for **3.21b** and δ 0.49, 2.36, and 2.05 for **3.21c** and by the presence of the corresponding carbon resonances in the ¹³C NMR spectrum at δ 42.6 and 96.1 for **3.21b** and δ 48.1 and 76.6 for **3.21c**. Second, the solubility properties of all three complexes are very

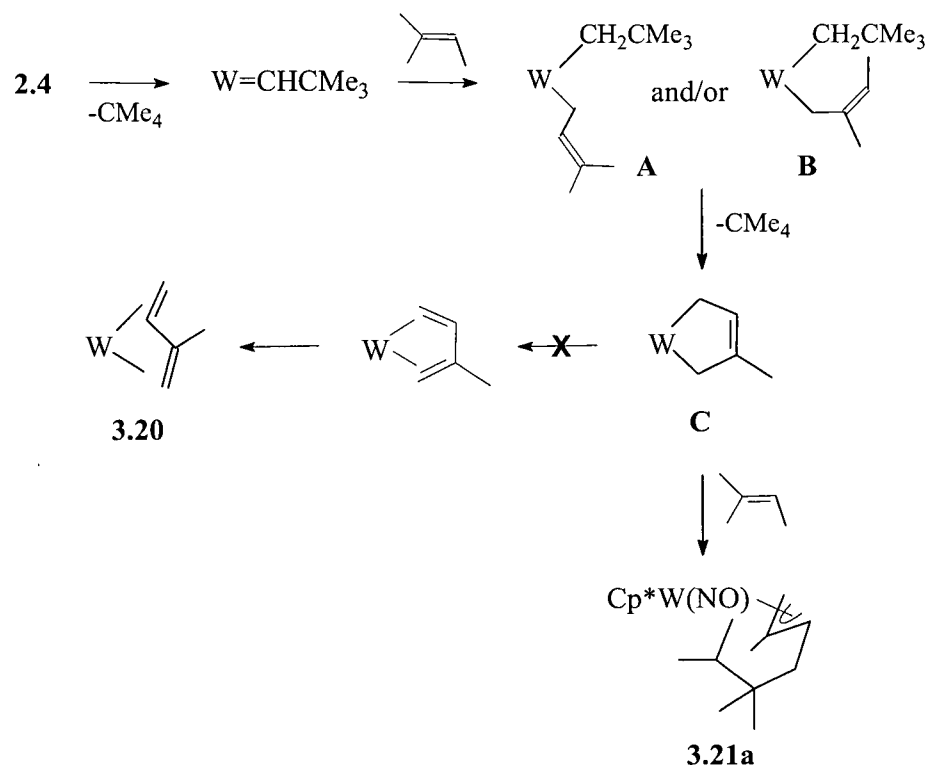
similar, as evidenced by the fact that they cannot be separated from one another by column chromatography and/or fractional crystallization. Third, elemental analysis and mass spectral data of a 1.9:1:1 mixture of **3.21a**, **3.21b**, and **3.21c** are consistent with the formula shown in eq 3.8.

Complexes **3.21a-c** are yellow, air-stable crystalline materials that can be heated in C_6D_6 at 70 °C without further transformation. Structurally, **3.21a-c** are related to the zirconocene and the $CpMo(NO) \eta^4(\sigma, \eta^3)$ -allyl complexes shown in Scheme 3.7, prepared by reaction of the *cis*- and *trans*- $Cp_2Zr(\eta^4$ -diene) complexes with alkenes³⁶ and of the $CpMo(NO)(\eta^4$ -2,5-dimethyl-2,4-hexadiene) complex with alkynes.³⁷ Taking into account the reactivity of these diene compounds, the formation of **3.21a** is proposed to proceed via the reaction sequence shown in Scheme 3.8. The initial step is allylic C–H activation leading to the η^1 -allyl neopentyl complexes **A** and/or **B**, which subsequently cyclometallate by a δ -elimination process to give the metallacyclopentene complex **C**. Rapid insertion of a second equivalent of 2-methyl-2-butene into the sterically less hindered W–C bond of **C** would then afford **3.21a**.

Scheme 3.7



Scheme 3.8



The proposal that **A** and/or **B** is unstable with respect to cyclometallation and formation of a five-membered tungstacycle, which can undergo further transformation in the presence of a Lewis base, is not unprecedented. Indeed, previous studies have shown that the bis(alkyl) complex, $\text{CpW}(\text{NO})(\text{CH}_2\text{SiMe}_3)(\text{CH}_2\text{CMe}_2\text{Ph})$, also cyclometallates readily under thermolytic conditions in the presence of PMe_3 to give the orthometallated complex $\text{CpW}(\text{NO})(\text{CH}_2\text{CMe}_2\text{-}o\text{-C}_6\text{H}_4)(\text{PMe}_3)$.³⁸ That this reaction proceeds via a metallacyclopentane intermediate will be demonstrated in Chapter 5 for the thermal decomposition of the Cp^* neopentyl neophyl derivative. Finally, since signals for complex **3.20** are not observed in the ^1H NMR spectrum of the crude reaction mixture and since **3.20** is thermally stable in the presence of 2-methyl-2-butene, isomerization of **C** to **3.20** followed by 2-methyl-2-butene insertion in a manner analogous to the CpMo system can be ruled out.

In contrast to **2.4**, the thermolysis of **2.1** in neat alkenes such as cyclopentene gives complex mixtures of products along with decomposition and formation of a brown-black precipitate. The $\text{CpMo}(\text{NO})(\text{CH}_2\text{CMe}_3)_2$ complex, on the other hand, shows little or no reactivity toward alkenes.^{15b}

3.4 Epilogue

In summary, $\text{Cp}'\text{W}(\text{NO})(\text{CH}_2\text{CMe}_3)_2$ and $\text{Cp}^*\text{W}(\text{NO})(\text{CH}_2\text{CMe}_3)(\text{CH}_2\text{Ph})$ complexes are thermally unstable with respect to α -abstraction of neopentane. This leads to the transient 16-electron alkylidene complexes $[\text{Cp}'\text{W}(\text{NO})(=\text{CHCMe}_3)]$ and $[\text{Cp}^*\text{W}(\text{NO})(=\text{CHPh})]$, respectively, which differ from the $[\text{CpMo}(\text{NO})(=\text{CHCMe}_3)]$ system in a number of ways.¹⁵ Notable differences and trends that emerge upon comparison of the trapping reactions of the neopentylidene systems with Lewis bases (L) are as follows. First, the rate of α -abstraction decreases significantly when the metal is changed from Mo to W and when Cp is replaced by Cp^* , though to a lesser extent. Second, only one ^1H NMR resonance is observed for the α -protons of the tungsten alkylidene complexes, indicating the presence of only the anti rotamer. Third, the tungsten complexes do not undergo dimerization in the absence of L, as observed for the CpMo system. Fourth, the trapping of $[\text{Cp}'\text{W}(\text{NO})(=\text{CHCMe}_3)]$ is markedly sensitive to the nature of L, favoring sterically undemanding and strong σ -donors such as phosphines, phosphites, and, in the case of the Cp^* system, amines. It is also strongly dependent on the choice of solvent. For example, when L = phosphine or phosphite, THF or 2,2,4,4-tetramethylpentane may be used as solvents with little or no deleterious effects. When L = amine, clean adduct formation is observed only when the amine also functions as the solvent. Fifth, the stability of the tungsten ligand-trapped complexes is sensitive to the nature of both L and Cp' , decreasing as the size and electron-donating ability of L increases and decreases, respectively, and as Cp' is changed from Cp^* to Cp. Finally, the syn-anti isomerization of the tungsten adducts can be effected photochemically but not thermally, as has been reported for the molybdenum counterparts.

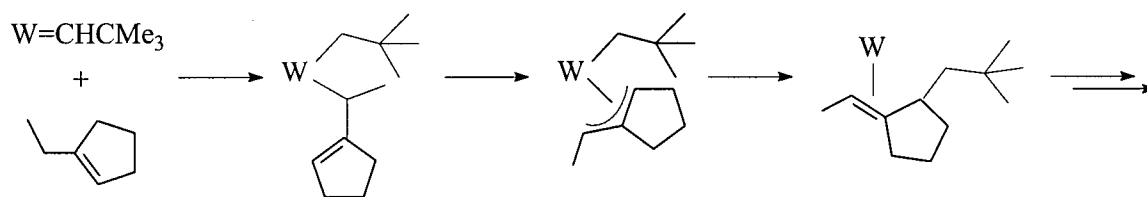
The thermal reactions of the $\text{Cp}'\text{W}(\text{NO})(\text{CH}_2\text{CMe}_3)_2$ complexes with a variety of heteroatom–hydrogen bonds has also been investigated. The reaction with dimethylamine demonstrates that $[\text{Cp}'\text{W}(\text{NO})(=\text{CHCMe}_3)]$ species are initially generated, which then effect the cleavage of the amine N–H bond to give cleanly the neopentyl amides **3.12** and **2.17**. With more acidic substrates such as methanol and benzoic acid, protonolysis of the bis(neopentyl) precursors occurs before generation of the $[\text{Cp}'\text{W}(\text{NO})(=\text{CHCMe}_3)]$ intermediates can take place.

Complexes **3.12** and **2.17** alternatively can be prepared by thermolysis of the PMe_3 -trapped alkylidene complexes $\text{Cp}'\text{W}(\text{NO})(=\text{CHCMe}_3)(\text{PMe}_3)$ in the presence of excess dimethylamine. When $\text{Cp}^*\text{W}(\text{NO})(=\text{CHCMe}_3)(\text{PMe}_3)$ is treated with methanol or benzoic acid, formation of the corresponding neopentyl alkoxide complex **2.16** and neopentyl carboxylate complex **3.13** is observed. Qualitatively, the rates of these reactions increase as the acidity of the organic substrates increases. The reaction of $\text{Cp}'\text{W}(\text{NO})(=\text{CHCMe}_3)(\text{PMe}_3)$ complexes with heteroatom-hydrogen bonds most likely involves an associative mechanism rather than a mechanism analogous to that previously proposed for $\text{CpMo}(\text{NO})(=\text{CHCMe}_3)(\text{Py})$, i.e. initial loss of PMe_3 , followed by N–H or O–H addition across the $\text{W}=\text{C}$ bond. This is based on the fact that all $\text{Cp}'\text{W}(\text{NO})(=\text{CHCMe}_3)(\text{L})$ complexes, including the amine adducts, are stable to thermolysis (70 °C, 1–4 d) in neat hydrocarbon solvents. If dissociation of L to form coordinatively unsaturated $[\text{Cp}'\text{W}(\text{NO})(=\text{CHCMe}_3)]$ were facile, then C–H bond activation of these solvents should be observed, as demonstrated recently in a communication¹⁸ of the reaction of $[\text{Cp}^*\text{W}(\text{NO})(=\text{CHCMe}_3)]$ with alkanes (full details of which are described in Chapters 4 and 5).

The thermal reactivity of the coordinatively unsaturated $[\text{Cp}'\text{W}(\text{NO})(=\text{CHCMe}_3)]$ complexes with alkenes has also been examined. This work demonstrates that, unlike the CpMo system which shows essentially no reactivity toward alkenes, both the CpW and Cp^*W complexes are reactive toward these substrates; only the Cp^*W complex yields tractable products, however. $[\text{Cp}^*\text{W}(\text{NO})(=\text{CHCMe}_3)]$ reacts with cyclic and acyclic alkenes to yield [2+2] cycloaddition and/or C–H activation products depending on the alkene structure.

Reactions with neohexene, cyclopentene, ethylcyclopentene, and norbornadiene give the tungstacyclobutane complexes **3.14**–**3.17**, respectively (Scheme 3.4). The formation of **3.14** is quantitative and indicative of a regio- and stereospecific [2+2] cycloaddition reaction. The formation of **3.15**–**3.17**, in contrast, is accompanied by side product formation and decomposition. In the norbornadiene reaction, an insoluble white rubber, presumably polynorbornadiene, is also produced. The reaction with cyclopentene, which contains unhindered allylic C–H bonds, yields 3-cyclopentylcyclopentene and 1,1'-bicyclopentyl as the major organic products. The formation of 3-cyclopentylcyclopentene can be rationalized by the multistep mechanism shown in Scheme 3.5. According to this mechanism, the key initial step is addition of a methylene C–H bond of cyclopentene (most likely at the allylic position) across the W=C bond of $[\text{Cp}^*\text{W}(\text{NO})(=\text{CHCMe}_3)]$. This leads to a mixed bis(alkyl) complex which can undergo further transformation in the presence of cyclopentene to give the observed product. The reaction with ethylcyclopentene, in contrast, yields two organic compounds whose masses strongly suggest that they are not formed by metathesis pathways but rather by coupling of a neopentylidene ligand to an ethylcyclopentene molecule and by a dehydrogenation of this coupled product.

The coupling of an alkylidene ligand to an alkene molecule via a non-metathesis route is extremely rare but not unprecedented. An example is the reactions of the neopentylidene complexes $\text{CpM}(=\text{CHCMe}_3)\text{Cl}_2$ ($\text{M} = \text{Ta}, \text{Nb}$) with terminal alkenes.³⁹ In this case, Schrock and coworkers showed that these reactions lead to new alkene products, formed by *selective insertion* of the neopentylidene ligand into an olefinic C–H bond of the alkene substrate. Although the identity of the organic products in the reaction of $[\text{Cp}^*\text{W}(\text{NO})(=\text{CHCMe}_3)]$ with ethylcyclopentene is unknown, it is unlikely that they are formed by a similar insertion process. This is especially so given the fact that cyclopentene, which is structurally more similar to ethylcyclopentene, does not give rise to such products, whereas acyclic 2-methyl-1-butene does. A common feature of ethylcyclopentene and 2-methyl-1-butene is the presence of an ethyl group at the double bond. Since the coupling of a neopentylidene ligand to a 2-methyl-1-butene molecule can be rationalized by a mechanism involving initial allylic C–H bond activation at the methylene position (Scheme 3.6c), an analogous proposed mechanism such as that shown below may be invoked for the ethylcyclopentene reaction.



Unlike neohexene and the cycloalkenes above, the reactions of $[Cp^*W(NO)(=CHCMe_3)]$ with acyclic alkenes containing allylic hydrogens are dominated by C–H bond activation pathways. In fact, no tungstacyclobutane complexes are detected from the reaction of this species with 2-methyl-1-butene. Instead, the major organometallic products are allyl neopentyl complex **3.18**, allyl hydride complex **3.19**, and diene complex **3.20** (eq 3.7). A small amount of an organic product whose mass equals the sum of a neopentylidene ligand and a molecule of 2-methyl-1-butene is also generated. The reaction of $[Cp^*W(NO)(=CHCMe_3)]$ with 2-methyl-2-butene similarly proceeds primarily by allylic C–H activation. However, unlike the 2-methyl-1-butene reaction, this leads to formation of the six-membered metallacycles **3.21a–c** as the major products (eq 3.8), formed by an unusual coupling of two molecules of 2-methyl-2-butene.

The formation of complexes **3.18–3.21** is significant, for it represents the first clear-cut examples of alkene C–H bond activation by a transition-metal alkylidene complex.⁴⁰ Further, it shows that activation of allylic C–H bonds is preferred, as would be expected on the basis of bond dissociation energies,⁴¹ and that allylic C–H activation is a facile process for *unstrained* alkenes. Thus, whether an alkene will undergo [2+2] cycloaddition and/or C–H activation reactions with $[Cp^*W(NO)(=CHCMe_3)]$ depends on the degree of strain of the alkene double bond and the presence and accessibility of allylic hydrogens.

3.5 References and Notes

- (1) Fischer, E. O.; Maasböl, A. *Angew. Chem. Int. Ed. Engl.* **1964**, *3*, 580.
- (2) For reviews, see: (a) Fischer, E. O. *Adv. Organomet. Chem.* **1976**, *14*, 1. (b) Gallop, M. A.; Roper, W. R. *Adv. Organomet. Chem.* **1986**, *25*, 121. (c) Dötz, K. H. *Angew. Chem., Int. Ed. Engl.* **1984**, *23*, 587. (d) Wulff, W. D.; Tang, P. C.; Chan, K. S.; McCallum, J. S.; Yang, D. C.; Gilbertson, S. R. *Tetrahedron* **1985**, *41*, 5813.
- (3) For reviews, see: (a) Schrock, R. R. In *Reactions of Coordinated Ligands*; Braterman, P. S.; Ed.; Plenum: New York, 1986; Vol. 1, pp 221–283. (b) Feldman, J.; Schrock, R. R. *Prog. Inorg. Chem.* **1991**, *39*, 1. (c) Beckhaus, R. *Angew. Chem. Int. Ed. Engl.* **1997**, *36*, 686.
- (4) (a) Dötz, K. H. *Pure Appl. Chem.* **1983**, *55*, 1689. (b) Hegedus, L. S.; McGuire, M. A.; Schultze, L. M.; Yijun, C.; Anderson, O. P. *J. Am. Chem. Soc.* **1984**, *106*, 2680. (c) Brookhart, M.; Studabaker, W. B. *Chem. Rev.* **1987**, *87*, 411.
- (5) Nugent, W. A.; Mayer, J. M. *Metal-Ligand Multiple Bonds*; John Wiley & Sons: New York, 1988; Chapter 3.
- (6) For leading references on the metathesis reaction, see: (a) Grubbs, R. H. In *Comprehensive Organometallic Chemistry*; Wilkinson, G., Ed.; Pergamon Press, Ltd.: New York, 1982; Vol. 8, pp 499–551. (b) Leconte, M.; Basset, J. M.; Quinard, F.; Larroche, C. In *Reactions of Coordinated Ligands*; Braterman, P. S., Ed.; Plenum: New York, 1986; Vol. 1, pp 371–420. (c) Schrock, R. R. *Pure Appl. Chem.* **1994**, *66*, 1447. (d) Schuster, M.; Blechert, S. *Angew. Chem. Int. Ed. Engl.* **1997**, *36*, 2036. (e) Grubbs, R. H.; Chang, S. *Tetrahedron* **1998**, *54*, 4413.
- (7) (a) Grubbs, R. H.; Tumas, W. *Science* **1989**, *243*, 907. (b) Bazan, G. C.; Khosravi, E.; Schrock, R. R.; Feast, W. J.; Gibson, V. C.; O'Regan, M. B.; Thomas, J. K.; Davis, W. M. *J. Am. Chem. Soc.* **1990**, *112*, 8378. (c) Schrock, R. R. *Acc. Chem. Res.* **1990**, *23*,

158. (d) Bazan, G. C.; Oskam, J. H.; Cho, H.-N.; Park, L. Y.; Schrock, R. R. *J. Am. Chem. Soc.* **1991**, *113*, 6899. (e) Conticello, V. P.; Gin, D. L.; Grubbs, R. H. *J. Am. Chem. Soc.* **1992**, *114*, 9708.
- (8) (a) Wagener, K. B.; Nel, J. G.; Konzelman, J.; Boncella, J. M. *Macromolecules* **1990**, *23*, 5155. (b) Wagener, K. B.; Smith, D. W. Jr. *Macromolecules* **1991**, *24*, 6073. (c) Wagener, K. B.; Boncella, J. M.; Nel, J. G. *Macromolecules* **1991**, *24*, 2649.
- (9) (a) Schlund, R.; Schrock, R. R.; Crowe, W. E. *J. Am. Chem. Soc.* **1989**, *111*, 8004. (b) Bazan, G. C.; Khosravi, E.; Schrock, R. R.; Feast, W. J.; Gibson, V. C.; O'Regan, M. B.; Thomas, J. K.; Davis, W. M. *J. Am. Chem. Soc.* **1990**, *112*, 8378. (c) Park, L. Y.; Schrock, R. R.; Stieglitz, S. G.; Crowe, W. E. *Macromolecules* **1991**, *24*, 3489. (d) Masuda, T.; Mishima, K.; Fujimori, J.; Nishida, M.; Muramatsu, H.; Higashimura, T. *Macromolecules* **1992**, *25*, 1401. (e) Makio, H.; Masuda, T.; Higashimura, T. *Polymer* **1993**, *34*, 2218. (f) Fox, H. H.; Wolf, M. O.; O'Dell, R.; Lin, B. L.; Schrock, R. R.; Wrighton, M. S. *J. Am. Chem. Soc.* **1994**, *116*, 2827. (g) Schrock, R. R.; Luo, S.; Lee, J. C.; Zanetti, N. C.; Davis, W. M. *J. Am. Chem. Soc.* **1996**, *118*, 3883.
- (10) (a) Fu, G. C.; Grubbs, R. H. *J. Am. Chem. Soc.* **1992**, *114*, 5426. (b) Fu, G. C.; Grubbs, R. H. *J. Am. Chem. Soc.* **1992**, *114*, 7324. (c) Fu, G. C.; Grubbs, R. H. *J. Am. Chem. Soc.* **1993**, *115*, 3800. (d) Fujimura, O.; Fu, G. C.; Grubbs, R. H. *J. Org. Chem.* **1994**, *59*, 4029. (e) Kim, S. H.; Bowden, N.; Grubbs, R. H. *J. Am. Chem. Soc.* **1994**, *116*, 10801. (f) Grubbs, R. H.; Miller, S. J.; Fu, G. C. *Acc. Chem. Res.* **1995**, *28*, 446. (g) Armstrong, S. K. *J. Chem. Soc., Perkin Trans.* **1998**, *1*, 371.
- (11) (a) Brown-Wensley, K. A.; Buchwald, S. L.; Cannizzo, L.; Clawson, L.; Ho, S.; Meinhardt, D.; Stille, J. R.; Strauss, D.; Grubbs, R. H. *Pure Appl. Chem.* **1983**, *55*, 1733. (b) Petasis, N. A.; Bzowej, E. I. *J. Am. Chem. Soc.* **1990**, *112*, 6392. (c) Bazan, G. C.; Schrock, R. R.; O'Regan, M. B. *Organometallics* **1991**, *10*, 1062. (d) Fujimura, O.; Fu, G. C.; Rothmund, R. W. K.; Grubbs, R. H. *J. Am. Chem. Soc.* **1995**, *117*,

2355. (e) Petasis, N. A.; Lu, S.-P.; Bzowej, E. I.; Fu, D.-K.; Staszewski, J. P.; Akritopoulou-Zanze, I.; Patane, M. A.; Hu, Y.-H. *Pure Appl. Chem.* **1996**, *67*, 667.
- (12) (a) Carter, E. A.; Goddard, W. A. *J. Am. Chem. Soc.* **1986**, *108*, 2180. (b) Carter, E. A.; Goddard, W. A. *J. Am. Chem. Soc.* **1986**, *108*, 4746.
- (13) (a) Clark, G. R.; Hoskins, S. V.; Jones, T. C.; Roper, W. R. *J. Chem. Soc., Chem. Commun.* **1983**, 719. (b) Brothers, P. J.; Roper, W. R. *Chem. Rev.* **1988**, *88*, 1293.
- (14) Casey, C. P.; Vosejka, P. C.; Askham, F. R. *J. Am. Chem. Soc.* **1990**, *112*, 3713.
- (15) (a) Legzdins, P.; Rettig, S. J.; Veltheer, J. E. *J. Am. Chem. Soc.* **1992**, *114*, 6922. (b) Legzdins, P.; Rettig, S. J.; Veltheer, J. E.; Batchelor, R. J.; Einstein, F. W. B. *Organometallics* **1993**, *12*, 3575.
- (16) Legzdins, P.; Rettig, S. J.; Veltheer, J. E.; Young, M. A.; Batchelor, R. J.; Einstein, F. W. B. *Organometallics* **1995**, *12*, 407.
- (17) (a) Legzdins, P.; Sayers, S. F. *Organometallics* **1996**, *15*, 3907. (b) Legzdins, P.; Sayers, S. F. *Chem. Eur. J.* **1997**, *3*, 1579.
- (18) Tran, E.; Legzdins, P. *J. Am. Chem. Soc.* **1997**, *119*, 5071.
- (19) Sayers, S. F. Ph.D. Dissertation, The University of British Columbia, 1997.
- (20) (a) *Eight Peak Index of Mass Spectra*; 2nd Ed.; Mass Spectrometry Data Center: Reading, UK; 1974; Vol. 2. (b) The NIST/EPA/NIH Online Mass Spectra Database; U. S. Department of Commerce, 1995.
- (21) For examples, see: (a) Kiel, W. A.; Lin, G.-Y.; Constable, A. G.; McCormick, F. B.; Strouse, C. E.; Eisenstein, O.; Gladysz, J. A. *J. Am. Chem. Soc.* **1982**, *104*, 4865. (b) Toreki, R.; Schrock, R. R.; Davis, W. M. *J. Am. Chem. Soc.* **1992**, *114*, 3367. (c) Johnson, L. K.; Frey, M.; Ulibarri, T. A.; Virgil, S. C.; Grubbs, R. H.; Ziller, J. W. *J. Am. Chem. Soc.* **1993**, *115*, 8167.

- (22) For comparison, the $^1J_{\text{CH}}$ values of idealized $\text{sp}^2\text{-CH}$ bonds are typically 140–150 Hz.
- (23) (a) Schrock, R. R. *Acc. Chem. Res.* **1979**, *12*, 98. (b) Pedersen, S. F.; Schrock, R. R. *J. Am. Chem. Soc.* **1982**, *104*, 7483. (c) Brookhart, M.; Green, M. L. H.; Wong, L.-L. *Prog. Inorg. Chem.* **1988**, *36*, 1.
- (24) Gibson, V. C. *J. Chem. Soc., Dalton Trans.* **1994**, 1607.
- (25) Tran, E.; Legzdins, P. Unpublished results.
- (26) The approximate pK_a values of phenylacetylene, methyl acetate, and dimethylamine are 29, 25, and 35, respectively. See: Bordwell, F. G. *Acc. Chem. Res.* **1988**, *21*, 456.
- (27) This polymer is also unaffected by strong bases (e.g. $\text{NaOH}/\text{H}_2\text{O}$ and KOH/EtOH). It, however, disintegrates upon contact with concentrated sulfuric acid.
- (28) For examples, see: (a) Schrock, R. R.; DePue, R.; Feldman, J.; Schaverien, C. J.; Dewan, J. C.; Liu, A. H. *J. Am. Chem. Soc.* **1988**, *110*, 1423. (b) Grubbs, R. H.; Gilliom, L. R. *J. Am. Chem. Soc.* **1986**, *108*, 733. (c) van Doorn, J. A.; van der Heijden, H.; Orpen, A. G. *Organometallics* **1995**, *14*, 1278.
- (29) For example, treatment of $\text{Cp}^*\text{W}(\text{NO})\text{X}_2$ [$\text{X} = \text{Cl}, \text{I}$] with 1,3-dimagnesiopropane or 1,3-dilithiopropene simply results formation of the monohalide dimer, $[\text{Cp}^*\text{W}(\text{NO})\text{X}]_2$, in high yield. Tran, E. Unpublished results.
- (30) Wallace, K. C.; Liu, A. H.; Dewan, J. C.; Schrock, R. R. *J. Am. Chem. Soc.* **1988**, *110*, 4964.
- (31) (a) Collman, J. P.; Hegedus, L. S.; Norton, J. R.; Finke, G. R. *Principles and Applications of Organotransition Metal Chemistry*, University Science Books: Mill Valley, CA, 1987; p. 176. (b) Ipaktschi, J.; Mirzaei, F.; Demuth-Eberle, G. J.; Beck, J.; Serafin, M. *Organometallics* **1997**, *16*, 3965. (c) Chapter 4 of this thesis.

- (32) (a) Hunter, A. D.; Legzdins, P.; Nurse, C. R.; Einstein, F. W. B.; Willis, A. C. *J. Am. Chem. Soc.* **1985**, *107*, 1791. (b) Christensen, N. J.; Hunter, A. D.; Legzdins, P. *Organometallics* **1989**, *8*, 930.
- (33) Faller, J. W.; Nguyen, J. T.; Ellis, W.; Mazzieri, M. R. *Organometallics* **1993**, *12*, 1434.
- (34) Greenhough, T. J.; Legzdins, P.; Martin, D. T.; Trotter, J. *Inorg. Chem.* **1979**, *11*, 3268.
- (35) (a) Ward, Y. D.; Villanueva, L. A.; Allred, G. D.; Payne, S. C.; Semones, M. A.; Liebeskind, L. S. *Organometallics* **1995**, *14*, 4132. (b) Villanueva, L. A.; Ward, Y. D.; Lachicotte, R.; Liebeskind, L. S. *Organometallics* **1996**, *15*, 4190.
- (36) (a) Erker, G.; Engel, K.; Dorf, U.; Atwood, J. L.; Hunter, W. E. *Angew. Chem. Int. Ed. Engl.* **1982**, *21*, 914. (b) Nakamura, A. *J. Organomet. Chem.* **1990**, *400*, 35 and references therein.
- (37) Christensen, N. J.; Legzdins, P.; Einstein, F. W. B.; Jones, R. H. *Organometallics* **1991**, *10*, 3070.
- (38) Brunet, N.; Debad, J. D.; Legzdins, P.; Trotter, J.; Veltheer, J. E.; Yee, V. C. *Organometallics* **1993**, *12*, 4572.
- (39) McLain, S. J.; Wood, C. D.; Schrock, R. R. *J. Am. Chem. Soc.* **1976**, *99*, 3519.
- (40) Although alkene C–H activation by transition-metal alkylidene complexes is unprecedented, activation of arene and even alkane C–H bonds by these species has previously been reported, see: (a) van der Heijden, H.; Hessen, B. *J. Chem. Soc., Chem. Commun.* **1995**, 145. (b) Coles, M. P.; Gibson, V. C.; Clegg, W.; Elsegood, M. R. J.; Porrelli, P. A. *Chem. Commun.* **1996**, 1963. (c) Cheon, J.; Rogers, D. M.; Girolami, G. S. *J. Am. Chem. Soc.* **1997**, *119*, 6814. (d) Reference 18.
- (41) McMillen, D. F.; Golden, D. M. *Ann. Rev. Phys. Chem.* **1982**, *33*, 493.

CHAPTER 4

Selective Activation of Aliphatic, Aromatic, and Benzylic C–H Bonds by [Cp*W(NO)(=CHCMe₃)] and Related Complexes

4.1 Introduction	105
4.2 Experimental Section	107
4.3 Results and Discussion	123
4.4 Conclusions	148
4.5 References and Notes	150

4.1 Introduction

The intermolecular activation of C–H bonds,¹ especially those of alkanes, by soluble organometallic complexes has been the subject of much experimental² and theoretical³ study in the last 20 years. Much of the impetus for this work has been provided by the search for reagents which can selectively convert alkanes, an abundant and cheap source of hydrocarbon feedstocks, into more valuable commodity chemicals. Although a large number of systems are now known which can effect the activation of C–H bonds intermolecularly, most are nonselective and involve the photochemical or thermal generation of a high-energy reactive intermediate.⁴

In general, organometallic complexes that can effect the activation of C–H bonds intermolecularly are of four main groups. First, there is the largest group which consists of low-valent late transition-metal complexes, and involves an oxidative-addition mechanism.⁵ Second is a group that consists of high-valent early transition-metal complexes,⁶ lanthanide complexes,⁷ and actinide complexes,⁸ and involves a σ -bond metathesis mechanism. In the

third and fourth group, the activation occurs as a result of H-atom abstraction by metallaradicals⁹ and C–H bond addition across a M=X bond (X = O,¹⁰ NR,^{11–15} CHR¹⁶).

Once rare, the reaction between a C–H bond and a metal-ligand multiple bond has flourished in recent years. However, while reactions of this type have become well established for transition-metal imido complexes, with specific examples now known for Ti,¹¹ Zr,¹² V,¹³ Ta,¹⁴ and W,¹⁵ there are at present few transition-metal oxo and alkylidene complexes that can effect the cleavage of C–H bonds intermolecularly.¹⁶ Fewer still are alkylidene complexes which can effect the cleavage of alkane C–H bonds. Indeed, prior to the preliminary report^{16c} of the work described in this chapter, alkylidene complexes were only known to activate aliphatic C–H bonds intramolecularly.^{17,18,19,20}

In the preceding chapter, it was shown that thermolysis of Cp*W(NO)(CH₂CMe₃)₂ leads to loss of neopentane and formation of the 16-electron neopentylidene complex, [Cp*W(NO)(=CHCMe₃)], as a highly reactive intermediate, which (a) can be trapped by a range of Lewis bases to yield the corresponding base adducts as the anti rotamer, (b) undergo addition reactions with the N–H and O–H bonds of amines and alcohols, respectively, and (c) react with alkenes to give novel [2+2] cycloaddition and/or C–H activation products depending on the alkene structure. The objective of this chapter is to report the full details of the reactivity of [Cp*W(NO)(=CHCMe₃)] with the C–H bonds of Me₄Si, alkanes, and arenes. As will soon be seen, these C–H activation reactions occur with some selectivity and lead to an array of C–H activation products depending on the alkane and arene structure. The reactivity of the neopentylidene complex, [CpW(NO)(=CHCMe₃)], and benzylidene complexes, [Cp*W(NO)(=CHAr)], with representative aliphatic and aromatic C–H bonds will also be reported and compared to that of the Cp* neopentylidene system.

4.2 Experimental Section

4.2.1 Methods

The synthetic methodologies employed throughout this thesis are described in detail in Section 2.2.1. GC–MS analyses were performed by Ms. L. Madilao of the UBC mass spectrometry facility using a Carlo Erba GC and Kratos MS-80 unit. ^{31}P and ^{19}F chemical shifts were recorded relative to $\text{P}(\text{OMe})_3$ (δ 141.0 in C_6D_6) and $\text{CF}_3\text{CO}_2\text{H}$ (δ 0.00) standards. All thermolyses were carried out in thick-walled glass vessels or J. Young NMR tubes immersed in an oil bath at 60–75 °C for ca. 1.5–2 d unless otherwise noted.

4.2.2 Reagents

The organometallic precursors $\text{CpW}(\text{NO})(\text{CH}_2\text{CMe}_3)_2$ (**2.1**), $\text{Cp}^*\text{W}(\text{NO})(\text{CH}_2\text{CMe}_3)_2$ (**2.4**), $\text{Cp}^*\text{W}(\text{NO})(\text{CH}_2\text{CMe}_3)(\text{CH}_2\text{CMe}_2\text{Et})$ (**2.7**), and $\text{Cp}^*\text{W}(\text{NO})(\text{CH}_2\text{CMe}_3)(\text{CH}_2\text{Ph})$ (**2.15**) were prepared as described in Section 2.2.2. Me_2NH (Aldrich, 99.9%) was used as received. 1,1,2,2-Tetramethylcyclopropane (Wiley Organics), tetramethylsilane, cyclopentane, neohexane, methylcyclopentane, methylcyclohexane, ethylcyclohexane, anisole, toluene, and mesitylene (Aldrich) were vacuum-transferred from sodium. PMe_3 , pentane, cyclohexane, *o*-xylene, *m*-xylene, and *p*-xylene (Aldrich) were vacuum-distilled from sodium benzophenone ketyl. α,α,α -Trifluorotoluene (Aldrich) was dried over activated 4 Å molecular sieves.

4.2.3 Preparation of $\text{Cp}^*\text{W}(\text{NO})(\text{CH}_2\text{CMe}_3)(\text{CH}_2\text{SiMe}_3)$ (**2.9**)

In the glovebox, a Pyrex vessel was charged with **2.4** (48 mg, 0.098 mmol) and tetramethylsilane (1 mL). The resulting wine-red solution was heated at ca. 70 °C for 2 d, during which time its color darkened. The organic volatiles were then removed in vacuo to obtain a red-black solid, which was extracted into pentane and filtered through Celite (1 × 1 cm). Concentration of the filtrate followed by cooling to –30 °C for 2 d provided **2.9** (45 mg,

90% yield) as maroon crystals. The identity of **2.9** was confirmed by comparison of its ^1H and ^{13}C NMR spectra to those of an authentic sample.²¹

4.2.4 Preparation of $\text{Cp}^*\text{W}(\text{NO})[\text{CH}_2\text{CMeCMe}_2\text{CH}]$ (**4.1**)

To Pyrex vessel containing **2.4** (35 mg, 0.071 mmol) was added 1,1,2,2-tetramethylcyclopropane (2 mL) by vacuum transfer. The resulting wine-red mixture was thawed and heated at ca. 70 °C for 2 d, during which time it became orange-yellow. The organic volatiles were then removed in vacuo to obtain an oily residue, which was redissolved in hexanes and filtered through alumina I (1 × 1 cm). The alumina column was washed with Et_2O until the filtrate was colorless. Concentration of the combined filtrates followed by cooling to -30 °C for several days afforded **4.1** (10 mg, 32% yield) as bright yellow crystals.

Anal. Calcd. for $\text{C}_{17}\text{H}_{27}\text{NOW}$: C, 45.85; H, 6.11; N, 3.15. Found: C, 45.55; H, 6.02; N, 3.00. IR (cm^{-1}) ν_{NO} 1588 (s). MS 445 [M^+ , ^{184}W]. ^1H NMR (400 MHz, C_6D_6) δ 0.72 (dd, $^2J_{\text{HH}} = 4.3$, $^3J_{\text{HH}} = 1.2$, 1H, $\text{CH}_{\text{syn}}\text{H}$ to Cp^*), 1.16 (br s, 1H, CH), 1.63 (s, 3H, CMe_2), 1.68 (s, 15H, C_5Me_5), 2.17 (s, 3H, CMe_2), 2.31 (s, 3H, CH_2CMe), 3.25 (d, $^2J_{\text{HH}} = 4.3$, 1H, $\text{CH}_{\text{anti}}\text{H}$ to Cp^*). $^{13}\text{C}\{^1\text{H}\}$ NMR (125 MHz, C_6D_6) δ 10.4 (C_5Me_5), 18.8 (CH_2CMe), 27.5 (1 CMe_2), 30.1 (1 CMe_2), 55.8 ($^1J_{\text{CW}} = 37$, WCH_2), 80.9 (CMe_2), 83.0 (WCH), 104.3 (C_5Me_5), 106.0 (CH_2CMe). NOEDS (400 MHz, C_6D_6) irradiat. at 0.72 ppm, NOEs at δ 1.16, 1.68, 3.25; irradiat. at 1.16 ppm, NOEs at δ 0.72, 1.68; irradiat. at 1.63 ppm, NOEs at δ 1.16, 2.17; irradiat. at 1.68 ppm, NOEs at δ 0.72, 1.16; irradiat. at 2.17 ppm, NOE at δ 1.63; irradiat. at 2.31 ppm, NOE at δ 3.25; irradiat. at 3.25 ppm, NOEs at δ 0.72, 2.31.

4.2.5 Preparation of $\text{Cp}^*\text{W}(\text{NO})(\eta^2\text{-alkene})(\text{PMe}_3)$ Complexes [alkene = cyclopentene (**4.2**), cyclohexene (**4.3**), neohexene (**4.4**)]

The reactions leading to complexes **4.2–4.4** were carried out in a similar manner. In each case, the neopentylidene complex $\text{Cp}^*\text{W}(\text{NO})(=\text{CHCMe}_3)(\text{PMe}_3)$ (**3.4**) (~10–30% yields) was detected as a minor product by ^1H and $^{31}\text{P}\{^1\text{H}\}$ NMR analyses of the crude reaction

mixture. The preparation of **4.2** is described as a representative example. To a Pyrex vessel containing **2.4** (56 mg, 0.11 mmol) was added cyclopentane (9 mL) and PMe_3 (5–10 equiv) by vacuum transfer. The resulting wine-red mixture was thawed and heated at ca. 70 °C for 2 d, during which time it became a dark yellow solution. Next, the organic volatiles were removed in vacuo to obtain a dark yellow oil, which was extracted into 5:1 hexanes/ Et_2O (2 mL) and filtered through alumina I (2×1 cm). The alumina column was washed with additional 5:1 hexanes/ Et_2O until the filtrate was colorless. Concentration of the combined filtrates followed by cooling to –30 °C for 2 d afforded **4.2** (25 mg, 44% yield) as pale yellow plates.

4.2.5.1 Complex 4.2. Anal. Calcd. for $\text{C}_{18}\text{H}_{32}\text{NOPW}$: C, 43.83; H, 6.54; N, 2.84. Found: C, 43.86; H, 6.61; N, 2.76. IR (cm^{-1}) ν_{NO} 1522 (s). MS 493 [M^+ , ^{184}W]. ^1H NMR (400 MHz, C_6D_6) δ 1.06 (m, 1H, $\alpha=\text{CH}$), 1.19 (d, $^2J_{\text{HP}} = 8.4$, 9H, PMe_3), 1.58 (m, 1H, γCH_2), 1.66 (s, 15H, C_5Me_5), 1.72 (m, 1H, γCH_2), 1.99 (m, 1H, $\alpha'=\text{CH}$), 2.34 (dd, $^2J_{\text{HH}} = 6.6$, $^3J_{\text{HH}} = 12.4$, 1H, βCH_2), 2.64 (m, 1H, $\beta'\text{CH}_2$), 3.00 (sept, 1H, $\beta'\text{CH}_2$), 3.26 (sept, 1H, βCH_2). $^{13}\text{C}\{^1\text{H}\}$ NMR (75 MHz, C_6D_6) δ 10.5 (C_5Me_5), 16.8 (d, $^1J_{\text{CP}} = 29$, PMe_3), 23.2 (γCH_2), 34.9 ($\beta'\text{CH}_2$), 35.4 (d, $^3J_{\text{CP}} = 4$, βCH_2), 44.2 ($^1J_{\text{CW}} = 40$, $\alpha'=\text{CH}$), 46.1 (d, $^2J_{\text{CP}} = 13$, $\alpha=\text{CH}$), 103.0 (C_5Me_5). $^{31}\text{P}\{^1\text{H}\}$ NMR (121 MHz, C_6D_6) δ –13.2 ($^1J_{\text{PW}} = 364$).

4.2.5.2 Complex 4.3 was prepared by heating **2.4** (81 mg, 0.16 mmol) in a cyclohexane solution (8 mL) of PMe_3 (5–15 equiv). It was crystallized from a 3:1 mixture of pentane/ Et_2O at –30 °C and isolated as pale yellow needles (32 mg, 51% yield).

Anal. Calcd. for $\text{C}_{19}\text{H}_{34}\text{NOPW}$: C, 44.98; H, 6.76; N, 2.76. Found: C, 44.20; H, 6.41; N, 2.75. IR (cm^{-1}) ν_{NO} 1518 (s). HRMS Calcd. for $\text{C}_{19}\text{H}_{34}\text{NOPW}$: 507.2881 [M^+ , ^{184}W]. Found: 507.1888. ^1H NMR (500 MHz, C_6D_6) δ 0.8 (m, 1H, $\alpha'=\text{CH}$), 1.22 (d, $^2J_{\text{HP}} = 9\text{H}$, PMe_3), 1.5 (m, 1H, $\alpha=\text{CH}$), 1.6 (m, 2H, $\gamma'\text{CH}_2$), 1.67 (s, 15H, C_5Me_5), 1.8 (m, 2H, γCH_2), 2.4 (m, 1H, $\beta'\text{CH}_2$), 2.8 (m, 2H, βCH_2), 3.1 (m, 1H, $\beta'\text{CH}_2$). $^{13}\text{C}\{^1\text{H}\}$ NMR (125 MHz, C_6D_6) δ 10.3 (C_5Me_5), 17.4 (d, $^2J_{\text{CP}} = 29$, PMe_3), 24.2 (γCH_2), 25.3 ($\gamma'\text{CH}_2$), 28.3 (βCH_2), 30.8 (d, $^3J_{\text{CP}} = 4$, $\beta'\text{CH}_2$), 36.9 ($^1J_{\text{CW}} = 39$, αCH), 40.0 (d, $^2J_{\text{CP}} = 12$, $\alpha'\text{CH}$), 103.0 (C_5Me_5). $^{31}\text{P}\{^1\text{H}\}$ NMR (202 MHz, C_6D_6) δ –13.2 (s, $^1J_{\text{PW}} = 373$).

4.2.5.3 Complexes 4.4 were prepared as a 5.7:1 mixture of **4.4_{syn}** and **4.4_{anti}** by heating **2.4** (66 mg, 0.13 mmol) in a neohexane solution (8 mL) of PMe_3 (0.38 mmol, 3 equiv). The two rotamers were isolated together as yellow blocks (38 mg, 56% yield) from a 4:1 mixture of hexanes/ Et_2O at -30°C .

Anal. Calcd. for $\text{C}_{19}\text{H}_{36}\text{NOPW}$: C, 44.80; H, 7.13; N, 2.75. Found: C, 44.95; H, 7.09; N, 2.68. IR (cm^{-1}) ν_{NO} 1513 (s). MS 509 [M^+ , ^{184}W]. ^1H NMR (400 MHz, C_6D_6) δ **4.4_{syn}**: 0.38 (m, 1H, $=\text{CH}_{\text{syn}}\text{H}$), 1.00 (s, 9H, CMe_3), 1.33 (d, $^2J_{\text{HP}} = 8.4$, 9H, PMe_3), 1.73 (s, 15H, C_5Me_5), 2.3 (m, 2H, $=\text{CH}_{\text{anti}}\text{H}$, $=\text{CHCMe}_3$). **4.4_{anti}**: -0.30 (m, 1H, $=\text{CH}_{\text{syn}}\text{H}$), 1.16 (d, $^2J_{\text{HP}} = 8.6$, 9H, PMe_3), 1.34 (s, 9H, CMe_3), 1.43 (m, 2H, $=\text{CH}_{\text{anti}}\text{H}$, $=\text{CHCMe}_3$), 1.67 (s, 15H, C_5Me_5). $^{13}\text{C}\{^1\text{H}\}$ NMR (75 MHz, C_6D_6) δ **4.4_{syn}**: 10.9 (C_5Me_5), 18.3 (d, $^1J_{\text{CP}} = 30$, PMe_3), 25.1 ($^1J_{\text{CW}} = 33$, $=\text{CH}_2$), 34.7 (CMe_3), 35.2 (d, $^2J_{\text{CP}} = 2$, CMe_3), 57.9 (d, $^1J_{\text{CP}} = 12$, $=\text{CHCMe}_3$), 103.9 (C_5Me_5). **4.4_{anti}**: 10.5 (C_5Me_5), 16.0 (d, $^1J_{\text{CP}} = 32$, PMe_3), 27.2 (d, $^2J_{\text{CP}} = 22$, $=\text{CH}_2$), 32.3 (CMe_3), 33.1 (CMe_3), 55.7 ($=\text{CHCMe}_3$), 103.0 (C_5Me_5). $^{31}\text{P}\{^1\text{H}\}$ NMR (202 MHz, C_6D_6) δ **4.4_{syn}**: -17.3 ($^1J_{\text{PW}} = 358$). **4.4_{anti}**: -9.6 ($^1J_{\text{PW}} = 361$). NOEDS (400 MHz, C_6D_6) **4.4_{syn}**: irradi. at 0.38 ppm, NOEs at δ 1.00, 1.73, 2.27; irradi. at 1.00 ppm, NOEs at δ 0.38, 1.33, 1.73, 2.27; irradi. at 1.73 ppm, NOEs at δ 0.38, 1.00, 1.33. **4.4_{anti}**: irradi. at -0.30 ppm, NOEs at δ 1.16, 1.43; irradi. at 1.16 ppm, NOEs at δ -0.30 , 1.67; irradi. at 1.34 ppm, NOE at δ 1.43; irradi. at 1.67 ppm, NOEs at δ 1.16.

4.2.6 Thermolysis of **2.4** in Cyclohexane in the Presence of PMe_3 : Effect of Varying PMe_3 Concentration

Into each of two J. Young NMR tubes was added 1.0 mL of a 0.020 M solution of **2.4** in cyclohexane. 6 equiv of PMe_3 were then added to one tube and 12 equiv to the other. The resulting solutions were heated side-by-side in 70°C bath and the reaction monitored periodically for 2 d by $^{31}\text{P}\{^1\text{H}\}$ NMR spectroscopy. In each case, formation of **3.4** and **4.3** as the sole products was observed; these were formed in a constant relative yield of 25% and 75% and 49% and 51%, respectively.

4.2.7 Kinetics of the Thermolysis of 2.4 in Neohexane in the Presence of PMe_3

Two J. Young NMR tubes, each containing **2.4** (16 mg, 0.033 mmol), neohexane (0.80 mL), PMe_3 (3.5 equiv), and a capillary tube of $\text{P}(o\text{-tolyl})_3$ in C_6D_6 , were heated to 70 °C in a constant-temperature bath and the reaction monitored periodically for 7 d by $^{31}\text{P}\{^1\text{H}\}$ NMR spectroscopy. In each case, parallel formations of **3.4** and **4.4_{syn}** were observed at early conversion. As the reaction progressed, the intensity of the signal due to **4.4_{anti}** appeared and increased at the expense of the intensity of the resonance due **4.4_{syn}**. The rate constant (average of the two runs) for the formation of **3.4** and **4.4_{syn}** was $4.22 \times 10^{-5} \text{ s}^{-1}$, while the rate constant for the isomerization of **4.4_{syn}** to **4.4_{anti}** was $7.41 \times 10^{-6} \text{ s}^{-1}$.

4.2.8 Thermolysis of $\text{Cp}^*\text{W}(\text{NO})(\text{CH}_2\text{CMe}_3)(\text{CH}_2\text{CMe}_2\text{Et})$ (**2.7**) in Neohexane in the Presence of PMe_3

This reaction was effected in a manner analogous to that described for reaction between **2.4**, neohexane, and PMe_3 . To a Pyrex bomb containing **2.7** (19 mg, 0.038 mmol) was added neohexane and excess PMe_3 by vacuum transfer. The resulting wine-red mixture was thawed and heated at ca. 70 °C for 2 d, during which time it became orange. The organic volatiles were then collected by vacuum transfer and were examined by GC-MS, which showed the presence of neopentane and neohexane but not neohexene, dimethylcyclopentane, or 2,2,6,6-tetramethyloctane. Analysis of the crude reaction mixture by $^{31}\text{P}\{^1\text{H}\}$ NMR spectroscopy indicated that **4.4_{syn}** and **4.4_{anti}** were formed as the major products. Several minor products were also observed, which gave rise to ^{31}P resonances at δ 35.6, 33.3, -5.7, -5.8, and -23.0 (relative to 85% H_3PO_4 at δ 0.00) in a ratio of about 1:1:0.5:0.5:0.8 based on relative ^{31}P NMR peak heights. The products with resonances at δ -5.6, -5.8, and -23.0 were assigned as $\text{Cp}^*\text{W}(\text{NO})(=\text{CHCMe}_3)(\text{PMe}_3)$ (**3.4**), $\text{Cp}^*\text{W}(\text{NO})(=\text{CHCMe}_2\text{Et})(\text{PMe}_3)$ (**4.5**), and $\text{Cp}^*\text{W}(\text{NO})(\text{PMe}_3)_2$ (**4.6**), respectively, on the basis of ^1H and ^{31}P NMR spectral data of the crude product mixtures (see below, Section 4.2.9). In the case of **4.6**, its identity was further confirmed by comparison of its ^1H and $^{31}\text{P}\{^1\text{H}\}$ NMR spectra to those of an authentic sample prepared by Na/Hg reduction of $\text{Cp}^*\text{W}(\text{NO})\text{Cl}_2$ in THF in the presence of PMe_3 .²²

4.2.9 Thermolysis of $\text{Cp}^*\text{W}(\text{NO})(\text{CH}_2\text{CMe}_3)(\text{CH}_2\text{CMe}_2\text{Et})$ (2.7) in THF in the Presence of PMe_3

This reaction was carried out in a manner analogous to that described above using THF as solvent. Analysis of the organic volatiles by GC-MS again showed peaks for neopentane and neohexane, but none for neohexene, dimethylcyclopentane, and 2,2,6,6-tetramethyloctane. Examination of the crude reaction mixture by ^1H and $^{31}\text{P}\{^1\text{H}\}$ NMR spectroscopies again indicated a complex mixture of products. In this case, complexes **3.4**, **4.5**, and **4.6** were observed as the major (and only identified) products in a ratio of about 1:1:1 based on relative ^{31}P NMR peak heights. The minor products gave rise to ^{31}P signals in the 10-18 ppm region. Signals consistent with the presence of **4.4** were not observed. The NMR mixture was then taken to dryness, extracted into 3:1 hexanes/ Et_2O , and filtered through alumina I (1×1 cm). The alumina column was washed with additional 3:1 hexanes/ Et_2O until the filtrate was colorless. Next, the combined filtrates were reduced in volume and stored at -30°C for several days to induce the deposition of **3.4**, **4.5**, and **4.6** as brown-orange crystals in a ratio of $\sim 1:1:3$.

$\text{Cp}^*\text{W}(\text{NO})(=\text{CHCMe}_2\text{Et})(\text{PMe}_3)$ (4.5). MS 509 [M^+ , ^{184}W]. ^1H NMR (500 MHz, C_6D_6) δ 1.06 (d, $^2J_{\text{HP}} = 9.0$, 9H, PMe_3), 1.40 (s, 3H, CMeMe), 1.46 (s, 3H, CMeMe), 1.86 (s, 15H, C_5Me_5), 11.27 (d, $^3J_{\text{HP}} = 3.3$, $\text{W}=\text{CH}$), CH_2CH_3 unobserved due to peak overlap. $^{13}\text{C}\{^1\text{H}\}$ NMR (125 MHz, C_6D_6) δ 9.7 (CCH_2CH_3), 10.71 (C_5Me_5), 19.4 (d, $^1J_{\text{CP}} = 32$, PMe_3), 28.7 (CMeMe), 28.8 (CMeMe), 36.6 (CH_2CH_3), 54.0 (CMeMe), 106.1 (C_5Me_5). $^{31}\text{P}\{^1\text{H}\}$ (121 MHz, C_6D_6 , referenced to external H_3PO_4) δ -7.6 ($^1J_{\text{PW}} = 445$).

$\text{Cp}^*\text{W}(\text{NO})(\text{PMe}_3)_2$ (4.6). MS 501 [M^+ , ^{184}W]. ^1H NMR (500 MHz, C_6D_6) δ (d, $^2J_{\text{HP}} = 7.2$, 18H, PMe_3), 1.92 (s, 15H, C_5Me_5). $^{13}\text{C}\{^1\text{H}\}$ NMR (125 MHz, C_6D_6) δ 11.9 (C_5Me_5), 24.0 (m, 2, 6, PMe_3), 98.8 (C_5Me_5). $^{31}\text{P}\{^1\text{H}\}$ (121 MHz, C_6D_6 , referenced to external H_3PO_4) δ -22.7 ($^1J_{\text{PW}} = 453$).

4.2.10 Preparation of $\text{Cp}^*\text{W}(\text{NO})(\text{cyclohexyl})(\text{NMe}_2)$ (4.7)

In a manner similar to the preparation of alkene complex **4.3**, a cyclohexane solution (10 mL) of **2.4** (60 mg, 0.12 mmol) and Me_2NH (5–10 equiv from a calibrated gas bulb) was heated at ca. 70 °C for 2 d, during which time its color changed from wine-red to dark yellow. The organic volatiles were then removed in vacuo to obtain a yellow-brown oil, which was triturated with pentane (3×5 mL), extracted into 3:1 pentane/ Et_2O , and filtered through alumina I (1×1 cm). The alumina column was washed with additional 3:1 pentane/ Et_2O until the filtrate was colorless. Concentration of the combined filtrates followed by cooling to –30 °C for several days provided **4.7** (31 mg, 54 % yield) as large, pale yellow needles. The needles were spectroscopically pure, but a satisfactory elemental analysis could not be obtained.

IR (CH_2Cl_2 , cm^{-1}) ν_{NO} 1529 (s). MS 476 [M^+ , ^{184}W]. ^1H NMR (500 MHz, C_6D_6) δ 1.17 (m, 1H, WCH), 1.45 (m, 3H, C_aHH , C_bHH , C_cHH), 1.66 (s, 15H, C_5Me_5), 1.72 (m, 1H, C_dH_2), 1.82 (m, 1H, C_aH_2), 1.98 (m, 2H, C_bHH , C_cHH), 2.27 (m, 1H, C_eH_2), 2.63 (s, 3H, NMe_a), 2.87 (br d, $J_{\text{HH}} = 14.0$, 1H, C_eH_2), 3.72 (s, 3H, NMe_b). $^{13}\text{C}\{^1\text{H}\}$ NMR (125 MHz, C_6D_6) δ 9.4 (C_5Me_5), 27.8 (C_aH_2), 32.9 (C_bH_2), 33.0 (C_cH_2), 37.2 (C_dH_2), 40.0 (C_eH_2), 51.1 (NMe_a), 52.1 (WCH, $^1J_{\text{CW}} = 94$ Hz), 60.6 (NMe_b), 109.9 (C_5Me_5).

4.2.11 Preparation of $\text{Cp}^*\text{W}(\text{NO})(\eta^3\text{-allyl})(\text{H})$ Complexes [$\eta^3\text{-allyl} = \eta^3\text{-C}_6\text{H}_9$ (4.8), $\eta^3\text{-C}_7\text{H}_{11}$ (4.9), $\eta^3\text{-C}_8\text{H}_{13}$ (4.10), $\eta^3\text{-C}_5\text{H}_9$ (4.11)].

The reactions leading to complexes **4.8–4.11** were all carried out in a similar manner. The preparation of **4.8** is described as a representative example. To a Pyrex vessel containing **2.4** (46 mg, 0.094 mmol) was added methylcyclopentane (2 mL) by vacuum transfer. The resulting wine-red mixture was thawed and heated at ca. 70 °C for 2 d, during which time it became a brown-yellow solution. The organic volatiles were then removed in vacuo to obtain a brown-yellow oil, which was extracted into 4:1 hexanes/ Et_2O (0.5 mL) and filtered through alumina I (2×1 cm). The alumina column was washed with additional 4:1 hexanes/ Et_2O (3

mL) followed by a minimum amount of Et₂O until the filtrate was colorless. The combined filtrates were concentrated at room temperature and then stored at -30 °C overnight to obtain **4.8_{endo}** and **4.8_{endo}*** as clusters of pale yellow needles (28 mg, 70% combined yield).

Complete NMR characterization of **4.8_{endo}*** could not be achieved due to inadequate signal-to-noise of its signals and to spectral overlap.

4.2.11.1 Complexes 4.8. Anal. Calcd. for C₁₆H₂₅NO: C, 44.56; H, 5.84; N, 3.25. Found: C, 44.68; H, 5.93; N, 3.29. IR (cm⁻¹) ν_{WH} 2161, 1911; ν_{NO} 1565, 1548 (s). MS 429 [M⁺-H₂, ¹⁸⁴W]. ¹H NMR (400 MHz, C₆D₆) δ **4.8_{endo}**: -1.05 (s, ¹J_{HW} = 119, WH), 0.68 (s, 1H, allyl CH_{anti}H), 1.69 (m, 1H, C_aH₂), 1.75 (s, 15H, C₅Me₅), 1.95 (m, 1H, C_aH₂), 2.44 (s, 1H, allyl CH), 2.51 (dd, ²J_{HH} = 8.2, ³J_{HH} = 14.5, 1H, C_bH₂), 2.83 (m, 2H, C_bHH, C_cHH), 2.95 (m, 1H, C_cH₂), 3.06 (m, 1H, allyl CH_{syn}H). **4.8_{endo}***: -0.69 (s, ¹J_{HW} = 121, 1H, WH), 0.96 (br s, 1H, allyl CH₂), 1.7 (m, 1H, allyl CH), 1.73 (s, 15H, C₅Me₅), 4.21 (br s, 1H, allyl CH₂), other resonances were masked by those of major isomer. ¹³C{¹H} (75 MHz, C₆D₆) δ **4.8_{endo}**: 10.7 (C₅Me₅), 23.8 (C_aH₂), 35.6 (C_bH₂), 35.9 (C_cH₂), 38.3 (allyl CH₂), 80.3 (allyl CH), 104.7 (C₅Me₅), 125.3 (allyl 4° C). **4.8_{endo}***: 10.4 (C₅Me₅), 23.2 (CH₂), 33.9 (CH₂), 36.2 (CH₂), 46.2 (allyl CH₂), 67.7 (allyl CH), 104.5 (C₅Me₅), 126.8 (allyl 4° C). NOEDS (400 MHz, C₆D₆) **4.8_{endo}**: irradi. at -1.05 ppm, NOEs at δ 1.95, 2.44, 2.83; irradi. at 0.68 ppm, NOEs at δ 2.44, 3.05; irradi. at 1.75 ppm, NOEs at δ -1.05, 0.68, 2.44; irradi. at 3.05 ppm, NOE at δ 0.68. **4.8_{endo}***: irradi. at 0.96 ppm, NOE at δ 4.21; irradi. at 4.21, NOEs at δ -0.69, 0.96.

4.2.11.2 Complex 4.9_{endo} was prepared by heating **2.4** in methylcyclohexane. It was isolated as clear pale yellow rods (57% yield) from 5:1 pentane/Et₂O at -30 °C.

Anal. Calcd. for C₁₇H₂₇NO: C, 45.86; H, 6.11; N, 3.15. Found: C, 45.99; H, 6.19; N, 2.97. IR (cm⁻¹) ν_{WH} 1905 (w); ν_{NO} 1564 (s). MS 443 [M⁺-H₂, ¹⁸⁴W]. ¹H NMR (500 MHz, C₆D₆) δ -0.73 (s, ¹J_{HW} = 123, 1H, WH), 0.31 (m, 1H, allyl CH_{anti}H), 1.39 (m, 1H, C_bH₂), 1.54 (m, 1H, C_aH₂), 1.71 (m, 1H, C_bH₂), 1.76 (s, 15H, C₅Me₅), 1.84 (m, 1H, C_aH₂), 2.28 (br s, 1H, allyl CH), 2.60 (m, 1H, allyl CH_{syn}H), 2.68 (m, 2H, C_cHH, C_dHH), 2.91 (q, ²J_{HH} = 7.9, C_cH₂),

2.97 (m, 1H, C_dH₂). ¹³C{¹H} (75MHz, C₆D₆) δ 10.7 (C₅Me₅), 22.1 (C_aH₂), 22.5 (C_bH₂), 28.8 (C_cH₂), 29.6 (C_dH₂), 41.3 (allyl CH₂), 80.0 (allyl CH), 104.9 (C₅Me₅), 121.1 (allyl 4° C).

4.2.11.3 Complexes 4.10 were prepared as a mixture of **4.10_{exo}** and **4.10_{endo}** by heating **2.4** in ethylcyclohexane. They were isolated as brown-yellow blocks (37% combined yield) from a minimum amount of pentane and 2 drops of Et₂O at -30 °C. Complete spectroscopic characterization of **4.10_{endo}** could not be achieved due to spectral overlap and to inadequate signal-to-noise of its NMR signals.

Anal. Calcd. for C₁₈H₂₉NO: C, 47.07; H, 6.36; N, 3.05. Found: C, 46.86; H, 6.42; N, 2.96. IR (cm⁻¹) **4.10_{exo}** ν_{WH} 1935 (m); ν_{NO} 1575 (br s). **4.10_{endo}**: ν_{WH} 2172 (m). MS 457 [M⁺-H₂, ¹⁸⁴W]. ¹H NMR (400 MHz, C₆D₆) δ **4.10_{exo}**: -0.92 (s, ¹J_{HW} = 125, 1H, WH), 1.42 (m, 1H, C_bH₂), 1.58 (m, 3H, C_aHH, C_cHH), 1.71 (s, 15H, C₅Me₅), 1.79 (m, 1H, C_bH₂), 1.90 (m, 1H, C_dH₂), 2.00 (m, 1H, C_cH₂), 2.15 (m, 3H, C_dHH, allyl CH_{syn}H, C_eHH), 2.44 (dd, 1H, ²J_{HH} = 3.1, ³J_{HH} = 13.3, allyl CH_{anti}H), 2.51 (m, 1H, C_eH₂), 2.66 (dd, ³J_{HH} = 7.8, ³J_{HH} = 13.3, 1H, allyl CH). **4.10_{endo}**: -0.71 (s, ¹J_{WH} = 126, 1H, WH), 0.60 (m, 1H, allyl CH_{anti}H), 2.87 (dd, ²J_{HH} = 3.3, ³J_{HH} = 7.2, 1H, allyl CH_{syn}H), 2.89 (m, 1H, CH₂), 4.69 (dd, ³J_{HH} = 7.2, ³J_{HH} = 11.8, 1H, allyl CH), other signals are obscured. ¹³C{¹H} (75 MHz, C₆D₆) δ **4.10_{exo}**: 10.7 (C₅Me₅), 27.1 (C_aH₂), 30.6 (C_bH₂), 32.6 (C_cH₂), 35.1 (C_dH₂), 37.2 (¹J_{CW} = 25, allyl CH₂), 41.0 (C_eH₂), 93.2 (allyl CH), 103.8 (C₅Me₅), 109.0 (allyl 4° C). **4.10_{endo}**: 10.5 (C₅Me₅), 27.0 (CH₂), 30.5 (CH₂), 32.5 (CH₂), 33.0 (CH₂), 40.9 (allyl CH₂), 42.8 (CH₂), 100.9 (allyl CH), 104.8 (C₅Me₅). NOEDS (400 MHz, C₆D₆) **4.10_{exo}**: irradi. at -0.92 ppm, NOEs at δ 2.01, 2.15, 2.51; irradi. at 2.51 ppm, NOEs at δ -0.92, 2.15; irradi. at 2.44 ppm, NOE at δ 2.15; irradi. at 2.66 ppm, NOE at δ 2.15.

4.2.11.4 Complex 4.11_{endo}. This compound was prepared by thermolysis of **2.4** in pentane. Crystallization of the filtered crude reaction mixture typically gave **4.11_{endo}** in 2–5% yield as bright yellow crystals.

MS 417 [$M^+ - H_2$, ^{184}W]. 1H NMR (500 MHz, C_6D_6) δ -1.40 (s, $^1J_{HW} = 120$, 1H, WH), 0.16 (dd, $^2J_{HH} = 1.3$, $^3J_{HH} = 10.1$, 1H, allyl C_bH_2), 1.09 (t, $^3J_{HH} = 7.0$, 3H, CH_2CH_3), 1.74 (s, 15H, C_5Me_5), 1.82 (m, 1H, α allyl C_cH), 2.34 (m, 1H, $C_aH_2CH_3$), 2.48 (m, 1H, $C_aH_2CH_3$), 2.79 (m, 1H, allyl C_bH_2), 4.59 (m, 1H, β allyl C_dH). $^{13}C\{^1H\}$ NMR (125 MHz, C_6D_6) δ 10.6 (C_5Me_5), 17.2 (CH_3), 27.8 (allyl C_aH_2), 38.9 (allyl C_bH_2), 84.4 (α allyl C_cH), 101.4 (β allyl C_dH), 104.5 (C_5Me_5).

4.2.12 Reactions of 2.4 with Arenes

The reactions of **2.4** with aromatic solvents were all effected in a similar manner. In all cases, the crude products were subjected to 1H NMR analysis (at either 400 or 500 MHz) prior to workup. The reaction with α,α,α -trifluorotoluene is described as a representative example.

4.2.12.1 Reaction with α,α,α -Trifluorotoluene. A solution of **2.4** (19 mg, 0.39 mmol) in α,α,α -trifluorotoluene (2 mL) in a Pyrex vessel was heated at 70–75 °C for 2 d, during which time it became brown-red. The organic volatiles were then removed in vacuo, and an NMR sample in C_6D_6 was prepared. The 1H NMR spectrum revealed the quantitative conversion of **2.4** into *o*-, *m*-, and *p*- $Cp^*W(NO)(CH_2CMe_3)(C_6H_4CF_3)$ (**4.13**) in a ratio of ~1:66:33, respectively (by integration of the methylene regions). **4.13_o** was identified by the doublets in the 1H NMR spectrum at δ -2.68 ($^2J_{HH} = 11.2$) and 5.05 ($^2J_{HH} = 11.6$) due to the presence of a CH_2CMe_3 group attached to a $[Cp^*W(NO)(aryl)]$ fragment. Next, the NMR mixture was taken to dryness, extracted into pentane, and then quickly filtered through a plug of alumina I (1 \times 1 cm). Concentration of the filtrate followed by cooling to -30 °C for 2 d afforded **4.13_m** and **4.13_p** as dark red crystals (38% combined yield).

Anal. Calcd. for $C_{22}H_{30}F_3NOW$: C, 46.74; H, 5.35; N, 2.48. Found: C, 46.43; H, 5.29; N, 2.48. IR (cm^{-1}) ν_{NO} 1575. MS 565 [M^+ , ^{184}W]. 1H NMR (300 MHz, $CDCl_3$) δ **4.13_m**: -2.58 (d, $^2J_{HH} = 10.9$, 1H, WCH_2), 1.12 (s, 9H, CMe_3), 1.84 (s, 15H, C_5Me_5), 5.11 (d, $^2J_{HH} = 10.8$, 1H, WCH_2), 7.31 (t, $^3J_{HH} = 7.3$, 1H, ArH), 7.38 (d, $^3J_{HH} = 7.3$, 1H, ArH), 7.65 (s, 1H, ArH), 7.77 (d, $^3J_{HH} = 7.2$, 1H, ArH). **4.13_p**: -2.61 (d, $^2J_{HH} = 10.4$, 1H, WCH_2), 1.12 (s,

9H, CMe₃), 1.842 (s, 15H, C₅Me₅), 5.13 (d, ²J_{HH} = 10.4, 1H, WCH₂), 7.41 (d, ³J_{HH} = 7.4, 2H, ArH), 7.59 (d, ³J_{HH} = 7.8, 2H, ArH). ¹³C{¹H} NMR (75 MHz, CDCl₃) δ 10.2 (C₅Me₅), 33.3 (CMe₃), 42.2 (CMe₃), 111.5 (C₅Me₅), 123.6 (m, Ar CH), 123.8 (m, Ar CH), 124.7 (q, ¹J_{CF} = 270, CF₃ of 4.12_m), 127.7 (WCH₂), 129.3 (q, ²J_{CF} = 30, CCF₃ of 4.12_m), 132.3 (d, ³J_{CF} = 14, Ar CH), 133.0 (m, Ar CH), 137.4 (Ar CH), 141.2 (Ar CH), 178.7 (WC_{ipso} of 4.12_m), 184.4 (WC_{ipso} of 4.12_p). CF₃ and CCF₃ resonances of 4.13_p were unobserved. ¹⁹F NMR (188 MHz, CDCl₃) δ 4.13_m: 13.6 (s). 4.13_p: 13.3 (s).

4.2.12.2 Reaction with Anisole cleanly produced a mixture of *o*-, *m*-, and *p*-Cp*W(NO)(CH₂CMe₃)(C₆H₄OCH₃) (4.12) in a ratio of approximately 88:7:5, respectively. After removal of C₆D₆ from the NMR sample, the residue was redissolved in hexanes (1 mL), and then stored at -30 °C overnight to obtain *o*-, *m*-, and *p*-4.12 (12 mg, 60% combined yield) as wine-colored crystals. Because of the low relative yields of 4.12_m and 4.12_p, spectral data other than ¹H NMR were not obtained.

Anal. Calcd. for C₂₂H₃₃NO₂W: C, 50.10; H, 6.31; N, 2.66. Found: C, 49.87; H, 6.61; N, 2.65. IR (cm⁻¹) ν_{NO} 1564 (s). MS 527 [M⁺, ¹⁸⁴W]. ¹H NMR (400 MHz, CDCl₃) δ 4.12_o: -2.90 (d, ²J_{HH} = 12.0, 1H, WCH₂), 1.05 (s, 9H, CMe₃), 1.83 (s, 15H, C₅Me₅), 3.89 (s, 3H, OCH₃), 4.91 (d, ²J_{HH} = 12.0, 1H, WCH₂), 6.78 (d, ³J_{HH} = 8.0, 1H, ArH), 6.88 (td, ³J_{HH} = 7.2, ⁴J_{HH} = 0.8, 1H, ArH), 7.19 (td, ³J_{HH} = 8.0, ⁴J_{HH} = 1.8, 1H, ArH), 7.97 (dd, ³J_{HH} = 7.1, ⁴J_{HH} = 2.0, 1H, ArH). 4.12_m: -1.92 (d, ²J_{HH} = 12.0, WCH₂), 1.06/1.07 (s, 9H, CMe₃), 1.85/1.86 (s, 15H, C₅Me₅), 3.77 (s, 3H, OCH₃), 4.15 (d, ²J_{HH} = 12.0, 1H, WCH₂), 6.68 (dd, ³J_{HH} = 8.4, ⁴J_{HH} = 2.4, 1H, ArH), 7.03 (d, ³J_{HH} = 7.2, 1H, ArH), other signals were obscured by signals of 4.12_o. 4.12_p: -2.21 (d, ²J_{HH} = 12.0, 1H, WCH₂), 1.06/1.07 (s, 9H, CMe₃), 1.85/1.86 (s, 15H, C₅Me₅), 3.75 (s, 3H, OCH₃), 4.66 (d, ²J_{HH} = 12.0, 1H, WCH₂), 6.76 (d, ³J_{HH} = 8.7, 2H, ArH), 7.56 (d, ³J_{HH} = 8.6, 2H, ArH). ¹³C{¹H} NMR (75 MHz, CDCl₃) δ 4.12_o: 10.5 (C₅Me₅), 33.7 (CMe₃), 41.3 (CMe₃), 54.6 (OCH₃), 108.9 (C₅Me₅), 111.1 (WCH₂), 121.2 (Ar CH), 128.9 (Ar CH), 130.5 (Ar CH), 140.9 (Ar CH), 159.8 (C_{ipso}OCH₃), 168.2 (WC_{ipso}).

4.2.12.3. Reaction with Toluene produced a mixture of ca. 82% *m*- and *p*-Cp*W(NO)(CH₂CMe₃)(C₆H₄Me) (**4.14**) in a 1.4:1 ratio and ca. 18% Cp*W(NO)(CH₂Ph)(C₆H₄Me). The latter species were identified by the doublets in the ¹H NMR spectrum at δ 2.38 (²J_{HH} = 6.1) and 3.35 (²J_{HH} = 6.1) due to the presence of a W–CH₂Ph group, and by mass spectral analysis, which showed a molecular ion peak at *m/z* 531. After removal of C₆D₆ from the NMR sample, the residue was chromatographed on alumina I (1 × 1 cm) by eluting with hexanes until a purple band became visible, and then with 4:1 hexanes/Et₂O to elute it. Next, the eluate was taken to dryness, redissolved in a minimum amount of pentane, and then stored at –30 °C for 1 d to obtain **4.14_m** and **4.14_p** as mauve microcrystals in 56% combined yield.

Anal. Calcd. for C₂₀H₃₀NO: C, 48.20; H, 6.07; N, 5.62. Found: C, 48.13; H, 5.97; N, 5.47. IR (cm^{–1}) ν_{NO} 1549 (s). MS 511 [M⁺, ¹⁸⁴W]. ¹H NMR (500 MHz, dioxane-*d*₈) δ **4.14_m**: –2.13 (d, ²J_{HH} = 11.5, 1H, WCH₂), 1.05 (s, 9H, CMe₃), 1.82 (s, 15H, C₅Me₅), 2.27 (s, 3H, ArMe), 4.45 (d, ²J_{HH} = 11.5, 1H, WCH₂), 6.95 (d, ³J_{HH} = 7.5, 1H, ArH), 7.09 (t, ³J_{HH} = 7.5, 1H, ArH), 7.21 (d, ³J_{HH} = 7.3, 1H, ArH), 7.39 (s, 1H, ArH). **4.14_p**: –2.05 (d, ²J_{HaHx} = 11.8, 1H, WCH₂), 1.07 (s, 9H, CMe₃), 1.83 (s, 15H, C₅Me₅), 2.22 (s, 3H, ArMe), 4.29 (d, ²J_{HaHx} = 11.8, 1H, WCH₂), 7.03 (d, ³J_{HH} = 7.5, 2H, ArH), 7.44 (d, ³J_{HH} = 7.8, 2H, ArH). ¹³C{¹H} NMR (125 MHz, dioxane-*d*₈) δ **4.14_m**: 10.02 (C₅Me₅), 21.4 (ArMe), 33.86 (CMe₃), 41.3 (CMe₃), 111.45 (C₅Me₅), 121.0 (WCH₂), 127.7 (Ar CH), 128.8 (Ar CH), 137.2 (C_{ipso}Me), 137.3 (Ar CH), 182.9 (WC_{ipso}). **4.14_p**: 10.00 (C₅Me₅), 21.5 (ArMe), 33.89 (CMe₃), 41.0 (CMe₃), 111.43 (C₅Me₅), 118.6 (WCH₂), 128.6 (Ar CH), 133.6 (Ar CH), 137.6 (C_{ipso}Me), 180.2 (WC_{ipso}).

4.2.12.4 Reaction with *o*-Xylene produced a mixture of Cp*W(NO)(CH₂CMe₃)(C₆H₃-3,4-Me₂) (**4.15**), Cp*W(NO)(CH₂CMe₃)(CH₂C₆H₄-2-Me) (**4.16**), and Cp*W(NO)(CH₂C₆H₄-2-Me)(C₆H₃-3,4-Me₂) (**4.17**) in ca. 66%, 19%, and 13% yields, respectively. A trace amount of a fourth product, tentatively assigned as Cp*W(NO)(CH₂C₆H₄-2-Me)₂, was identified by a doublet in the ¹H NMR spectrum at δ 3.43 (²J_{HH} = 6.0). After removal of C₆D₆ from the NMR sample, the residue was dissolved in a minimum amount of Et₂O and stored at –30 °C overnight to obtain **4.16** as dark orange crystals (20% yield). Next, the mother liquor was

chromatographed on alumina I (2×1 cm) by developing with hexanes until a purple band became visible, and then with 3:1 hexanes/Et₂O to elute it. Concentration of the eluate in vacuo, followed by cooling to -30 °C for several days afforded **4.15** as mauve needles (39% yield).

Cp*W(NO)(CH₂CMe₃)(C₆H₃-3,4-Me₂) (4.15): Anal. Calcd. for C₂₃H₃₅NO: C, 52.58; H, 6.72; N, 2.67. Found: C, 52.79; H, 6.78; N, 2.90. IR (cm⁻¹) ν_{NO} 1559. MS 525 [M⁺, ¹⁸⁴W]. ¹H NMR (300 MHz, C₆D₆) δ -1.76 (d, ²J_{HH} = 11.7, 1H, WCH₂), 1.28 (s, 9H, CMe₃), 1.59 (s, 15H, C₅Me₅), 1.99 (s, 3H, ArMe), 2.08 (s, 3H, ArMe), 4.26 (d, ²J_{HH} = 11.7, 1H, WCH₂), 7.04 (d, ³J_{HH} = 7.5, 1H, ArH), 7.47 (d, ³J_{HH} = 7.2, 1H, ArH), 7.82 (s, 1H, ArH). ¹³C{¹H} NMR (75 MHz, C₆D₆) δ 10.1 (C₅Me₅), 19.7 (ArMe), 20.0 (ArMe), 34.0 (CMe₃), 40.7 (CMe₃), 110.6 (C₅Me₅), 117.4 (¹J_{CW} = 90, WCH₂), 128.9 (Ar CH), 134.0 (Ar CH), 135.7 (C_{ipso}Me), 136.3 (C_{ipso}Me), 139.4 (Ar CH), 181.0 (WC_{ipso}).

Cp*W(NO)(CH₂CMe₃)(CH₂C₆H₄-2-Me) (4.16): Anal. Calcd. for C₂₃H₃₅NO: C, 52.58; H, 6.72; N, 2.67. Found: C, 52.72; H, 6.54; N, 2.55. IR (cm⁻¹) ν_{NO} 1543. MS 525 [M⁺, ¹⁸⁴W]. ¹H NMR (400 MHz, CDCl₃) δ -2.75 (d, ²J_{HH} = 13.5, 1H, CH₂CMe₃), 0.72 (s, 9H, CMe₃), 1.60 (d, ²J_{HH} = 13.5, 1H, CH₂CMe₃), 1.91 (s, 15H, C₅Me₅), 2.13 (d, ²J_{HH} = 7.6, 1H, CH₂Ar), 2.26 (s, 3H, ArMe), 3.01 (d, ²J_{HH} = 7.6, 1H, CH₂Ar), 6.00 (d, ³J_{HH} = 7.4, 1H, ArH), 6.62 (t, ³J_{HH} = 7.4, 1H, ArH), 7.00 (d, ³J_{HH} = 7.5, 1H, ArH), 7.58 (t, ³J_{HH} = 7.5, 1H, ArH). ¹³C{¹H} NMR (75 MHz, CDCl₃) δ 10.6 (C₅Me₅), 20.1 (ArMe), 33.8 (CMe₃), 37.3 (CMe₃), 44.8 (CH₂Ar), 70.0 (br s, CH₂CMe₃), 108.5 (C₅Me₅), 121.2 (CH₂C_{ipso}), 125.4 (Ar CH), 128.0 (Ar CH), 129.6 (Ar CH), 133.4 (Ar CH), 145.5 (C_{ipso}Me).

Cp*W(NO)(CH₂C₆H₄-2-Me)(C₆H₃-3,4-Me₂) (4.17): ¹H NMR (500 MHz, C₆D₆) δ 1.61 (s, 15H, C₅Me₅), 2.10 (s, 3H, ArMe), 2.19 (s, 3H, ArMe), 2.31 (s, 3H, ArMe), 3.53 (d, ²J_{HH} = 6.0, 1H, WCH₂), 6.08 (d, ³J_{HH} = 7.3, 1H, ArH), 6.33 (d, ³J_{HH} = 7.5, 1H, ArH), 6.62 (t, ³J_{HH} = 7.5, 1H, ArH), 6.87 (d, ³J_{HH} = 7.4, 1H, ArH). Others resonances were obscured by peak overlap.

4.2.12.5 Reaction with *m*-Xylene produced a mixture of $\text{Cp}^*\text{W}(\text{NO})(\text{CH}_2\text{CMe}_3)(\text{C}_6\text{H}_3\text{-}3,5\text{-Me}_2)$ (**4.18**) and $\text{Cp}^*\text{W}(\text{NO})(\text{CH}_2\text{C}_6\text{H}_4\text{-}3\text{-Me})(\text{C}_6\text{H}_4\text{-}3,5\text{-Me}_2)$ (**4.19**) in ca. 50% and 41% yields, respectively. A third product, tentatively assigned as $\text{Cp}^*\text{W}(\text{NO})(\text{CH}_2\text{C}_6\text{H}_4\text{-}3\text{-Me})_2$ based on the presence of a benzylic methylene doublet in the ^1H NMR spectrum at δ 0.65 ($^2J_{\text{HH}} = 6.0$), was detected in 9% yield. After removal of C_6D_6 from the NMR sample, the residue was dissolved in a minimum amount of hexanes, and then stored at -30°C overnight to obtain **4.19** as bright yellow crystals (33% yield). Next, the mother liquor was chromatographed on alumina I (1.5×0.7 cm) by developing with hexanes until a purple band became visible, and then with 3:1 hexanes/ Et_2O to elute it. Concentration of the eluate in vacuo, followed by cooling to -30°C for several days afforded **4.18** as mauve rosettes (33% yield).

$\text{Cp}^*\text{W}(\text{NO})(\text{CH}_2\text{CMe}_3)(\text{C}_6\text{H}_3\text{-}3,5\text{-Me}_2)$ (4.18**):** Anal. Calcd. for $\text{C}_{23}\text{H}_{35}\text{NOW}$: C, 52.58; H, 6.72; N, 2.67. Found: C, 52.63; H, 6.87; N, 2.60. IR (cm^{-1}) ν_{NO} 1550 (s). MS 525 [M^+ , ^{184}W]. ^1H NMR (300 MHz, CD_2Cl_2) δ -2.14 (d, $^2J_{\text{HH}} = 11.4$, 1H, WCH_2), 1.09 (s, 9H, CMe_3), 1.83 (s, 15H, C_5Me_5), 2.25 (s, 3H, ArMe), 4.55 (d, $^2J_{\text{HH}} = 11.4$, 1H, WCH_2), 6.80 (s, 1H, ArH), 7.07 (s, 2H, ArH). $^{13}\text{C}\{^1\text{H}\}$ NMR (75 MHz, CDCl_3) δ 10.1 (C_5Me_5), 21.4 (ArMe), 33.6 (CMe_3), 41.1 (CMe_3), 111.2 (C_5Me_5), 122.3 (WCH_2), 129.1 (Ar CH), 134.2 (2 Ar CH), 136.2 (2 $\text{C}_{\text{ipso}}\text{Me}$), 181.7 (WC_{ipso}).

$\text{Cp}^*\text{W}(\text{NO})(\text{CH}_2\text{C}_6\text{H}_4\text{-}3\text{-Me})(\text{C}_6\text{H}_4\text{-}3,5\text{-Me}_2)$ (4.19**):** Anal. Calcd. for $\text{C}_{26}\text{H}_{33}\text{NOW}$: C, 55.82; H, 5.95; N, 2.50. Found: C, 54.31; H, 5.78; N, 2.30. IR (cm^{-1}) ν_{NO} 1546 (s). HRMS Calcd. for $\text{C}_{26}\text{H}_{33}\text{NOW}$: 559.2072 [M^+ , ^{184}W]. Found: 559.2080. ^1H NMR (300 MHz, CDCl_3) δ 1.80 (s, 15H, C_5Me_5), 1.92 (s, 3H, ArMe), 2.07 (s, 6H, 2 ArMe), 2.30 (d, $^2J_{\text{HH}} = 6.0$, 1H, WCH_2), 3.23 (d, $^2J_{\text{HH}} = 6.0$, 1H, WCH_2), 6.35 (br hump, 1H, ArH), 6.43 (s, 1H, ArH), 6.59 (s, 1H, ArH), 6.70 (s, 2H, ArH), 6.73 (t, $^3J_{\text{HH}} = 7.5$, 1H, ArH), 7.09 (br d, $^3J_{\text{HH}} = 6.3$, 1H, ArH). $^{13}\text{C}\{^1\text{H}\}$ NMR (75 MHz, CDCl_3) δ 10.6 (C_5Me_5), 20.7 (2 ArMe), 33.6 (ArMe), 46.9 (WCH_2), 108.8 (C_5Me_5), 113.2 ($\text{CH}_2\text{C}_{\text{ipso}}$), 125.9 (Ar CH), 129.1 (Ar CH), 132.5 (Ar CH), 132.7 (Ar CH), 134.0 (Ar CH), 135.0 ($\text{C}_{\text{ipso}}\text{Me}$), 136.3 (v br s, Ar CH), 139.6 ($\text{C}_{\text{ipso}}\text{Me}$), 171.9 (WC_{ipso}).

4.2.12.6 Reaction with *p*-Xylene produced a mixture of $\text{Cp}^*\text{W}(\text{NO})(\text{CH}_2\text{CMe}_3)(\text{C}_6\text{H}_4\text{-2,5-Me}_2)$ (**2.11'**) and $\text{Cp}^*\text{W}(\text{NO})(\text{CH}_2\text{C}_6\text{H}_4\text{-4-Me})(\text{C}_6\text{H}_4\text{-2,5-Me}_2)$ (**4.21**), and $\text{Cp}^*\text{W}(\text{NO})(\text{CH}_2\text{C}_6\text{H}_4\text{-4-Me})_2$ (**4.22**) in ca. 44%, 33%, and 13% yields, respectively, the last of which was identified by comparison of its ^1H NMR data to those of an authentic sample prepared by a metathesis route.²⁴ After removal of C_6D_6 from the NMR sample, the residue was chromatographed on alumina I (1×1 cm) by developing with hexanes until a purple band became visible, and then with 3:1 hexanes/ Et_2O to elute it. Concentration of the eluate in vacuo, followed by cooling to -30°C for several days afforded **2.11'** as mauve rods (33% yield). A second orange-yellow band was eluted with 2:1 hexanes/ Et_2O . This fraction was then stored at -30°C overnight to induce the deposition of **4.21** as yellow-orange blocks (23% yield).

$\text{Cp}^*\text{W}(\text{NO})(\text{CH}_2\text{CMe}_3)(\text{C}_6\text{H}_4\text{-2,5-Me}_2)$ (2.11'**):** Anal. Calcd. for $\text{C}_{23}\text{H}_{35}\text{NOW}$: C, 52.58; H, 6.72; N, 2.67. Found: C, 52.43; H, 6.59; N, 2.52. IR (cm^{-1}) ν_{NO} 1538 (s). MS 525 [M^+ , ^{184}W]. ^1H NMR (500 MHz, $\text{tol-}d_8$, 213K) δ **major rotamer:** -0.98 (d, $^2J_{\text{HH}} = 11.5$, 1H, WCH_2), 1.34 (s, 9H, CMe_3), 1.47 (s, 15H, C_5Me_5), 2.20 (s, 3H, ArMe), 2.89 (s, 3H, ArMe), 4.08 (d, $^2J_{\text{HH}} = 11.5$, 1H, WCH_2), 6.54 (s, 1H, ArH), 6.85 (d, $^3J_{\text{HH}} = 7.6$, 1H, ArH), 7.17 (d, $^3J_{\text{HH}} = 7.9$, 1H, ArH). **minor rotamer:** -3.28 (d, $^2J_{\text{HH}} = 10.4$, 1H, WCH_2), 1.33 (s, 9H, CMe_3), 1.48 (s, 15H, C_5Me_5), 1.73 (s, 3H, ArMe), 2.31 (s, 3H, ArMe), 5.02 (d, $^2J_{\text{HH}} = 10.4$, 1H, WCH_2), 8.34 (s, 1H, ArH), 7.04 (d, $^3J_{\text{HH}} = 7.4$, 1H, ArH), 7.21 (d, $^3J_{\text{HH}} = 7.7$, 1H, ArH). $^{13}\text{C}\{^1\text{H}\}$ NMR (125 MHz, CD_2Cl_2) δ **major rotamer:** 9.8 (C_5Me_5), 21.0 (ArMe), 25.5 (ArMe), 33.1 (CMe_3), 40.0 (CMe_3), 110.8 (C_5Me_5), 111.2 (WCH_2), 127.7 (Ar CH), 128.1 (Ar CH), 129.9 (Ar CH), 130.9 ($\text{C}_{\text{ipso}}\text{Me}$), 146.0 ($\text{C}_{\text{ipso}}\text{Me}$), 185.6 (WC_{ipso}). **minor rotamer:** 10.0 (C_5Me_5), 20.6 (ArMe), 27.7 (ArMe), 32.7 (CMe_3), 42.2 (CMe_3), 109.5 (C_5Me_5), 127.8 (Ar CH), 129.5 (Ar CH), 133.2 ($\text{C}_{\text{ipso}}\text{Me}$), 134.7 (WCH_2), 136.3 ($\text{C}_{\text{ipso}}\text{Me}$), 140.5 (Ar CH), 180.8 (WC_{ipso}).

$\text{Cp}^*\text{W}(\text{NO})(\text{CH}_2\text{C}_6\text{H}_4\text{-4-Me})(\text{C}_6\text{H}_4\text{-2,5-Me}_2)$ (4.21**):** Anal. Calcd. for $\text{C}_{26}\text{H}_{33}\text{NOW}$: C, 55.82; H, 5.95; N, 2.50. Found: C, 55.54; H, 6.06; N, 2.68. IR (cm^{-1}) ν_{NO} 1548 (s). MS 559 [M^+ , ^{184}W]. ^1H NMR (400 MHz, C_6D_6) δ 1.57 (s, 15H, C_5Me_5), 1.58 (s, 3H, ArMe), 1.99

(s, 3H, ArMe), 2.38 (d, $^2J_{\text{HH}} = 6.1$, 1H, WCH₂), 2.93 (s, 3H, ArMe), 3.35 (d, $^2J_{\text{HH}} = 6.1$, 1H, WCH₂), 5.33 (br s, 1H, ArH), 6.35 (d, $^3J_{\text{HH}} = 7.8$, 2H, ArH), 6.66 (d, $^3J_{\text{HH}} = 7.5$, 1H, ArH), 6.94 (d, $^3J_{\text{HH}} = 7.8$, 2H, ArH), 7.04 (d, $^3J_{\text{HH}} = 7.5$, 1H, ArH). $^{13}\text{C}\{^1\text{H}\}$ NMR (75 MHz, CDCl₃) δ 10.5 (C₅Me₅), 20.5 (ArMe), 21.4 (ArMe), 28.2 (ArMe), 49.1 (br s, 2 WCH₂), 108.9 (C₅Me₅), 111.7 (WCH₂C_{ipso}), 124.6 (Ar CH), 127.5 (Ar CH), 129.8 (2 Ar CH), 130.1 (C_{ipso}Me), 135.2 (2 Ar CH), 142.5 (C_{ipso}Me), 146.9 (C_{ipso}Me), 180.8 (WC_{ipso}).

4.2.12.7 Reaction with Mesitylene produced Cp*W(NO)(CH₂C₆H₃-3,5-Me₂)₂ (**4.23**) as the only detectable organometallic product in addition to decomposition, which gave rise to broad featureless peaks in the Cp* region. After removal of C₆D₆ from the NMR sample, the oily brown-yellow residue was redissolved in 4:1 hexanes/Et₂O and filtered through a plug of alumina I (1 × 1 cm). The filtrate was reduced in volume and then stored at -30 °C to induce the deposition of **4.23** as long orange-yellow needles (43% yield).

Anal. Calcd. for C₂₄H₃₇NO: C, 57.25; H, 6.35; N, 2.38. Found: C, 57.14; H, 6.42; N, 2.42. IR (cm⁻¹) ν_{NO} 1547 (s). MS 587 [M⁺, ¹⁸⁴W]. ^1H NMR (300 MHz, CDCl₃) δ 0.81 (d, $^2J_{\text{HH}} = 8.7$, 2H, WCH₂), 2.11 (s, 15H, C₅Me₅), 2.46 (d, $^2J_{\text{HH}} = 8.7$, 2H, WCH₂), 2.50 (s, 12H, ArMe), 6.68 (s, 4H, ArH), 7.24 (s, 2H, ArH). $^{13}\text{C}\{^1\text{H}\}$ NMR (75 MHz, CDCl₃) δ 10.3 (C₅Me₅), 21.2 (4 ArMe), 41.3 ($^1J_{\text{CW}} = 66$, 2 WCH₂), 107.7 (C₅Me₅), 128.7 (2 Ar CH), 129.1 (4 Ar CH), 132.9 (4 C_{ipso}Me), 137.7 (br, 2 CH₂C_{ipso}).

4.2.13 Thermolysis of CpW(NO)(CH₂CMe₃)₂ in Neat Me₄Si, C₆D₆, and *p*-Xylene

Each of these reactions was carried out in a manner similar to the reaction of **2.4** with tetramethylsilane except the reaction was carried out at 60 °C for ca. 5–15 h. In all cases the ^1H NMR spectrum of the crude reaction mixture revealed primarily decomposition.

4.2.14 Thermolysis of $\text{CpW}(\text{NO})(\text{CH}_2\text{CMe}_3)_2$ in Cyclohexane in the Presence of PMe_3

In a manner analogous to the Cp^* reaction described above, a 0.01 M solution of **2.1** in cyclohexane in the presence of excess PMe_3 was heated at 60 °C overnight, during which time it changed color from wine-red to yellow. The organic volatiles were then removed in vacuo, and an NMR sample in C_6D_6 was prepared. The ^1H NMR spectrum of the crude reaction mixture revealed the clean conversion of **2.1** into an ca. 3:2 mixture of $\text{CpW}(\text{NO})(=\text{CHCMe}_3)(\text{PMe}_3)$ (**3.1**) and $\text{CpW}(\text{NO})(\text{cyclohexene})(\text{PMe}_3)$, respectively. The identity of **3.1** was confirmed by comparison of its ^1H NMR data to those of an authentic sample, while that of $\text{CpW}(\text{NO})(\text{cyclohexene})(\text{PMe}_3)$ was established on the basis of mass spectral and ^1H and ^{13}C NMR analyses of the crude reaction mixture.

$\text{CpW}(\text{NO})(\text{cyclohexene})(\text{PMe}_3)$: MS 437 [M^+ , ^{184}W]. ^1H (400 MHz, C_6D_6) δ 1.13 (d, $^2J_{\text{HP}} = 8.8$, 9H, PMe_3), 1.6–1.8 (m, 5H), 1.9 (m, 1H), 2.25 (m, 1H), 2.43 (m, 1H), 2.95 (m, 1H), 3.10 (m, 1H), 4.87 (s, 5H, C_5H_5). $^{13}\text{C}\{^1\text{H}\}$ (100 MHz, C_6D_6) δ 18.2 (d, $^1J_{\text{CP}} = 30.8$, PMe_3), 24.6 (CH_2), 24.8 (CH_2), 30.6 (d, $^2J_{\text{CP}} = 3.9$, $=\text{CH}$), 30.7 (CH_2), 32.6 (CH_2), 33.9 (d, $^2J_{\text{CP}} = 10.6$, $=\text{CH}$), 95.4 (C_5H_5).

4.3 Results and Discussion

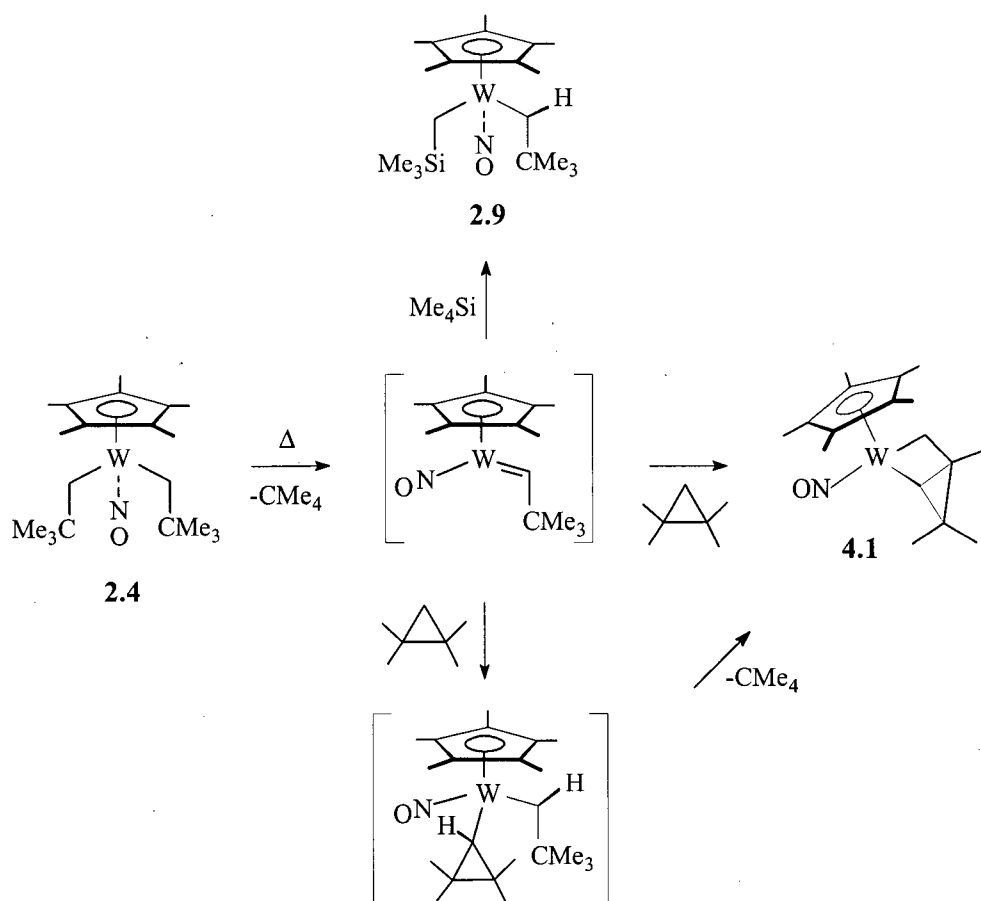
4.3.1 Thermal Reactions of $\text{Cp}^*\text{W}(\text{NO})(\text{CH}_2\text{CMe}_3)_2$ (**2.4**) with Tetramethylsilane and Alkanes

As noted in the Introduction, thermolysis of the bis(neopentyl) complex $\text{Cp}^*\text{W}(\text{NO})(\text{CH}_2\text{CMe}_3)_2$ (**2.4**) leads to the formation of $[\text{Cp}^*\text{W}(\text{NO})(=\text{CHCMe}_3)]$ as a highly reactive intermediate. In the following section, it is shown that $[\text{Cp}^*\text{W}(\text{NO})(=\text{CHCMe}_3)]$ reacts rapidly with the C–H bonds of tetramethylsilane and alkanes and that the

thermodynamic product of C–H activation often involves subsequent rearrangement of the initially formed complex.

As shown in Scheme 4.1, thermolysis of **2.4** in tetramethylsilane at 70 °C for ca. 2 d leads to formation of the known bis(alkyl) complex $\text{Cp}^*\text{W}(\text{NO})(\text{CH}_2\text{CMe}_3)(\text{CH}_2\text{SiMe}_3)$ (**2.9**) in 90% isolated yield. Thermolysis in 1,1,2,2-tetramethylcyclopropane, in contrast, gives a complex mixture containing $\text{Cp}^*\text{W}(\text{NO})[\text{CH}_2\text{C}(\text{Me})\text{C}(\text{Me})_2\text{CH}]$ (**4.1**) as the major and only identified product. The formation of **4.1** most likely proceeds via the intermediacy of $\text{Cp}^*\text{W}(\text{NO})(\text{CH}_2\text{CMe}_3)(2,2,3,3\text{-tetramethylcyclopropyl})$, which then rapidly rearranges to **4.1** by γ -hydrogen abstraction. The driving force presumably is derived from the formation of a

Scheme 4.1



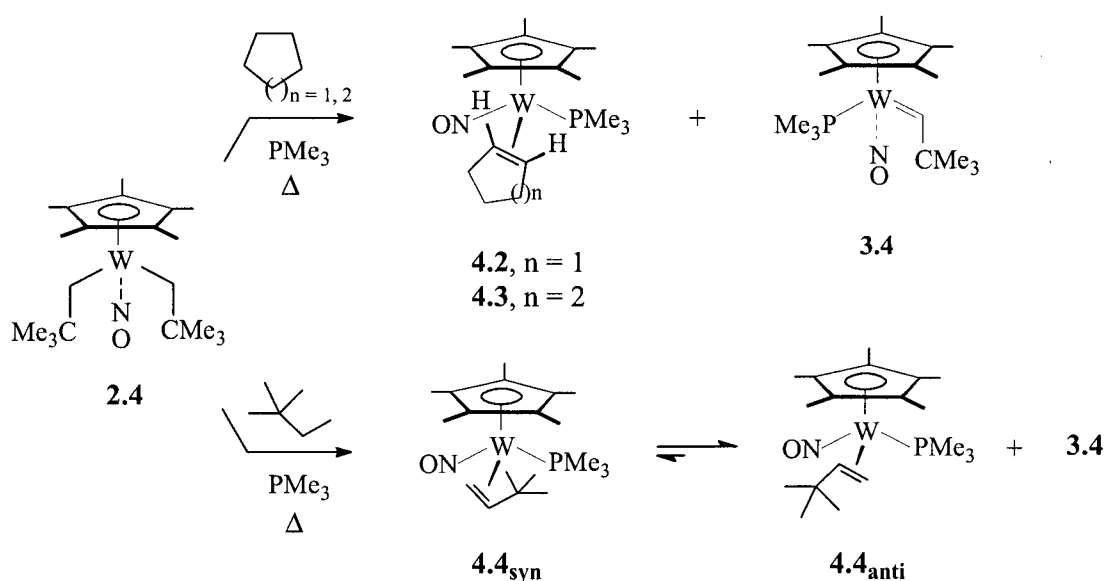
strong W–^cPr bond in the first step and the release of severe steric congestion between the cyclopropyl and neopentyl groups in the second. The alternative possibility involving initial formation of Cp*W(NO)(CH₂CMe₃)[(1,2,2-trimethylcyclopropyl)methyl] (not shown) appears highly unlikely, since it would involve activation a strong cyclopropyl C–H bond to form a highly strained product, and since γ -hydrogen abstraction has so far not been observed with other Cp*W(NO)(R)(R') complexes in which R and R' are primary alkyl ligands (and neopentyl-like).

Complex **4.1** was isolated as bright yellow crystals in 32% yield. It is stable to air and moisture and can be stored indefinitely at 25 °C under nitrogen. In the ¹³C{¹H} NMR spectrum (C₆D₆), the W–CH₂ and W–CH carbons resonate at δ 55.8 (¹J_{CW} = 37 Hz) and 83.0, respectively. In the ¹H NMR spectrum, the corresponding methine proton appears as a broad singlet at δ 1.16, while the diastereotopic methylene protons appear as a doublet and a doublet of doublets at δ 3.25 (²J_{HH} = 4.3 Hz) and δ 0.72 (²J_{HH} = 4.3 Hz, ⁴J_{HH} = 1.2 Hz). That the cyclopropyl group points away from the Cp* ligand has been confirmed by an NOE difference experiment, which shows a strong enhancement of the methine resonance upon irradiation of the Cp* methyl protons, and vice versa.

In contrast to reactions with tetramethylsilane and 1,1,2,2-tetramethylcyclopropane, only decomposition is observed upon thermolysis of **2.4** in neat cyclopentane, cyclohexane, or neohexane. More tractable chemistry, however, is observed in the presence of a trapping agent such as PMe₃. As shown in Scheme 4.2, thermolysis of **2.4** in cyclopentane, cyclohexane, or neohexane in the presence of excess PMe₃ at 70 °C for ca. 2 d cleanly produces the η^2 -alkene complexes **4.2–4.4**, respectively, and Cp*W(NO)(=CHCMe₃)(PMe₃) (**3.4**), in ratios that depend on the amount of PMe₃ used. From the crude reaction mixtures, it can be observed by ¹H and ³¹P{¹H} NMR spectroscopies that **4.2** and **4.3** exist as a single isomer, whereas **4.4** exists as a 5:1 mixture of syn and anti rotamers,²³ respectively, which have proven to be inseparable by physical means. Complex **3.4** was identified by comparison of its NMR spectral data to those of an authentic sample prepared by thermolysis of a THF or 2,2,4,4-tetramethylpentane solution of **2.4** in the presence of excess PMe₃ (see Chapter 3). Complexes

4.2–4.4, on the other hand, were isolated as air-stable yellow crystalline materials by chromatography on alumina I, followed by crystallization from hexanes/Et₂O at –30 °C. They were characterized by standard spectroscopic and analytical methods, aided by HMQC, HMBC, and/or NOE difference experiments, and in the case of **4.3** and **4.4_{syn}** also by X-ray diffraction.

Scheme 4.2

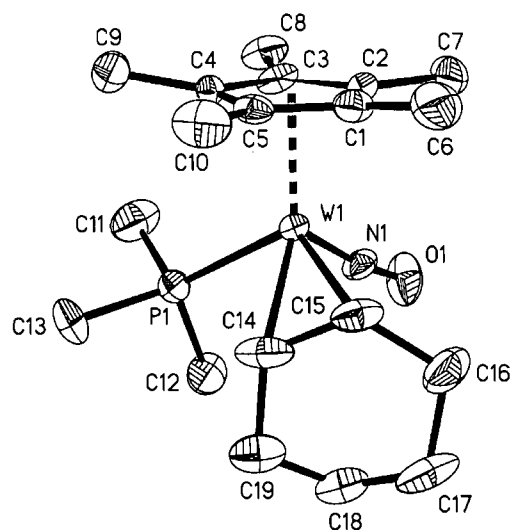


Spectroscopically, complexes **4.2–4.4** are very similar to the rhenium alkene complexes, [CpRe(NO)(CH₂=CHR)(PPh₃)]⁺X[–],²⁴ synthesized by Gladysz and coworkers. In the ¹H NMR spectra (C₆D₆), the olefinic proton resonances appear at about δ –0.3 to 1.0 and δ 1.4 to 2.3. In all cases, the upfield signals correspond to the protons lying *syn* to the Cp* ligand and *cis* to NO. In the ¹³C{¹H} NMR spectra (C₆D₆), the corresponding carbon resonances appear as a doublet and a singlet at δ 40.0–46.1 (²J_{CP} = 12–13 Hz) and δ 36.9–44.2 (¹J_{CW} = 39–40 Hz), respectively. These upfield shifts are indicative of substantial metallacyclopropane character and can be ascribed to strong π -backbonding by tungsten.^{25,26} Key to the stereochemical assignment of **4.4_{syn}** in solution is the observation of a strong NOE

enhancement of the *tert*-butyl resonance upon irradiation of the Cp* and PMe₃ signals. In the case of **4.4_{anti}**, irradiation of the PMe₃ signal leads to an NOE enhancement of the =CH₂ signal at δ -0.30 and irradiation of either the Cp* or =CH₂ signal at δ -0.30 leads to an enhancement of the signal for the =CHCMe₃ proton at δ 1.43.²⁷

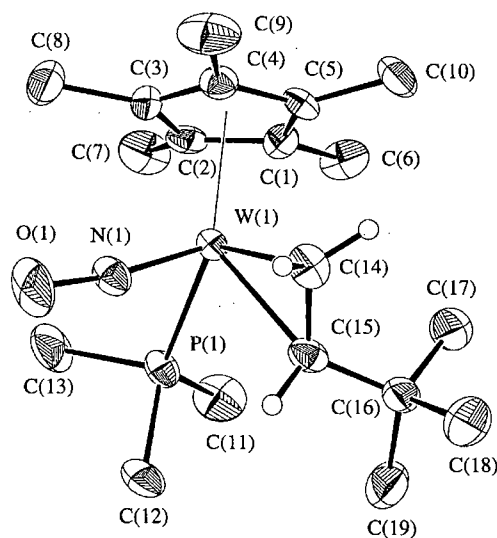
Shown in Figure 4.1 are the ORTEP diagrams of the solid-state molecular structures of complexes **4.3** and **4.4_{syn}** along with selected bond distances and angles. As in the case of the [CpRe(NO)(CH₂=CHR)(PPh₃)]⁺X⁻ complexes, the nitrosyl ligand in each of **4.3** and **4.4_{syn}** is essentially linear, while the alkene ligand is oriented such that its C=C bond axis is perpendicular to the W-N-O vector, as would be expected for maximum π -bonding.²⁸ The alkene ligand is coordinated in a manner such that the two W-C _{α} distances are unequal. In each complex, the bond cis to NO is shorter than that cis to PMe₃. This asymmetry appears to be due to steric crowding by the alkene substituents, since the opposite trend is observed for the [CpRe(NO)(CH₂=CHR)(PPh₃)]⁺X⁻ complexes, where the =CHR group is cis to NO, and since in **4.3** and **4.4_{syn}** the W-C _{α} distance also increases as the size of the substituent on carbon increases. Finally, as expected from the NMR experiments, there is a substantial lengthening of the carbon double bonds in **4.3** and **4.4_{syn}**. In both compounds, the C(14)-C(15) bond distances are essentially identical at 1.447 Å.²⁹

A



W(1)–N(1)	2.444(2) Å
N(1)–O(1)	1.768(6) Å
W(1)–P(1)	1.251(8) Å
W(1)–C(14)	2.246(9) Å
W(1)–C(15)	2.193(9) Å
C(14)–C(15)	1.447(12) Å
N(1)–W(1)–C(14)	105.8(3)°
N(1)–W(1)–C(15)	96.3(3)°
N(1)–W(1)–P(1)	87.1(2)°
W(1)–N(1)–O(1)	172.6(6)°

B



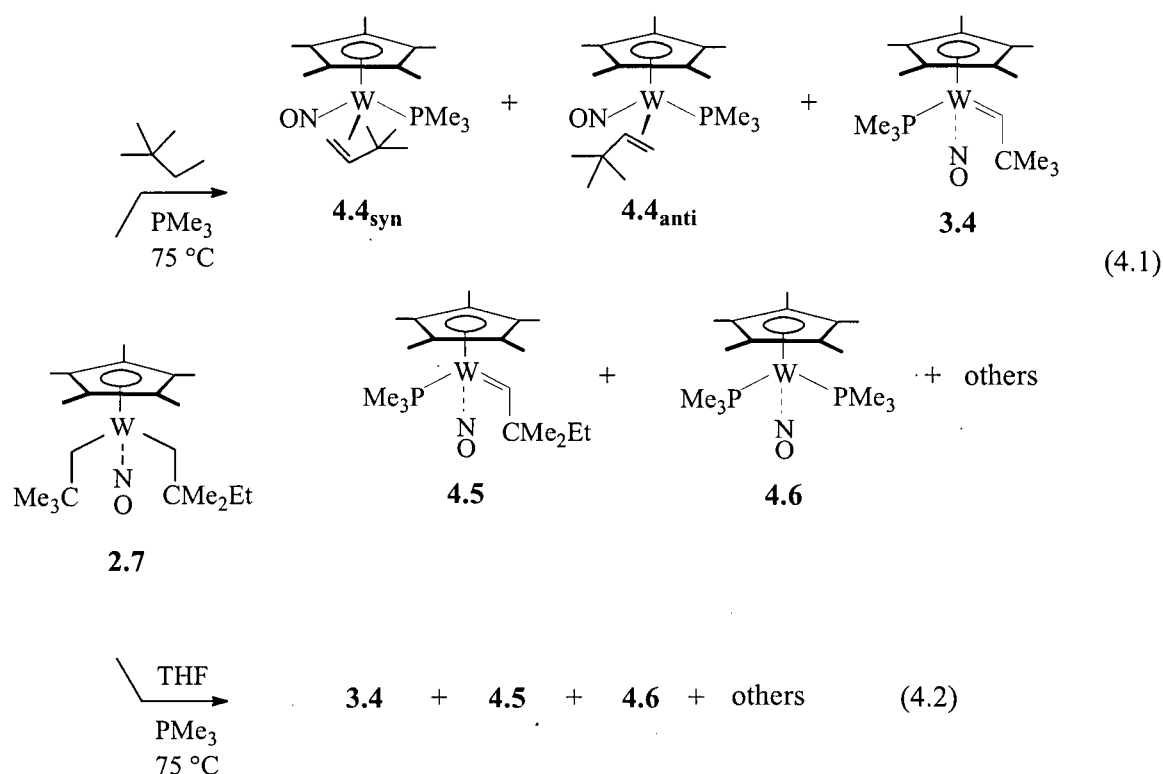
W(1)–N(1)	2.441(2) Å
N(1)–O(1)	1.770(5) Å
W(1)–P(1)	1.227(6) Å
W(1)–C(14)	2.173(6) Å
W(1)–C(15)	2.298(6) Å
C(14)–C(15)	1.446(8) Å
N(1)–W(1)–C(14)	93.0(3)°
N(1)–W(1)–C(15)	94.6(2)°
N(1)–W(1)–P(1)	82.5(2)°
W(1)–N(1)–O(1)	170.7(5)°

Figure 4.1. ORTEP diagrams and selected bond distances and angles for complexes (A) $\text{Cp}^*\text{W}(\text{NO})(\text{cyclohexene})(\text{PMe}_3)$ (**4.3**) and (B) $\text{Cp}^*\text{W}(\text{NO})(\text{neohexene})(\text{PMe}_3)$ (**4.4_{syn}**).

In order to gain insight into the reactions outlined in Scheme 4.2, the thermolysis of **2.4** in cyclohexane in the presence of various amounts of PMe_3 was monitored by $^{31}\text{P}\{^1\text{H}\}$ NMR spectroscopy. This showed that the ratio of the neopentylidene complex **3.4** to the cyclohexene complex **4.3** is independent of the reaction time and that this ratio increases as the initial concentration of PMe_3 increases. These results thus indicate that **3.4** and **4.3** are formed as a result of a competition between PMe_3 and cyclohexane for reaction with $[\text{Cp}^*\text{W}(\text{NO})(=\text{CHCMe}_3)]$ and that these complexes do not interconvert.

The thermolysis of **2.4** in neohexane in the presence of excess PMe_3 was also monitored by $^{31}\text{P}\{^1\text{H}\}$ NMR spectroscopy. In this case, parallel formation of **3.4** and **4.4_{syn}** was observed at early conversion. As the reaction progressed, **4.4_{anti}** was generated at the expense of **4.4_{syn}**. At 70 °C, the isomerization of **4.4_{syn}** to **4.4_{anti}** ($k_{\text{obs}} \sim 7.41 \times 10^{-6} \text{ s}^{-1}$) is independent of PMe_3 concentration and occurs at a rate that is approximately one order of magnitude lower than that for formation of **4.4_{syn}** ($k_{\text{obs}} \sim 4.22 \times 10^{-5} \text{ s}^{-1}$). In addition, it may be effected in neat C_6D_6 or in C_6D_6 in the presence of a large excess of PMe_3 without solvent activation or formation of the known bis(phosphine) complex $\text{Cp}^*\text{W}(\text{NO})(\text{PMe}_3)_2$.² These results therefore suggest that **4.4_{syn}** is the kinetic product of the double C–H activation of neohexane and that, in contrast to the $[\text{CpRe}(\text{NO})(\text{CH}_2=\text{CHR})(\text{PPh}_3)]^+\text{X}^-$ complexes, which upon thermolysis undergo exchange of alkene enantioface by way of a $\sigma\text{-C-H}$ complex,³⁰ the isomerization of **4.4_{syn}** to **4.4_{anti}** occurs by simple rotation and without phosphine or alkene ligand dissociation.

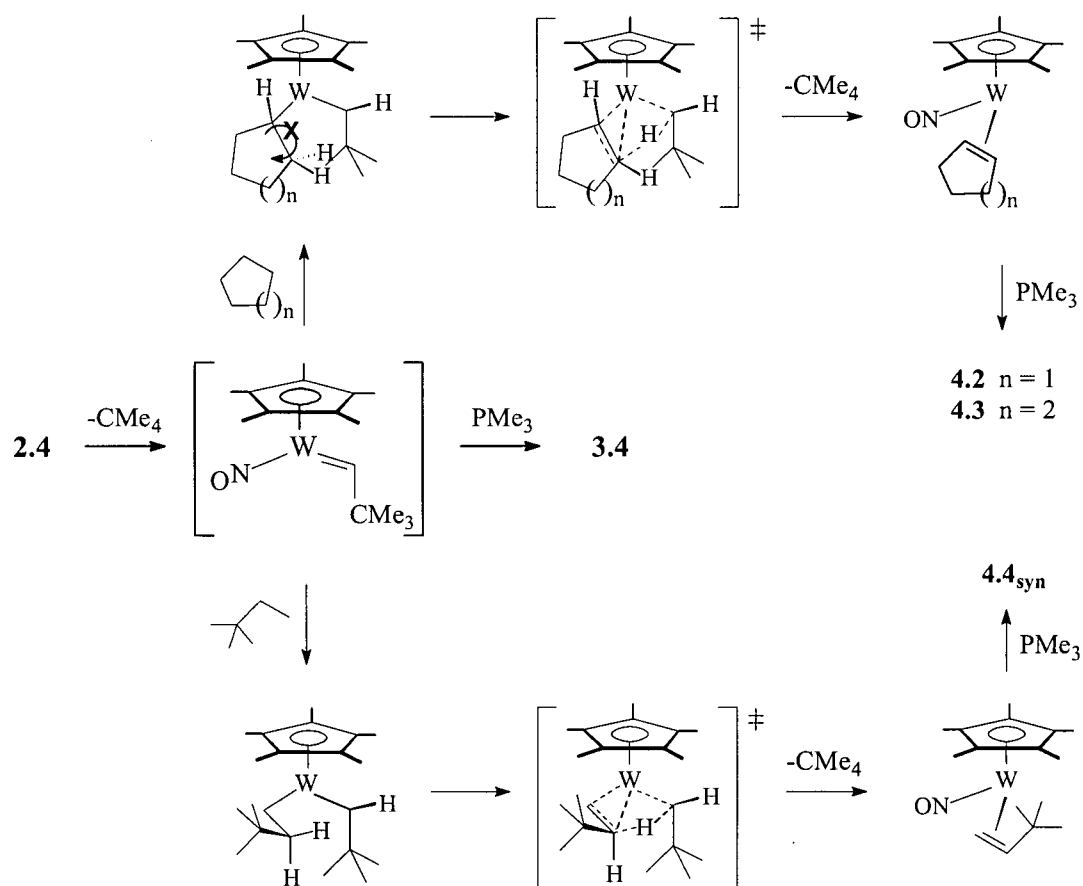
To determine whether the formation of **4.4** occurs with concomitant reversible *tert*-butyl C–H activation, the bis(alkyl) complex $\text{Cp}^*\text{W}(\text{NO})(\text{CH}_2\text{CMe}_3)(\text{CH}_2\text{CMe}_2\text{Et})$ (**2.7**) was prepared and its thermal decomposition investigated. If **2.7**, the expected product of *tert*-butyl C–H activation, was formed reversibly, then heating a solution of **2.7** and PMe_3 should cleanly produce complexes **3.4** and **4.4** when the solvent is neohexane, and complex **3.4** when the solvent is THF. This was not the case, however, when the thermolysis of **2.7** in the presence of excess PMe_3 was performed. As shown in eq 4.1, the thermolysis of **2.7** in neohexane is complex, producing not only **4.4** and **3.4** as major products but also



$\text{Cp}^*\text{W}(\text{NO})(=\text{CH}_2\text{CMe}_2\text{Et})(\text{PMe}_3)$ (**4.5**) and $\text{Cp}^*\text{W}(\text{NO})(\text{PMe}_3)_2$ (**4.6**), along with several unidentified minor products which display ^{31}P NMR signals in the δ 33–36 region. The thermolysis of **2.7** in THF is similarly complex, affording an approximately 1:1:1 mixture of **3.4**, **4.5**, and **4.6** based on relative ^{31}P NMR peak heights, as well as several minor unidentified products which display ^{31}P NMR signals in the δ 10–18 region (eq 4.2). In this case, **4.4** could not be observed by $^{31}\text{P}\{^1\text{H}\}$ NMR spectroscopy, most likely because the concentration of free neohexane was too low to compete with PMe_3 for reaction with $[\text{Cp}^*\text{W}(\text{NO})(=\text{CHMe}_3)]$.

Although complexes **4.4**, **3.4**, **4.5** and **4.6** could not be isolated pure, their identities could be established by ^1H NMR, ^{13}C NMR, and/or ^{31}P NMR analyses of semi-purified product mixtures. Spectroscopically, **4.5** is very similar to **3.4**; it was thus identified by the characteristic signals of its alkylidene α -proton and PMe_3 phosphorus at δ 11.27 ($^3J_{\text{HP}} = 3.3$ Hz) and δ -7.6 ($^1J_{\text{PW}} = 445$ Hz), respectively. In the case of **4.6**, its identity was confirmed by

Scheme 4.3

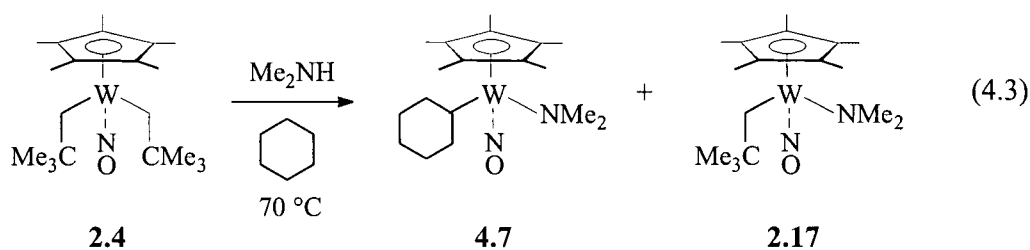


comparison of its ¹H, ¹³C, and ³¹P NMR spectral data to those of an authentic sample³⁵ prepared by reducing Cp*W(NO)Cl₂ with sodium amalgam in the presence of excess PMe₃. Together these results strongly suggest that in the activation of neohexane by [Cp*W(NO)(=CHCMe₃)] attack at the *tert*-butyl position occurs rarely, if at all. The activation of neohexane is therefore regiospecific and involves initial attack at the CH₂CH₃ position.

The observation that **4.2**, **4.3**, and **4.4_{syn}** are formed stereospecifically can be rationalized in terms of a mechanism in which the initially formed complex eliminates neopentane by a direct β-hydrogen abstraction reaction. As illustrated in Scheme 4.3, a

bicyclic transition state with little conformational freedom is involved. In this transition state, in order to minimize unfavorable steric interactions with the neopentyl *tert*-butyl group, rotation about the neohexyl C $_{\alpha}$ –C $_{\beta}$ bond occurs so as to place the *tert*-butyl syn with respect to the Cp* ligand. Subsequent β -hydrogen abstraction leading to **4.4_{syn}** therefore occurs stereospecifically for steric reasons. In the formation of **4.2** and **4.3**, on the other hand, such a rotation is not possible due to the geometric constraints imposed by the cycloalkyl rings. Consequently, β -hydrogen abstraction leads to formation of alkene complexes in which the =CHR hydrogen points toward the Cp* ligand.

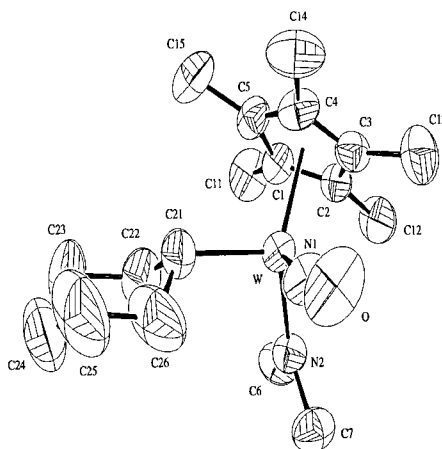
The trapping of the above double C–H-activated intermediates is not limited to phosphine ligands. As shown in eq 4.3, thermolysis of **2.4** in cyclohexane in the presence of excess Me₂NH also occurs cleanly, yielding Cp*W(NO)(cyclohexyl)(NMe₂) (**4.7**) and Cp*W(NO)(CH₂CMe₃)(NMe₂) (**2.17**) (see Chapter 3), in ratios that depend upon the amount of amine added. As noted in Chapter 3, complex **2.17** can also be generated upon thermolysis of **2.4** or Cp*W(NO)(=CHCMe₃)(PMe₃) (**3.4**) in THF in the presence of excess Me₂NH. Since the conversion of **2.4** to **2.17** involves initial formation of [Cp*W(NO)(=CHCMe₃)] as the reactive intermediate rather than σ -bond metathesis, the formation of **4.7** therefore is in the same manner as that proposed above for reaction in the presence of PMe₃. An exception is that amine coordination is followed by conversion of the cyclohexene moiety into a cyclohexyl group by α -hydrogen migration.



Complex **4.7** was isolated as a yellow crystalline solid by chromatography on alumina I, followed by crystallization from hexanes/Et₂O. It was then characterized by ¹H and ¹³C NMR spectroscopies and by an X-ray crystallographic study. Spectroscopically, **4.7** is very

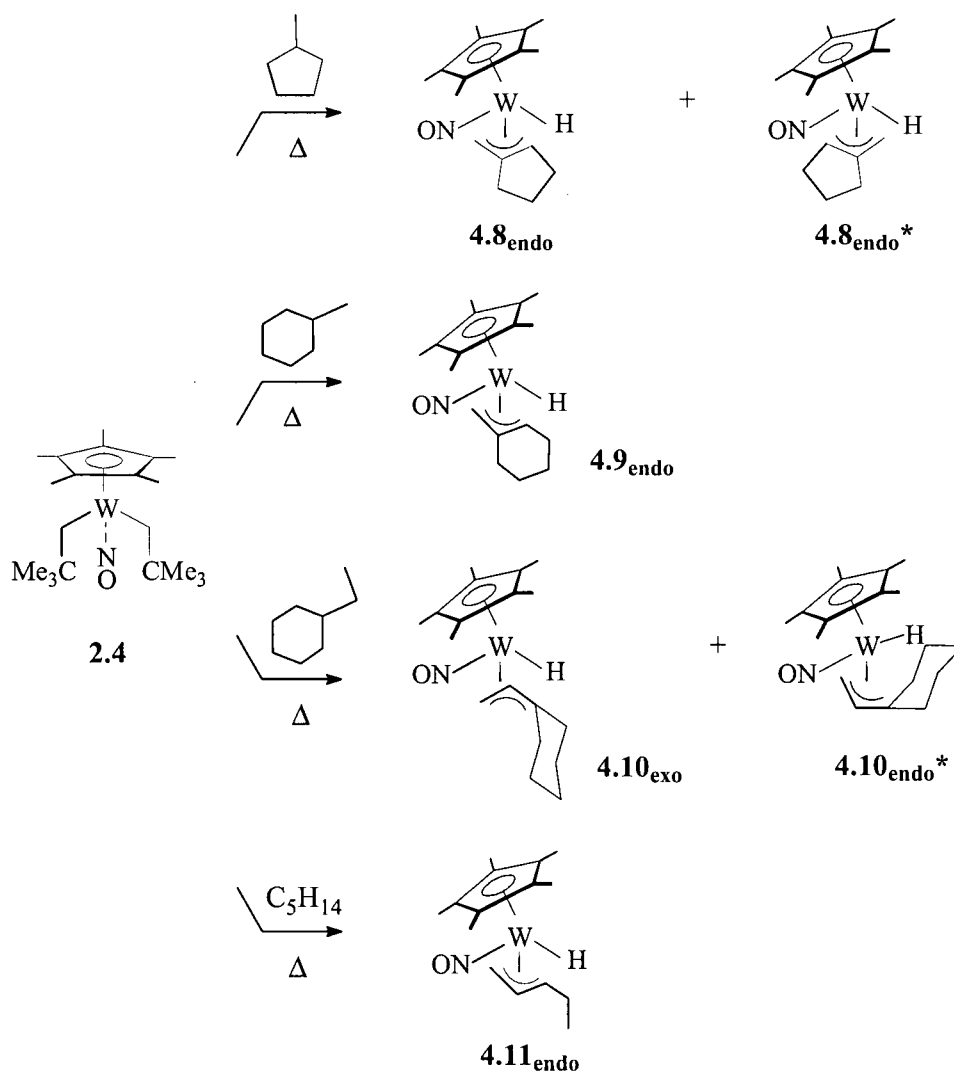
similar to **2.17**. In addition to peaks due to the Cp* and NMe₂ ligands, the ¹³C{¹H} NMR spectrum of **4.7** in C₆D₆ contains signals attributable to the cyclohexyl methine carbon at δ 52.1 (¹J_{CW} = 94 Hz) and methylene carbons at δ 27.8, 32.9, 33.0, 37.2, and 40.0. In the ¹H NMR spectrum, the cyclohexyl methine proton resonates as a multiplet at δ 1.17, while the amido methyl groups resonate as two sharp singlets at δ 2.63 and 3.72 even at 70 °C. This suggests that the amido ligand is functioning as a strong π -donor toward the tungsten center.

Shown in Figure 4.2 is an ORTEP diagram of the solid-state molecular structure of **4.7** along with selected bond distances and angles. Like the structure of **2.17**, the amido ligand of **4.7** adopts a planar geometry with bonding parameters consistent with it acting as a π -donor. For example, the W–NMe₂ distance of 1.924(8) Å is indicative of considerable multiple bond character and the N(1)–W–N(2)–C(7) and N(1)–W–N(2)–C(6) torsion angles of –8(4)° and 177.1(6)°, respectively, are of proper magnitude for maximum π -bonding.



methylcyclohexane, ethylcyclohexane, or pentane (70 °C, 2 d) results in the formation of the η^3 -allyl hydride complexes **4.8–4.11** in low to moderate yields in both the presence and absence of PMe_3 (Scheme 4.5). Reactions in the absence of PMe_3 proceed with concomitant decomposition, while reactions in the presence of PMe_3 proceed with some decomposition (especially in the case of pentane) as well as give **3.4** and PMe_3 -trapped alkene complexes as minor products.

Scheme 4.5 (* = minor isomer detectable by ^1H and ^{13}C NMR spectroscopies)



Complexes **4.8–4.11** were isolated as yellow crystalline materials by crystallization from hexanes or pentane/Et₂O. They are thermally quite stable; for example, **4.8** and **4.10** can be heated in toluene-*d*₈ for several hours at 70–90 °C without detectable decomposition or reaction with solvent. The formulation of **4.8–4.11** is supported by NMR, IR, and mass spectroscopies. The highest peak in the electron-impact mass spectra corresponds to the molecular ion minus H₂. The W–H stretch in the Nujol-mull IR spectra appears as a weak absorbance at 1900–2200 cm⁻¹. In the ¹H NMR spectra, the hydride resonance appears as a singlet at δ –0.7 to –1.4 with ¹J_{HW} = 119–123 Hz.

The ¹H and ¹³C NMR spectra of **4.9** and **4.11** indicate the presence of one isomer. In the ¹H and ¹³C NMR spectra of **4.8** and **4.10**, two isomers were observed in ratios of >85:15. The major and minor isomers of **4.8** were assigned endo structures in which the hydride ligand is cis and trans, respectively, to the substituted end of the allyl ligand based on ¹H NOE difference measurements (see the Experimental Section), ¹H and ¹³C NMR chemical shifts for the allyl fragment, and comparison of these NMR data to those of **4.9**, which has been characterized by X-ray diffraction (see below). The isomers of **4.10**, in contrast, differ from one another in the orientation of the allyl fragment relative to the Cp* ligand. The assignment of the major isomer as an exo complex in which the hydride ligand is cis to the substituted end of the allyl was based on results of an NOE difference experiment and an X-ray diffraction study. In the case of the minor isomer of **4.10**, its assignment as an endo complex in which the hydride ligand is cis to the substituted end of the allyl was based on the fact that its allyl proton and carbon resonances appear at chemical shifts that are very similar to those of **4.8**_{endo} and **4.9**_{endo}, and quite different from those of **4.10**_{exo}. As shown in Table 4.1, the chemical shifts for the allyl protons and carbons are particularly diagnostic of the orientation of the allyl ligand with respect to the Cp* ligand. In general the chemical shift difference for the α -CH₂ resonances of the endo isomer ($\Delta\delta \approx 2.3$ –3.3 ppm) is much larger than that of the exo isomer ($\Delta\delta \approx 0.3$ ppm). In addition, the resonance for the central proton of the endo isomer appears at much lower field than that of the exo isomer.

Table 4.1. Selected ^1H and ^{13}C NMR Data for the η^3 -Allyl Moieties of Complexes **4.8–4.11**^a

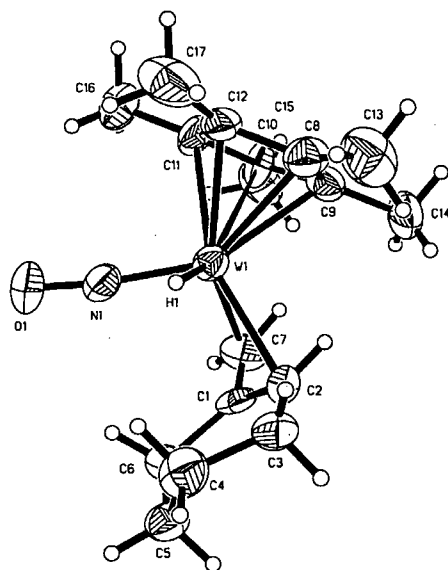
compd	^1H NMR (δ)				^{13}C NMR (δ)		
	$\alpha\text{-CH}_2$ (anti)	$\alpha\text{-CH}_2$ (syn)	$\alpha\text{-CH}$ (anti)	$\beta\text{-CH}$	$\alpha\text{-CH}_2$	$\alpha\text{-CH}$	$\beta\text{-CH}$
4.8 _{endo} ^b	0.68	3.06	2.44		38.3	80.3	
4.8 _{endo} ^{*c}	0.96	4.21	1.7		46.2	67.7	
4.9 _{endo} ^d	0.31	2.60	2.28		41.3	80.0	
4.11 _{endo} ^d	0.16	2.79	1.82	4.59	38.9	84.4	101.4
4.10 _{endo} ^c	0.60	2.87		4.69	40.9		100.9
4.10 _{exo} ^b	2.44	2.15		2.66	37.2		109.0

^aIn C_6D_6 . ^bMajor isomer. ^cMinor isomer. ^dOnly one isomer was detected in the NMR spectra of purified samples.

As mentioned above, the solid-state molecular structures of **4.9**_{endo} and **4.10**_{exo} have been determined by X-ray diffraction. Shown in Figure 4.3 are the ORTEP representations of these structures along with selected bond distances and angles. Structurally, **4.9**_{endo} and **4.10**_{exo} are very similar to the σ, η^3 (endo) complex, $\text{Cp}^*\text{W}(\text{NO})[\text{CH}_2\text{C}(\text{Me})\text{CHCH}_2\text{C}(\text{Me})_2\text{CH}(\text{Me})]$, reported in Chapter 3. Noteworthy are the following features. First, in contrast to the allyl ligands in nitrosyl complexes such as $\text{CpM}(\text{NO})(\eta^3\text{-allyl})(\text{halide})$ ($\text{M} = \text{Mo},^{31} \text{W}^{32}$), $\text{CpW}(\text{NO})(\eta^3\text{-allyl})(\eta^1\text{-alkynyl})$,³³ and $\text{TpMo}(\text{NO})(\eta^3\text{-allyl})(\text{CO})$,³⁴ which exhibit $\eta^3 \rightarrow \sigma, \eta^2$ distortion, the allyl C–C distances in **4.9**_{endo} and **4.10**_{exo} (1.37–1.39 Å) are all within 0.02 Å of one another and in the range intermediate of double and single bonds. Second, in each complex the substituted allyl terminus is cis to the hydride ligand, which was located but not refined, and is farther from the metal center than the unsubstituted terminus, presumably in order to minimize steric repulsion between the allyl substituents and the $[\text{Cp}^*\text{W}(\text{NO})(\text{H})]$ fragment.

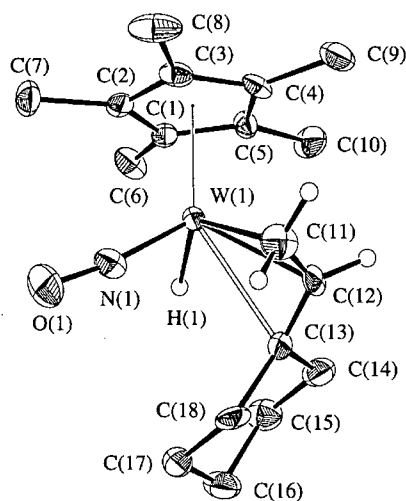
The observation that **4.8–4.11** are formed in low to moderate yields in both the presence and absence of excess PMe_3 and that, in all but the case of **4.8**_{endo}^{*}, the hydride and the substituted end of the allyl ligand are adjacent to one another can be explained in terms of

A



W(1)–C(7)	2.234(11) Å
W(1)–C(1)	2.369(9) Å
W(1)–C(2)	2.397(11) Å
C(1)–C(2)	1.366(14) Å
C(1)–C(7)	1.39(2) Å
W(1)–N(1)	1.787(9) Å
N(1)–O(1)	1.216(11) Å
C(2)–C(1)–C(7)	118.7(10)°
C(2)–C(1)–C(6)	120.5(9)°
C(1)–C(2)–C(3)	123.8(10)°
C(7)–C(1)–C(6)	119.7(10)°
C(2)–C(3)–C(4)	111.5(10)°
O(1)–N(1)–W(1)	172.8(9)°

B



W(1)–C(11)	2.267(8) Å
W(1)–C(12)	2.275(7) Å
W(1)–C(13)	2.476(7) Å
C(11)–C(12)	1.390(11) Å
C(12)–C(13)	1.380(10) Å
W(1)–N(1)	1.768(6) Å
N(1)–O(1)	1.227(7) Å
C(11)–C(12)–C(13)	125.7(7)°
C(12)–C(13)–C(18)	122.7(7)°
O(1)–N(1)–W(1)	172.8(9)°

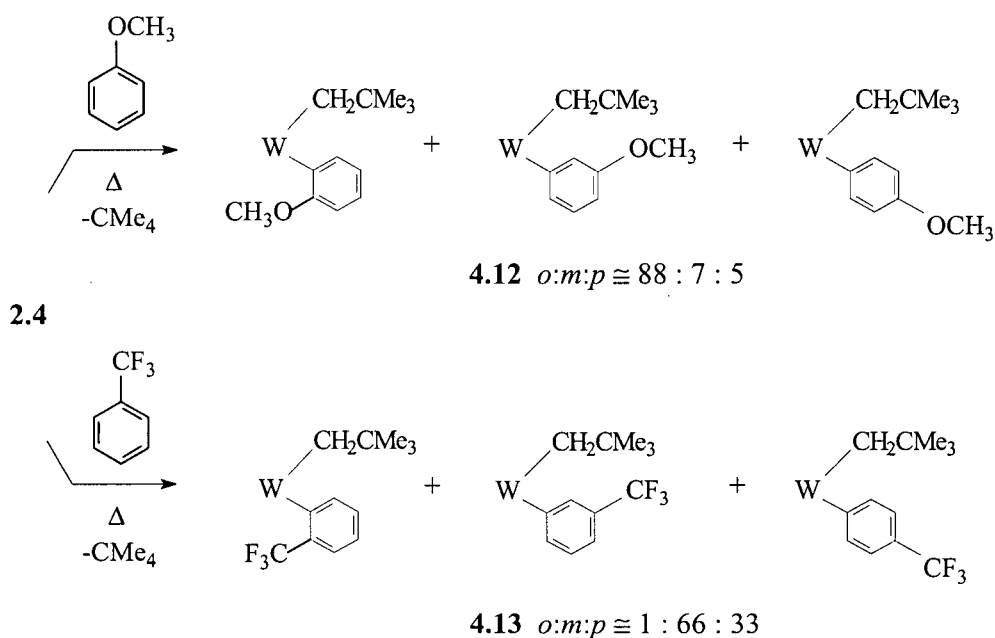
Figure 4.3. ORTEP drawings and selected bond distances and angles of (A) $\text{Cp}^*\text{W}(\text{NO})(\eta^3\text{-C}_7\text{H}_{11})(\text{H})$ (**4.9_{endo}**) and (B) $\text{Cp}^*\text{W}(\text{NO})(\eta^3\text{-C}_8\text{H}_{13})(\text{H})$ (**4.10_{exo}**).

formation of bis(alkyl) complexes **A** and **A'**, which rearrange to the alkene intermediates **B**, **B'**, and **B''** in a manner analogous that described above for the activation of neohexane, cyclopentane, and cyclohexane. Allylic C–H activation then ensues depending on the structure and orientation of the alkene ligand. For intermediate **B**, allylic C–H activation is apparently fast and irreversible, yielding the observed product **4.11_{endo}** even in the presence of PMe_3 . In the case of intermediate **B''**, the orientation of its alkene ligand does not permit such a transformation; adduct formation therefore occurs when the reaction is carried out in the presence of PMe_3 . Intermediate **B'**, on the other hand, is structurally similar to the alkene intermediates in the cyclopentane and cyclohexane reactions with one exception. Subsequent allylic C–H activation in **B'** would lead to formation of a 1,3-disubstituted allyl ligand in an endo and not an exo conformation. As noted above, thermolysis of **2.4** in cyclopentane or cyclohexane in the presence of PMe_3 leads to the clean formation of alkene complexes **4.3** and **4.4**, respectively, whereas use of pentane as solvent results in concomitant decomposition. A possible explanation for these observations therefore is that allylic C–H activation in $[\text{Cp}^*\text{W}(\text{NO})(\text{alkene})]$ complexes is stereospecific,³⁵ occurring only when it leads to formation of an endo allyl ligand, and that 1,3-disubstituted allyl ligands are unstable, decomposing at the temperature at which they form.

4.3.2 Thermal Reactions of **2.4** with Arenes

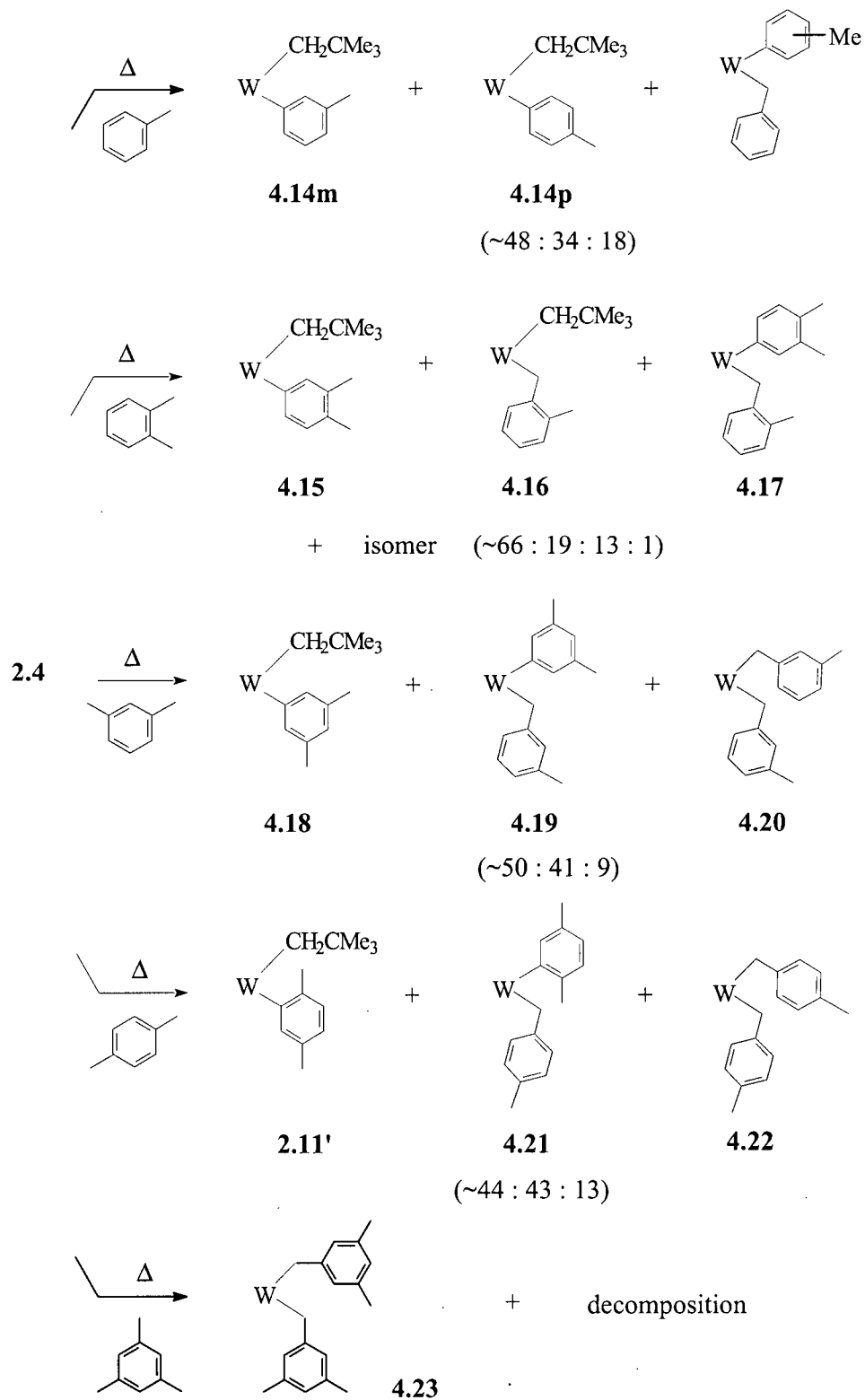
In addition to its reactions with alkanes, the unsaturated neopentylidene complex $[\text{Cp}^*\text{W}(\text{NO})(=\text{CHCMe}_3)]$ is also highly reactive toward aromatic solvents. As shown in Scheme 4.6, thermolysis of **2.4** in neat α,α,α -trifluorotoluene or anisole at 70–75 °C for ~1.5 d leads to formation of products resulting from aryl C–H bond addition across the $\text{W}=\text{C}$ linkage. In α,α,α -trifluorotoluene, the products are *o*-, *m*-, and *p*- $\text{Cp}^*\text{W}(\text{NO})(\text{CH}_2\text{CMe}_3)(\text{C}_6\text{H}_5\text{CF}_3)$ (**4.12**), formed in a ratio of ~1:66:33 by integration of the methylene regions of the ^1H NMR spectrum (C_6D_6). Similarly, the reaction with anisole yields the corresponding *o*-, *m*-, and *p*- $\text{Cp}^*\text{W}(\text{NO})(\text{CH}_2\text{CMe}_3)(\text{C}_6\text{H}_5\text{OCH}_3)$ complexes (**4.13**) in a ratio of ~88:7:5.

Scheme 4.6



The thermolysis of **2.4** in methylated benzenes at 70–75 °C yields both aryl and benzyl C–H activation products as shown in Scheme 4.7. The thermolysis in toluene produces a mixture of ca. 82% *m*- and *p*-Cp*W(NO)(CH₂CMe₃)(C₆H₄Me) (**4.14**) in a ratio of 1.4:1 and ca. 18% Cp*W(NO)(CH₂Ph)(C₆H₄Me). The formation of Cp*W(NO)(CH₂Ph)(C₆H₄Me) occurs with Cp*W(NO)(CH₂CMe₃)(CH₂Ph) as an observable intermediate. As noted in the Introduction, Cp*W(NO)(CH₂CMe₃)(CH₂Ph) is unstable with respect to α -abstraction of neopentane. This leads to formation of the benzyldiene complex, [Cp*W(NO)(=CHPh)], which apparently is also capable of cleaving C–H bonds intermolecularly. Because of the low yields of Cp*W(NO)(CH₂Ph)(C₆H₄Me), isolation was not attempted; assignment of their structures therefore is only tentative and rests primarily on the fact that the W–CH₂Ph resonances exhibit chemical shifts and coupling constants very similar to those of other benzyl-containing complexes such as **4.17**, **4.19**, **4.21**, and **4.22** (see below).³⁶ Complexes **4.14**, on the other hand, were purified as a mixture by crystallization and characterized fully by spectroscopic and analytical methods (see below).

Scheme 4.7



Heating **2.4** in *o*-xylene results in the formation of complexes **4.15**, **4.16**, and **4.17** in ca. 66%, 19%, and 13% yields, respectively, and a trace amount of a product tentatively assigned as the bis(benzyl), $\text{Cp}^*\text{W}(\text{NO})(\text{CH}_2\text{C}_6\text{H}_4\text{-2-Me})_2$ (by ^1H NMR). Complete conversion of **4.16** to **4.17** and $\text{Cp}^*\text{W}(\text{NO})(\text{CH}_2\text{C}_6\text{H}_4\text{-2-Me})_2$ was not possible, as decomposition of **4.16** to unknown products became competitive at longer reaction times.

The reaction with *m*-xylene gives complexes **4.18**, **4.19**, and **4.20** in respective yields of ca. 50%, 41%, and 9%, according to ^1H NMR analysis, while the reaction with *p*-xylene produces **2.11'**, **4.21**, and **4.22** in ca. 44%, 33%, and 13% yields, respectively. The intermediates $\text{Cp}^*\text{W}(\text{NO})(\text{CH}_2\text{CMe}_3)(\text{CH}_2\text{C}_6\text{H}_4\text{-3-Me})$ and $\text{Cp}^*\text{W}(\text{NO})(\text{CH}_2\text{CMe}_3)(\text{CH}_2\text{C}_6\text{H}_4\text{-4-Me})$ were not observed, presumably because they decomposed too rapidly to allow build up during the reaction. The reaction with mesitylene, in contrast, proceeds with concomitant decomposition and yields the benzyl-activated complex, $\text{Cp}^*\text{W}(\text{NO})(\text{CH}_2\text{C}_6\text{H}_3\text{-3,5-Me}_2)_2$ (**4.23**), as the only identifiable product in 43% isolated yield.

In order to confirm the identity of several of the products produced in the reactions of **2.4** with *o*-, *m*-, and *p*-xylenes, the ^1H NMR data of **4.22** were compared to those of an authentic sample, while complexes **4.15**, **4.16**, **4.18**, **4.19**, **4.20**, **4.21**, and **2.11'** were purified and characterized fully by spectroscopic and analytical techniques. With the exception of **4.19** and **2.11'**, the remaining isolated products exhibit straightforward NMR spectra,³⁷ which indicate the presence of a methylene agostic³⁸ interaction ($^1J_{\text{C}\alpha\text{-H}} \leq 90$ Hz) in **4.15** and **4.18**, and an η^2 -benzyl interaction in **4.16** ($^2J_{\text{HH}} = 6$ Hz, $\delta\text{C}_{\text{ipso}} = 111$) and **4.21** ($^2J_{\text{HH}} = 7$ Hz, $\delta\text{C}_{\text{ipso}} = 121$).³⁹ Broad features, on the other hand, complicate the NMR spectra of **4.19** and **2.11'**. Variable-temperature NMR studies of **4.19** suggest that it undergoes two separate dynamic processes in solution. The room-temperature process involves an $\eta^2 \rightarrow \eta^3 \rightarrow \eta^2$ interconversion of the *m*-methylbenzyl ligand. This is supported by the observation of (1) a structureless hump at δ 6.35 that can be ascribed to the aromatic proton that is at the 6-position, (2) a severely broad signal at δ 136.3 due to the carbon to which this proton is attached, and (3) a sharp upfield signal at δ 113.2 due to $\text{WCH}_2\text{C}_{\text{ipso}}$.⁴⁰ At temperatures below -50 °C, the η^2 -benzyl interaction is frozen out, and a second fluxional process that involves hindered rotation about

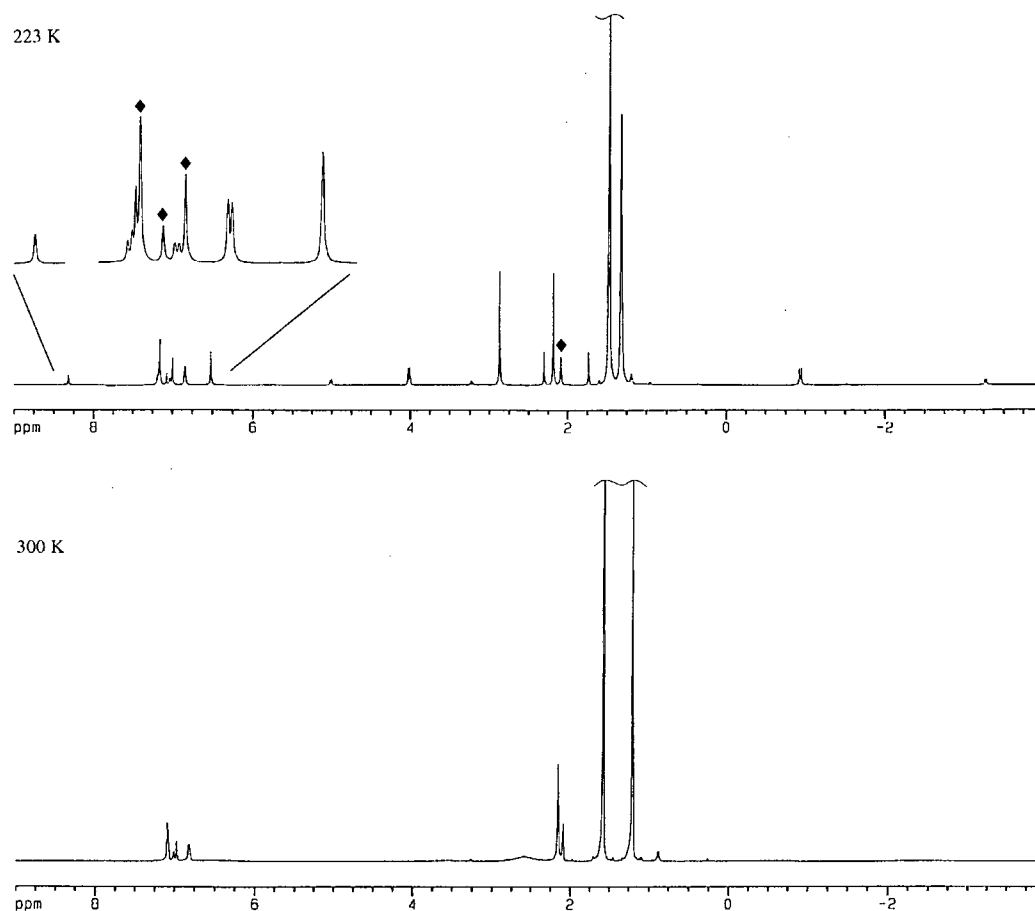


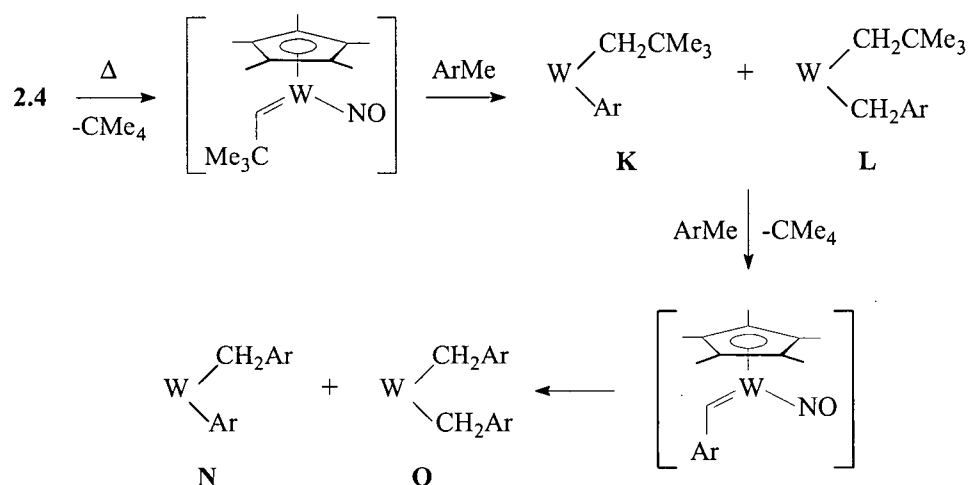
Figure 4.4. Variable-temperature 500-MHz ^1H NMR spectra of **2.11'** in toluene- d_8 (♦).

the 3,5-xylyl ligand is observed. For complex **2.11'**, hindered rotation about the 2,5-xylyl ligand is evidenced at room temperature. As the sample is cooled to $-30\text{ }^\circ\text{C}$, two sets of well-resolved resonances, consistent with the presence of two conformational isomers of **2.11'**, appear in the ^1H NMR spectrum (Figure 4.4). The two isomers exist in a 3:1 ratio that is invariant to temperatures between -20 and $-80\text{ }^\circ\text{C}$. A ^1H - ^1H EXSY experiment (mixing time = 75 ms) in toluene- d_8 at $-50\text{ }^\circ\text{C}$ reveals that they are not static structures but are in fact interconverting on the NMR time scale (see the Appendix).

The above benzyl-containing products are in general relatively stable. There is no evidence of isomerization during the reaction, and arene exchange is not observed. The neopentyl aryl complexes behave similarly. An exception is that these latter complexes are less stable than their benzyl analogues, often decomposing in trace amounts to unknown products under the conditions of the experiment. Under these conditions no appreciable change in the product ratios is observed. The selectivity with which the reactive intermediates $[\text{Cp}^*\text{W}(\text{NO})(=\text{CHCMe}_3)]$ and $[\text{Cp}^*\text{W}(\text{NO})(=\text{CHAr})]$ react with different types of aryl and benzyl C–H bonds therefore can be calculated from these ratios by correcting for the number of each type of bond (see Tables 4.4 and 4.5).

With regard to reactions with methylated arenes, Table 4.2 shows that $[\text{Cp}^*\text{W}(\text{NO})(=\text{CHAr})]$ is significantly more discriminating than $[\text{Cp}^*\text{W}(\text{NO})(=\text{CHCMe}_3)]$ with respect to aryl vs benzyl C–H activation and that, in all but the case of mesitylene, both species favor the former over the latter, despite the latter being much weaker bonds. Comparison of the reactions of $[\text{Cp}^*\text{W}(\text{NO})(=\text{CHCMe}_3)]$ indicates a strong preference for activation of the meta and para C–H bonds relative to the bonds at the ortho and benzylic position. Attack at the ortho position, in fact, is significant only when the ortho C–H bond is not too sterically hindered and the meta and para C–H bonds are absent. Thus, in the absence of severe steric hindrance there is a strong preference for aryl activation over benzyl activation, presumably because of initial formation of η^2 -arene complexes prior to C–H activation and because of formation of a much stronger metal–aryl bond. The observation that $[\text{Cp}^*\text{W}(\text{NO})(=\text{CHAr})]$ is more reactive toward aryl C–H bonds than $[\text{Cp}^*\text{W}(\text{NO})(=\text{CHCMe}_3)]$ can be attributed to the presence of the α -aryl group, which mediates the alkylidene's nucleophilicity. It can also be attributed to the fact that the α -aryl group is less sterically demanding than the *tert*-butyl group in $[\text{Cp}^*\text{W}(\text{NO})(=\text{CHCMe}_3)]$, thereby making it easier for arenes to form η^2 -complexes prior to C–H activation.

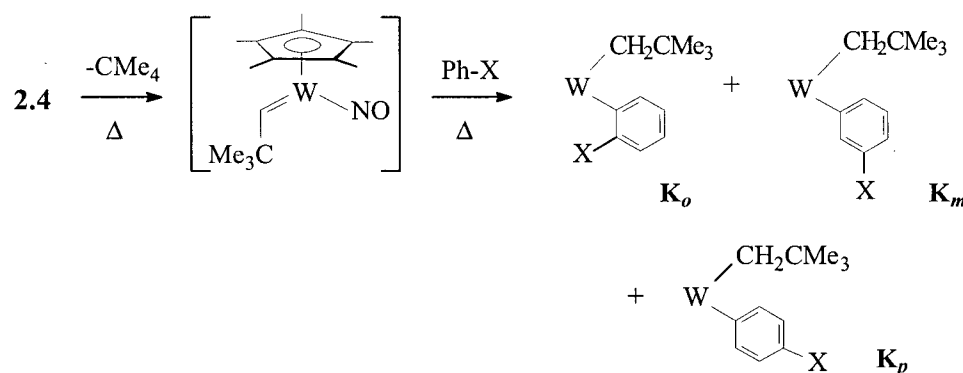
Table 4.2. Relative Kinetic Selectivities of $[\text{Cp}^*\text{W}(\text{NO})(=\text{CHCMe}_3)]$ and $[\text{Cp}^*\text{W}(\text{NO})(=\text{CHAr})]$ for Activation of Aryl and Benzyl C–H Bonds



ArMe	relative product yields (%) ^a				$\Sigma \text{aryl}:\Sigma \text{benzyl}$	$[\text{Cp}^*\text{W}(\text{NO})(=\text{CHCMe}_3)]^c$	$[\text{Cp}^*\text{W}(\text{NO})(=\text{CHAr})]^c$
	K	L	N	O			
toluene	82	0	18	0	82:18	2.73:1	>99:1
<i>o</i> -xylene ^b	66	19	14	1	66:34	2.91:1	19.5:1
<i>m</i> -xylene ^b	50	0	41	9	50:50	1.50:1	6.83:1
<i>p</i> -xylene ^b	44	0	43	13	44:56	1.18:1	4.96:1
mesitylene	<20	0	0	>80	~20:80	~1:1.33	~0:100

^aDetermined by repeated integration of the ¹H NMR spectra recorded at either 400 or 500 MHz; errors are to ca. 3–5%. ^bProduct distributions obtained from side-by-side thermolyses at 75.0 °C. ^cStatistically corrected.

Table 4.3. Kinetic Selectivities of $[\text{Cp}^*\text{W}(\text{NO})(=\text{CHCMe}_3)]$ for Activation of Aryl C–H Bonds in Monosubstituted Benzenes



X	relative product yields ^a			<i>o:m:p</i> ^b
	K_o	K_m	K_p	
CF_3	~1	66	33	0:1:1
OCH_3	88	7	5	12.5:1:1.4
CH_3	~0 ^c	66	33	0:1:1.4

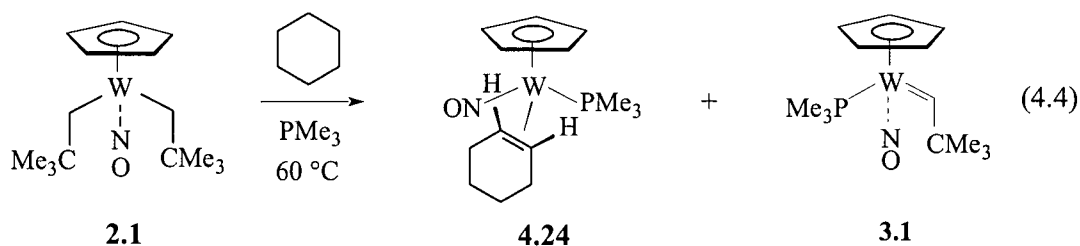
^aDetermined by repeated integration of the ^1H NMR spectra recorded at either 400 or 500 MHz; errors are to ca. 3–5%. ^bStatistically corrected. ^cNot detected, but possibly present at 5% of total product.

In general, transition-metal complexes whose aryl C–H activation reactivity is electronically controlled exhibit high selectivity for para vs meta activation. For example, Mayer and co-workers have shown that the $(\text{HBpz}_3)\text{Re}(\text{O})(\text{Cl})(\text{I})$ complex [HBpz_3 = hydridotris(1-pyrazolyl)borate] reacts with toluene to give the meta- and para-activated products in a 1:10.5 ratio and with more electron-rich substrates such as anisole, only the product of para activation is observed.⁴¹ Similarly, Graham and Sweet have reported that the $[\text{CpRe}(\text{NO})(\text{CO})][\text{BF}_4]$ complex activates toluene to give a 1:31 mixture of meta:para products, but with α,α,α -trifluorotoluene the reverse trend is observed as would be expected since CF_3 is an electron-withdrawing group.⁴² With regard to reactions of $[\text{Cp}^*\text{W}(\text{NO})(=\text{CHCMe}_3)]$ with monosubstituted benzenes, Table 4.3 shows that para C–H

bonds react only *slightly* faster than meta C–H bonds when the benzene substituent is electron-donating. When the benzene substituent is electron-withdrawing, no significant difference in rates between meta and para activation is observed. This suggests that electronic effects play a very minor role (if at all) in controlling the selectivity of the aryl C–H reaction of the neopentylidene intermediate. Consistent with this proposal, both α,α,α -trifluorotoluene and toluene, which differ markedly in electronic properties, show nearly identical reactivity toward ortho C–H bonds. That both give essentially no ortho C–H activation strongly suggests that these reactions are governed primarily by steric effects. However, unlike α,α,α -trifluorotoluene and toluene, anisole reacts to give mostly ortho C–H-activated products, despite having meta/para selectivity essentially identical with that observed for toluene. Clearly, steric effects are not operative in this case. A more reasonable explanation is that anisole reacts by way of a site-directed⁴³ reaction in which prior coordination of the methoxy group to the metal center of $[\text{Cp}^*\text{W}(\text{NO})(=\text{CHCMe}_3)]$ directs attack at the ortho position.⁴⁴

4.3.3 Thermal Reactions of $\text{CpW}(\text{NO})(\text{CH}_2\text{CMe}_3)_2$ (**2.1**) with Aliphatic and Aromatic C–H Bonds: Qualitative Observations

In order to study the effect of the Cp' ligand on the C–H activation chemistry described above, the thermolysis of the Cp complex **2.1** in cyclohexane in the presence of excess PMe_3 and in neat *p*-xylene, C_6D_6 , and tetramethylsilane was examined. In contrast to **2.4**, thermolysis of **2.1** in neat *p*-xylene or tetramethylsilane to 60 °C yields a complex mixture of intractable products. In the case of C_6D_6 , only decomposition is observed, as judged by ^1H NMR monitoring of the reaction. When **2.1** is heated in cyclohexane in the presence of excess PMe_3 , on the other hand, the reaction proceeds in the same manner as that described above



for **2.4** with one exception. The expected C–H activation product, $\text{CpW}(\text{NO})(\text{cyclohexene})(\text{PMe}_3)$ (**4.24**), is generated as a minor product unless the amount (and concentration) of PMe_3 added is very low compared to that used in the Cp^* experiments. Taking together, these observations can be interpreted as follows. The reactivity of the Cp intermediate $[\text{CpW}(\text{NO})(=\text{CHCMe}_3)]$ is analogous to that of the Cp^* system, except (a) it does not yield stable products with substrates such as *p*-xylene, C_6D_6 , and tetramethylsilane, and (b) its selectivity for PMe_3 coordination vs cyclohexane activation is significantly greater than that observed with its Cp^* counterpart, presumably for electronic as well as steric reasons.

4.4 Conclusions

In summary, the highly reactive neopentylidene intermediate $[\text{Cp}^*\text{W}(\text{NO})(=\text{CHCMe}_3)]$ has been shown to undergo rapid addition reactions with the C–H bonds of Me_4Si , alkanes, and arenes. The reaction with Me_4Si produces the bis(alkyl) complex **2.9** in high yield. The reactions with alkanes, in contrast, lead to different types of rearranged products depending on the alkane structure. In addition, they demonstrate that, in the absence of severe steric hindrance, the C–H bonds that are preferentially attacked are generally those having the highest bond dissociation energies: i.e., cyclopropyl $>$ 1° alkyl \sim 2° alkyl $>$ cycloalkyl \gg *tert*-butyl. This is based on the following observations. The major product in the reaction with 1,1,2,2-tetramethylcyclopropane is the metallacycle complex **4.1**, formed by initial addition of a cyclopropyl C–H bond across the $\text{W}=\text{C}$ bond followed by γ -cyclometalation. Neohexane, which contains three different types of C–H bonds, is activated regiospecifically at the CH_2CH_3 position. In this case, the initially formed complex then undergoes β -hydrogen abstraction in a stereospecific manner, yielding an η^2 -alkene complex having the *tert*-butyl group syn to the Cp^* ligand. In the presence of added PMe_3 , this alkene complex can be trapped and isolated as **4.4_{syn}**. Cyclopentane and cyclohexane react similarly in the presence of excess PMe_3 to give the corresponding cycloalkene complexes **4.2** and **4.3** as a single isomer. The reactions with methylcyclopentane, methylcyclohexane, ethylcyclohexane, and pentane, in contrast, give complex mixtures containing the η^3 -allyl hydride complexes **4.8–4.11**, respectively, in *both* the presence and absence of PMe_3 . The formation of **4.8–4.11**

is proposed to proceed via the reaction sequence outlined in Scheme 4.6. This proposed mechanism assumes that (1) β -hydrogen abstraction occurs with the same stereospecificity as that observed for the neohexane reaction, (2) subsequent allylic C–H activation is also stereospecific, occurring only when it leads to formation of an endo and acyclic allyl ligand, and (3) 1,3-disubstituted allyl ligands are unstable, decomposing at the temperature at which they form. Although rare, the conversion of an alkane molecule into a π -coordinated ligand by multiple H-atom loss (i.e., dehydrogenation) is precedented. However, in contrast to the formation of **4.2–4.11**, where the neopentylidene ligand accepts two hydrogens from the alkane solvent, most systems in the literature require an added alkene as hydrogen acceptor.⁴⁵

In the reactions of $[\text{Cp}^*\text{W}(\text{NO})(=\text{CHCMe}_3)]$ with arenes, meta- and para-C–H bonds are preferentially attacked, followed by ortho and benzyl C–H bonds. Exceptions are the reaction with anisole, where ortho attack predominates, presumably because of prior coordination of the oxygen atom to metal center, and the reaction with mesitylene, where benzylic activation is strongly favored, presumably because all the aryl hydrogens in this molecule are in sterically hindered environments. Like the $\text{Cp}^*\text{W}(\text{NO})(\text{CH}_2\text{CMe}_3)(\text{CH}_2\text{Ph})$ complex reported in Chapter 3, the benzyl-activated products are unstable with respect to α -abstraction of neopentane. This leads to formation of $[\text{Cp}^*\text{W}(\text{NO})(=\text{CHAr})]$ complexes which favor aryl C–H bonds significantly more than $[\text{Cp}^*\text{W}(\text{NO})(=\text{CHCMe}_3)]$.

Finally, the above study also shows that the Cp neopentylidene complex, $[\text{CpW}(\text{NO})(=\text{CHCMe}_3)]$, is also capable of cleaving C–H bonds intermolecularly. However, unlike the Cp^* system, it is significantly more reactive toward PMe_3 than the C–H bonds of cyclohexane and its C–H activation products are in general not stable at the temperature at which they form.

4.5 References and Notes

- (1) The term "activation" of a σ -bond has two meanings in organometallic chemistry: (a) an increase in reactivity of a bond due to some action, and (b) the cleavage of a bond. In this thesis, all "C-H activation reactions" are processes in which the C-H bond is broken.
- (2) For reviews, see: (a) Shilov, A. E. *Activation of Saturated Hydrocarbons by Transition Metal Complexes*; D. Reidel: Boston, 1984. (b) Crabtree, R. H. *Chem. Rev.* **1985**, *85*, 245. (c) *Activation and Functionalization of Alkanes*; Hill, C. H., Ed.; Wiley, 1989. (d) *Selective Hydrocarbon Activation, Principles and Progress*; Davies, J. A., Watson, P. L., Liebman, J. F., Greenberg, A., Eds.; VCH: NY, 1990. (e) Arndtsen, B. A.; Bergman, R. G.; Mobley, T. A.; Peterson, T. H. *Acc. Chem. Res.* **1995**, *28*, 154. (f) Bengali, A. A.; Arndtsen, B. A.; Burger, P. M.; Schultz, R. H.; Weiller, B. H.; Kyle, K. R.; Moore, C. B.; Bergman, R. G. *Pure Appl. Chem.* **1995**, *67*, 281. (g) Shilov, A. E.; Shul'pin, G. B. *Chem. Rev.* **1997**, *97*, 2879. (h) Stahl, S. S.; Labinger, J. A.; Bercaw, J. E. *Angew. Chem., Int. Ed. Engl.* **1998**, *37*, 2180.
- (3) (a) Saillard, J.-Y.; Hoffmann, R. *J. Am. Chem. Soc.* **1984**, *106*, 2006. (b) Cundari, T. R. *J. Am. Chem. Soc.* **1994**, *116*, 340. (c) Siegbahn, P. E. M.; Svensson, M. *J. Am. Chem. Soc.* **1994**, *116*, 10124. (d) Siegbahn, P. E. M. *J. Am. Chem. Soc.* **1996**, *118*, 1487. (e) Niu, S.; Hall, M. B. *J. Am. Chem. Soc.* **1999**, *121*, 3992.
- (4) For an example of an exception, see: Arndtsen, B. A.; Bergman, R. G. *Science* **1995**, *270*, 1970.
- (5) (a) Wenzel, T. T.; Bergman, R. G. *J. Am. Chem. Soc.* **1986**, 4856. (b) Desrosiers, P. J.; Shinomoto, R. S.; Flood, T. C. *J. Am. Chem. Soc.* **1986**, *108*, 1346. (b) Hackett, M.; Whitesides, G. M. *J. Am. Chem. Soc.* **1988**, *110*, 1449.
- (6) (a) Jordan, R. F.; Guram, A. S. *Organometallics* **1990**, *9*, 2116. (b) Guram, A. S.; Jordan, R. F.; Taylor, D. F. *J. Am. Chem. Soc.* **1991**, *113*, 1833. (c) Lécuyer, C.;

- Quignard, F.; Choplin, A.; Olivier, D.; Bassett, J. M. *Angew. Chem., Int. Ed. Engl.* **1991**, *30*, 1660. (d) Quignard, F.; Choplin, A.; Bassett, J. M. *J. Chem. Soc., Chem. Commun.* **1991**, 1589.
- (7) (a) Watson, P. L. *J. Am. Chem. Soc.* **1983**, *105*, 6491. (b) Watson, P. L.; Parshall, G. W. *Acc. Chem. Res.* **1985**, *18*, 51. (c) Thompson, M. E.; Bercaw, J. E. *Pure Appl. Chem.* **1984**, *56*, 1. (d) Thompson, M. E.; Baxter, S. M.; Bulls, A. R.; Burger, B. J.; Nolan, M. C.; Santarsiero, B. D.; Schaefer, W. R.; Bercaw, J. E. *J. Am. Chem. Soc.* **1987**, *109*, 203. (e) Bunel, E.; Burger, B. J.; Bercaw, J. E. *J. Am. Chem. Soc.* **1988**, *110*, 976. (f) Evans, W. J.; Chamberlain, L. R.; Ulibarri, T. A.; Ziller, J. W. *J. Am. Chem. Soc.* **1988**, *110*, 6423.
- (8) (a) Bruno, J. W.; Marks, T. J.; Day, V. W. *J. Am. Chem. Soc.* **1982**, *104*, 7357. (b) Fendrick, C. M.; Marks, T. J. *J. Am. Chem. Soc.* **1986**, *108*, 425.
- (9) (a) Groves, J. T.; Nemo, T. E. *J. Am. Chem. Soc.* **1983**, *105*, 6243. (b) Traylor, T. G. *J. Chem. Soc., Chem. Commun.* **1984**, 279. (c) Wayland, B. B.; Del Rossi, K. J. *J. Organomet. Chem.* **1984**, *276*, C47. (d) Wayland, B. B.; Ba, S.; Sherry, A. E. *J. Am. Chem. Soc.* **1991**, *113*, 5305. (e) Zhang, X.-X.; Wayland, B. B. *J. Am. Chem. Soc.* **1994**, *116*, 7897. (f) Brown, S. N.; Mayer, J. M. *J. Am. Chem. Soc.* **1994**, *116*, 2219.
- (10) (a) Cook, G. K.; Mayer, J. M. *J. Am. Chem. Soc.* **1994**, *116*, 1855. (b) Brown, S. N.; Myers, A. W.; Fulton, J. R.; Mayers, J. M. *Organometallics* **1998**, *17*, 3364.
- (11) (a) Cummins, C. C.; Schaller, C. P.; Van Duyne, G. D.; Wolczanski, P. T.; Chan, E. A.-W.; Hoffmann, R. *J. Am. Chem. Soc.* **1991**, *113*, 2985. (b) Bennett, J. L.; Wolczanski, P. T. *J. Am. Chem. Soc.* **1994**, *116*, 2179. (c) Bennett, J. L.; Wolczanski, P. T. *J. Am. Chem. Soc.* **1997**, *119*, 10696.
- (12) (a) Walsh, P. J.; Hollander, F. J.; Bergman, R. G. *J. Am. Chem. Soc.* **1988**, *110*, 8730. (b) Cummins, C. C.; Baxter, S. M.; Wolczanski, P. T. *J. Am. Chem. Soc.* **1988**, *110*, 8731. (c) Walsh, P. J.; Hollander, F. J.; Bergman, R. G. *Organometallics* **1993**, *12*,

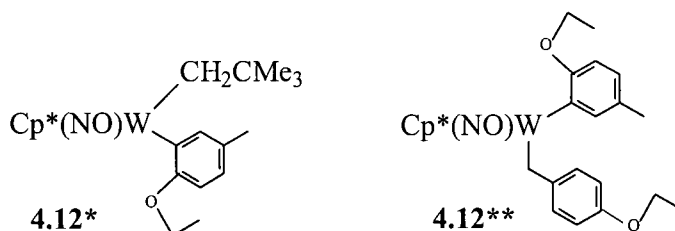
3705. (d) Lee, S. Y.; Bergman, R. G. *J. Am. Chem. Soc.* **1995**, *117*, 5877. (e) Schaller, C. P.; Bonanno, J. B.; Wolczanski, P. T. *J. Am. Chem. Soc.* **1994**, *116*, 4133. (f) Schaller, C. P.; Cummins, C. C.; Wolczanski, P. T. *J. Am. Chem. Soc.* **1996**, *118*, 591.
- (13) de With, J.; Horton, A. D. *Angew. Chem., Int. Ed. Engl.* **1993**, *32*, 903.
- (14) Schaller, C. P.; Wolczanski, P. T. *Inorg. Chem.* **1993**, *32*, 131.
- (15) Schafer, D. F.; Wolczanski, P. T. *J. Am. Chem. Soc.* **1998**, *120*, 4881.
- (16) (a) van der Heijden, H.; Hessen, B. *J. Chem. Soc., Chem. Commun.* **1995**, 145. (b) Coles, M. P.; Gibson, V. C.; Clegg, W.; Elsegood, M. R. J.; Porrelli, P. A. *Chem. Commun.* **1996**, 1963. (c) Tran, E.; Legzdins, P. *J. Am. Chem. Soc.* **1997**, *119*, 5071. (d) Cheon, J.; Rogers, D. M.; Girolami, G. S. *J. Am. Chem. Soc.* **1997**, *119*, 6814.
- (17) (a) McDade, C.; Green, J. C.; Bercaw, J. E. *Organometallics* **1987**, *1*, 1629. (b) van Doorn, J. A.; van der Heijden, H.; Orpen, A. G. *Organometallics* **1994**, *13*, 4271.
- (18) Bulls, A. R.; Schaefer, W. P.; Serfas, M.; Bercaw, J. E. *Organometallics* **1987**, *6*, 1219.
- (19) (a) Chamberlain, L.; Rothwell, I. P.; Huffman, J. C. *J. Am. Chem. Soc.* **1982**, *104*, 7338. (b) Chamberlain, L. R.; Rothwell, I. P.; Huffman, J. C. *J. Am. Chem. Soc.* **1986**, *108*, 1502. (c) Lockwood, M. A.; Clark, J. R.; Parkin, B. C.; Rothwell, I. P. *Chem. Commun.* **1996**, 1973.
- (20) Schrock, R. R.; DePue, R. T.; Feldman, J.; Yap, K. B.; Yang, D. C.; Davis, W. M.; Park, L.; DiMare, M.; Schofield, M.; Anhaus, J.; Walborsky, E.; Evitt, E.; Krüger, C.; Betz, P. *Organometallics* **1990**, *9*, 2262.
- (21) (a) Debad, J. D.; Legzdins, P.; Batchelor, R. J.; Einstein, F. W. B. *Organometallics* **1993**, *12*, 2094. (b) For complete spectroscopic and structural characterizations, see Chapter 2 of this thesis.
- (22) Martin, J. T. Ph.D. Thesis, University of British Columbia, 1988.

- (23) The syn and anti notation simply represents the orientation of the neohexene *tert*-butyl group with respect to the Cp* ligand.
- (24) Bodner, G. S.; Peng, T.-S.; Arif, A. M.; Gladysz, J. A. *Organometallics* **1990**, *9*, 1191.
- (25) For comparison, the olefinic carbons of free cyclopentane and cyclohexane resonate at about δ 130. See: Silverstein, R. M.; Bassler, G. C.; Morrill, T. C. *Spectrometric Identification of Organic Compounds*; John Wiley & Sons, Inc.: New York, 1991; pp 217 and 238.
- (26) The exceptionally strong π -donor ability of the related Cp*W(NO)(PPh₃) fragment has recently been documented, see: Burkey, D. J.; Debad, J. D.; Legzdins, P. *J. Am. Chem. Soc.* **1997**, *119*, 1139.
- (27) Irradiation of the *tert*-butyl group was not feasible since its chemical shift is too close to that of =CH_{anti}H and =CHCMe₃.
- (28) (a) Schilling, B. E. R.; Hoffmann, R.; Faller, J. W. *J. Am. Chem. Soc.* **1979**, *101*, 592. (b) Kiel, W. A.; Lin, G.-Y.; Constable, A. G.; McCormick, F. B.; Strouse, C. E.; Eisenstein, O.; Gladysz, J. A. *J. Am. Chem. Soc.* **1982**, *104*, 4865. (c) Peng, T.-S.; Pu, J.; Gladysz, J. A. *Organometallics* **1994**, *13*, 929. (d) Gibson, V. C. *J. Chem. Soc., Dalton Trans.* **1994**, 1607. (e) Peng, T.-S.; Winter, C. H.; Gladysz, J. A. *Inorg. Chem.* **1994**, *33*, 2534.
- (29) For comparison, typical C–C single and C=C double bond distances are 1.54 Å and 1.34 Å, respectively.
- (30) (a) Peng, T.-S.; Gladysz, J. A. *J. Chem. Soc., Chem. Commun.* **1990**, 902. (b) Peng, T.-S.; Gladysz, J. A. *J. Am. Chem. Soc.* **1992**, *114*, 4174. (c) Peng, T.-S.; Arif, A. M.; Gladysz, J. A. *Helv. Chim. Acta* **1992**, *75*, 442.
- (31) Faller, J. W.; Nguyen, J. T.; Ellis, W.; Mazzieri, M. R. *Organometallics* **1993**, *12*, 1434.

- (32) Greenhough, T. J.; Legzdins, P.; Martin, D. T.; Trotter, J. *Inorg. Chem.* **1979**, *11*, 3268.
- (33) Ipatkschi, J.; Mirzaei, F.; Demuth-Eberle, G. J.; Beck, J.; Serafin, M. *Organometallics* **1997**, *16*, 3965.
- (34) (a) Ward, Y. D.; Villanueva, L. A.; Allred, G. D.; Payne, S. C.; Semones, M. A.; Liebeskind, L. S. *Organometallics* **1995**, *14*, 4132. (b) Villanueva, L. A.; Ward, Y. D.; Lachicotte, R.; Liebeskind, L. S. *Organometallics* **1996**, *15*, 4190.
- (35) Although less likely, it cannot be ruled out that allylic C-H activation is simply highly stereoselective.
- (36) In general, the resonances for the W-CH₂Ar protons of the benzyl aryl complexes Cp*W(NO)(CH₂Ar)(Ar) appear as two doublets at δ 2 and 3 ($^2J_{\text{HH}} \sim 8$ Hz), whereas those of the bis(benzyl) Cp*W(NO)(CH₂Ar)₂ appear at δ 0.8 and 3 ($^2J_{\text{HH}} \sim 8$ Hz).
- (37) In general, the resonances for the W-CH₂CMe₃ protons of neopentyl aryl complexes appear as two doublets at δ -2 and 4 ($^2J_{\text{HH}} \sim 12$ Hz), whereas those of neopentyl benzyl complexes appear at δ -2 and 2 ($^2J_{\text{HH}} \sim 12$ Hz).
- (38) (a) Brookhart, M.; Green, M. L. H. *J. Organomet. Chem.* **1983**, *250*, 395. (b) Brookhart, M.; Green, M. L. H.; Wong, L.-L. *Prog. Inorg. Chem.* **1988**, *36*, 1. (c) Crabtree, R. H.; Hamilton, D. G. *Adv. Organomet. Chem.* **1988**, *28*, 299.
- (39) For comparison, the corresponding $^2J_{\text{HH}}$ values of η^1 -benzyl ligands in related complexes are ~ 10 Hz, while the ipso carbons are located at δ 150–160. For examples, see: (a) Legzdins, P.; Jones, R. H.; Phillips, E. C.; Yee, V. C.; Trotter, J.; Einstein, F. W. B. *Organometallics* **1991**, *10*, 986. (b) Dryden, N. H.; Legzdins, P.; Trotter, J.; Yee, V. C. *Organometallics* **1991**, *10*, 2857.
- (40) Because the remaining ^1H and ^{13}C resonances are sharp, it is unlikely that the broadness of the ortho CH group is due to a fluxional process involving either a γ -

agostic C–H interaction or a slow rotation about the C $_{\alpha}$ –C $_{\beta}$ bond of the *m*-methylbenzyl ligand.

- (41) Brown, S. N.; Myers, A. W.; Fulton, J. R.; Mayer, J. M. *Organometallics* **1998**, *17*, 3364.
- (42) Sweet, J. R.; Graham, W. A. G. *J. Am. Chem. Soc.* **1983**, *105*, 305.
- (43) For a review of substrate-directable chemical reactions, see: Hoveyda, A. H.; Fu, G. C.; Evans, D. A. *Chem. Rev.* **1993**, *93*, 1307.
- (44) In further support of this proposal, thermolysis of **2.4** in 1-ethoxy-4-methylbenzene (see below) has been found to produce complexes **4.12*** and **4.12**** in ~90% and 10% yields, respectively. **4.12***: Anal. Calcd. for C₂₄H₃₇NO₂W: C, 51.90; H, 6.72; N, 2.52. Found: C, 51.63; H, 6.78; N, 2.53. IR (cm⁻¹) ν_{NO} 1565 (s). MS 555 [M⁺, ¹⁸⁴W]. ¹H NMR (400 MHz, C₆D₆) δ -2.63 (d, ²J_{HH} = 11.6, 1H, WCH₂), 1.03 (t, ³J_{HH} = 6.8, 3H, OCH₂CH₃), 1.33 (s, 9H, CMe₃), 1.65 (s, 15H, C₅Me₅), 2.23 (s, 3H, ArMe), 3.50 (q, ³J_{HH} = 7.1, 2H, OCH₂CH₃), 4.98 (d, ²J_{HH} = 11.6, 1H, WCH₂), 6.52 (d, ³J_{HH} = 8.1, 1H, ArH), 6.96 (dd, ³J_{HH} = 8.1, ⁴J_{HH} = 1.9, 1H, ArH), 8.21 (br s, 1H, ArH). ¹³C{¹H} (75 MHz, CDCl₃) δ 10.2 (C₅Me₅), 15.3 (OCH₂CH₃), 20.5 (ArMe), 33.4 (CMe₃), 41.6 (CMe₃), 62.9 (OCH₂CH₃), 109.6 (Ar CH), 111.0 (C₅Me₅), 129.8 (WCH₂), 134.0 (C_{ipso}Me), 141.0 (Ar CH), 157.1 (C_{ipso}OEt), 168.5 (WC_{ipso}). NOEDS (400 MHz, C₆D₆) irradi. at 2.23 ppm, NOEs at δ 6.96, 8.15. **4.12****: MS 619 [M⁺, ¹⁸⁴W]. ¹H NMR (300 MHz, C₆D₆) δ 1.45 (t, ³J_{HH} = 6.8, 3H, OCH₂CH₃), 4.10 (m, 2H, OCH₂CH₃), 6.25 (d, ³J_{HH} = 8.1, 1H, ArH), 6.49 (d, ³J_{HH} = 8.1, ArH). Other signals were obscured.



- (45) For examples, see: (a) Crabtree, R. H.; Mellea, M. F.; Mihelcic, J. M.; Quirk, J. M. *J. Am. Chem. Soc.* **1982**, *104*, 107. (b) Burk, M. J.; Crabtree, R. H.; McGrath, D. V.; J. *Chem. Soc., Chem. Comm.* **1985**, 1829. (c) Baudry, D.; Ephritikhine, M.; Felkin, H.; Holmes-Smith, R. *J. Chem. Soc., Chem. Commun.* **1983**, 788. (d) McGhee, W. D.; Bergman, R. G. *J. Am. Chem. Soc.* **1988**, *110*, 4246.

CHAPTER 5

Kinetic and Mechanistic Studies of the Generation and C–H Activation Reactions of the $[\text{Cp}'\text{W}(\text{NO})(=\text{CHCMe}_3)]$ Fragments

5.1 Introduction	157
5.2 Experimental Section	160
5.3 Results and Discussion	170
5.4 Conclusions	189
5.5 References and Notes	190

5.1 Introduction

α -Hydrogen abstraction from an alkyl ligand is a fundamental process in organometallic chemistry and has played an important role in the development of transition-metal alkylidene¹/carbene² complexes. As with the more ubiquitous β -hydrogen abstraction reaction, an α -hydrogen may be abstracted by an external reagent,³ the metal,⁴ or a neighboring ligand.⁵ Abstraction of an α -hydrogen by the metal is often reversible, only takes place in coordinatively unsaturated d^n complexes, where $n \geq 2$, and may or may not be followed by reductive elimination of HX, where X is a ligand originally attached to the metal. Direct transfer of an α -hydrogen atom to a neighboring ligand on the other hand occurs with no formal change in the metal oxidation state, is rarely reversible, and has a rate that often depends on factors such as the degree of steric congestion at the metal center, the solvent, and the presence of added donor ligands. More complicated pathways involving initial Cp^* ring-metallation or γ -C–H activation followed by α -hydrogen abstraction have also been noted. For example, it has been shown that (1) the reaction of the bis(alkyl) $\text{Cp}^*\text{W}(\text{NO})(\text{CH}_2\text{SiMe}_3)_2$ with LDA leads to formation of an “ate” alkylidene complex in which the ring-metallated species $[(\eta^5, \eta^1-$

$\text{C}_5\text{Me}_4\text{CH}_2\text{W}(\text{NO})(\text{CH}_2\text{SiMe}_3)_2[\text{Li}_2(\text{THF})_3]$ is an observable intermediate,⁶ and (2) thermolysis of $(\text{PMe}_3)_2\text{Ta}(\text{Me})(\text{Mes})\text{Br}_3$ ($\text{Mes} = \text{C}_6\text{H}_3\text{-2,4,6-Me}_3$) leads to loss of methane and formation of a substituted benzylidene complex via abstraction of a γ -hydrogen atom and subsequent rearrangement of an unobserved benzotantalacyclobutene compound.⁷

In the preceding chapters, it was reported that the bis(alkyl) complexes $\text{Cp}^*\text{W}(\text{NO})(\text{CH}_2\text{CMe}_3)_2$ and its Cp analogue exhibit α -agostic structures in solution and solid states and that they decompose readily at elevated temperatures to give neopentane and presumably the coordinatively unsaturated neopentylidene fragments, $[\text{Cp}^*\text{W}(\text{NO})(=\text{CHCMe}_3)]$, which can effect the C–H bond cleavage of alkanes, arenes, and certain alkenes. In the activation of alkanes and arenes, several remarkable selectivity features of $[\text{Cp}^*\text{W}(\text{NO})(=\text{CHCMe}_3)]$ have been noted (see Chapter 4). First, this intermediate can activate aliphatic C–H bonds even in the presence of excess PMe_3 .⁸ Second, it reacts most rapidly with aromatic compounds, showing a strong preference for activation of the meta and para C–H bonds relative to the bonds at the ortho and benzylic positions. Attack at the ortho position, in fact, is significant only when the reaction is site-directed or when the ortho C–H bond is not too sterically hindered and the meta and para C–H bonds are absent. Third, in the activation of alkanes the C–H bonds that are preferentially attacked are generally those having the highest bond dissociation energies; the qualitative order of reactivity, for example, is cyclopropyl > 1° alkyl ~ 2° alkyl > cycloalkyl >> *tert*-butyl.

There are a number of cases now known in which the kinetic selectivity for different types of C–H bonds is similar to that of $[\text{Cp}^*\text{W}(\text{NO})(=\text{CHCMe}_3)]$.⁹ For many of these systems, it has been found that strong M–C bonds are formed when strong C–H bonds are broken and that the relative ease of C–H activation is determined largely by the strengths of the product M–C bonds and by the binding affinities of the hydrocarbon to the metal center prior to activation.^{10,11} For example, arenes are generally more reactive than alkanes because of prior coordination of the metal to the π -electrons to give η^2 -arene complexes and because of formation of a much stronger M–C bond.

Molecular complexes in which an arene is weakly coordinated to an unsaturated metal center in an η^2 -fashion were first formulated as early as the mid-1960s.¹² Since then, the area of arene as well as alkane coordination has grown steadily, and has led to the discovery that such adducts not only exist as independent entities^{11,13} but also as metastable intermediates in a number of C–H bond making and breaking reactions.¹⁴ For reactions involving C–H activation, the initial formation of alkane σ -complexes and η^2 -arene complexes is apparently necessary for two reasons: (1) to allow the metal to coordinate interchangeably (and hence discriminate) different types of C–H bonds, and (2) to provide a lower energy pathway for the bond-breaking step.¹⁵

Recently, there has been considerable research effort devoted to understanding the mechanisms of intermolecular C–H activation by soluble transition-metal complexes. However, in few of these investigations has it been possible to obtain direct information about the reactive intermediates without examining also the reverse reactions. Much of the current understanding of C–H activation by way of oxidative addition, for example, has come from mechanistic studies of alkane reductive elimination reactions, where several lines of evidence based on isotope effect and isotope tracer experiments have implicated the existence of alkane σ -complexes.

With respect to the mechanism by which the $\text{Cp}'\text{W}(\text{NO})(\text{CH}_2\text{CMe}_3)_2$ complexes decompose and react, no intermediates have yet been directly observed, although several trapping reactions with phosphines and alkenes (see Chapter 3) have strongly implicated the intermediacy of $[\text{Cp}'\text{W}(\text{NO})(=\text{CHCMe}_3)]$ in which the *tert*-butyl group points away from Cp' ligand. In this chapter, the first part reports an in-depth study of the kinetics and mechanisms of the thermal decompositions and subsequent C–H activation reactions of the bis(neopentyl) complexes. Specifically, kinetic isotope effect and labeling studies are described which not only further support the intermediacy of $[\text{Cp}'\text{W}(\text{NO})(=\text{CHCMe}_3)]$, but which also strongly implicate the intermediacy of alkane adducts, $[\text{Cp}'\text{W}(\text{NO})(=\text{CHCMe}_3)(\eta^2\text{-R-H})]$, along the pathway for both the forward and reverse reactions. A mechanism involving a net transfer of an α -hydrogen from one neopentyl group to the α -carbon of the adjacent neopentyl group is proposed; whether

neopentane is lost by direct α -hydrogen abstraction or by α -hydride elimination followed by reductive elimination could not be distinguished. In the second part of this chapter, an investigation of the thermal stabilities of a series $\text{Cp}'\text{W}(\text{NO})(\text{R})(\text{R}')$ complexes that are electronically and structurally analogous to the bis(neopentyl) compounds is described. Two major conclusions from this work are the following: (1) the pathway by which these compounds decompose is governed primarily by the strengths of the M–C bond formed and broken, and (2) the presence of α -agostic interactions in the ground state structures has little, if any, effect on the rate and pathway of decomposition.

5.2 Experimental Section

5.2.1 Methods

The synthetic methodologies employed throughout this thesis are described in detail in Section 2.2.1. Unless otherwise stated, all thermolyses were carried out in J. Young NMR tubes or thick-walled glass vessels immersed in an oil bath at 65–70 °C for ca. 2 d.

5.2.2 Reagents

THF and cyclohexane used in kinetic experiments were distilled from Na/benzophenone ketyl and then stored in glass bombs under dinitrogen. Dimethylphenylphosphine, trimethylphosphine, triethylphosphine, *n*-butyl ether (Aldrich), C_6D_6 (Cambridge Isotopes), $\text{C}_6\text{H}_3\text{D}_3$ (98 %, Aldrich), and tetramethylsilane- d_{12} were dried over sodium. Dimethyldichlorosilane (Aldrich) was freshly distilled. CD_3I (99.5+ atom % D, Aldrich) was dried over 4-Å molecular sieves. The organometallic complexes $\text{CpW}(\text{NO})(\text{CH}_2\text{CMe}_3)_2$ (**2.1**), $\text{Cp}^*\text{W}(\text{NO})(\text{CH}_2\text{CMe}_3)_2$ (**2.4**), $\text{Cp}^*\text{W}(\text{NO})(\text{CH}_2\text{CMe}_3)(\text{CH}_2\text{CMe}_2\text{Ph})$ (**2.8**), and $\text{Cp}^*\text{W}(\text{NO})(\text{CH}_2\text{CMe}_3)(\text{CH}_3)$ (**2.10**) were prepared as described in Section 2.2.1. The α -deuterated complexes $\text{CpW}(\text{NO})(\text{CD}_2\text{CMe}_3)_2$ (**2.1-*d*₄**), $\text{Cp}^*\text{W}(\text{NO})(\text{CD}_2\text{CMe}_3)_2$ (**2.4-*d*₄**), and $\text{Cp}^*\text{W}(\text{NO})(\text{CH}_2\text{CMe}_3)(\text{CD}_2\text{CMe}_2\text{Ph})$ (**2.8-*d*₂**) were prepared in a similar manner using the dialkylmagnesium reagents $\text{R}_2\text{Mg} \cdot (\text{dioxane})$ ($\text{R} = \text{CD}_2\text{CMe}_3, \text{CD}_2\text{CMe}_2\text{Ph}$); an exception is that

the crude product mixtures were filtered through Celite instead of alumina I prior to crystallization. In all cases, ^1H NMR spectroscopy at 300 MHz revealed no detectable methylene proton signals, thus indicating at least 98% D incorporation at C_α .

5.2.3 NMR and Mass Spectral Data for $\text{Cp}^*\text{W}(\text{NO})(\text{CH}_2\text{CMe}_3)(\text{CD}_2\text{CMe}_2\text{Ph})$ (2.8- d_2)

MS 555 [M^+ , ^{184}W]. ^1H NMR (500 MHz, CDCl_3) δ -2.18 (d, $^2J_{\text{HH}} = 12.5$, 1H, WCH_2), 1.27 (s, 9H, CMe_3), 1.45 (s, 15H, C_5Me_5), 1.74 (s, 3H, CMeMe), 1.85 (s, 3H, CMeMe), 3.16 (d, $^2J_{\text{HH}} = 12.4$, 1H, WCH_2), 7.06 (t, $^3J_{\text{HH}} = 7.3$, 1H, H_p), 7.23 (t, $^3J_{\text{HH}} = 7.4$, 2H, H_m), 7.50 (d, $^3J_{\text{HH}} = 7.4$, 2H, H_o). $^2\text{H}\{^1\text{H}\}$ NMR (77 MHz, C_6H_6) δ -0.54 (s, 1D, WCD_2), 2.47 (s, 1D, WCD_2).

5.2.4 Preparation of $(\text{CH}_3)_2\text{Si}(\text{CD}_3)_2$

Mg turnings (4.00 g, 167 mmol) and *n*-butyl ether (350 mL) were added to a 500-mL three-necked flask equipped with a stir-bar and a reflux condenser. The flask was cooled to -78°C and CD_3I (6.0 mL, 94.4 mmol) was added dropwise by syringe. The resulting mixture was stirred at room temperature for 3.5 h, during which time its color changed to grey-black. The supernatant solution was filtered through Celite (2×2 cm) into a 500-mL two-necked flask and cooled to -40°C . Freshly distilled Me_2SiCl_2 (5.10 mL, 42.0 mmol) was added dropwise by syringe. Once the addition was complete, the flask was removed from the cold bath, wrapped with aluminum foil, and the contents were stirred (under a static atmosphere of argon) for another 16 h. A pale brown-yellow solution resulted which contained an off-white precipitate in suspension. At this point, the contents of the flask were quickly transferred to a one-necked flask equipped with a short-path distillation head. Under a flow of argon, colorless $(\text{CH}_3)_2\text{Si}(\text{CD}_3)_2$ (~1–2 mL, b.p. $28\text{--}32^\circ\text{C}$) was distilled into a receiving flask immersed in a dry ice/acetone bath (Care should be taken to avoid bumping!). To remove iodide byproducts, the distillate was transferred to a Pyrex bomb containing PPh_3 (~200 mg), degassed, and stored in the dark for ~5 d. Next, it was vacuum transferred into another bomb containing a Na mirror and allowed to dry for 4 d before use. The purity of $(\text{CH}_3)_2\text{Si}(\text{CD}_3)_2$ was established by ^1H NMR spectroscopy and by GC-MS m/z 94 [M^+].

5.2.5 Preparation of $\text{Cp}^*\text{W}(\text{NO})(\text{CH}_2\text{CMe}_3)(\text{C}_6\text{D}_5)$ (**2.11-*d*₅**)

A wine-red solution of **2.4** (60 mg, 0.12 mmol) in C_6D_6 (~1 mL) was heated at 70 °C for ~2 d, during which time its color changed to purple-red. ^1H NMR analysis of the sample revealed the formation of free neopentane and the known $\text{Cp}^*\text{W}(\text{NO})(\text{CHDCMe}_3)(\text{C}_6\text{D}_5)$ (**2.11-*d*₆**)¹⁶ (~95%) along with a small amount of unidentified products, which displayed signals in the range δ 1–2. The organic volatiles were then removed in vacuo to obtain an oily residue, which was chromatographed on alumina I (1 × 1.5 cm) by eluting with hexanes. The first band to appear, a pink fraction, was collected by eluting with 4:1 hexanes/ Et_2O . Concentration of this fraction, followed by cooling to –30 °C for 1 d provided **2.11-*d*₅** as dark wine-red needles (18 mg, 30% yield) [Occasionally, a residual amount of **2.11-*d*₆** could still be detected by ^1H NMR]. The ^1H NMR spectrum of **2.11-*d*₅** is identical to that of the protio analogue **2.11** (see Chapter 2), except it does not display aromatic resonances.

5.2.6 Kinetic Measurements

All kinetic experiments were performed by UV-vis spectroscopy. Spectra were recorded on a HP 8452A Diode Array UV-vis spectrophotometer equipped with a deuterium lamp and a thermostated cell holder connected to a VWR Scientific constant-temperature bath (model 1160A) filled with ethylene glycol/water and maintained to ± 0.05 °C. The spectrophotometer was interfaced to a 586 PC computer using HP 89531A operating software. Stock solutions of organometallic reagent were prepared in the appropriate solvent in the glovebox and stored at –30 °C between runs. A representative stock solution of **2.1**, **2.1-*d*₄**, **2.4**, or **2.4-*d*₄** contained 0.013 mmol of the complex dissolved in 25.0 mL of solvent in a volumetric flask. In a typical experiment, a UV-vis cell equipped with a Kontes Teflon stopcock was charged sequentially with 3.0 mL of the solution of the organometallic reagent and a measured amount of trapping reagent where required. Each run was monitored for >3 half-lives. In all but a few cases, each rate constant was determined at least three times for each system and each temperature studied. Spectra were recorded at regular time intervals after the solutions had been allowed to reach the desired temperatures (5–15 min). The absorbance intensities of **2.1**, **2.4**, and their deuterated

analogues at $\lambda = 486$ nm were monitored in all cases and then plotted versus time. Infinity values were determined by non-linear regression with least-squares fitting of the raw data using SigmaPlot 3.0; Jandsen Graphing Software, 1987–1992. Using Microsoft Excel, the observed rate constants (k_{obs}) were then calculated from the slope of the plots of $\ln[(A_t - A_\infty)/(A_t - A_0)]$ versus time, which displayed excellent linearity with correlation coefficients typically 0.995 or better. Activation parameters, ΔH^\ddagger and ΔS^\ddagger , were determined from Eyring plots of $\ln(k_{\text{obs}}/T)$ versus $1/T$, where $\Delta H^\ddagger = -R \times \text{slope}$, $\Delta S^\ddagger = R[\text{intercept} - \ln(k_B/h)]$ and R , k_B , and h are the gas constant, Boltzmann's constant, and Planck's constant, respectively. Errors are 95% confidence limits of linearly regressed lines.

5.2.7 ^1H and $^2\{^1\text{H}\}$ NMR Analyses of the Thermolysis of (a) **2.1-*d*₄** and **2.4-*d*₄** in THF in the Presence of PMe_3 and (b) **2.4-*d*₄** in C_6D_6

In a typical reaction, a J. Young NMR tube containing 10–20 mg of organometallic reagent was charged with ca. 0.5 mL of solvent and, where needed, an excess amount of PMe_3 by vacuum transfer. The resulting mixture was heated in a constant-temperature bath at 65.0 °C in the case of **2.1-*d*₄** and 75.0 °C in the case of **2.4-*d*₄** and monitored periodically by ^1H (C_6D_6) and $^2\text{H}\{^1\text{H}\}$ (C_6H_6) NMR spectroscopies. In all cases, the thermolyses were relatively clean and H/D exchange between the α - and γ -positions of the neopentyl ligands of the starting materials during the course of the thermolyses was evidenced by the presence of low-intensity ^1H NMR signals in the methylene regions. At >90% conversion, the ^1H and ^2H NMR spectrum of the reactions of **2.1-*d*₄** and **2.4-*d*₄** with PMe_3 showed peaks consistent with the presence of both $\text{Cp}'\text{W}(\text{NO})(=\text{CDCMe}_3)(\text{PMe}_3)$ (major) and $\text{Cp}'\text{W}(\text{NO})[=\text{CHCMe}_2(\text{CD}_3)](\text{PMe}_3)$ (minor). The ^1H and $^2\text{H}\{^1\text{H}\}$ NMR spectra of the C_6D_6 reaction of **2.4-*d*₄** similarly revealed the formation of $\text{Cp}^*\text{W}(\text{NO})(\text{CHDCMe}_3)(\text{C}_6\text{D}_5)$ along with a small amount of $\text{Cp}^*\text{W}(\text{NO})[\text{CH}_2\text{CMe}_2(\text{CD}_3)](\text{C}_6\text{D}_5)$.

5.2.8 Thermolysis of 2.4 in THF in the Presence of Excess PMe_3 and C_6D_6

In the glovebox, a small Pyrex vessel was charged with **2.4** (24 mg, 0.049 mmol), THF (2–3 mL), and C_6D_6 (21 μL , 0.24 mmol, 5 equiv). The wine-red solution was then degassed by three freeze-pump-thaw cycles. Next, PMe_3 (>10 equiv) was added by vacuum transfer and the resulting solution was heated at 70 °C for ca. 16 h, after which time the organic volatiles were removed in vacuo. ^1H NMR spectroscopy showed that $\text{Cp}^*\text{W}(\text{NO})(=\text{CHCMe}_3)(\text{PMe}_3)$ (**3.1**) was the only product formed. An identical result was also obtained when $\text{Si}(\text{CH}_3)_4$ was substituted for C_6D_6 .

5.2.9 GC–MS Analysis of Neopentane Generated from the Thermolysis of (a) **2.1- d_4** and **2.4- d_4** in THF in the Presence of Excess PMe_3 and (b) **2.4- d_4** in Neat PMe_3

These experiments were carried out in 0.4–0.5 mL of solvent and were stopped after 2–3 d at 65 °C in the case of **2.1- d_4** and 75 °C in the case of **2.4- d_4** . The organic volatiles were then removed in vacuo and analyzed by GC–MS, which showed the absence of dineopentyl. The mass spectra of the reaction of **2.1- d_4** with PMe_3 in THF showed the presence of neopentane- d_0 , - d_1 , - d_2 , and - d_3 in respective yields of ca. 2%, 17%, 4%, and 77% (see Table 5.1). In the case of **2.4- d_4** , the corresponding isotopic distribution was ca. 0%, 18%, 3%, and 79% in THF and ca. 0%, 10%, 0%, and 90% in neat PMe_3 . As expected, ^1H NMR (C_6D_6) analysis of the nonvolatiles of the reaction of **2.4- d_4** in neat PMe_3 revealed the presence of a small amount of hydrogen at the α -position.

5.2.10 Thermolysis of **2.4** in $\text{Si}(\text{CD}_3)_4$

A sample of **2.4** (29 mg, 0.057 mmol) in tetramethylsilane- d_{12} (0.5 mL) in a J. Young NMR tube was heated in an oil bath at 70 °C for 2.5 d, during which time its color became deep purple red. A ^1H NMR spectrum of this solution showed the clean formation of $\text{Cp}^*\text{W}(\text{NO})(\text{CHDCMe}_3)[\text{CD}_2\text{Si}(\text{CD}_3)_3]$ (**2.9- d_{12}**) and 1 equiv of neopentane. The organic volatiles were removed in vacuo. The remaining red-black solid was extracted with pentane and

filtered through Celite. Cooling this filtrate to $-30\text{ }^{\circ}\text{C}$ overnight afforded **2.9-*d*₁₂** (27 mg, 93% yield) as mauve crystals.

Anal. Calcd. for $\text{C}_{19}\text{H}_{25}\text{D}_{12}\text{NOSiW}$: C, 43.94; H, 7.13; N, 2.70. Found: C, 44.26; H, 7.09; N, 2.74. IR (cm^{-1}) ν_{NO} 1554 (s), ν_{CD} 2204 (w). MS 519 [M^+ , ^{184}W]. ^1H NMR (300 MHz, C_6D_6) δ 1.36 (s, 9H, CMe_3), 1.51 (s, 15H, C_5Me_5), 3.19 (br s, 1H, WCHDC). $^2\text{H}\{^1\text{H}\}$ NMR (77 MHz, C_6H_6) δ -2.16 (s, 1D, WCHDC), -1.38 (s, 1D, WCD_2Si), 0.33 (s, 9D, $\text{Si}(\text{CD}_3)_3$), 1.06 (s, 1D, WCD_2Si). $^{13}\text{C}\{^1\text{H}\}$ NMR (75 MHz, C_6D_6) δ 9.9 (C_5Me_5), 34.2 (CMe_3), 39.7 (CMe_3), 104.8 (t, $^1J_{\text{CD}} = 14.9$, WCHDC), 109.8 (C_5Me_5). ^{13}C resonances attributable to CD_2 and $\text{Si}(\text{CD}_3)_3$ could not be observed, presumably due to C–D coupling, quadrupolar effect, and lack of nuclear Overhauser enhancement.

5.2.11 Thermolysis of **2.4** in C_6D_6

See the first part of Section 5.2.5.

5.2.12 Thermolysis of **2.4** in $(\text{CH}_3)_2\text{Si}(\text{CD}_3)_2$

A sample of **2.4** (14 mg, 0.025 mmol) in a J. Young NMR tube was dissolved in $(\text{CH}_3)_2\text{Si}(\text{CD}_3)_2$ (~0.3 mL) and then heated in a constant-temperature bath at $70.0\text{ }^{\circ}\text{C}$ for 1.5 d, after which time the volatiles were removed in vacuo. The residue was dissolved in C_6D_6 and two ^1H NMR spectra (400 MHz, pulse delay of 10 seconds) were recorded. The ratio of $\text{Cp}^*\text{W}(\text{NO})(\text{CH}_2\text{CMe}_3)[\text{CH}_2\text{Si}(\text{CH}_3)(\text{CD}_3)_2]$ (**2.9-*d*₆-H**) to $\text{Cp}^*\text{W}(\text{NO})(\text{CHDCMe}_3)[\text{CD}_2\text{Si}(\text{CD}_3)(\text{CH}_3)_2]$ (**2.9-*d*₆-D**) was determined to be 1.35(5):1 by integration of the methylene signals at δ 3.20 and 3.27.

^1H NMR (500 MHz, C_6D_6) δ -2.11 (dd, $^2J_{\text{HH}} = 12.4$, $^4J_{\text{HH}} = 1.4$, 1H, WCH_2C), -1.30 (dd, $^2J_{\text{HH}} = 12.0$, $^4J_{\text{HH}} = 1.4$, WCH_2Si), 0.38 [s, $\text{SiMe}(\text{CD}_3)_2$ and $\text{SiMe}_2(\text{CD}_3)$], 1.07 (s, CMe_3), 1.35 (d, $^2J_{\text{HH}} = 12.4$, WCH_2Si), 1.52 (s, C_5Me_5), 3.20 (s, WCHDC), 3.27 (d, $^2J_{\text{HH}} = 12.4$, 1H, WCH_2C).

5.2.13 Thermolysis of 2.4 in 1:1 C₆H₆/C₆D₆

Two samples of **2.4** (16 mg, 0.033 mmol) in J. Young NMR tubes were dissolved in an equimolar mixture of C₆H₆/C₆D₆ (0.4 mL). The tubes were then heated side by side in a constant-temperature bath at 70.0 °C for ~1.5 d. After removal of the organic volatiles in vacuo, the residues were dissolved in C₆D₆ and two ¹H NMR spectra (400 MHz, pulse delay of 10 s) were recorded for each experiment. The average ratio of Cp*W(NO)(CH₂CMe₃)(C₆H₅) (**2.11**) to Cp*W(NO)(CHDCMe₃)(C₆D₅) (**2.11-d₆**) was determined to be 1.05(5):1 by integration of the methylene signals at δ 4.37 and 4.50.

¹H NMR (500 MHz, C₆D₆) δ -2.05 (d, ²J_{HH} = 11.4, 1H, WCH₂), 1.26 (s, CMe₃), 1.53 (s, C₅Me₅), 4.37 (s, WCHD), 4.50 (d, ²J_{HH} = 11.4, 1H, WCH₂), 7.08 (t, ³J_{HH} = 7.4, ArH), 7.19 (t, ³J_{HH} = 7.4, ArH), 7.71 (d, ³J_{HH} = 7.7, ArH).

5.2.14 Thermolysis of 2.4 in 1,3,5-C₆H₃D₃-d₃

Two samples of **2.4** (14 mg, 0.025 mmol) in J. Young NMR tubes were dissolved in 1,3,5-C₆H₃D₃ (~0.3 mL). Each sample was heated in a constant-temperature bath at 70.0 °C for ~1.5 d, after which time the organic volatiles were removed in vacuo. The residues were then dissolved in C₆D₆ and two ¹H NMR spectra (400 MHz, pulse delay of 10 seconds) were recorded for each experiment. The average ratio of Cp*W(NO)(CH₂CMe₃)(C₆H₂D₃) (**2.11-d₃-H**) to Cp*W(NO)(CHDCMe₃)(C₆H₃D₂) (**2.11-d₃-D**) was determined to be 1.35(5):1 by integration of the methylene signals at δ 4.34 and δ 4.48.

¹H NMR (400 MHz, C₆D₆) δ -2.02 (d, ²J_{HH} = 11.4, 1H, WCH₂), 1.25 (s, CMe₃), 1.54 (s, C₅Me₅), 4.34 (s, WCHD), 4.48 (d, ²J_{HH} = 11.4, 1H, WCH₂), 7.08 (s, ArH), 7.18 (s, ArH), 7.71 (s, ArH).

5.2.15 Thermolysis of $\text{Cp}^*\text{W}(\text{NO})(\text{CH}_2\text{CMe}_3)(\text{CH}_2\text{CMe}_2\text{Ph})$ (**2.8**) in THF in the Presence of Added PMe_3

To a Pyrex reactor containing **2.8** (50 mg, 0.090 mmol) was added THF (2 mL) and excess PMe_3 by vacuum transfer. The resulting mixture was thawed and heated at 75 °C overnight, during which time its color changed from brown-red to yellow-orange. The organic volatiles were removed in vacuo and the residue was analyzed by ^1H NMR (C_6D_6) spectroscopy, which showed the presence of $\text{Cp}^*\text{W}(\text{NO})(\text{CH}_2\text{CMe}_2\text{-}o\text{-C}_6\text{H}_4)(\text{PMe}_3)$ (**5.1**) as the major species along with $\text{Cp}^*\text{W}(\text{NO})(=\text{CHCMe}_2)(\text{PMe}_3)$ (**3.4**) and $\text{Cp}^*\text{W}(\text{NO})(\text{CH}_2\text{CMe}_3)(\text{C}_6\text{H}_4\text{CMe}_3)$ (**5.2**) (as a ~1.4:1 mixture of *m*- and *p*-isomers) in a combined yield of ~15%. Next, the crude product sample was redissolved in a minimum amount of Et_2O and stored at -30 °C for 2 d to obtain **5.1** (15 mg, 30% yield) as yellow-orange blocks. The mother liquor was taken to dryness and chromatographed on alumina I by eluting with hexanes. The first band to appear, a pink fraction, was collected by eluting with 4:1 hexanes/ Et_2O . Concentration of this fraction, followed by cooling to -30 °C for 2 d afforded **5.2** (~2 mg) as mauve needles contaminated by a trace amount of **5.1**.

$\text{Cp}^*\text{W}(\text{NO})(\text{CH}_2\text{CMe}_2\text{-}o\text{-C}_6\text{H}_4)(\text{PMe}_3)$ (5.1**):** Anal. Calcd. for $\text{C}_{23}\text{H}_{36}\text{NOPW}$: C, 49.56; H, 6.51; N, 2.51. Found: C, 49.78; H, 6.54; N, 2.52. MS 557 [M^+ , ^{184}W]. ^1H NMR (500 MHz, CDCl_3) δ 1.18 (s, 3H, CMeMe), 1.21 (d, $^2J_{\text{HP}} = 8.9$, 9H, PMe_3), 1.36 (s, 3H, CMeMe), 1.49 (d, $^2J_{\text{HH}} = 8.8$, 1H, WCH_2), 1.65 (dd, $^2J_{\text{HH}} = 8.8$, $^3J_{\text{HP}} = 2.3$, 1H, WCH_2), 1.87 (s, 15H, C_5Me_5), 6.84 (m, 1H, ArH), 6.94 (m, 2H, ArH), 7.11 (d, $^3J_{\text{HH}} = 7.6$, 1H, ArH). $^{13}\text{C}\{^1\text{H}\}$ NMR (75 MHz, CDCl_3) δ 10.5 (C_5Me_5), 14.1 (d, $^1J_{\text{CP}} = 29$, PMe_3), 30.6 (CMeMe), 36.1 (d, $^4J_{\text{CP}} = 3$, CMeMe), 51.5 (d, $^3J_{\text{CP}} = 3$, CMeMe), 57.4 ($^2J_{\text{CP}} = 7$, WCH_2), 107.0 (C_5Me_5), 122.7 (Ar CH), 123.0 (Ar CH), 124.2 (Ar CH), 138.4 (d, $^3J_{\text{CP}} = 13$, Ar CH), 165.9 (d, $^3J_{\text{CP}} = 9$, C_{ipso}), 173.2 (d, $^2J_{\text{CP}} = 21$, WC_{ipso}). $^{31}\text{P}\{^1\text{H}\}$ NMR (202 MHz, C_6D_6) δ -20.4 ($^1J_{\text{PW}} = 211$).

$\text{Cp}^*\text{W}(\text{NO})(\text{CH}_2\text{CMe}_3)(\text{C}_6\text{H}_4\text{CMe}_3)$ (5.2**):** ^1H NMR (500 MHz, C_6D_6) δ **5.2_m**: -1.82 (d, $^2J_{\text{HH}} = 11.5$, 1H, WCH_2), 1.26 (s, 9H, CH_2CMe_3), 1.29 (s, 9H, $\text{C}_{\text{ipso}}\text{CMe}_3$), 1.58 (s, 15H, C_5Me_5), 4.38 (d, $^2J_{\text{HH}} = 11.6$, 1H, WCH_2), 7.19 (d, $^3J_{\text{HH}} = 7.2$, 1H, ArH), 7.22 (t, $^3J_{\text{HH}} = 7.4$, 1H,

ArH), 7.62 (d, $^3J_{\text{HH}} = 7.5$, 1H, ArH), 7.84 (s, 1H, ArH). **5.2_p**: -1.92 (d, $^2J_{\text{HH}} = 11.5$, 1H, WCH₂), 1.22 (s, 9H, C_{ipso}CMe₃) 1.26 (s, 9H, CH₂CMe₃), 1.58 (s, 15H, C₅Me₅), 4.38 (d, $^2J_{\text{HH}} = 11.6$, 1H, WCH₂), 7.29 (d, $^3J_{\text{HH}} = 8.0$, 2H, ArH), 7.78 (d, $^3J_{\text{HH}} = 7.9$, 2H, ArH).

5.2.16 Thermolysis of Cp*W(NO)(CH₂CMe₃)(CD₂CMe₂Ph) (**2.8-d₂**) in THF in the Presence of Added PMe₃

This reaction was carried out in the same manner as that described above for the protio complex **2.8**. Analysis of the crude reaction mixture by ¹H NMR spectroscopy indicated the presence of Cp*W(NO)(CD₂CMe₂-*o*-C₆H₄) (**5.1-d₂**), Cp*W(NO)(=CHCMe₃)(PMe₃) (**3.4**) (W=CH δ 11.2), and Cp*W(NO)(CH₂CMe₃)[C₆H₄CMe₂(CD₂H)] (**5.2-d₂**). Complexes **5.1-d₂** and **5.2-d₂** were purified, respectively, by crystallization from Et₂O and by chromatography on alumina I with hexanes and hexanes/Et₂O as described above.

5.1-d₂: MS *m/z* 559 [M⁺, ¹⁸⁴W]. ¹H NMR (500 MHz, C₆D₆) δ 0.89 (d, $^2J_{\text{HP}} = 8.8$, 9H, PMe₃), 1.58 (s, 15H, C₅Me₅), 1.68 (s, 3H, CMeMe), 1.75 (s, 3H, CMeMe), 7.06 (t, $^3J_{\text{HH}} = 6.9$, 1H, ArH), 7.10 (d, $^3J_{\text{HH}} = 6.9$, 1H, ArH), 7.16 (t, $^3J_{\text{HH}} = 7.1$, 1H, ArH), 7.23 (d, $^3J_{\text{HH}} = 7.5$, 1H, ArH). ²H{¹H} NMR (77 MHz, C₆H₆) δ 1.80 (br s, 2D, WCD₂). ¹³C{¹H} (CDCl₃) δ 10.5 (C₅Me₅), 14.1 (d, $^1J_{\text{CP}} = 29$, PMe₃), 30.6 (CMeMe), 36.1 (CMeMe), 51.3 (CMeMe), 107.0 (C₅Me₅), 122.6 (Ar CH), 123.0 (Ar CH), 124.2 (Ar CH), 138.4 (d, $^3J_{\text{CP}} = 13$, Ar CH), 165.9 (C_{ipso}), 173.2 (d, $J_{\text{CP}} = 21$, WC_{ipso}).

5.2-d₂: ¹H NMR (500 MHz, C₆D₆) δ **5.2-*m*-d₂**: -1.82 (d, $^2J_{\text{HH}} = 11.5$, 1H, WCH₂), 1.26 (s, 9H, CH₂CMe₃), 1.29 [s, 7H, C_{ipso}CMe₂(CD₂H)], 1.58 (s, 15H, C₅Me₅), 4.38 (d, $^2J_{\text{HH}} = 11.6$, 1H, WCH₂), 7.19 (d, $^3J_{\text{HH}} = 7.2$, 1H, ArH), 7.22 (t, $^3J_{\text{HH}} = 7.4$, 1H, ArH), 7.62 (d, $^3J_{\text{HH}} = 7.5$, 1H, ArH), 7.84 (s, 1H, ArH). **5.2-*p*-d₂**: -1.82 (d, $^2J_{\text{HH}} = 11.5$, 1H, WCH₂), 1.26 [s, 7H, C_{ipso}Me₂(CD₂H)], 1.29 (s, 9H, CH₂CMe₃), 1.58 (s, 15H, C₅Me₅), 4.38 (d, $^2J_{\text{HH}} = 11.6$, 1H, WCH₂), 7.29 (d, $^3J_{\text{HH}} = 7.8$, 2H, ArH), 7.78 (d, $^3J_{\text{HH}} = 7.9$, 2H, ArH). ²H{¹H} NMR (77 MHz, C₆H₆) δ 1.26 [br s, CMe₂(CD₂H)].

5.2.17 Thermolysis of $\text{Cp}^*\text{W}(\text{NO})(\text{CHDCMe}_3)[\text{CD}_2\text{Si}(\text{CD}_3)_3]$ (**2.9-*d*₁₂**) in $\text{Si}(\text{CH}_3)_4$

A solution of **2.9-*d*₁₂** in ~0.5 mL of tetramethylsilane was heated in a J. Young NMR tube at ~70 °C for 2 d. Neither reaction nor H/D exchange could be detected in the ^1H and $^2\text{H}\{^1\text{H}\}$ NMR spectra of a C_6D_6 sample of the crude reaction mixture.

5.2.18 Thermolysis of $\text{Cp}^*\text{W}(\text{NO})(\text{CH}_2\text{CMe}_3)(\text{CH}_3)$ (**2.10**)

To a C_6D_6 solution (~0.5 mL) of freshly sublimed **2.10** in a J. Young NMR tube was added PMe_3 (~1.2 equiv) by vacuum transfer. An immediate color change from dark red to yellow resulted. Inspection of the ^1H NMR spectrum at room temperature revealed the presence of an equilibrium mixture containing $\text{Cp}^*\text{W}(\text{NO})(\text{CH}_2\text{CMe}_3)(\text{CH}_3)(\text{PMe}_3)$, **2.10**, and free PMe_3 . Only one isomer of $\text{Cp}^*\text{W}(\text{NO})(\text{CH}_2\text{CMe}_3)(\text{CH}_3)(\text{PMe}_3)$ was detected at 400 MHz, namely that in which the PMe_3 is coordinated between the methyl and nitrosyl ligands.

$\text{Cp}^*\text{W}(\text{NO})(\text{CH}_2\text{CMe}_3)(\text{CH}_3)(\text{PMe}_3)$: ^1H NMR (400 MHz, C_6D_6) δ 0.00 (d, $^3J_{\text{HP}} = 16.7$, 3H, WCH_3), 0.61 (dd, $^2J_{\text{HH}} = 11.5$, $^3J_{\text{HP}} = 5.9$, 1H, WCH_2), 1.03 (d, $^2J_{\text{HP}} = 8.7$, 9H, PMe_3), 1.42 (d, $^2J_{\text{HH}} = 11.5$, 1H, WCH_2), 1.52 (s, 9H, CMe_3), 1.54 (s, 15H, C_5Me_5). $^{13}\text{C}\{^1\text{H}\}$ NMR (75 MHz, C_6D_6) δ 9.8 (C_5Me_5), 11.6 (d, $^1J_{\text{CP}} = 28$, PMe_3), 12.8 (d, $^2J_{\text{CP}} = 21$, $^1J_{\text{CH}} = 128$, WCH_3), 35.4 (CMe_3), 38.4 (CMe_3), 54.6 (d, $^2J_{\text{CP}} = 11$, $^1J_{\text{CH}} = 120$, WCH_2), 106.0 (C_5Me_5). $^{31}\text{P}\{^1\text{H}\}$ NMR (202 MHz, C_6D_6) δ -17.4 ($^1J_{\text{PW}} = 140$). NOEDS (400 MHz) irradiat. at 0.00 ppm, NOEs at δ 0.61 and 1.03; irradiat. at 0.61 ppm, NOEs at δ 0.00 and 1.42; irradiat. at 1.03 ppm, NOEs at δ 0.00 and 1.54.

When $\text{THF-}d_8$ was used in place of C_6D_6 as solvent, an immediate color change from dark red to yellow also resulted. Thermolysis of this mixture to 70 °C in the dark showed no noticeable reaction after 2 days. After an additional 3 d at ~85 °C, traces of **3.4** ($\text{W}=\text{CH}$ δ 11.25) was detected by ^1H NMR spectroscopy (C_6D_6) along with similar amounts of unidentified decomposition products, which displayed broadened peaks in the Cp^* region. No methyldiene products were observed.

5.2.19 Thermolysis of $\text{Cp}^*\text{W}(\text{NO})(\text{CH}_2\text{CMe}_3)(\text{C}_6\text{D}_5)$ (**2.11-*d*₅**) in C_6D_6

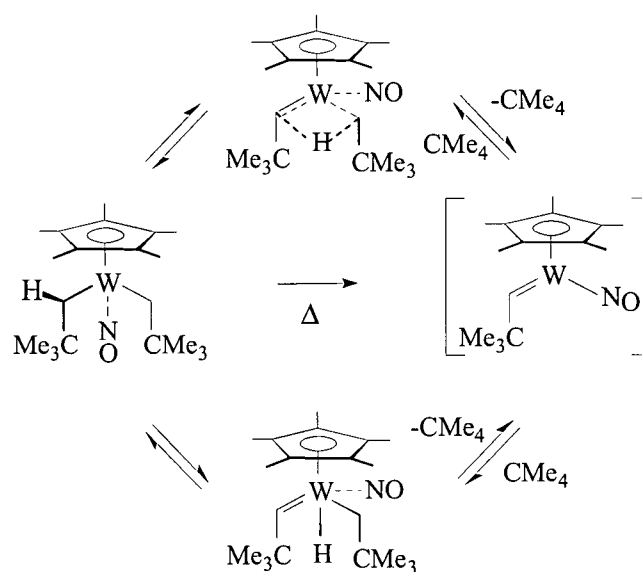
A C_6D_6 solution (~0.4 mL) of **2.11-*d*₅** in a J. Young NMR tube was prepared. The tube was then placed in an NMR probe at 70 °C. ^1H NMR spectra were acquired at regular time intervals over the course of ~10 h. Although a small amount of decomposition was observed, neither arene exchange nor H/D scrambling was evident.

5.3 Results and Discussion

5.3.1 Isotopic Labeling Studies

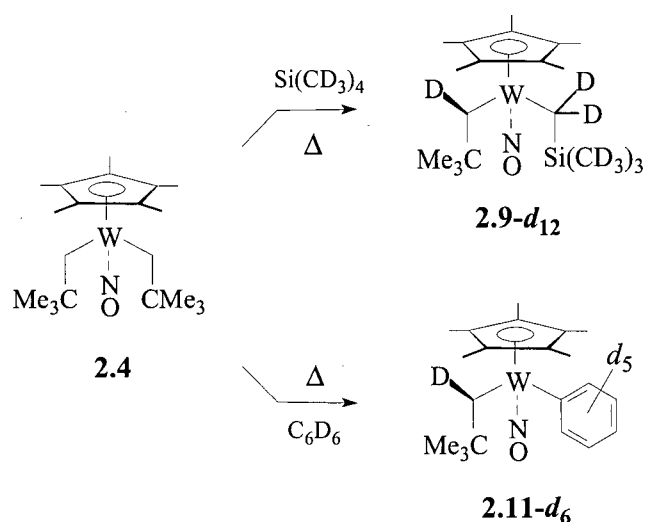
The most straightforward mechanism for the thermal decomposition and C–H activation reaction of $\text{Cp}'\text{W}(\text{NO})(\text{CH}_2\text{CMe}_3)_2$ [$\text{Cp}' = \text{Cp}$ (**2.1**), Cp^* (**2.4**)] is that shown in Scheme 5.1. Because this reaction sequence involves both C–H bond scission and formation, valuable mechanistic information may be obtained by replacement of the migrating hydrogen with deuterium. In this context, two types of deuterium-labeling experiments have been carried out in order to probe this mechanistic possibility.

Scheme 5.1



First, thermolysis of **2.4** in neat $\text{Me}_4\text{Si-}d_{12}$ at $\sim 70^\circ\text{C}$ for 2.5 d results in the quantitative formation of neopentane and the mixed bis(alkyl) complex $\text{Cp}^*\text{W}(\text{NO})(\text{CHDCMe}_3)[\text{CD}_2\text{Si}(\text{CD}_3)_3]$ (**2.9-}d_{12}**) in which a deuterium is incorporated into the α -position of the neopentyl ligand (Scheme 5.2). Similarly, thermolysis of **2.4** in neat C_6D_6 at $\sim 70^\circ\text{C}$ for 2 d produces the phenyl neopentyl derivative $\text{Cp}^*\text{W}(\text{NO})(\text{CHDCMe}_3)(\text{C}_6\text{D}_5)$ (**2.11-}d_6**) in which the α -carbon of the neopentyl ligand is monodeuterated. Minor resonances downfield of the Cp^* region are also detected in the ^1H NMR spectrum in this case and are assignable to products arising from slow decomposition of **2.11-}d_6 during the late stages of the reaction (see later). For both complexes **2.9-}d_{12}** and **2.11-}d_6**, analysis of the crude product mixture by NMR spectroscopy indicates that only one of the neopentyl methylene protons is replaced by deuterium. Particularly indicative of the structures illustrated in Scheme 5.2 is the ^1H NMR resonance of the remaining proton, which appears as a singlet and is shifted upfield relative to the resonance observed in the unlabeled complex by ca. 0.07 ppm for **2.9-}d_{12}** and 0.14 ppm for **2.11-}d_6**. Thus, although no intermediates could be detected when the reaction with C_6D_6 was followed by ^1H NMR spectroscopy, these results unambiguously demonstrate that $[\text{Cp}^*\text{W}(\text{NO})(=\text{CHCMe}_3)]$ is a key intermediate in the thermal decomposition of **2.4**, that (in agreement with the results of the trapping reactions with phosphines and certain alkenes) the**

Scheme 5.2

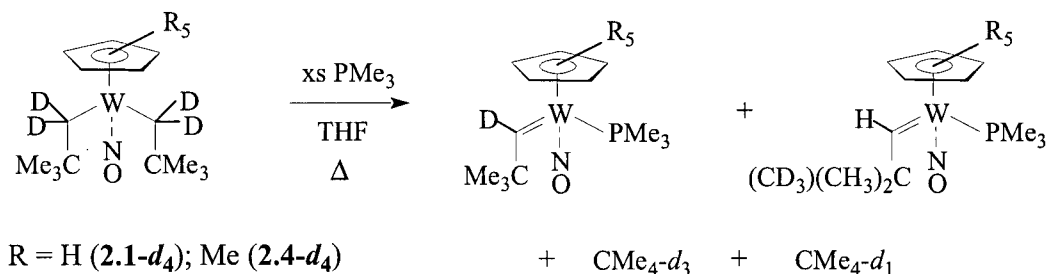


neopentylidene moiety is anti with respect to the Cp* ligand, and that **2.9-*d*₁₂** and **2.11-*d*₆** are formed as a result of a *cis* C–D addition across the tungsten-carbon double bond in this unobserved unsaturated intermediate.

In the second type of deuterium-labeling study, the preparation and thermal decomposition of the α -deuterated derivatives Cp'W(NO)(CD₂CMe₃)₂ [Cp' = Cp (**2.1-*d*₄**), Cp* (**2.4-*d*₄**)] were carried out. The preparation of **2.1-*d*₄** and **2.4-*d*₄** can be carried out in a manner analogous to that for **2.1** and **2.4** using (Me₃CCD₂)₂Mg·(dioxane) as the alkylating agent. These deuterium-containing compounds, however, undergo H/D exchange with Et₂O/pentane and Et₂O/hexanes when filtered slowly through alumina I. Their purification therefore is best achieved by filtration of the crude product mixtures through Celite followed by crystallization. For both compounds, the methylene resonances were the only signals observed in the ²H{¹H}NMR spectrum. No corresponding methylene signals were observed in the ¹H NMR spectrum, indicating an isotopic purity of at least 98%.

To determine the fate of the α -hydrogen abstracted and the source of the hydrogen consumed in converting one neopentyl group to neopentane, the thermal decompositions of **2.1-*d*₄** and **2.4-*d*₄** were performed in THF in the presence of excess PMe₃ for 2–3 d at 65 °C and 75 °C, respectively. As can be seen from Scheme 5.3 and Table 5.1, analysis of the crude reaction mixtures by ¹H and ²H NMR spectroscopies and the organic volatiles by GC/mass spectrometry shows the formation of Cp'W(NO)(=CDCMe₃)(PMe₃) and neopentane-*d*₃ as the major products

Scheme 5.3



in these reactions. In each case, small quantities of $\text{Cp}^*\text{W}(\text{NO})[=\text{CHCMe}_2(\text{CD}_3)](\text{PMe}_3)$ and neopentane- d_1 are also observed, with the latter constituting 17–18% of the neopentane mixture. A reasonable explanation for these observations is that loss of neopentane from **2.1- d_4** and **2.4- d_4** occurs reversibly during the course of the thermolysis and that this process involves an α -hydrogen abstraction/elimination pathway in which an α -deuterium (hydrogen) from one neopentyl group is transferred to the α -carbon atom of the other. Since neopentane- d_2 is not observed as a product, it can also be concluded that neither ring metalation nor γ -hydrogen activation is a competitive side-reaction.

Table 5.1. Isotopic Composition of Neopentane Derived from Thermal Decompositions of **2.1- d_4** and **2.4- d_4**

compd	reaction medium	isotopic composition of neopentane (%) ^a			
		- d_0^b	- d_1	- d_2^b	- d_3
2.1-d_4	THF, excess PMe_3	2	17	4	77
2.4-d_4	THF, excess PMe_3	0	18	3	79
2.4-d_4	neat PMe_3	0	10	0	90

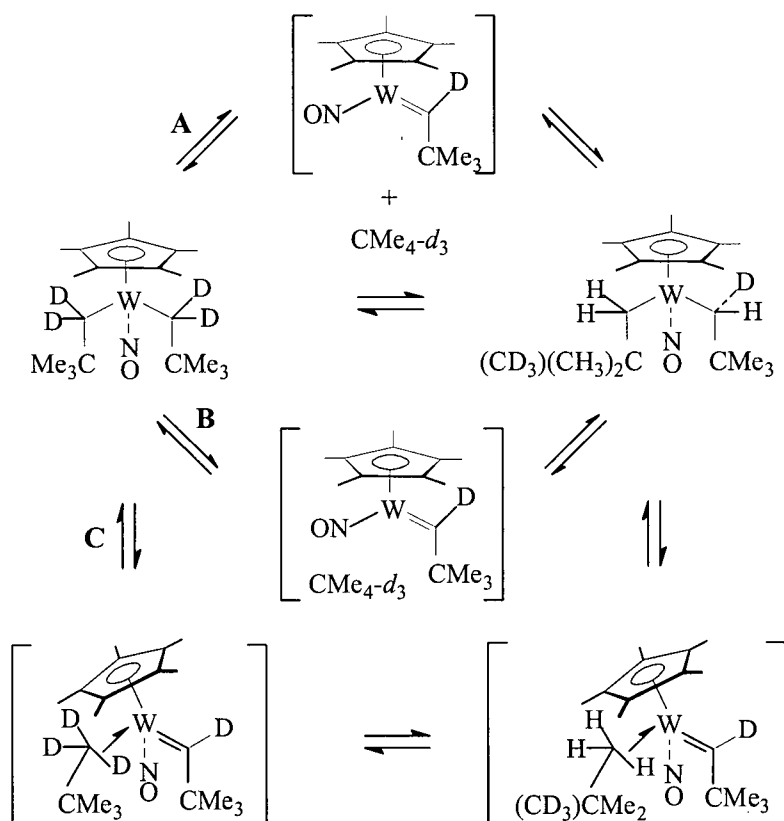
^aThese are *estimates* derived directly from the GC–MS data (see the Appendix); they are not corrected for isotopic impurities present in the starting materials. ^bThese percentages are within experimental error.

Further evidence that loss of neopentane occurs reversibly during the thermolysis of **2.1** and **2.4** comes from reaction of **2.4- d_4** with C_6D_6 . When **2.4- d_4** is heated in neat C_6D_6 at 70 °C, H/D exchange between the α - and γ -positions of the neopentyl ligands in **2.4- d_4** is again found to occur, as judged by ^1H and $^2\text{H}\{^1\text{H}\}$ NMR spectroscopies. Concurrently, neopentane and the benzene-activated isotopomer $\text{Cp}^*\text{W}(\text{NO})(\text{CD}_2\text{CMe}_3)(\text{C}_6\text{D}_5)$ form. A small quantity of $\text{Cp}^*\text{W}(\text{NO})[\text{CHDCMe}_2(\text{CD}_3)](\text{C}_6\text{D}_5)$ is also observed with deuterium incorporated into the *same* α -position as that described above for **2.11- d_6** . This is based on the observation that the W–CHD resonance appears exclusively as a low-intensity broad singlet at δ 4.37. This demonstrates that the thermal decomposition of **2.4- d_4** proceeds by an α -H abstraction route

wherein isotopic label scrambling between the α - and γ -positions of the neopentyl ligands occurs prior to product formation.

The H/D exchange described above in principle could occur inter- or intramolecularly as depicted in Scheme 5.4. Path A can be discounted since thermolysis of **2.4** (70 °C, 16 h) in THF in the presence of excess PMe_3 (>10 equiv) and 5 equiv of Me_4Si or C_6D_6 produces $\text{Cp}^*\text{W}(\text{NO})(=\text{CHCMe}_3)(\text{PMe}_3)$, with no detectable products resulting from intermolecular C–H(D) activation. This is not unexpected and can be attributed to the fact that the added hydrocarbon in each case is too low in concentration to compete with PMe_3 for reaction with intermediate $[\text{Cp}^*\text{W}(\text{NO})(=\text{CHCMe}_3)]$. The possibility of a solvent-caged mechanism (i.e. path B) can also be tested by a competition experiment. When **2.4- d_4** is heated to 75 °C in *neat* PMe_3 , $\text{Cp}^*\text{W}(\text{NO})(=\text{CDCMe}_3)(\text{PMe}_3)$ is observed with detectable proton incorporation in the α -position. In addition, the neopentane produced is approximately 90% d_3 and 10% d_1 as determined by GC/MS analysis (see Table 5.1). This strongly suggests that neopentane does *not* react as a solvent-caged species. More likely is that the H/D exchange occurs intramolecularly via path C. According to this path, the starting bis(neopentyl) does *not* decompose to give $[\text{Cp}^*\text{W}(\text{NO})(=\text{CDCMe}_3)]$ directly. Rather, the initial step involves *reversible* formation of the σ -complex, $[\text{Cp}^*\text{W}(\text{NO})(=\text{CDCMe}_3)(\eta^2\text{-D-CD}_2\text{CMe}_3)]$. The observation of neopentane- d_1 , in addition to the expected neopentane- d_3 , indicates that the metal in this complex also migrates readily and intramolecularly from complexation with an α -C–D bond to complexation with a γ -C–H bond with eventual formation of $\text{Cp}^*\text{W}(\text{NO})(\text{CHDCMe}_3)[\text{CH}_2\text{CMe}_2(\text{CD}_3)]$. It also strongly suggests that this exchange process occurs competitively with loss of neopentane from $[\text{Cp}^*\text{W}(\text{NO})(=\text{CDCMe}_3)(\eta^2\text{-D-CD}_2\text{CMe}_3)]$ and that the latter process is *irreversible*. This leads to formation of the $[\text{Cp}^*\text{W}(\text{NO})(=\text{CDCMe}_3)]$ intermediate, which then coordinates PMe_3 or another (and more concentrated) hydrocarbon.

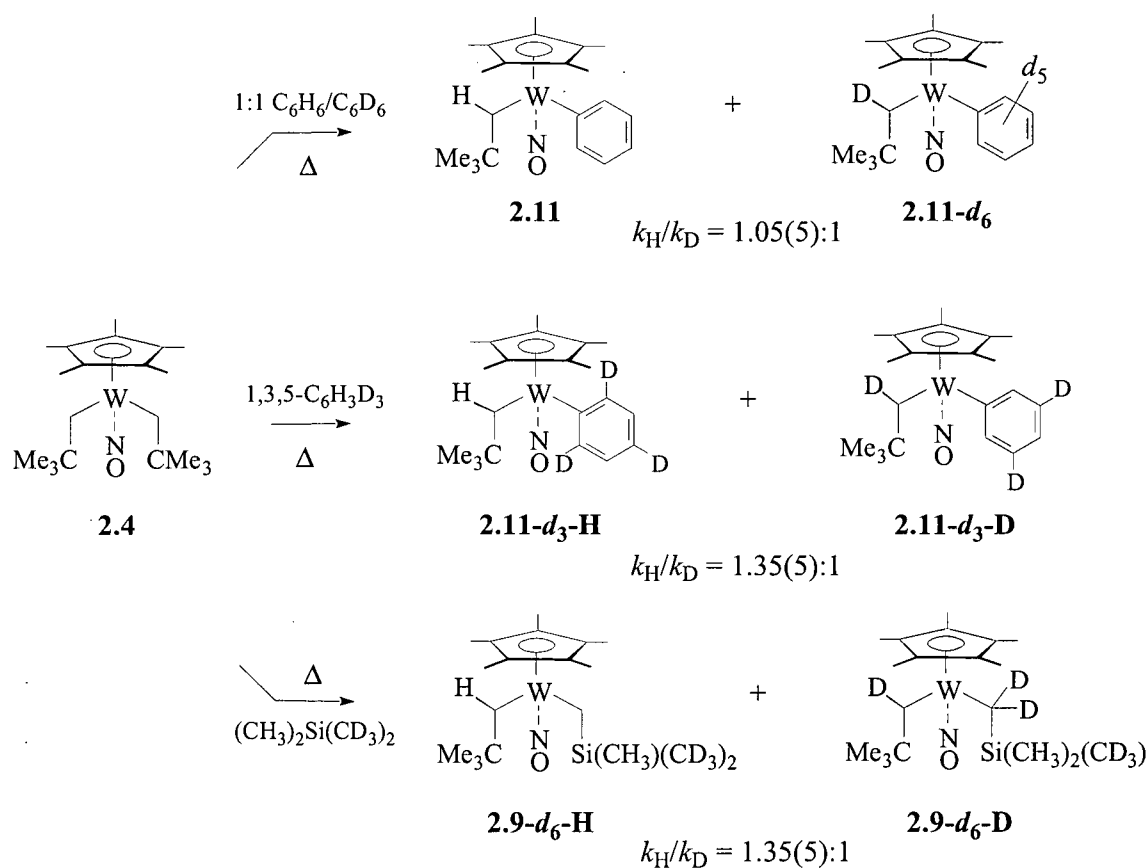
Scheme 5.4



5.3.2 Isotope Effect Studies

Additional evidence that an intermediate alkane σ -complex exists along the pathway by which **2.1** and **2.4** eliminate neopentane comes from studies of the isotope effects on the reverse reaction, i.e., the C-H activation reaction of $[\text{Cp}^*\text{W}(\text{NO})(=\text{CHCMe}_3)]$. The isotope effects on the C-H activation reaction of $[\text{Cp}^*\text{W}(\text{NO})(=\text{CHCMe}_3)]$ were measured as shown in Scheme 5.5. Thermolysis of **2.4** in a mixture of 1:1 $\text{C}_6\text{H}_6/\text{C}_6\text{D}_6$ at 70.0 °C for 1.5 d results in the formation of the benzene C-H and C-D activation products, **2.11** and **2.11- d_6** . By integration of the methylene proton signals at δ 4.50 and 4.37 (Figure 5.1A), the ratio of **2.11** to **2.11- d_6** , was found to be 1.05(5):1. Similarly, the thermolysis of **2.4** in 1,3,5- $\text{C}_6\text{H}_3\text{D}_3$ at 70.0 °C for 1.5 d produces $\text{Cp}^*\text{W}(\text{NO})(\text{CH}_2\text{CMe}_3)(2,4,6\text{-C}_6\text{H}_2\text{D}_3)$ (**2.11- d_3 -H**) and $\text{Cp}^*\text{W}(\text{NO})(\text{CHDCMe}_3)(3,5\text{-}$

Scheme 5.5



$\text{C}_6\text{H}_3\text{D}_2$) (**2.11- d_3 -D**). The ratio of the benzene products in this case (Figure 5.1B) is 1.35(5):1, indicating a slight preferential activation of a C–H bond over a C–D bond. An analogous result is obtained when $(\text{CH}_3)_2\text{Si}(\text{CD}_3)_2$ is substituted for 1,3,5- $\text{C}_6\text{H}_3\text{D}_3$ as solvent. $(\text{CH}_3)_2\text{Si}(\text{CD}_3)_2$ was prepared in a straightforward manner as shown in eq 5.1. Thermolysis of **2.4** in $(\text{CH}_3)_2\text{Si}(\text{CD}_3)_2$ at 70.0 °C for 1.5 d leads to the formation of $\text{Cp}^*\text{W}(\text{NO})(\text{CH}_2\text{CMe}_3)[\text{CH}_2\text{Si}(\text{CH}_3)(\text{CD}_3)_2]$ (**2.9- d_6 -H**) and $\text{Cp}^*\text{W}(\text{NO})(\text{CHDCMe}_3)[\text{CD}_2\text{Si}(\text{CH}_3)_2(\text{CD}_3)]$ (**2.9- d_3 -D**) in a 1.35(5):1 ratio by integration of the methylene proton resonances at δ 3.27 and 3.20, respectively.

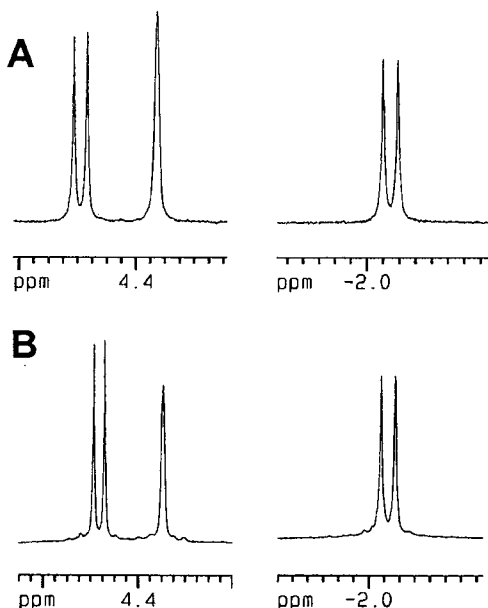
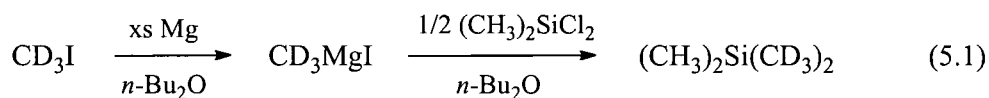


Figure 5.1. 500-MHz ^1H NMR spectra of the methylene regions of (A) $\text{Cp}^*\text{W}(\text{NO})(\text{CH}_2\text{CMe}_3)(\text{C}_6\text{H}_5)$ (**2.11**) and $\text{Cp}^*\text{W}(\text{NO})(\text{CHDCMe}_3)(\text{C}_6\text{D}_5)$ (**2.11-d₆**) and (B) $\text{Cp}^*\text{W}(\text{NO})(\text{CH}_2\text{CMe}_3)(2,4,6\text{-C}_6\text{H}_2\text{D}_3)$ (**2.11-d₃-H**) and $\text{Cp}^*\text{W}(\text{NO})(\text{CHDCMe}_3)(3,5\text{-C}_6\text{H}_3\text{D}_2)$ (**2.11-d₃-D**).

Each of the experiments outlined in Scheme 5.5 was carried out under conditions that ensure that once C–H or C–D cleavage has occurred isomerization of the initially formed product is not followed. The observed product ratios therefore reflect the kinetic isotope effects for activation of benzene and tetramethylsilane by $[\text{Cp}^*\text{W}(\text{NO})(=\text{CHCMe}_3)]$. This demonstrates that a small but real isotope effect ($k_{\text{H}}/k_{\text{D}} = 1.35(5)$) is observed when $[\text{Cp}^*\text{W}(\text{NO})(=\text{CHCMe}_3)]$ has to compete for C–H/C–D bonds in the *same* molecule. When the C–H/C–D bonds belong to *separate* molecules, the isotope effect ($k_{\text{H}}/k_{\text{D}} = 1.05(5)$) is negligible, if present at all. These results require that direct C–H bond addition across the tungsten neopentylidene moiety is not occurring and that an intermediate σ -complex is involved. The involvement of an intermediate

σ -complex allows the C–H(D) bonds in the same molecule to coordinate interchangeably with the metal center prior to bond activation. Since the zero-point energy of a C–H bond is higher than that of a C–D and since this energy difference is greatest when the two bonds are terminal, there is a thermodynamic preference for the former to coordinate to the metal and undergo subsequent bond cleavage.

Similar isotope effects have been reported by Jones *et. al.*, Bergman *et. al.*, and Flood *et. al.* for the thermal activation of benzene by $[\text{Cp}^*\text{Rh}(\text{PMe}_3)]$, $[\text{Cp}^*\text{Ir}(\text{PMe}_3)(\eta^2\text{-C}_3\text{H}_6)]$, and $[\text{CnRh}(\text{PMe}_3)][\text{BAr}_4]$ [Cn = 1,4,7-trimethyl-1,4,7-triazacyclononane; Ar = $\text{C}_6\text{H}_3\text{-3,5-(CF}_3)_2$], respectively. Bergman and Flood proposed that their observed isotope effects could be due to initial formation of either a σ -complex or an η^2 -arene complex. Jones and Feher, on the other hand, postulated the intermediacy of an η^2 -arene complex for their reactions. As additional evidence, they found that when benzene is replaced by *p*-di-*tert*-butylbenzene, an η^2 complex can be directly observed by ^1H NMR spectroscopy at low temperatures. In the activation of benzene by $[\text{Cp}^*\text{W}(\text{NO})(=\text{CHCMe}_3)]$, the presence of an intermediate η^2 -arene complex would provide a lower energy pathway for the interconversion of one σ -complex to another. Unfortunately, such a species can neither be proved nor disproved based on the observed kinetic isotope effects discussed above. The fact that the $k_{\text{H}}/k_{\text{D}}$ values for reactions with 1,3,5- $\text{C}_6\text{H}_3\text{D}_3$ and $(\text{CH}_3)_2\text{Si}(\text{CD}_3)_2$ are identical may simply be coincidental.

5.3.3 Kinetic Studies

Kinetic studies were carried out on the thermal decomposition of $\text{CpW}(\text{NO})(\text{CH}_2\text{CMe}_3)_2$ (**2.1**) and $\text{Cp}^*\text{W}(\text{NO})(\text{CH}_2\text{CMe}_3)_2$ (**2.4**) in THF and cyclohexane in the presence of greater than 5-fold excess of phosphine, where phosphine = PMe_3 , PMe_2Ph , or PEt_3 . The rates of disappearance of **2.1** and **2.4** were measured by UV-vis spectroscopy by monitoring the decrease in absorbance intensity at 486 nm; measured rate constants are given in Tables 5.2 and 5.3. In all cases examined, the rates of decomposition were first-order in metal complex for >3 half-lives and showed no dependence on the concentration and nature of added phosphine.

Table 5.2. Rate Constants for the Decomposition of **2.1** and **2.4** as a Function of Phosphine and Phosphine Concentration

entry	compd ^a	solvent	temp (°C) ^b	phosphine	[phosphine] (M)	k_{obs} (s ⁻¹) ^c
1	2.4	cyclohexane	91.0	PMe ₃	0.0032	$4.84(10) \times 10^{-4}$
2			91.0	PMe ₃	0.016	$4.72(7) \times 10^{-4}$
3			91.0	PMe ₃	0.16	$4.55(7) \times 10^{-4}$
4	2.4	THF	81.5	PMe ₃	0.016	$2.16(4) \times 10^{-4}$
5			81.5	PMe ₂ Ph	0.016	$2.30(3) \times 10^{-4}$
6			81.5	PEt ₃	0.016	$2.13(2) \times 10^{-4}$
7	2.1	THF	81.0	PMe ₃	0.016	$5.72(5) \times 10^{-4}$
8			81.0	PMe ₂ Ph	0.016	$5.75(4) \times 10^{-4}$
9			81.0	PEt ₃	0.016	$5.52(4) \times 10^{-4}$

^a[organometallic] $\sim 5.2 \times 10^{-4}$ M. ^bError ~ 1 °C. ^cEntries 1-3 were obtained from 2-3 runs and entries 4-9 were obtained from 3-4 runs; errors were calculated according to $[\sum(s_i)^2]^{1/2}/n$, where s_i is the standard deviation of k_i .

Comparison of the rate data of entries 4 and 7 of Table 5.2 indicates that **2.4** decomposes slower than **2.1** by a factor of ca. 2.7 (Figure 5.2); the latter in turn decomposes at a rate ca. 10 times slower than the previously reported CpMo(NO)(CD₂CMe₃)₂¹⁷ system.

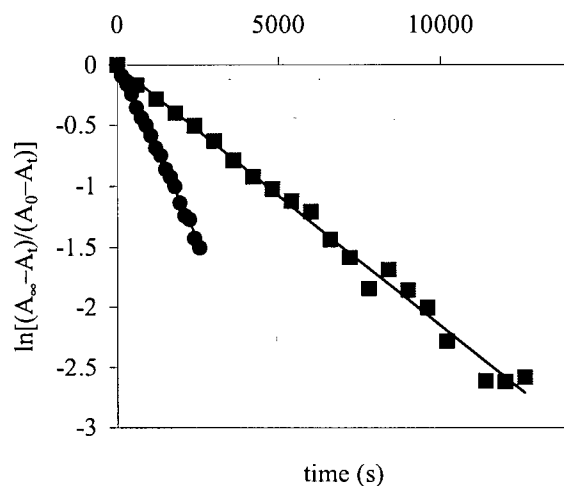


Figure 5.2. Representative first-order kinetic plots for the decomposition of **2.1** (●) and **2.4** (■) in THF in the presence of excess PMe_3 at 81 °C.

For both compounds **2.1** and **2.4**, the decomposition is slightly faster in THF solvent than in cyclohexane (Table 5.3). By arbitrarily setting the k_{obs} value derived from reaction in cyclohexane at 81 °C to 1.0, the relative rates of decomposition of **2.1** and **2.4** in THF are 2.7 and 1.3, respectively. These results stand in contrast to the rate of decomposition of $\text{CpTa}(\text{CH}_2\text{CMe}_3)_2\text{Cl}_2$ ¹⁸ reported by Schrock and co-workers, which is slowed by donor solvents, and to the rate of decomposition of $\text{CpMo}(\text{NO})(\text{CD}_2\text{CMe}_3)_2$,¹⁶ which is invariant to changes in solvent polarity and donor ability.

Table 5.3. Rate Constants for the Thermal Decompositions of **2.1** and **2.4** in the Presence of Excess PMe_3^a

entry	compd ^a	temp (°C) ^b	solvent	k_{obs} (s ⁻¹) ^c	solvent	k_{obs} (s ⁻¹) ^c
1	2.4	71.5	THF	$8.43(11) \times 10^{-5}$	cyclohexane	$5.23(3) \times 10^{-5}$
2		81.5		$2.16(4) \times 10^{-4}$		$1.67(2) \times 10^{-4}$
3		91.0		$5.61(8) \times 10^{-4}$		$4.58(5) \times 10^{-4}$
4		99.0		$1.20(6) \times 10^{-3}$		$1.23(2) \times 10^{-3}$
5	2.1	62.0	THF	$8.74(12) \times 10^{-5}$	cyclohexane	$2.46(1) \times 10^{-5}$
6		71.0		$2.31(5) \times 10^{-4}$		$6.48(3) \times 10^{-5}$
7		81.0		$5.72(5) \times 10^{-4}$		$2.09(2) \times 10^{-4}$
8		90.0		$1.42(4) \times 10^{-3}$		$4.90(7) \times 10^{-4}$

^a[organometallic] $\sim 5.2 \times 10^{-4}$ M. ^bError ~ 1 °C. ^cObtained from 3-4 runs; errors were calculated according to $[\sum(s_i)^2]^{1/2}/n$, where s_i is the standard deviation of k_i .

The rates of thermal decomposition of **2.1** between 60 and 90 °C and of **2.4** between 71 and 99 °C in THF and cyclohexane gave linear Eyring plots as shown in Figure 5.2. From these plots, the activation parameters listed in Table 5.4 were determined. The close to zero entropies of activation for both **2.1** and **2.4** in cyclohexane are comparable to those observed by Bercaw and co-workers for the α -hydrogen transfer reactions involving $\text{Cp}^*\text{M}(\text{CH}_2\text{R})_2$ compounds [$\text{M} = \text{Ti}$ ($\Delta S^\ddagger = -2.85(71)$ eu),¹⁹ Hf ($\Delta S^\ddagger = 1(3)$ eu)²⁰], and suggest that there is little reorganization on approach to the transition state in this solvent.

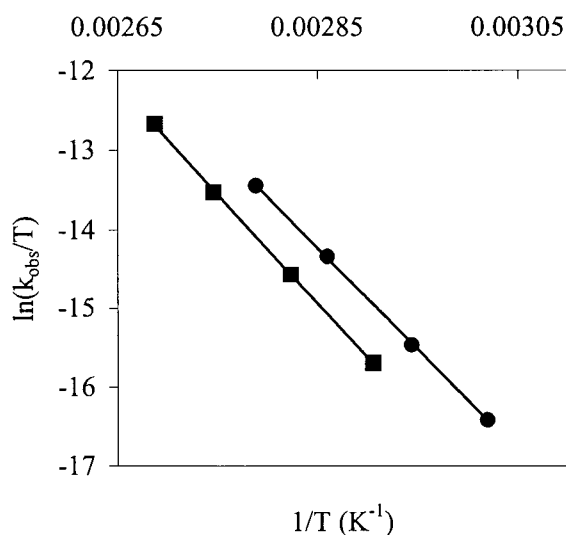


Figure 5.3. Eyring plots for the thermal decompositions of **2.1** (●) and **2.4** (■) in cyclohexane in the presence of excess PMe_3 .

Table 5.4. Activation Parameters for the Thermal Decompositions of **2.1** and **2.4** in THF and Cyclohexane in the Presence of Excess PMe_3 ^a

Entry	compd ^a	solvent	ΔH^\ddagger (kcal/mol) ^b	ΔS^\ddagger (eu) ^{b,c}
1	2.4	THF	24.0(2.2)	-7.9(6.1)
2		cyclohexane	28.3(3.5)	3.6(9.8)
3	2.1	THF	23.3(1.7)	-7.9(4.9)
4		cyclohexane	25.1(2.1)	-4.8(6.1)

^a[Organometallic] $\sim 5.2 \times 10^{-4}$ M. ^bErrors are 95% confidence limits. ^c1 eu = 1 cal/K·mol = 4.184 J/K·mol.

An examination of the kinetics of the thermal decomposition of $\text{CpW}(\text{NO})(\text{CD}_2\text{CMe}_3)_2$ (**2.1-*d*₄**) and $\text{Cp}^*\text{W}(\text{NO})(\text{CD}_2\text{CMe}_3)_2$ (**2.4-*d*₄**) reveals a decrease in rate compared to **2.1** and **2.4** (Table 5.5). At ca. 81 °C, the $k_{\text{H}}/k_{\text{D}}$ values for decompositions of **2.1/2.1-*d*₄** and **2.4/2.4-*d*₄** in THF are 2.86 and 2.50, respectively, indicating that an $\alpha\text{-C-H(D)}$ bond is being broken in the transition state of the rate-determining step. These isotope effects are smaller than values of

3–5,^{5a,21} which are generally observed for simple intramolecular α -hydrogen abstraction reactions. They are, however, similar in magnitude to those reported for the thermal decompositions of $\text{Cp}^*\text{Ti}(\text{CH}_3)_2$ ($k_{\text{H}}/k_{\text{D}} = 2.92(10)$ at 110°C)¹⁸ and $\text{Ta}(\text{CH}_2\text{CMe}_3)_5$ ($k_{\text{H}}/k_{\text{D}} = 2.7$ at 60°C).²² A common feature of $\text{Cp}^*\text{Ti}(\text{CH}_3)_2$ and $\text{Ta}(\text{CH}_2\text{CMe}_3)_5$ is that when deuterium is substituted for hydrogen in the α -position of the alkyl groups, they undergo alkane elimination not only by α -deuterium abstraction but also by ring metallation and γ -hydrogen abstraction, respectively. The slightly reduced $k_{\text{H}}/k_{\text{D}}$ values observed in these reactions therefore can be ascribed to the lack of kinetic contributions from these side reactions.

In contrast to $\text{Cp}^*\text{Ti}(\text{CD}_3)_2$ and $\text{Ta}(\text{CD}_2\text{CMe}_3)_5$, abstraction of a γ -hydrogen or a hydrogen from a Cp or Cp^* ring is not observed in the thermal decompositions of $\text{CpW}(\text{NO})(\text{CD}_2\text{CMe}_3)_2$ (**2.1-*d*₄**) and $\text{Cp}^*\text{W}(\text{NO})(\text{CD}_2\text{CMe}_3)_2$ (**2.4-*d*₄**) (see above). Instead, thermolyses of these tungsten complexes show that H/D exchange between the α - and γ -positions of the neopentyl ligands, leading to formation of $\text{Cp}'\text{W}(\text{NO})(\text{CDH}\text{CMe}_3)[\text{CH}_2\text{CMe}_2(\text{CD}_3)]$, occurs competitively with loss of neopentane-*d*₃ from the starting compounds. The origin of the normal but relatively small isotope effects observed in the decomposition of $\text{Cp}'\text{W}(\text{NO})(\text{CD}_2\text{CMe}_3)_2$ therefore is due to the kinetic contribution from loss of neopentane from $\text{Cp}'\text{W}(\text{NO})(\text{CD}_2\text{CMe}_3)_2$ and $\text{Cp}'\text{W}(\text{NO})(\text{CDH}\text{CMe}_3)[\text{CH}_2\text{CMe}_2(\text{CD}_3)]$. Since the latter species can only undergo α -C–H bond cleavage, the overall deuterium isotope effect is diluted by its decomposition.

Table 5.5. Rate Constants for Thermolyses of **2.1-*d*₄** and **2.4-*d*₄** in the Presence of Excess PMe_3

compd ^a	solvent	temp ($^\circ\text{C}$) ^b	k_{obs} (s^{-1}) ^c	$k_{\text{H}}/k_{\text{D}}$
2.1-<i>d</i>₄	THF	81.5	$2.00(4) \times 10^{-4}$	2.86(6)
2.4-<i>d</i>₄	THF	81.5	$8.64(24) \times 10^{-5}$	2.50(8)
2.4-<i>d</i>₄	cyclohexane	91.0	$1.92(3) \times 10^{-4}$	2.39(5)

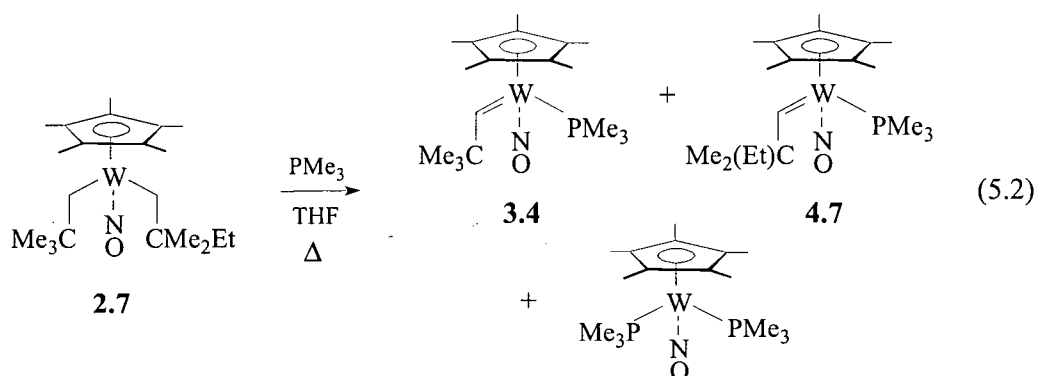
^a[Organometallic] $\sim 5.2 \times 10^{-4}$ M. ^bError $\sim 1^\circ\text{C}$. ^cObtained from duplicate runs; errors were calculated according to $[\sum(s_i/k_i)^2]^{1/2}(k_{\text{H}}/k_{\text{D}})$, where s_i is the standard deviation of k_i .

5.3.4 Thermolyses of Other Cp'W(NO)(R)(R') Complexes: Qualitative Observations

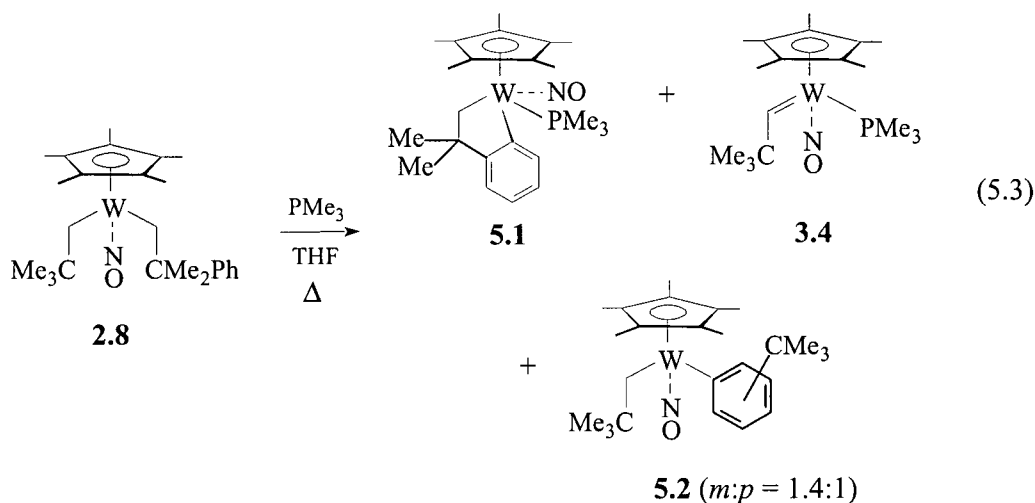
In the preceding chapters it was shown that the benzyl neopentyl complexes, $\text{Cp}^*\text{W}(\text{NO})(\text{CH}_2\text{CMe}_3)(\text{CH}_2\text{Ar})$ ($\text{Ar} = \text{Ph}, \text{C}_6\text{H}_4\text{-}o\text{-Me}, \text{C}_6\text{H}_4\text{-}m\text{-Me}, \text{C}_6\text{H}_4\text{-}p\text{-Me}$) also decompose by α -hydrogen abstraction to give neopentane. Significantly, it was found that while the benzyl, *m*-methylbenzyl, and *p*-methylbenzyl complexes decompose cleanly and readily at a rate that is comparable to that of **2.4** (i.e., 1.5–2 d at 70 °C), the *o*-methylbenzyl complex decomposes partially (<20%) and rather messily under similar conditions. Two features of these results are significant. First, although the neopentyl but not the benzyl ligand is involved in α -agostic bonding (see Chapter 2), α -hydrogen abstraction from a benzyl ligand is more facile than α -hydrogen abstraction from a neopentyl ligand. This selectivity presumably is driven by the breaking of a relatively weak W–neopentyl bond and the formation of a strong $\text{W}=\text{C}(\text{H})\text{Ar}$ bond. Second, even when the benzyl methylene hydrogens are hindered by *o*-methyl substitution, α -hydrogen abstraction from the neopentyl ligand does not take place. This result suggests that the presence of an α -agostic interaction in the ground state structure is *not* a prerequisite for the cleavage of an α -C–H bond.

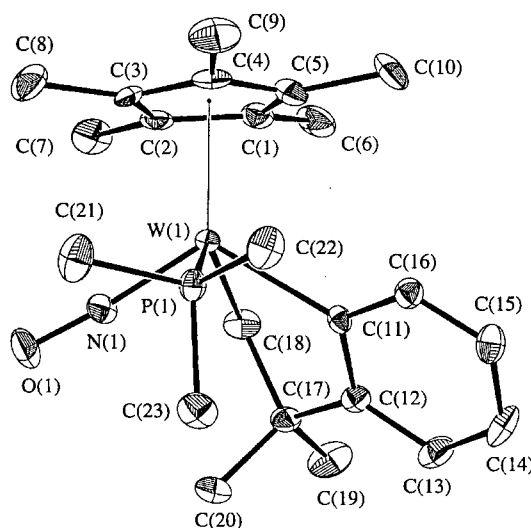
To gain additional insight into the structural features which determine the thermal reactivity of other $\text{Cp}^*\text{W}(\text{NO})(\text{R})(\text{R}')$ complexes, the thermolyses of the bis(alkyl) and alkyl aryl complexes $\text{Cp}^*\text{W}(\text{NO})(\text{CH}_2\text{CMe}_3)(\text{CH}_2\text{CMe}_2\text{Et})$ (**2.7**) (described in detail in Chapter 4), $\text{Cp}^*\text{W}(\text{NO})(\text{CH}_2\text{CMe}_3)(\text{CH}_2\text{CMe}_2\text{Ph})$ (**2.8**), $\text{Cp}^*\text{W}(\text{NO})(\text{CHDCMe}_3)[\text{CD}_2\text{Si}(\text{CD}_3)_3]$ (**2.9-d₁₂**), $\text{Cp}^*\text{W}(\text{NO})(\text{CH}_2\text{CMe}_3)(\text{CH}_3)$ (**2.10**), and $\text{Cp}^*\text{W}(\text{NO})(\text{CH}_2\text{CMe}_3)(\text{C}_6\text{D}_5)$ (**2.11-d₅**) were carried out. Qualitatively **2.7** and **2.8** decompose at a rate comparable to that observed for **2.4**, whereas the sterically less bulky **2.9-d₁₂**, **2.10**, and **2.11-d₅** are significantly more stable.

As noted in Chapter 4, thermolysis of **2.7** in THF in the presence of excess PMe_3 at 70–75 °C for 1.5 d produces a mixture containing as the major (and only identified) products $\text{Cp}^*\text{W}(\text{NO})(=\text{CHCMe}_3)(\text{PMe}_3)$ (**3.4**) and $\text{Cp}^*\text{W}(\text{NO})(=\text{CHCMe}_2\text{Et})(\text{PMe}_3)$ (**4.7**) in a ratio of ~1:1, and $\text{Cp}^*\text{W}(\text{NO})(\text{PMe}_3)_2$, whose mechanism of formation is not yet known (eq 5.2). Under similar reaction conditions, thermolysis of the neophyl neopentyl complex **2.8** at 75 °C



overnight in the presence of excess PMe_3 results in the formation of a yellow-orange mixture containing the ortho-metalated complex $\text{Cp}^*\text{W}(\text{NO})(\text{CH}_2\text{CMe}_2\text{-}o\text{-C}_6\text{H}_4)(\text{PMe}_3)$ (**5.1**) as the major product (eq 5.3). The minor products, formed in trace amounts and identified on the basis of their ^1H NMR spectral data, are **3.4** and a 1.4:1 mixture of *m*- and *p*- $\text{Cp}^*\text{W}(\text{NO})(\text{CH}_2\text{CMe}_3)(\text{C}_6\text{H}_4\text{CMe}_3)$ (**5.2**). Complex **5.1** was isolated as yellow-orange blocks in 30% yield. Its structure was confirmed by X-ray diffraction. As shown in Figure 5.4, the ORTEP diagram of **5.1** clearly shows that the phenyl ring is orthometalated. The $\text{W}(1)\text{-C}(18)$ and $\text{W}(1)\text{-C}(11)$ bond lengths are 2.244(5) and 2.236(4) Å, respectively, and are slightly longer than those in previously characterized $\text{CpW}(\text{NO})(\text{CH}_2\text{CMe}_2\text{-}o\text{-C}_6\text{H}_4)(\text{NCMe})$ (2.232(8) and 2.201(8) Å).²³ In addition, the PMe_3 is coordinated cis to the $\text{W-C}(\text{sp}^2)$ bond, and not cis to the $\text{W-C}(\text{sp}^3)$ bond as observed for the NCMe ligand in the Cp compound.

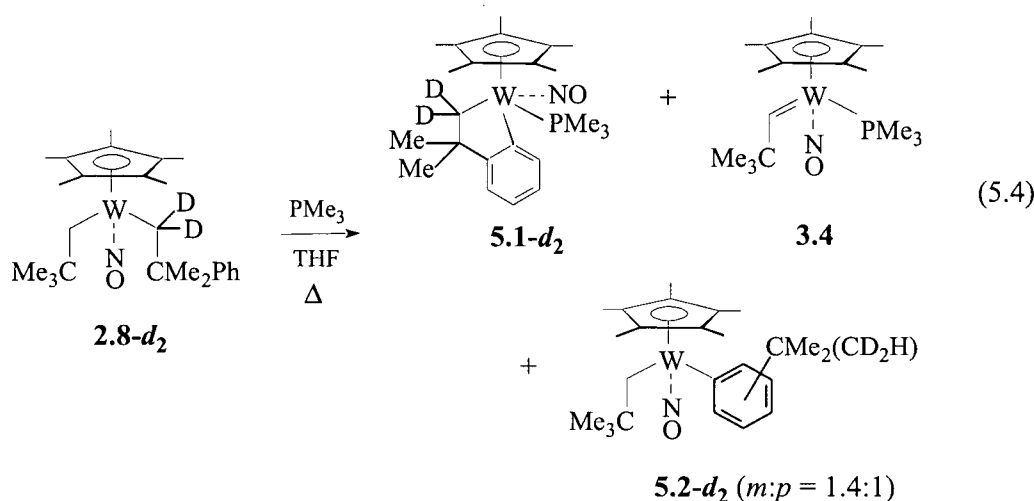




W(1)–N(1)	1.793(4)
W(1)–P(1)	2.5089(11)
W(1)–C(18)	2.244(5)
W(1)–C(11)	2.236(4)
N(1)–O(1)	1.216(5)
C(17)–C(18)	1.539(7)
C(11)–C(12)	1.498(7)
W(1)–N(1)–O(1)	174.6(4)
N(1)–W(1)–C(11)	115.74(19)
N(1)–W(1)–C(18)	84.47(19)
N(1)–W(1)–P(1)	77.30(13)
C(17)–C(18)–W(1)	112.8(3)

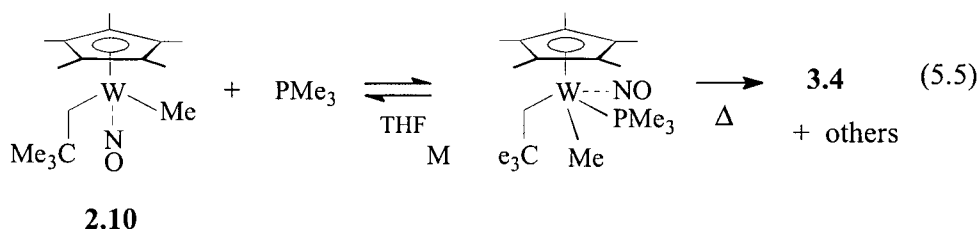
Figure 5.4. ORTEP diagram and selected bond distances and angles of complex $\text{Cp}^*\text{W}(\text{NO})(\text{CH}_2\text{CMe}_2\text{-}o\text{-C}_6\text{H}_4)(\text{PMe}_3)$ (**5.1**).

To determine whether **5.1** is formed by δ -hydrogen abstraction in unobserved intermediate, $[\text{Cp}^*\text{W}(\text{NO})(=\text{CHCMe}_2\text{Ph})]$, the α -deuterated complex $\text{Cp}^*\text{W}(\text{NO})(\text{CH}_2\text{CMe}_3)(\text{CD}_2\text{CMe}_2\text{Ph})$ (**2.8-d₂**) was prepared and its thermal reactivity examined. The thermolysis of **2.8-d₂** was carried out in THF in the presence of excess PMe_3 and afforded a mixture containing **3.4**, **5.1-d₂**, and **5.2-d₂** in yields similar to those observed in the reaction of **2.8** (eq 5.4). Complex **5.2-d₂** was isolated in >90% purity by chromatography on alumina I and characterized by ^1H and $^2\text{H}\{^1\text{H}\}$ NMR spectroscopies. Complex **5.1-d₂** was isolated by crystallization from Et_2O and characterized by mass spectrometry and by ^1H , $^2\text{H}\{^1\text{H}\}$, and $^{13}\text{C}\{^1\text{H}\}$ NMR spectroscopies. Key to the identification of **5.1-d₂** is the absence of methylene resonances in its ^1H and ^{13}C NMR spectra and the presence of a peak (m/z 559) corresponding to the molecular ion in its EI mass spectrum. This demonstrates that **5.1-d₂** is formed as a result of metalation at the δ -position of the neophyl ligand, followed by coordination of PMe_3 , and that α -hydrogen abstraction from CH_2CMe_3 and δ -hydrogen abstraction from $\text{CH}_2\text{CMe}_2\text{Ph}$ are competitive processes in the thermal decomposition of **2.8**. The observation that δ -hydrogen abstraction from a neophyl ligand is preferred over α -hydrogen



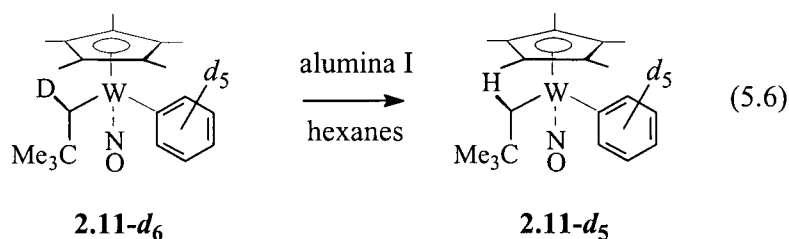
abstraction is not without precedent. The thermal decompositions of $(\text{dppe})\text{Pt}(\text{CH}_2\text{CMe}_2\text{Ph})_2$ ²⁴ and $\text{CpV}(\text{CH}_2\text{CMe}_2\text{Ph})_2(\text{PMe}_3)$,²⁵ for example, have been shown to cyclometalate exclusively through δ -H activation. In the case of **2.8**, δ -H activation is preferred even though both alkyl ligands are involved in α -agostic bonding with the metal (see Chapter 2). This kinetic preference presumably is driven by the formation of a strong M–C(aryl) bond.

In contrast to the above bis(alkyls), $\text{Cp}^*\text{W}(\text{NO})(\text{CHDCMe}_3)[\text{CD}_2\text{Si}(\text{CD}_3)_3]$ (**2.9-*d*₁₂**) shows no evidence of decomposition or H/D scrambling analogous to that observed for **2.4-*d*₄** after a sample was heated in neat Me_4Si at $\sim 70^\circ\text{C}$ for 2 d. In the case of $\text{Cp}^*\text{W}(\text{NO})(\text{CH}_2\text{CMe}_3)(\text{CH}_3)$ (**2.10**), it reacts instantaneously with PMe_3 in either C_6D_6 or THF at ambient temperature to give a yellow solution whose ^1H NMR spectrum is consistent with the formation of $\text{Cp}^*\text{W}(\text{NO})(\text{CH}_2\text{CMe}_3)(\text{CH}_3)(\text{PMe}_3)$ as an equilibrium mixture (eq 5.5). Only one isomer of $\text{Cp}^*\text{W}(\text{NO})(\text{CH}_2\text{CMe}_3)(\text{CH}_3)(\text{PMe}_3)$ is formed, namely that in which the PMe_3 is cis to the methyl and nitrosyl ligands, according to NOE difference data. Like **2.9-*d*₁₂**, both **2.10** and its PMe_3 adduct are fairly stable thermally. They decompose partially in THF at $\sim 85^\circ\text{C}$ for 3 d to give traces of $\text{Cp}^*\text{W}(\text{NO})(=\text{CHCMe}_3)(\text{PMe}_3)$ (**3.4**) and unidentified products. Although the methyldiene complex $\text{Cp}^*\text{W}(\text{NO})(=\text{CH}_2)(\text{PMe}_3)$ was not apparent in the ^1H NMR spectrum of the crude reaction mixture, it is possible that $[\text{Cp}^*\text{W}(\text{NO})(=\text{CH}_2)]$ was also generated but that this species was too reactive to be trapped by PMe_3 . Thus it appears that while α -abstraction of



alkane occurs readily in **2.4**, **2.7**, **2.8**, and certain neopentyl benzyl derivatives, this process is at best sluggish for **2.9-*d*₁₂** and **2.10** under similar experimental conditions. While it can be argued that loss of tetramethylsilane from **2.9-*d*₁₂** or methane from **2.10** is highly unfavorable because it would involve the breaking of fairly strong M-CD₂Si(CD₃)₃ and M-CH₃ bonds,²⁶ the reason why these complexes do not undergo facile loss of neopentane as observed for Cp*W(NO)(CH₂CMe₃)(CH₂Ar) is at present unclear.

Finally, in the above section it was shown that thermolysis of **2.4** in C₆D₆ at 70 °C results in the formation of Cp*W(NO)(CHDCMe₃)(C₆D₅) (**2.11-*d*₆**). To determine whether benzene is activated reversibly, the thermolysis of isotopically labeled Cp*W(NO)(CH₂CMe₃)(Ph-*d*₅) (**2.11-*d*₅**) was investigated. This compound was prepared as shown in eq 5.6 by taking advantage of the acidic nature of the agostic C-D bond. The thermolysis of **2.11-*d*₅** was carried out in neat C₆D₆ and monitored periodically by ¹H NMR spectroscopy at 70 °C. Throughout the course of the thermolysis (~10 h), slow decomposition was evidenced by the appearance minor peaks in the Cp* region. Arene exchange and H/D exchange between the neopentyl and phenyl ligands, however, were not observed. This result demonstrates that **2.11-*d*₅** does not decompose by an α-hydrogen abstraction pathway, presumably because this would require the breaking of the strong M-C(aryl) bond. To gain additional insight into the thermal decomposition of **2.11**, the thermolysis of **2.4** in C₆D₆ was carried out at 70-75 °C for 3 d. The organic volatiles were then analyzed by GC/MS, which indicated the presence of neopentane-*d*₀, -*d*₁, and *d*₂ in approximately 81%, 11%, and 7% yields, respectively. The formation of neopentane-*d*₁ and -*d*₂ strongly suggests that Cp*W(NO)(CHDCMe₃)(Ph-*d*₅) (**2.11-*d*₆**) decomposes by two competitive pathways, namely ring metalation and β-hydrogen abstraction.



5.4 Conclusions

The thermal decompositions of the bis(neopentyl) complexes $\text{Cp}'\text{W}(\text{NO})(\text{CH}_2\text{CMe}_3)_2$ have been shown to proceed by a reversible, rate-determining formation of a neopentane σ -complex, $[\text{Cp}'\text{W}(\text{NO})(=\text{CHCMe}_3)(\eta^2\text{-H-CH}_2\text{CMe}_3)]$, in which the metal can coordinate interchangeably to the α - and γ -C-H bonds of the neopentane molecule. Concurrently, neopentane dissociates irreversibly from the metal center to give the 16-electron intermediate, $[\text{Cp}'\text{W}(\text{NO})(=\text{CHCMe}_3)]$, which can coordinate to another hydrocarbon or to a Lewis base such as PMe_3 .

Comparison of the relative rates and products of the thermal decompositions of **2.7**, **2.8**, **2.9- d_{12}** , **2.10** and **2.11- d_5** with those of **2.4** and the benzyl neopentyl complexes $\text{Cp}^*\text{W}(\text{NO})(\text{CH}_2\text{CMe}_3)(\text{CH}_2\text{Ar})$ demonstrates that (1) **2.4** and the benzyl neopentyl complexes are unstable with respect to neopentane loss by α -hydrogen abstraction, (2) **2.7** and **2.8** decompose at a rate comparable to that of **2.4** but give several products as a result of competitive α -hydrogen abstraction from CH_2CMe_3 and $\text{CH}_2\text{CMe}_2\text{Et}$ and competitive α -hydrogen abstraction from CH_2CMe_3 and δ -hydrogen abstraction from $\text{CH}_2\text{CMe}_2\text{Ph}$, and (3) **2.9- d_{12}** , **2.10**, and **2.11- d_5** are thermally robust; thermolysis of **2.10** and **2.11- d_5** at extended times demonstrates that α -hydrogen abstraction resulting in loss of neopentane is a very minor reaction at best.

5.5 References and Notes

- (1) (a) Schrock, R. R. In *Reactions of Coordinated Ligands*; Braterman, P. S.; Ed.; Plenum: New York, 1986; Vol. 1, pp 221–223. (b) Feldman, J.; Schrock, R. R. *Prog. Inorg. Chem.* **1991**, *39*, 1. (c) LaPointe, A. M.; Schrock, R. R.; Davis, W. M. *J. Am. Chem. Soc.* **1995**, *117*, 4802.
- (2) Luecke, H. F.; Arndtsen, B. A.; Burger, P.; Bergman, R. G. *J. Am. Chem. Soc.* **1996**, *118*, 2517.
- (3) For examples, see: (a) Schrock, R. R. *J. Am. Chem. Soc.* **1975**, *97*, 6577. (b) Schrock, R. R.; Sharp, P. R. *J. Am. Chem. Soc.* **1978**, *100*, 2389. (c) Schrock, R. R.; Messerle, L. W.; Wood, C. D.; Guggenberger, L. J. *J. Am. Chem. Soc.* **1978**, *100*, 3793. (d) Kiel, W. A.; Lin, G.-Y.; Constable, A. G.; McCormick, F. B.; Strouse, C. E.; Eisenstein, O.; Gladysz, J. A. *J. Am. Chem. Soc.* **1982**, *104*, 4865. (e) Kiel, W. A.; Lin, G.-Y.; Bodner, G. S.; Gladysz, J. A. *J. Am. Chem. Soc.* **1983**, *105*, 4958.
- (4) For examples, see: (a) Cooper, N. J.; Green, M. L. H. *J. Chem. Soc., Dalton Trans.* **1979**, 1121. (b) Fellmann, J. D.; Turner, H. W.; Schrock, R. R. *J. Am. Chem. Soc.* **1980**, *102*, 6608. (c) Fellmann, J. D.; Schrock, R. R.; Traficante, D. D. *Organometallics* **1982**, *1*, 481. (d) Turner, H. W.; Schrock, R. R.; Fellmann, J. D.; Holmes, S. J. *J. Am. Chem. Soc.* **1983**, *105*, 4942. (e) Parkin, G.; van Asselt, A.; Leahy, D. J.; Whinnery, L.; Hua, N. G.; Quan, R. W.; Henling, L. M.; Schaefer, W. P.; Santarsiero, B. D.; Bercaw, J. E. *Inorg. Chem.* **1992**, *31*, 82. (f) Schrock, R. R.; Shih, K.-Y.; Dobbs, D. A.; Davis, W. M. *J. Am. Chem. Soc.* **1995**, *117*, 6609. (g) Schrock, R. R.; Seidel, S. W.; Mösch-Zanetti, N. C.; Shih, K.-Y.; O'Donoghue, M. B.; Davis, W. M.; Reiff, W. M. *J. Am. Chem. Soc.* **1997**, *119*, 11876. (h) Schrock, R. R.; Seidel, S. W.; Mösch-Zanetti, N. C.; Dobbs, D. A.; Shih, K.-Y.; Davis, W. M. *Organometallics* **1997**, *16*, 5195.
- (5) For examples, see: (a) Caulton, K. G.; Chisholm, M. H.; Streib, W. E.; Ziling, X. *J. Am. Chem. Soc.* **1991**, *113*, 6082. (b) References 1a and 1b.
- (6) Legzdins, P.; Sayers, S. F. *Chem. Eur. J.* **1997**, *3*, 1579.

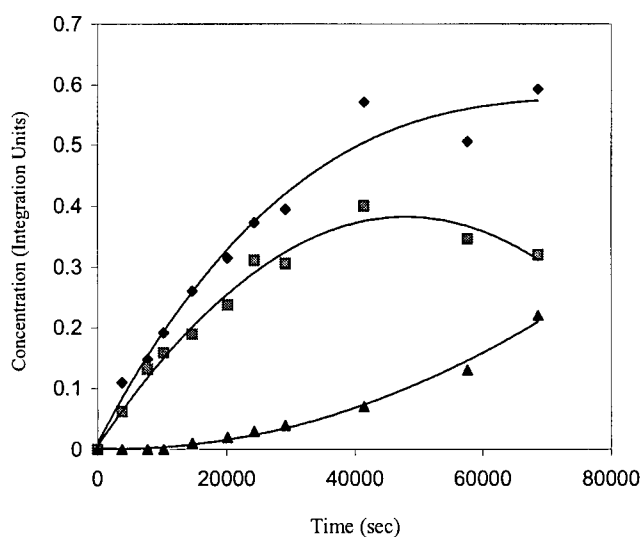
- (7) Sharp, P. R.; Astruc, D.; Schrock, R. R. *J. Organomet. Chem.* **1979**, 182, 477.
- (8) Tran, E.; Legzdins, P. *J. Am. Chem. Soc.* **1997**, 119, 5071.
- (9) Jones, W. D.; Hessell, E. T. *J. Am. Chem. Soc.* **1993**, 115, 554.
- (10) (a) McNamara, B. K.; Yeston, J. S.; Bergman, R. G.; Moore, C. B. *J. Am. Chem. Soc.* **1999**, 121, 6437.
- (11) Brown, C. E.; Ishikawa, Y.; Hackett, P. A.; Rayner, D. M. *J. Am. Chem. Soc.* **1990**, 112, 2530.
- (12) (a) Chatt, J.; Davidson, J. M. *J. Chem. Soc.* **1965**, 843. (b) Hodges, R. J.; Garnett, J. L. *J. Phys. Chem.* **1968**, 72, 1969.
- (13) (a) Graham, M. A.; Perutz, R. N.; Poliakoff, M.; Turner, J. J. *J. Organomet. Chem.* **1972**, 34, C34. (b) Perutz, R. N.; Turner, J. J. *J. Am. Chem. Soc.* **1975**, 97, 4791. (c) Hall, C.; Perutz, R. *Chem. Rev.* **1996**, 96, 3125. (d) Sun, X.-Z.; Grills, D. C.; Nikiforov, S. M.; Poliakoff, M.; George, M. W. *J. Am. Chem. Soc.* **1997**, 119, 7521. (e) Evans, D. R.; Drovetskaya, T.; Bau, R.; Reed, C. A.; Boyd, P. D. W. *J. Am. Chem. Soc.* **1997**, 119, 3633. (f) Geftakis, S.; Ball, G. E. *J. Am. Chem. Soc.* **1998**, 120, 9953.
- (14) (a) Buchanan, J. M.; Stryker, J. M.; Bergman, R. G. *J. Am. Chem. Soc.* **1986**, 108, 1537. (b) Jones, W. D.; Feher, F. J. *J. Am. Chem. Soc.* **1986**, 108, 4814. (c) Periana, R. A.; Bergman, R. G. *J. Am. Chem. Soc.* **1986**, 108, 7332. (d) McGhee, W. D.; Bergman, R. G. *J. Am. Chem. Soc.* **1988**, 110, 4226. (e) Bullock, R. M.; Headford, C. E. L.; Hennessy, K. M.; Kegley, S. E.; Norton, J. R. *J. Am. Chem. Soc.* **1989**, 111, 3897. (f) Parkin, G.; Bercaw, J. E. *Organometallics* **1989**, 8, 1172. (g) Gould, G. L.; Heinekey, D. M. *J. Am. Chem. Soc.* **1989**, 111, 5502. (h) Wang, C.; Ziller, J. W.; Flood, T. C. *J. Am. Chem. Soc.* **1995**, 117, 1647. (i) Stahl, S. S.; Labinger, J. A.; Bercaw, J. E. *J. Am. Chem. Soc.* **1996**, 118, 5961. (j) Schafer, D. F.; Wolczanski, P. T. *J. Am. Chem. Soc.* **1998**, 120, 4881. (k) Gross, C. L.; Girolami, G. S. *J. Am. Chem. Soc.* **1998**, 120, 6605.

- (l) Mobley, T. A.; Schade, C.; Bergman, R. G. *Organometallics* **1998**, *17*, 3574. (m) Wick, D. D.; Reynolds, K. A.; Jones, W. D. *J. Am. Chem. Soc.* **1999**, *121*, 3974.
- (15) Jones, W. D.; Feher, F. J. *J. Am. Chem. Soc.* **1984**, *106*, 1650.
- (16) This reaction was reported previously by former group member, K. J. Ross. The product, $\text{Cp}^*\text{W}(\text{NO})(\text{CHDCMe}_3)(\text{C}_6\text{D}_5)$, was fully characterized by ^1H and ^2H NMR spectroscopies, but no minor products were suggested. Ross, K. J. Ph.D. Dissertation, University of British Columbia, 1994.
- (17) Legzdins, P.; Veltheer, J. E.; Young, M. A. *Organometallics* **1995**, *14*, 407.
- (18) Wood, C. D.; McLain, S. J.; Schrock, R. R. *J. Am. Chem. Soc.* **1979**, *101*, 3210.
- (19) McDade, C.; Green, J. C.; Bercaw, J. E. *Organometallics* **1982**, *1*, 1629.
- (20) Bulls, A. R.; Schaefer, W. P.; Serfas, M.; Bercaw, J. E. *Organometallics* **1987**, *6*, 1219.
- (21) (a) Cheon, J.; Rogers, D. M.; Girolami, G. S. *J. Am. Chem. Soc.* **1997**, *119*, 6804. (b) Ajou, J. A. N.; Rice, G. L.; Scott, S. L. *J. Am. Chem. Soc.* **1998**, *120*, 13436.
- (22) Schrock, R. R.; Fellmann, J. D. *J. Am. Chem. Soc.* **1978**, *100*, 3359.
- (23) Brunet, N.; Debad, J. D.; Legzdins, P.; Trotter, J.; Veltheer, J. E.; Yee, V. C. *Organometallics* **1993**, *12*, 4572.
- (24) Ankianiec, B. C.; Hardy, D. T.; Thomson, S. K.; Watkins, W. N.; Young, G. B. *Organometallics* **1992**, *11*, 2591.
- (25) Hessen, B.; Buijink, J. K. F.; Meetsa, A.; Teuben, J. H.; Helgesson, G.; Håkansson, M.; Jagner, S.; Spek, A. L. *Organometallics* **1993**, *12*, 2268.
- (26) Bruno, J. W.; Marks, T. J.; Morss, L. R. *J. Am. Chem. Soc.* **1983**, *105*, 6824.

APPENDIX

Table A1. Selected IR Spectral Data for Complexes **2.1–2.11**^a

cmpd	R	R'	Nujol		KBr	
			ν_{NO}	$\nu_{\text{C}\alpha\text{H}}$	ν_{NO}	$\nu_{\text{C}\alpha\text{H}}$
2.1	CH ₂ CMe ₃	CH ₂ CMe ₃	1558 (s)		1555 (s)	
2.2	CH ₂ CMe ₂ Ph	CH ₂ CMe ₂ Ph	1554 (s)	2690, 2719 (br)	1560 (s)	2690, 2719 (br)
2.3	CH ₂ SiMe ₃	CH ₂ SiMe ₃	1596 (s)		<i>c</i>	
2.4	CH ₂ CMe ₃	CH ₂ CMe ₃	1551 (s)		1551 (s)	
2.5	CH ₂ CMe ₂ Ph	CH ₂ CMe ₂ Ph	1547 (s)	2478 (sh w)	1551 (s)	2478 (sh w)
2.6	CH ₂ SiMe ₃	CH ₂ SiMe ₃	1549 (s)		<i>c</i>	
2.7	CH ₂ CMe ₃	CH ₂ CMe ₂ Et	1576 (s)		1554 (s)	
2.8	CH ₂ CMe ₃	CH ₂ CMe ₂ Ph	1574 (s)		1557 (s)	
2.9	CH ₂ CMe ₃	CH ₂ SiMe ₃	1553 (s)		1552 (s)	
2.10	CH ₂ CMe ₃	CH ₃	1587 (s)		1551 (s)	
2.11	CH ₂ CMe ₃	Ph	1547 (s)	2529 (br w)	1551 (s)	

^a ν in cm⁻¹. ^bNot observed. ^cNot determined.**Figure A1.** Plot of the kinetic data for the products of the thermolysis of **2.4** in neoheptane in the presence of excess PMe₃: Cp*W(NO)(=CHCMe₃)(PMe₃) (**3.4**) = ♦; Cp*W(NO)(*syn*-neoheptene)(PMe₃) (**4.4_{syn}**) = ■; Cp*W(NO)(*anti*-neoheptene)(PMe₃) (**4.4_{anti}**) = ▲.

Since $k_{4.4\text{syn}} = k_{3.4}$, $k_{4.4\text{anti}}$ can be calculated according to the equation: $t_{4.4\text{syn}}^{\text{max}} = [1/(k_{4.4\text{syn}} - k_{4.4\text{anti}})] \ln(k_{4.4\text{syn}}/k_{4.4\text{anti}})$, where $t_{4.4\text{syn}}^{\text{max}}$ is the time at which $[4.4_{\text{syn}}]$ reaches its maximum value.

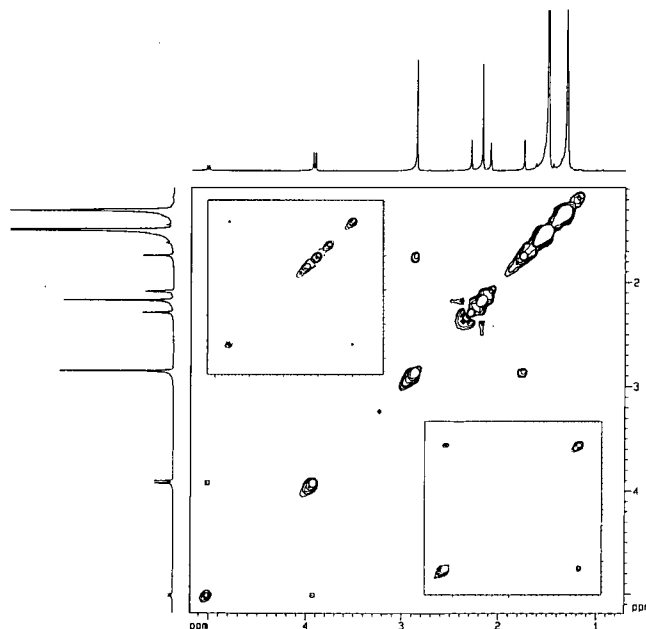


Figure A2. ^1H - ^1H EXSY spectrum of $\text{Cp}^*\text{W}(\text{NO})(\text{CH}_2\text{CMe}_3)(\text{C}_6\text{H}_3\text{-2,5-Me}_2)$ (**2.11'**) in toluene- d_8 at $-50\text{ }^\circ\text{C}$.

GC-MS Analysis of Neopentane- d_x : Neopentane does not give a molecular ion on electron impact; the base peak is $[\text{M} - \text{methyl}]^+$ (i.e., C_4H_9 , m/z 57). Assuming that (a) neopentane- d_3 is solely $(\text{CH}_3)_3\text{C}(\text{CD}_3)$, neopentane- d_2 is solely $(\text{CH}_3)_3\text{C}(\text{CD}_2\text{H})$, etc., (b) there are no isotope effects for methyl- and hydrogen-losses, and (c) the highest mass peak in the ^{13}C corrected data corresponds to the amount of that isotope, the isotopic distribution in the neopentanes produced from thermolyses of **2.1- d_4** , **2.4- d_4** , and **2.11- d_6** can be calculated by subtracting the appropriate theoretical amount from all the lower mass peak totals; three such operations would give the amounts of neopentane- d_3 , - d_2 , and - d_1 . The amount remaining in the m/z 57 column is due to neopentane- d_0 ; however, this must be normalized by multiplying by 0.75 since an m/z 57 fragment is generated 4 times out of 4 but neopentane- d_1 , - d_2 , or - d_3 gives m/z 58, 59, and 60

fragments, respectively, only 3 times out of 4. See, Schrock, R. R.; Fellmann, J. D. *J. Am. Chem. Soc.* **1978**, *100*, 3359.

Table A2. *tert*-Butyl Ions in the Mass Spectra of Neopentanes

m/z^a	57	58	59	60
2.1-d₄ /THF/PMe ₃	45.07	25.96	8.62	100.00
2.4-d₄ /THF/PMe ₃	37.73	28.52	7.74	100.00
2.4-d₄ /PMe ₃	32.63	14.91	5.85	100.00
2.11-d₆ /C ₆ D ₆	100.00	~9.60	~6.58	0
Neopentane-d ₀ ^b	100.00	0.13		
Neopentane-d ₁ ^b	35.07	100.00		
Neopentane-d ₂ ^b	34.66	3.29	100.00	
Neopentane-d ₃ ^b	32.66	3.30	2.71	100.00

^aAll corrected for ¹³C. ^bCalculated spectra. Schrock, R. R.; Fellmann, J. D. *J. Am. Chem. Soc.* **1978**, *100*, 3359.

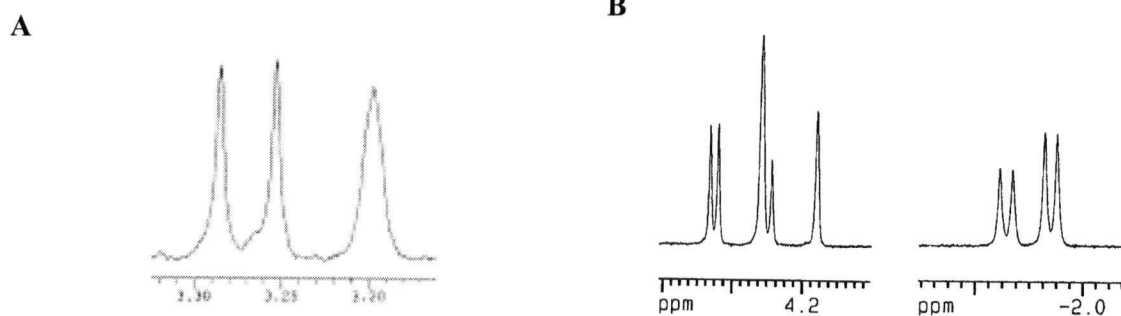


Figure A3. ¹H NMR spectra of the methylene regions of (A) Cp*W(NO)(CH₂CMe₃)[CH₂Si(CH₃)(CD₃)₂] (**2.9-d₆-H**) and Cp*W(NO)(CHDCMe₃)[CD₂Si(CH₃)₂(CD₃)] (**2.9-d₃-D**) [obtained from thermolysis of **2.4** in (CH₃)₂Si(CD₃)₂, $k_H/k_D = 1.35(5)$], and (B) *m*- and *p*-isomers of Cp*W(NO)(CH₂CMe₃)(C₆H₄Me) and Cp*W(NO)(CHDCMe₃)(C₆D₄Me) [obtained from thermolysis of **2.4** in 1:1 toluene/toluene-*d*₈, $k_H/k_D = 1.04(5)$, unpublished].

Table A3. Crystallographic Data for Complexes 2.4-d₄, 2.4, 2.9, 2.11', 2.17, and 3.1

Compound	2.4-d ₄	2.4 (neutron)	2.9	2.11'	2.17	3.1
Empirical formula	C ₂₀ H ₃₃ D ₄ NOW	C ₂₀ H ₃₇ NOW	C ₁₉ H ₃₇ NOSiW	C ₂₃ H ₃₅ NOW	C ₁₇ H ₃₂ N ₂ OW	C ₁₃ H ₂₄ NOPW
Formula weight	495.38	491.38	507.44	525.39	464.30	425.16
Crystal color, habit	red, irregular	red, irregular	red, rod	mauve, plate	orange, needle	orange-brown, irregular
Crystal size (mm ³)	0.30 × 0.10 × 0.06	0.48 × 1.8 × 4.8	0.40 × 0.19 × 0.13	0.02 × 0.25 × 0.35	0.23 × 0.05 × 0.03	0.17 × 0.25 × 0.35
Crystal system	monoclinic	Monoclinic	orthorhombic	monoclinic	orthorhombic	monoclinic
Space group	P2 ₁ /n	P2 ₁ /n	Pnma	P2 ₁ /n (#14)	P2 ₁ 2 ₁ 2 ₁	P2 ₁ /n (#14)
a (Å)	8.9342(2)	8.8644(3)	9.4941(2)	15.1357(14)	8.1536(4)	9.477(3)
b (Å)	21.7953(5)	21.7233(8)	19.1577(3)	14.476(2)	10.4139(6)	13.815(1)
c (Å)	11.3422(1)	11.2865(4)	12.3282(2)	20.9921(6)	22.2664(12)	12.512(3)
β (°)	105.528(1)	105.555(2)	90	103.8596(6)	90	98.04(2)
Z value	4	4	4	8	4	4
D _{calc} (mg/m ³)	1.546	0.768	1.503	1.563	1.631	1.741
F ₀₀₀	984	196	1016	2096	920	824
Diffractionmeter	Siemens SMART Platform CCD	D19 at Institut Laue-Langevin, Grenoble	Siemens SMART Platform CCD	Rigaku ADSC CCD	Siemens SMART Platform CCD	Rigaku AFC6S
Temperature (K)	173(2)	120	173(2)	180(1)	173(2)	294(1)
Reflections collected	10477	4557	20540	37183	14051	331184
Unique reflections	3717	2940 [R _{int} = 0.0465]	3357	10796	3355	2989
Structure solution	direct methods	direct methods	direct methods	Patterson methods	direct methods	Patterson methods
Residuals (all data): R, R _w	0.0997; 0.1046	0.0633; 0.1506	0.0300; 0.0582	0.067; 0.057	0.0284; 0.0445	0.039; 0.036
Goodness of fit on F ²	1.009	1.310	5.973	1.64	0.996	1.39

Table A4. Crystallographic Data for Complexes **3.4**, **3.14**, **3.15**, **3.17**, and **3.21a**

Compound	3.4	3.14	3.15	3.17	3.21a
Empirical formula	C ₁₈ H ₃₄ NOPW	C ₂₁ H ₃₇ NOW	C ₂₀ H ₃₃ NOW	C ₂₂ H ₃₃ NOW	C ₂₀ H ₃₃ NOW
Formula weight	495.28	503.38	487.32	511.34	487.32
Crystal color, habit	yellow, irregular	yellow–orange, plate	orange–yellow, plate	orange-red, block	yellow, block
Crystal size (mm ³)	0.13 × 0.11 × 0.09	0.03 × 0.25 × 0.40	0.22 × 0.20 × 0.04	0.15 × 0.15 × 0.05	0.08 × 0.06 × 0.03
Crystal system	Monoclinic	orthorhombic	triclinic	monoclinic	Monoclinic
Space group	P2 ₁	Pbca (#61)	P1 [−]	P2 ₁ /c	P2 ₁ /n
a (Å)	8.5740(3)	17.0638(6)	8.3212(2)	10.5083(6)	8.8932(5)
b (Å)	13.9660(5)	14.3890(14)	8.4603(1)	14.6572(8)	14.9128(9)
c (Å)	8.9140(3)	17.6135(5)	14.5189(1)	14.1654(8)	14.6821(9)
β (°)	98.804(1)	90	85.809(1)	109.973(1)	101.653(1)
Z value	2	8	2	4	4
D _{calc} (mg/m ³)	1.559	1.546	1.712	1.656	1.697
F ₀₀₀	492	2016	484	1016	968
Diffractometer	Siemens SMART Platform CCD	Rigaku / ADSC CCD	Siemens SMART Platform CCD	Siemens SMART Platform CCD	Siemens SMART Platform CCD
Temperature (K)	173(2)	180(1)	173(2)	173(2)	173(2)
Reflections collected	6896	41411	5403	11588	14279
Unique reflections	3562	6065	3234	3634	3385
Structure solution	Direct methods	Patterson methods	direct methods	direct methods	direct methods
Residuals (all data): R; R _w	0.0499; 0.1202	0.049; 0.053	0.0239; 0.0567	0.0238; 0.0498	0.0570; 0.0831
Goodness of fit on F ²	1.051	1.45	1.041	0.999	1.014

Table A5. Crystallographic Data for Complexes **4.3**, **4.4_{syn}**, **4.7**, **4.9_{endo}**, **4.11_{exo}**, and **5.1**

Compound	4.3	4.4_{syn}	4.7	4.9_{endo}	4.11_{exo}	5.1
Empirical formula	C ₁₉ H ₃₄ NOPW	C ₁₉ H ₃₆ NOPW	C ₁₈ H ₃₀ N ₂ OW	C ₁₇ H ₂₇ NOW	C ₁₈ H ₂₉ NOW	C ₂₃ H ₃₆ NOPW
Formula weight	507.29	509.32	474.30	445.25	459.28	557.35
Crystal color, habit	orange, plate	Yellow, prism	yellow, needle	yellow, plate	yellow, irregular	yellow-orange, irregular
Crystal size (mm ³)	0.50 × 0.35 × 0.02	0.20 × 0.30 × 0.35	0.44 × 0.34 × 0.16	0.28 × 0.20 × 0.20	0.20 × 0.25 × 0.30	0.40 × 0.35 × 0.30
Crystal system	monoclinic	monoclinic	monoclinic	monoclinic	monoclinic	Orthorhombic
Space group	C2/c	P2 ₁ /c (#14)	P2 ₁ /c	P2 ₁ /c	P2 ₁ /n (#14)	P212121 (no. 19)
a (Å)	30.6298(7)	9.0797(8)	15.366(2)	7.5179(2)	8.4943(13)	9.7565(11)
b (Å)	8.2908(2)	16.930(3)	8.123(1)	13.8169(3)	13.8052(12)	14.2763(4)
c (Å)	16.6982(4)	14.4809(5)	17.292(3)	16.1151(4)	14.9389(5)	16.5299(3)
β (°)	108.4520(10)	107.3047(9)	113.34(1)	98.424(1)	95.5851(8)	90
Z value	8	4	4	4	4	4
D _{calc} (mg/m ³)	1.675	1.592	1.590	1.786	1.751	1.608
F ₀₀₀	2016	1016	935.70	872	904	1112
Diffractionmeter	Siemens SMART Platform CCD	Rigaku ADSC CCD	Enraf Nonius CAD4F	Siemens SMART Platform CCD	Rigaku ADSC CCD	Rigaku ADSC CCD
Temperature (K)	173(2)	180(1)	293(1)	173(2)	180(1)	180(2)
Reflections collected	9770	19699	3514	8282	16138	17859
Unique reflections	3514	4959	2526	2905	4516	6213
Structure solution	direct methods	Patterson methods	Patterson methods	direct methods	Patterson methods	Patterson methods
Residuals (all data): R; R _w	0.0713; 0.0862	0.077; 0.084	0.037; 0.046 (2.5σ)	0.0729; 0.1519	0.099; 0.099	0.0350; 0.0583
Goodness of fit on F ²	0.963	1.77	1.20	1.012	1.87	1.137

Table A6. Fractional coordinates and equivalent isotropic displacement parameters for $\text{Cp}^*\text{W}(\text{NO})(\text{CD}_2\text{CMe}_3)_2$ (**2.4-*d*₄**)

	x	y	z		U(eq)
W(1)	7797(1)	1370(1)	6588(1)	27(1)	1
N(1)	5765(10)	1327(4)	6170(7)	38(2)	1
O(1)	4356(8)	1233(4)	5706(7)	53(2)	1
C(1)	8040(12)	2318(5)	6918(9)	42(3)	1
C(2)	6942(11)	2866(4)	6582(8)	38(3)	0.54(3)
C(3)	5199(17)	2690(10)	6230(3)	62(8)	0.54(3)
C(4)	7240(3)	3191(11)	5466 (18)	58(8)	0.54(3)
C(5)	7180(3)	3318(11)	7654(19)	75 (9)	0.54(3)
C(2')	6942(11)	2866(4)	6582(8)	38 (3)	0.46(3)
C(3')	5500(3)	2765(12)	7010(3)	60(10)	0.46(3)
C(4')	6520(4)	2984(14)	5205(14)	66(10)	0.46(3)
C(5')	7810(3)	3438(9)	7250(2)	54(9)	0.46(3)
C(6)	8258(11)	931(5)	8365(8)	30(2)	1
C(7)	7105(10)	768(4)	9041(9)	41(3)	1
C(8)	6009(12)	260(5)	8408(10)	56(3)	1
C(9)	7968(12)	543(5)	10351(9)	54(3)	1
C(10)	6131(12)	1330(5)	9222(10)	48(3)	1
C(11)	7958(12)	767(5)	4948(9)	39(3)	1
C(12)	8492(11)	1369(4)	4736(9)	28(2)	1
C(13)	9893(11)	1477(4)	5627(9)	32(2)	1
C(14)	10245(10)	950(5)	6397(8)	29(2)	1
C(15)	9056(11)	511(4)	5971(9)	31(2)	1
C(16)	6550(12)	434(6)	4144(11)	58(3)	1
C(17)	7716(13)	1747(6)	3628(10)	62(4)	1
C(18)	10957(12)	2018(5)	5698(11)	52(3)	1
C(19)	11682(11)	867(6)	7436(9)	49(3)	1
C(20)	9006(13)	138(5)	6435(11)	52(3)	1

Table A7. Fractional coordinates and equivalent isotropic displacement parameters for $\text{Cp}^*\text{W}(\text{NO})(\text{CH}_2\text{CMe}_3)_2$ (2.4)

	x	y	z	U(eq)
W(1)	7802(3)	1371(1)	6593(2)	22(1)
N(1)	5730(2)	1318(1)	6163(1)	28(1)
O(1)	4337(3)	1225(1)	5703(3)	39(1)
C(1)	8051(3)	2323(1)	6930(2)	34(1)
C(2)	6929(3)	2871(1)	6591(2)	33(1)
C(3)	5143(10)	2680(5)	6266(11)	54(2)
C(4)	7140(12)	3174(4)	5433(10)	51(2)
C(5)	7195(15)	3323(4)	7648(9)	72(3)
C(3')	5544(14)	2776(5)	6962(17)	58(3)
C(4')	6722(32)	2963(12)	5232(21)	84(4)
C(5')	7794(19)	3448(5)	7242(17)	69(3)
C(6)	8302(3)	926(1)	8377(2)	26(1)
C(7)	7088(2)	768(1)	9076(2)	25(1)
C(8)	6010(3)	259(1)	8408(2)	43(1)
C(9)	7960(3)	541(1)	10371(2)	34(1)
C(10)	6110(3)	1328(1)	9223(2)	40(1)
C(11)	7950(3)	764(1)	4936(2)	28(1)
C(12)	8481(3)	1364(1)	4723(2)	26(1)
C(13)	9924(2)	1478(1)	5634(2)	26(1)
C(14)	10274(2)	955(1)	6411(2)	26(1)
C(15)	9074(3)	509(1)	5970(2)	26(1)
C(16)	6565(3)	440(1)	4126(2)	41(1)
C(17)	7708(4)	1755(1)	3637(2)	40(1)
C(18)	10975(3)	2021(1)	5706(3)	38(1)
C(19)	11727(3)	878(1)	7445(2)	36(1)
C(20)	9025(3)	-135(1)	6431(3)	37(1)

Table A8. Fractional coordinates and equivalent isotropic displacement parameters for $\text{Cp}^*\text{W}(\text{NO})(\text{CH}_2\text{CMe}_3)(\text{CH}_2\text{SiMe}_3)$ (**2.9**)

	x	y	z		U(eq)
W(1)	1576(1)	7500	4928(1)	28(1)	1
N(1)	3324(4)	7500	5428(3)	34(1)	1
O(1)	4412(5)	7500	5958(4)	58(1)	1
C(1)	1687(19)	6652(5)	3795(7)	39(2)	0.50
Si(1)	3091(6)	5998(3)	3944(4)	45(1)	0.50
C(2)	4825(22)	6418(16)	3888(20)	76(4)	0.50
C(3)	2936(27)	5389(12)	2800(16)	73(3)	0.50
C(4)	3024(21)	5459(5)	5199(12)	62(2)	0.50
C(1')	1815(19)	6545(5)	4037(7)	39(2)	0.50
C(1'')	3032(20)	6003(10)	3939(14)	45(1)	0.50
C(2')	4479(24)	6350(16)	3691(21)	76(4)	0.50
C(3')	2722(28)	5440(13)	3057(18)	73(3)	0.50
C(4')	3069(21)	5653(5)	5086(13)	62(2)	0.50
C(11)	586(4)	7128(2)	6543(2)	36(1)	1
C(12)	-394(4)	6897(2)	5737(3)	43(1)	1
C(13)	-980(5)	7500	5230(5)	49(1)	1
C(14)	1376(6)	6679(3)	7333(3)	60(1)	1
C(15)	-855(7)	6157(3)	5544(6)	74(2)	1
C(16)	-2092(7)	7500	4353(8)	91(4)	1

Table A9. Fractional coordinates and equivalent isotropic displacement parameters for $\text{Cp}^*\text{W}(\text{NO})(\text{CH}_2\text{CMe}_3)(\text{C}_6\text{H}_3\text{-2,5-Me}_2)$ (**2.11'**)

atom	x	y	z	B_{eq}
W(1)	-0.29851(3)	0.11513(4)	0.20928(2)	1.509(10)
W(2)	0.22121(3)	0.11527(4)	0.28286(2)	1.597(10)
O(1)	-0.2504(6)	-0.0809(6)	0.2474(4)	3.7(2)
O(2)	0.2387(6)	-0.0787(6)	0.2391(4)	3.6(2)
N(1)	-0.2610(6)	0.0018(7)	0.2349(5)	2.2(2)
N(2)	0.2400(7)	0.0040(7)	0.2547(5)	3.3(3)
C(1)	-0.4252(6)	0.1339(8)	0.1147(5)	1.5(2)
C(2)	-0.4421(8)	0.0634(9)	0.1532(6)	2.6(3)
C(3)	-0.4499(7)	0.1041(9)	0.2176(6)	2.2(3)
C(4)	-0.4329(8)	0.2020(8)	0.2112(6)	2.3(3)
C(5)	-0.4207(7)	0.2198(8)	0.1484(5)	1.5(2)
C(6)	-0.4261(8)	0.1265(10)	0.0443(6)	3.5(3)
C(7)	-0.4623(9)	-0.0347(9)	0.1353(7)	3.2(3)
C(8)	-0.4751(9)	0.0568(10)	0.2756(7)	3.8(4)
C(9)	-0.4405(8)	0.2728(8)	0.2654(6)	2.3(3)
C(10)	-0.4076(8)	0.3136(9)	0.1210(6)	2.8(3)
C(11)	-0.2243(7)	0.1379(9)	0.1367(6)	2.0(3)
C(12)	-0.1989(8)	0.0739(9)	0.0923(6)	2.3(3)
C(13)	-0.1480(8)	0.1054(10)	0.0500(6)	2.8(3)
C(14)	-0.1226(8)	0.1969(11)	0.0479(6)	3.0(3)
C(15)	-0.1468(8)	0.2610(9)	0.0900(6)	2.6(3)
C(16)	-0.1978(7)	0.2296(9)	0.1326(5)	1.9(3)
C(17)	-0.2237(10)	-0.0279(9)	0.0909(7)	3.6(4)
C(18)	-0.1202(8)	0.3624(10)	0.0922(6)	3.5(3)

Table A10. Fractional coordinates and equivalent isotropic displacement parameters for $\text{Cp}^*\text{W}(\text{NO})(\text{CH}_2\text{CMe}_3)(\text{NMe}_2)$ (**2.17**)

	x	y	z	U (eq)	SOF
W (1)	7668 (1)	9528 (1)	8843 (1)	18 (1)	1
O (1)	4412 (5)	8430 (4)	9183 (2)	40 (1)	1
N (1)	5741 (5)	8789 (4)	8982 (2)	25 (1)	1
N (2)	8873 (6)	8009 (4)	8613 (2)	26 (1)	1
C (1)	9528 (6)	10124 (5)	9622 (2)	23 (1)	1
C (2)	9811 (6)	11026 (5)	9157 (2)	23 (1)	1
C (3)	8377 (7)	11755 (5)	9084 (2)	26 (1)	1
C (4)	7168 (6)	11317 (5)	9490 (2)	25 (1)	1
C (5)	7873 (6)	10266 (5)	9819 (2)	23 (1)	1
C (6)	10773 (8)	9236 (7)	9904 (3)	35 (2)	1
C (7)	11436 (7)	11300 (7)	8861 (4)	38 (1)	1
C (8)	8253 (10)	12924 (6)	8685 (3)	40 (2)	1
C (9)	5476 (9)	11832 (8)	9575 (4)	45 (2)	1
C (10)	7077 (9)	9571 (8)	10330 (3)	44 (2)	1
C (11)	7085 (6)	10423 (5)	7980 (2)	23 (1)	1
C (12)	6090 (6)	9741 (5)	7489 (2)	23 (1)	1
C (13)	6139 (8)	10551 (8)	6914 (3)	37 (1)	1
C (14)	4295 (7)	9597 (7)	7678 (3)	32 (1)	1
C (15)	6787 (9)	8407 (7)	7339 (3)	36 (2)	1
C (16)	10590 (7)	8082 (7)	8421 (3)	38 (2)	1
C (17)	8338 (11)	6680 (7)	8626 (4)	40 (2)	1

Table A11. Fractional coordinates and equivalent isotropic displacement parameters for $\text{CpW(NO)(=CHCMe}_3\text{)(PMe}_3\text{)}$ (**3.1**)

	x	y	z	U(eq)
W(l)	0.56731(7)	0.35417(4)	0.27778(5)	3.99(1)
P(l)	0.7964(4)	0.3512(3)	0.3905(3)	4.36(9)
O(1)	0.639(1)	0.1799(7)	0.1519(9)	6.0(3)
N(1)	0.611(1)	0.2494(9)	0.2078(9)	40(3)
C(1)	0.572(4)	0.481(2)	0.152(2)	88(8)
C(2)	0.432(4)	0.452(1)	0.151(2)	8.7(7)
C(3)	0.385(3)	0.475(2)	0.246(3)	90(8)
C(4)	0.491(3)	0.518(1)	0.307(2)	69(6)
C(5)	0.607(3)	0.524(1)	0.252(3)	7.5(7)
C(6)	0.469(2)	0.2983(9)	0.388(1)	47(4)
C(7)	0.419(2)	0.199(1)	0.424(1)	5.9(5)
C(8)	0.467(3)	0.194(1)	0.543(2)	11.5(9)
C(9)	0.479(2)	0.115(1)	0.366(2)	71(6)
C(10)	0.259(2)	0.198(1)	0.404(2)	10.0(7)
C(11)	0.804(2)	0.416(1)	0.516(1)	93(6)
C(12)	0.945(2)	0.401(1)	0.334(2)	81(6)
C(13)	0.861(2)	0.234(1)	0.433(2)	79(6)

Table A12. Fractional coordinates and equivalent isotropic displacement parameters for $\text{Cp}^*\text{W}(\text{NO})(=\text{CHCMe}_3)(\text{PMe}_3)$ (**3.4**)

	x	y	z	U(eq)
W(1)	2584(1)	7503(2)	8145(1)	32(1)
N(1)	1248(13)	6735(14)	8898(13)	85(6)
O(1)	95(15)	6260(12)	9063(16)	107(5)
C(1)	1642(9)	7463(13)	5468(9)	49(3)
C(2)	2515(16)	8288(11)	5859(21)	46(4)
C(3)	4155(13)	8009(11)	6336(18)	40(4)
C(4)	4177(13)	6978(11)	6218(21)	39(4)
C(5)	2644(17)	6655(12)	5704(21)	49(5)
C(6)	-104(11)	7399(26)	4811(11)	99(8)
C(7)	2017(30)	9308(12)	5497(18)	110(12)
C(8)	5570(21)	8632(18)	6594(16)	98(12)
C(9)	5657(23)	6403(14)	6610(15)	79(9)
C(10)	2138(32)	5614(14)	5492(25)	133(15)
P(1)	1449(4)	8963(3)	9327(4)	45(1)
C(11)	2630(18)	10022(12)	9594(20)	74(5)
C(12)	-462(19)	9389(16)	8346(19)	86(6)
C(13)	913(17)	8655(13)	11157(14)	68(5)
C(14)	4388(11)	7389(17)	9777(10)	28(4)
C(15)	4914(15)	7008(10)	11253(14)	50(3)
C(16)	3621(18)	6467(11)	11840(16)	62(4)
C(17)	6271(18)	6339(14)	11142(18)	79(5)
C(18)	5533(16)	7784(12)	12495(13)	67(6)

Table A13. Fractional coordinates and equivalent isotropic displacement parameters for $\text{Cp}^*\text{W}(\text{NO})[\text{CH}(\text{CMe}_3)\text{CH}_2(\text{CMe}_3)\text{CH}]$ (**3.14**)

	x	y	z	U(eq)
W(1)	0.201815(11)	0.148487(12)	0.182473(12)	1.283(6)
O(1)	0.2461(3)	0.3412(2)	0.2014(3)	3.27(11)
N(1)	0.0837(3)	0.2588(3)	0.1928(3)	2.02(10)
C(1)	0.0788(3)	0.0797(4)	0.2345(4)	2.74(14)
C(2)	0.0780(3)	0.1790(4)	0.2379(4)	2.92(14)
C(3)	0.0832(3)	0.2117(4)	0.1618(4)	3.10(15)
C(4)	0.0874(3)	0.1357(4)	0.1107(3)	2.15(12)
C(5)	0.0793(4)	0.0537(3)	0.1564(4)	2.41(12)
C(6)	0.0712(5)	0.0139(7)	0.2979(5)	6.8(3)
C(7)	0.0668(4)	0.2380(7)	0.3064(5)	7.6(3)
C(8)	0.0762(5)	0.1856(5)	0.1388(7)	6.9(2)
C(9)	0.0890(4)	0.1396(6)	0.0265(5)	5.8(2)
C(10)	0.3308(4)	0.0436(4)	0.1247(5)	5.2(2)
C(11)	0.2730(3)	0.1227(4)	0.0424(3)	2.17(12)
C(12)	0.3142(4)	0.0854(3)	0.1007(3)	1.44(10)
C(13)	0.2675(3)	0.0511(4)	0.1798(3)	2.36(13)
C(14)	0.3207(3)	0.0707(3)	0.2590(3)	1.32(10)
C(15)	0.3919(4)	0.0980(4)	0.3252(3)	1.93(12)
C(16)	0.3734(4)	0.0470(4)	0.0232(3)	3.12(14)
C(17)	0.2835(4)	0.2105(4)	0.0687(4)	3.29(15)
C(18)	0.2686(4)	0.1458(4)	-0.0294(4)	3.1(2)
C(19)	0.3758(3)	0.1143(4)	0.3947(4)	2.83(14)
C(20)	0.3701(4)	0.0158(4)	0.3428(4)	2.90(14)
C(21)	0.3701(4)	0.1856(5)	0.3105(3)	2.70(14)

Table A14. Fractional coordinates and equivalent isotropic displacement parameters for $\text{Cp}^*\text{W}(\text{NO})(\text{C}_{10}\text{H}_{18})$ (**3.15**)

	x	y	z	U(eq)	SOF
W(1)	5150(1)	2760(1)	2065(1)	17(1)	1
N(1)	6788(5)	3618(4)	1854(3)	21(1)	1
O(1)	8003(4)	4069(5)	1569(3)	35(1)	1
C(1)	3210(6)	4977(6)	2467(3)	24(1)	1
C(2)	1256(6)	5420(6)	2547(4)	33(1)	1
C(3)	799(6)	5474(6)	3581(4)	33(1)	1
C(4)	2225(6)	3905(6)	3972(4)	31(1)	1
C(5)	3914(6)	3904(6)	3497(3)	20(1)	1
C(6)	5416(5)	2109(5)	3490(3)	18(1)	1
C(7)	6935(6)	1801(6)	4118(3)	24(1)	1
C(8)	6287(7)	1857(7)	5131(3)	34(1)	1
C(9)	7838(6)	3086(6)	3914(3)	29(1)	1
C(10)	8284(7)	12(6)	3963(4)	39(1)	1
C(11)	6433(6)	489(6)	1104(3)	22(1)	1
C(12)	5301(6)	1891(6)	565(3)	23(1)	1
C(13)	3565(6)	2193(6)	900(3)	22(1)	1
C(14)	3622(6)	968(5)	1660(3)	20(1)	1
C(15)	5393(6)	-91(5)	1775(3)	22(1)	1
C(16)	8368(6)	-246(7)	943(4)	34(1)	1
C(17)	5853(7)	2774(6)	-276(3)	30(1)	1
C(18)	1967(6)	3494(6)	473(4)	29(1)	1
C(19)	2100(6)	698(6)	2180(3)	28(1)	1
C(20)	6020(6)	-1663(6)	2436(3)	28(1)	1

Table A15. Fractional coordinates and equivalent isotropic displacement parameters for Cp*W(NO)(C₁₂H₁₈) (3.17)

	x	y	z	U (eq)	SOF
W(1)	7336(1)	2185(1)	8834(1)	21(1)	1
O(1)	6175(3)	1602(2)	6690(2)	44(1)	1
N(1)	6565(3)	1919(2)	7544(2)	28(1)	1
C(1)	7862(4)	663(2)	9325(3)	37(1)	1
C(2)	8976(4)	1047(3)	9110(3)	38(1)	1
C(3)	9574(3)	1725(2)	9852(3)	32(1)	1
C(4)	8844(3)	1739(2)	10532(2)	28(1)	1
C(5)	7777(4)	1093(2)	10195(3)	32(1)	1
C(6)	6984(8)	-101(3)	8752(4)	63(2)	1
C(7)	9498(6)	740(4)	8299(4)	60(1)	1
C(8)	10814(4)	2282(4)	9930(4)	49(1)	1
C(9)	9255(4)	2219(3)	11532(3)	36(1)	1
C(10)	6843(4)	849(3)	10756(3)	42(1)	1
C(11)	5684(3)	2762(2)	9114(3)	25(1)	1
C(12)	6279(3)	3628(2)	8745(3)	27(1)	1
C(13)	6628(4)	4425(2)	9517(3)	35(1)	1
C(14)	6852(5)	5261(3)	8972(3)	45(1)	1
C(15)	8009(5)	5163(3)	8848(3)	47(1)	1
C(16)	8620(4)	4261(2)	9288(3)	36(1)	1
C(17)	7762(3)	3522(2)	8564(2)	26(1)	1
C(18)	8096(5)	4211(3)	10173(3)	43(1)	1
C(19)	4145(4)	2627(3)	8610(3)	33(1)	1
C(20)	3767(5)	1756(3)	9042(4)	53(1)	1
C(21)	3695(4)	2530(4)	7476(3)	43(1)	1
C(22)	3390(4)	3428(3)	8871(4)	46(1)	1

Table A16. Fractional coordinates and equivalent isotropic displacement parameters for $\text{Cp}^*\text{W}(\text{NO})(\eta^3\text{-C}_{10}\text{H}_{18})$ (**3.21a**)

	x	y	z	U (eq)	SOF
W(1)	1213 (1)	4078 (1)	2930 (1)	25 (1)	1
O(1)	2190 (7)	5741 (3)	4015 (4)	54 (2)	1
N(1)	1920 (6)	5040 (3)	3579 (4)	35 (1)	1
C(1)	-1044 (7)	4724 (4)	2140 (4)	28 (1)	1
C(2)	-1275 (7)	4489 (4)	3038 (4)	29 (1)	1
C(3)	-1248 (7)	3532 (4)	3096 (4)	29 (1)	1
C(4)	-1040 (7)	3183 (4)	2220 (4)	30 (2)	1
C(5)	-955 (7)	3923 (4)	1624 (4)	28 (1)	1
C(6)	-1136 (9)	5667 (4)	1753 (6)	43 (2)	1
C(7)	-1603 (9)	5120 (5)	3775 (5)	42 (2)	1
C(8)	-1623 (9)	2976 (4)	3883 (5)	40 (2)	1
C(9)	-1088 (9)	2207 (5)	1954 (5)	46 (2)	1
C(10)	-1069 (9)	3884 (5)	584 (5)	43 (2)	1
C(11)	2527 (8)	4501 (4)	1796 (5)	41 (2)	1
C(12)	3577 (9)	3751 (5)	1500 (5)	44 (2)	1
C(13)	4469 (9)	3302 (6)	2393 (5)	52 (2)	1
C(14)	3298 (7)	3069 (4)	2958 (5)	36 (2)	1
C(15)	3299 (8)	3313 (4)	3875 (5)	34 (2)	1
C(16)	1879 (8)	3156 (4)	4149 (4)	36 (2)	1
C(17)	3351 (12)	5354 (6)	2009 (8)	71 (3)	1
C(18)	4657 (11)	4081 (6)	892 (7)	65 (3)	1
C(19)	2555 (9)	3039 (5)	905 (5)	51 (2)	1
C(20)	4547 (9)	3837 (5)	4471 (5)	44 (2)	1

Table A17. Fractional coordinates and equivalent isotropic displacement parameters for Cp*W(NO)(cyclohexene)(PMe₃) (**4.2**)

	x	y	z	U(eq)
W(1)	1305(1)	3312(1)	634(1)	22(1)
P(1)	1754(1)	4776(3)	-105(1)	34(1)
N(1)	1605(2)	1560(8)	507(4)	30(2)
O(1)	1840(2)	321(7)	518(4)	52(2)
C(1)	944(3)	3315(10)	1706(5)	30(2)
C(2)	1402(3)	2782(9)	2051(5)	28(2)
C(3)	1709(3)	4070(9)	2029(5)	22(2)
C(4)	1422(3)	5430(8)	1675(5)	23(2)
C(5)	954(3)	4960(9)	1459(5)	25(2)
C(6)	521(4)	2404(14)	1735(7)	57(3)
C(7)	1551(4)	1108(10)	2420(7)	53(3)
C(8)	2216(3)	4030(12)	2422(6)	42(2)
C(9)	1594(4)	7127(9)	1653(6)	38(2)
C(10)	552(4)	6033(12)	1110(7)	47(3)
C(11)	2329(4)	5472(14)	521(7)	57(3)
C(12)	1914(4)	3513(11)	-873(6)	48(3)
C(13)	1528(5)	6612(12)	682(7)	62(3)
C(14)	752(3)	3687(11)	-608(5)	4e(3)
C(15)	619(3)	2463(11)	114(6)	38(2)
C(16)	555(4)	687(12)	-410(7)	54(3)
C(17)	445(4)	556(14)	1357(6)	62(3)
C(18)	791(4)	1521(11)	1653(6)	50(3)
C(19)	736(3)	3269(11)	1523(6)	43(2)

Table A18. Fractional coordinates and equivalent isotropic displacement parameters for Cp*W(NO)(neohexene)(PMe₃) (**4.4_{syn}**)

atom	x	y	z	B _{eq}
W(1)	0.18313(2)	0.147497(14)	0.24211(2)	2.452(5)
P(1)	0.3870(2)	0.19188(11)	0.38425(13)	3.63(4)
O(1)	0.2053(7)	0.3122(3)	0.1733(4)	6.8(2)
N(1)	0.2076(6)	0.2432(3)	0.1996(4)	3.75(13)
C(1)	0.0292(7)	0.0576(4)	0.3079(5)	3.42(15)
C(2)	0.0029(7)	0.1376(4)	0.3322(5)	3.51(15)
C(3)	-0.0671(7)	0.1794(4)	0.2471(6)	3.9(2)
C(4)	-0.0810(7)	0.1260(4)	0.1676(5)	3.50(15)
C(5)	-0.0275(6)	0.0515(4)	0.2079(4)	3.19(14)
C(6)	0.0770(8)	-0.0099(5)	0.3787(5)	5.2(2)
C(7)	0.0132(10)	0.1629(5)	0.4337(6)	6.3(3)
C(8)	-0.1239(9)	0.2633(5)	0.2383(8)	7.2(3)
C(9)	-0.1563(9)	0.1433(5)	0.0637(6)	6.6(2)
C(10)	-0.0486(8)	-0.0251(4)	0.1516(6)	5.5(2)
C(11)	0.4646(10)	0.1301(5)	0.4907(6)	6.5(2)
C(12)	0.5578(8)	0.2303(5)	0.3574(6)	5.4(2)
C(13)	0.3285(10)	0.2789(5)	0.4380(7)	6.7(3)
C(14)	0.2350(8)	0.0898(4)	0.1214(4)	3.9(2)
C(15)	0.3818(7)	0.0925(4)	0.1961(5)	3.5(2)
C(16)	0.4711(7)	0.0154(4)	0.2253(5)	4.1(2)
C(17)	0.3830(9)	-0.0475(5)	0.2626(6)	5.4(2)
C(18)	0.5161(10)	-0.0167(5)	0.1386(7)	6.9(3)
C(19)	0.6242(9)	0.0281(5)	0.3075(7)	6.6(2)

Table A19. Fractional coordinates and equivalent isotropic displacement parameters for Cp*W(NO)(cyclohexyl)(NMe₂) (**4.7**)

	x	y	z	U(eq)
W	0.30124(2)	0.16682(4)	0.08101(2)	0.0425
O	0.3916(6)	-0.1617(8)	0.1310(6)	0.087
N(1)	0.3568(5)	-0.0263(8)	0.1036(5)	0.057
N(2)	0.3937(5)	0.2761(8)	0.0498(5)	0.049
C(1)	0.2168(6)	0.3906(10)	0.1164(6)	0.048
C(2)	0.3034(5)	0.3620(9)	0.1842(5)	0.047
C(3)	0.3019(6)	0.1985(10)	0.2135(5)	0.053
C(4)	0.2119(6)	0.1305(10)	0.1634(6)	0.053
C(5)	0.1600(6)	0.2438(11)	0.1051(6)	0.051
C(6)	0.3882(7)	0.4521(10)	0.0270(6)	0.062
C(7)	0.4810(7)	0.2108(12)	0.0484(7)	0.070
C(11)	0.1816(7)	0.5532(11)	0.0723(7)	0.066
C(12)	0.3816(7)	0.4849(13)	0.2255(6)	0.071
C(13)	0.3795(8)	0.1213(15)	0.2892(7)	0.086
C(14)	0.1779(8)	-0.0392(12)	0.1787(8)	0.077
C(15)	0.0583(6)	0.2382(14)	0.0472(8)	0.075
C(21)	0.1982(7)	0.0864(15)	-0.0386(6)	0.070
C(22)	0.1664(9)	0.2168(22)	-0.1014(8)	0.105
C(23)	0.0886(11)	0.1550(28)	-0.1863(10)	0.132
C(24)	0.1242(14)	0.0220(33)	-0.2233(10)	0.130
C(25)	0.1593(15)	-0.1211(25)	-0.1588(12)	0.140
C(26)	0.2348(12)	-0.0546(19)	-0.0805(9)	0.109

Table A20. Fractional coordinates and equivalent isotropic displacement parameters for $\text{Cp}^*\text{W}(\text{NO})(\eta^3\text{-C}_7\text{H}_{11})(\text{H})$ (**4.9_{endo}**)

	x	y	z	U(eq)
W(1)	3433(1)	6447(1)	2047(1)	36(1)
C(1)	3341(13)	7560(7)	924(6)	37(2)
C(2)	2630(14)	6721(8)	571(7)	38(2)
C(3)	774(16)	6639(9)	96(8)	49(3)
C(4)	-442(15)	7436(9)	339(8)	58(3)
C(5)	464(17)	8404(8)	278(9)	52(3)
C(6)	2179(15)	8480(7)	914(8)	42(3)
C(7)	5008(15)	7530(8)	1426(8)	53(3)
C(8)	4147(17)	4761(9)	2080(8)	52(3)
C(9)	5794(13)	5261(8)	2020(7)	42(3)
C(10)	6333(11)	5814(9)	2795(7)	41(3)
C(11)	4911(15)	5742(9)	3271(7)	50(3)
C(12)	3645(16)	5059(9)	2873(9)	55(3)
C(13)	3313(21)	4036(11)	1463(11)	82(5)
C(14)	6940(17)	5143(9)	1323(9)	62(4)
C(15)	7923(18)	6414(8)	2938(11)	66(4)
C(16)	4964(24)	6177(12)	4130(9)	84(5)
C(17)	2035(20)	4691(10)	3228(12)	85(5)
N(1)	2300(12)	7312(7)	2608(6)	44(2)
O(1)	1620(12)	7847(8)	3072(6)	74(3)

Table A21 Fractional coordinates and equivalent isotropic displacement parameters for $\text{Cp}^*\text{W}(\text{NO})(\eta^3\text{-C}_8\text{H}_{13})(\text{H})$ (**4.11_{exo}**)

	x	y	z	U(eq)
W(1)	0.64157(3)	0.17219(2)	0.36499(2)	2.012(6)
O(1)	0.7957(7)	-0.0135(4)	0.3192(4)	5.5(2)
N(1)	0.7258(7)	0.0622(5)	0.3323(4)	3.18(14)
C(1)	0.5883(7)	0.1911(5)	0.5156(4)	2.32(14)
C(2)	0.7467(8)	0.1610(5)	0.5140(4)	2.45(14)
C(3)	0.8301(7)	0.2353(5)	0.4724(5)	2.87(15)
C(4)	0.7204(8)	0.3132(5)	0.4500(5)	2.56(15)
C(s)	0.5711(7)	0.2831(5)	0.4770(5)	2.34(14)
C(6)	0.4598(9)	0.1388(6)	0.5636(5)	37(2)
C(7)	0.8188(11)	0.0698(6)	0.5556(6)	4.5(2)
C(8)	1.0043(8)	0.2377(8)	0.4632(6)	5.0(2)
C(9)	0.7587(11)	0.4104(6)	0.4129(6)	4.2(2)
C(10)	0.4227(9)	0.3450(6)	0.4724(6)	4.2(2)
C(11)	0.7270(9)	0.2429(7)	0.2416(5)	4.0(2)
C(12)	0.5651(10)	0.2593(5)	0.2389(4)	33(2)
C(13)	0.4491(9)	0.1890(5)	0.2304(5)	2.9(2)
C(14)	0.2778(9)	0.2157(7)	0.2386(5)	40(2)
C(15)	0.1744(9)	0.1336(7)	0.2640(6)	40(2)
C(16)	0.1892(9)	0.0475(6)	0.2026(6)	43(2)
C(17)	0.3569(9)	0.0161(6)	0.1978(5)	35(2)
C(18)	0.4612(9)	0.0993(6)	0.1729(5)	33(2)

Table A22. Fractional coordinates and equivalent isotropic displacement parameters for $\text{Cp}^*\text{W}(\text{NO})(\text{CH}_2\text{CMe}_2\text{-}o\text{-C}_6\text{H}_4)(\text{PMe}_3)$ (**5.1**)

	x	y	z	U (eq)
W(1)	1757(1)	1247(1)	1918(1)	13(1)
P(1)	3741(1)	1248(1)	952(1)	18(1)
O(1)	1243(4)	2996(3)	951(2)	33(1)
N(1)	1502(4)	2312(3)	1362(2)	20(1)
C(1)	145(6)	221(3)	2586(3)	22(1)
C(2)	-526(5)	721(3)	1940(3)	19(1)
C(3)	75(6)	404(3)	1194(3)	20(1)
C(4)	1109(6)	-270(4)	1391(3)	24(1)
C(5)	1166(6)	-371(4)	2253(3)	24(1)
C(6)	-284(7)	221(4)	3455(3)	31(1)
C(7)	-1713(5)	1371(3)	2011(3)	29(1)
C(8)	-421(6)	666(4)	376(3)	35(1)
C(9)	1811(7)	-898(4)	802(3)	39(1)
C(10)	1984(6)	-1074(3)	2726(3)	35(1)
C(11)	3553(4)	1234(4)	2758(2)	14(1)
C(12)	3677(5)	1975(3)	3309(3)	17(1)
C(13)	4805(6)	2014(4)	3825(3)	26(1)
C(14)	5771(5)	1313(5)	3839(3)	28(1)
C(15)	5610(5)	538(4)	3336(3)	24(1)
C(16)	4541(5)	516(3)	2790(3)	20(1)
C(17)	2534(5)	2676(3)	3317(3)	18(1)
C(18)	1280(5)	2133(3)	3004(3)	21(1)
C(19)	2209(6)	3049(4)	4175(3)	31(1)
C(20)	2872(6)	3530(3)	2789(3)	27(1)
C(21)	3161(6)	1439(4)	-83(3)	33(1)
C(22)	5022(6)	330(4)	798(3)	31(1)
C(23)	4823(6)	2258(4)	1128(3)	29(1)